CODON AND AMINO ACID USAGE ANALYSIS IN THE GENUS *ACINETOBACTER*

Thesis Submitted for the Award of the Degree of

DOCTOR OF PHILOSOPHY
in

Biochemistry

By

Ujwal Dahal

Registration Number: 12111181

Supervised By
Dr. Anu Bansal (21971)
Department of Biochemistry
(Associate professor)
Lovely Professional University

LOVELY PROFESSIONAL UNIVERSITY, PUNJAB
2025

DECLARATION

I, hereby declare that the presented work in the thesis entitled "**Codon and amino acid usage analysis in the genus *Acinetobacter***" in fulfillment of my degree of **Doctor of Philosophy (Ph. D.)** is outcome of research work carried out by me under the supervision of Dr. Anu Bansal, working as Assistant Professor and Cultural Coordinator, in the Department of Biochemistry, School of Bioengineering and Biosciences of Lovely Professional University, Punjab, India. In keeping with the general practice of reporting scientific observations, due acknowledgments have been made whenever the work described here has been based on the findings of another investigator. This work has not been submitted in part or full to any other University or Institute for the award of any degree.

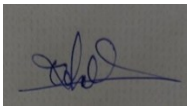

Name of the scholar: Ujwal Dahal

Registration No.: 12111181

Department/School: Department of Biochemistry, School of Bioengineering and Biosciences

Lovely Professional University,

Punjab, India

CERTIFICATE

This is to certify that the work reported in the Ph. D. thesis entitled "**Codon and amino acid usage analysis in the genus *Acinetobacter***" submitted in fulfillment of the requirement for the award of degree of **Doctor of Philosophy (Ph.D.)** in the Department of Biochemistry, is a research work carried out by Ujwal Dahal (12111181), is bonafide record of his/her original work carried out under my supervision and that no part of thesis has been submitted for any other degree, diploma or equivalent course.

Name of supervisor: Anu Bansal

Designation: Associate Professor

Department/school: Department of Biochemistry, School of Bioengineering and Biosciences

Lovely Professional University, 144411 Phagwara, Punjab, India

ABSTRACT

Discovered in the early 1900s, *Acinetobacter* was initially regarded as an insignificant bacterium, with only *A. baumannii* identified as an opportunistic pathogen and susceptible to all available antibiotics. However, during the 1990s, advancements in hospital technologies and the increased use of catheters and ventilators led to a significant rise in *Acinetobacter* infections globally. During this period, additional species, such as *A. calcoaceticus, A. nosocomialis, and A. pittii*, were also found to be infectious. The infection rate surged dramatically by the early 2010s, with reports identifying over 21 pathogenic species of *Acinetobacter*. Following 2010 to the present date, cases of antibiotic resistance emerged within this genus. This prompted the World Health Organization to classify *A. baumannii* as one of the ESKAPE pathogens, known for its ability to evade available antibiotics. Given this background, we sought to understand how this previously insignificant genus gave rise to multiple pathogenic and antibiotic-resistant members. To explore this, we conducted codon and amino acid analysis across the entire *Acinetobacter* genus as well as on their antibiotic resistance and virulence genes to uncover the mechanisms underlying the pathogenicity, antibiotic resistance, and evolutionary changes within the genus.

Our investigation encompassed a majority of *Acinetobacter* species, totaling 56, with available genome data sourced from Ensembl bacteria. Through systematic analysis and comparison, we identified and scrutinized various factors including RSCU, RAAU, optimal and favored codons, GC content, CAI, ENC plot, parity plot, and codon pairs, as well as GC3 variation. Notably, each organism displays a preference for a pair of adjacent codons, known as a codon pair. Consequently, we endeavored to compute the relative synonymous codon pair usage (RSCPU) across all members of the genus. Additionally, we sought to delineate the overarching evolutionary driving forces and offer a more intricate understanding of the distinct evolutionary statuses of all selected species through the use of neutrality plots and translational selection assessment. The detailed analysis of *gyrB* sequence alignment and phylogeny within this diverse genus is

poised to make a significant contribution to understanding this genus. Additionally, we conducted a whole genome sequence analysis of selected members of the genus to detect antibiotic resistance and virulence genes and integrated codon usage analysis with phylogenetic data to get insights into the adaptive strategies of *Acinetobacter* species and uncover how these strategies contributed during the evolution of virulence and resistance genes in the genus.

The analysis revealed a dynamic range of GC composition from 35.71% to 46.21%, highlighting the interplay of selective pressures and mutational bias in shaping genomic characteristics. Within the *Acinetobacter baumannii* complex, a balanced distribution of nucleotides at third codon positions reflected genomic stability. The preference for AT-rich codons in all the members of the genus indicated selection pressures favoring specific codons, while the observed correlation of GC content with codon usage emphasizes the influence of compositional bias on preferences. Furthermore, Codon Adaptation Index (CAI) values > 0.5 revealed a high bias towards the use of favored and optimal codons in highly expressed genes. Species-specific variations in codon pair preferences, along with shared similarities within the ACB complex, suggested functional congruence. *gyrB* gene phylogenetic analysis clustered ACB complex despite different levels of evolutionary divergence. This study provides a quantitative overview of various factors influencing codon and amino acid usage bias in the genus *Acinetobacter*. The absence of substantial genomic disparities between pathogenic and non-pathogenic species suggested potential virulence factors across all *Acinetobacter* members, warranting further investigation into their pathogenic potential. Therefore, we conducted whole comparative genome sequence analysis of clinically significant *Acinetobacter baumannii* and environmentally prevalent *Acinetobacter baylyi* to shed light on their genetic landscapes. Sequencing revealed 59,373 and 58,729 SNPs, alongside 33 and 27 Indels respectively. Notably, virulence gene profiling highlighted both shared and unique gene presence patterns, with all virulence genes present except the absence of *hemO* in *A. baumannii* and *basC* in *A. baylyi* when compared with pathogenic *A. baumannii* strain AB00057. Crucial antibiotic resistance genes like *blaADC-25* and *blaOXA-98* were

identified, with sequence similarity of 96.9% and 99.88% respectively with their reference sequence. It was discovered that β-lactamase genes such as *blaADC-25* (36%) and *blaOXA-98* (39%) have lower GC contents, whereas biofilm-associated gene clusters, such as *pga* (39% to 43%) gene cluster, exhibit higher GC contents. Codon usage bias across specific gene clusters was found to be consistent, with minimal effect of mutational pressure (6%-28%) and a significant effect of translational selection (0.31 to 0.50). Overall, the codon usage signatures across specific gene cluster and across functionally related genes were found to be very similar. Leucine and alanine predominated in the genes, reflecting their functional association. Phylogenetic analysis showed that gene clustering correlates with codon usage patterns. Protein interaction network analysis supported the notion that both codon usage and selective pressures like mutation and translational selection influence the evolution of antibiotic resistance and virulence genes in *A. baumannii and A. baylyi.*

This study not only enhanced our understanding of how *Acinetobacter* species evolve, adapt, and diversify in response to selective pressures encountered in various ecological niches and host environments but also showed the unique genomic signature of ACB complex entirely different from other members of the genus. These findings contribute valuable insights into the genomic strategies underpinning the pathogenic potential of ACB complex, metabolic versatility, and evolutionary success, with implications for biomedical research, antibiotic resistance studies, and public health interventions targeting *Acinetobacter* infections. Additionally, the comprehensive analysis of *A. baumannii* 1425 ARGs and VRGs shed light on the intricate genetic landscape underlying its adaptability and pathogenicity. The study identified a diverse array of ARGs and VRGs, such as *blaADC-25* and *blaOXA-98* in *A. baumannii and A. baylyi*, which contribute to the resistant against treatment and its ability to cause severe infections. The identification of these genes especially in environmentally prevalent *A. baylyi* suggests its pathogenicity in the near future. Moreover, the genetic variability observed among these genes underscores the complex evolutionary mechanisms through which *Acinetobacter* acquires virulence and resistance. Furthermore, the examination of

codon usage patterns has revealed crucial genomic signatures within specific gene clusters and functionally related genes. Additionally, the phylogenetic clustering of genes with similar codon usage patterns revealed how *Acinetobacter* optimizes the expression of ARGs and VRGs for its survival in virulence and antibiotic-resistant environments during the time of evolution. Future research could further explore these genomic insights to develop targeted therapies and mitigate the impact of *Acinetobacter*-associated infections.

ACKNOWLEDGMENT

I would like to express my sincere gratitude to the following individuals and organizations for their invaluable support and contribution to the completion of my PhD thesis:

My supervisor Dr. Anu Bansal for her guidance, encouragement, and unwavering support throughout my research journey. Her expertise, knowledge, and experience have been instrumental in shaping my research and helping me navigate the challenges that arose during my Ph.D journey. I am deeply grateful for her time, patience, and commitment to my success.

I would like to express my profound gratitude to Dr. Minhaj Ahmad Khan, Dr. Gurmeen Rakhra, Dr. Arvind Kumar, and Dr. Jeena Gupta for their insightful advice and intellectual assistance during my ETP evaluation. The staff and faculty at Lovely Professional University, Punjab, India, and DAV University, Jalandhar, India, for providing me with the resources, facilities, and opportunities to pursue my research interests. Their expertise, knowledge, and support have been invaluable in my research journey. I am grateful for their guidance, and mentorship, and for creating an environment that fosters learning and growth.

My family and all the relatives for their love, patience, and understanding during the ups and downs of my Ph.D journey. Their unwavering support and encouragement have been a constant source of strength and motivation for me. My friends, Dr. Bhumandeep Kour, Dr. Bhusan Laxman Sonawane, Sourarabh Garg, Er. Ujjwal Mishra and Sushma Sigdel for their unwavering support, and encouragement, and for always being there to listen and provide a much-needed break from my research. Their friendship and camaraderie have been a source of joy and comfort during my Ph.D journey. I am grateful for their understanding when I needed to focus on my research and for their celebration when I achieved milestones.

I would also like to express my appreciation to Eurofins Analytical Services India Pvt Ltd, Banglore, India, Institute of Microbial Technology, Chandigarh as well as Dr. Shelly

Gupta, Dr. Karan Paul, Dr. Anuj Sharma and Dr. Dheeraj Chitara for their research support and assistance.

I would also like to thank Almighty, for giving me strength and encouragement throughout all the challenging moments of completing my work. I am truly grateful for his unconditional and endless love, mercy, and grace.

I am truly grateful to every one of you for your contributions, whether big or small, to this significant milestone in my academic journey.

Ujwal Dahal

Table of Contents

List of Tables

List of Figures

CHAPTER 1: INTRODUCTION

The *Acinetobacter* genus encompasses a cohesive monophyletic group of over 59 species, both pathogenic and nonpathogenic, distinctly categorized into four clades based on 550 core protein-coding genes (Vijayakumar et al., 2019). The first clade comprises 28 species, spanning from *A. schindleri* to *A. radioresistens*. The second clade features the ACB complex as a sub-clade, encompassing 22 species, starting from *A. proteolyticus* to *A. ursingii*. The "ACB complex" consists of *A. calcoaceticus*, *A. baumannii*, *A. pitti*, *A. nosocomialis*, *A. oleivorans*, A. *lactucae*, and *A. seifertii* which cannot be differentiated by simple phenotypic methods and needs genotypic identification methods. The third clade consists of four species, spanning from *A. boissieri* to *A.brisouii* while the last clade is composed by *A. puyangensis, A. populi*, and A. *qingfengensis*,(Almeida et al., 2021). Recently, new species, including *A. silvestris* (Nemec et al., 2022), *A. sedimenti* (Zheng et al., 2022), *A. amyesii* (Nemec et al., 2022), *A. faecalis* (Chen et al., 2023), *A. tibetensis* (Pan et al., 2023), and *A. ihumii* (Yacouba et al., 2022), have also been discovered. All members of this genus are exclusively aerobic, exhibiting characteristics such as being catalase-positive (Dahal et al., 2023), oxidase-negative, (Touchon et al., 2014) and non-motile (Patel et al., 2021). The importance of *Acinetobacter* spp. as a notable nosocomial bacteria responsible for hospital outbreaks is increasingly recognized, especially in intensive care and ventilator units across hospitals, where they swiftly develop resistance even against the most robust antimicrobials (Antunes et al., 2014; Manchanda et al., 2010). Meningitis by *A. baumannii* (Xiao et al., 2019), pneumonia by *A. calcoaceticus* (El Gharib et al., 2021), bacteremia by *A. bereziniae* (Lee et al., 2020), *A. seifertii* (Kishii et al., 2016) and *A. urisingii* (Daniel et al., 2019), urinary and respiratory tract infections by *A. junnii* (Kollimuttathuillam et al., 2021) and *A. baumannii* (Chakraborty et al., 2019) are some of the most frequent illnesses associated with various *Acinetobacter* species.

Acinetobacter spp infections have caused higher death rates in several parts of the world during the previous decade, ranging from 35% in Mexico and Ecuador (Elbehiry et al., 2023) to 66 % in Brazil (John et al., 2020). Meanwhile, the death rate reports as high as 42.8% in China (John et al., 2020) and 57.6% in developing nations like India (John et

al., 2020; Vijay et al., 2018). These global death rates are mainly due to Ventilator-associated pneumonia (VAP). *A. baumannii* is the main cause of VAP globally accounting for 47% of VAP cases in India (Vijay et al., 2018), 26.9% and 14.6% in Poland and Ukaraine (Huang et al., 2019) respectively. Up to 84.3% of VAP cases caused by multi-drug-resistant *A. baumannii* have been reported to be fatal in the intensive care unit (Adukauskiene et al., 2022). The range of crude mortality for individuals with *Acinetobacter* bacteremia is 37% to 52% in the United States (C. Ma & McClean, 2021) and 78.48% in India (Mathai et al., 2012). Moreover, *Acinetobacter* meningitis being very uncommon, poses a growing risk to individuals who have had neurosurgery because of its fatality rate (>70%) (Adukauskiene et al., 2022; C. Ma & McClean, 2021).

Given this alarming clinical impact, a comprehensive and multi-pronged strategy is required (Rebic et al., 2018). Promising avenues include the development of novel antimicrobials and antibiotic adjuvants that can either bypass or inhibit known resistance mechanisms (Ayoub Moubareck & Hammoudi Halat, 2020). In parallel, alternative therapeutic approaches such as phage therapy, antimicrobial peptides, and immunotherapeutic interventions are gaining attention (Almeida et al., 2021; Mateo-Estrada et al., 2019). Infection prevention and control measures remain central to containment efforts, especially in nosocomial settings, and must be rigorously implemented through standardized protocols and sustained training. Surveillance systems to track resistance trends and detect outbreaks at early stages are equally critical, as are the deployment of rapid diagnostic platforms that can enable timely and targeted therapeutic interventions (Ayoub Moubareck & Hammoudi Halat, 2020). Equally important is the reinforcement of antimicrobial stewardship programs to preserve the efficacy of existing drugs. In recent years, genomic and transcriptomic investigations have provided valuable insights into the resistance determinants, virulence factors, and adaptive mechanisms employed by Acinetobacter. These omics-based approaches hold substantial potential for the identification of novel drug targets and vaccine candidates, thereby contributing to the long-term control and prevention of Acinetobacter-associated infections (Rebic et al., 2018).

Apart from its pathogenicity profile, the genus *Acinetobacter* also displays physiological traits that are linked to critical microbiological and biotechnological processes, including biofilm formation (Yang et al., 2019), quorum sensing (the process by which *Acinetobacter* species communicate with each other to maintain population density) (Zhong & He, 2021), production of lipase, biosurfactants like Alasan and Emulsan (Mujumdar et al., 2019), biopolymeric substances like polyhydroxy butyrate (Anburajan et al., 2019), biodiesel, wax, and dye degradation (Dahal et al., 2023; Patel et al., 2021; Snellman & Colwell, 2004). These bioproducts from *Acinetobacter* are used in the food industry (lipase), textiles (dyes), biofuel (biodiesel), cosmetic (wax esters), and pharmaceutical industry (lipases) (Dahal et al., 2023; Patel et al., 2021; Snellman & Colwell, 2004).

1.1 Phylogeny

Utilizing 275 meticulously selected high-quality protein sequences, extracted from a consensus dataset of 550 core protein-coding genes, the construction of the core genome maximum likelihood (cgML) tree for over 80 *Acinetobacter* species unveiled four prominent clades, offering an extensive perspective on *Acinetobacter*'s evolutionary history. These species were demonstrated to form a cohesive monophyletic group, distinctly categorized into four clades. The first clade comprised 28 species, spanning from *A. schindleri* to *A. radioresistens*. The second clade featured the ACB complex, encompassing 22 species, from *A. proteolyticus* to *A. ursingii*. The fourth clade was constituted by *A. populi, A. puyangensis*, and *A. qingfengensis*, while the third clade included four species, ranging from *A. boissieri* to *A. brisouii* (Almeida et al., 2021). Additionally, *A. radioresistens* emerged as the earliest lineage among the sequenced *Acinetobacter* genomes, boasting the smallest genome size, whereas the ACB complex exhibited the largest genome size. This conclusion was drawn from an extensive evaluation of several conserved genes (Sahl et al., 2013; Touchon et al., 2014b). Furthermore, species originating from non-human vertebrates, the environment, and insects displayed smaller genome sizes than those isolated from humans. Nevertheless,

no significant discrepancies were observed in the distribution of amino acid usage and virulence genes across the various species. Every *Acinetobacter* species was found to harbor at least one virulence gene. Within the ACB sub-clade, numerous virulence factors associated with functions like iron absorption, pathogenesis, biofilm development, and adhesion were identified (Almeida et al., 2021).

Most advanced molecular diagnostic techniques have been forwarded for the identification of species of the genus *Acinetobacter*. Some of them are: Amplified 16S rRNA gene restriction analysis (ARDRA), High-resolution fingerprint analysis by amplified fragment length polymorphism (AFLP), tRNA spacer fingerprinting and Sequencing of the rpoB gene(RNA polymerase β-subunit) (Dahal et al., 2023). Due to the similarity in phenotypic characteristics DNA printing finger-printing techniques are used to separate *Acinetobacter species*. RNA polymerase subunit (ropB) gene-based phylogenic study matches the results from DNA-DNA hybridization and average nucleotide index and is proved as co-standard for previously used rRNA based gene-based phylogeny. DNA gyrase subunit B also gave insights into the taxonomy of *Acinetobacter* despite poor resolution compared to the ropB gene. These methods have not completely solved the diversity of *Acinetobacter* taxonomy the result of which increased the phylogenic analysis of housekeeping genes. Therefore, considering the resolution high-resolution investigations other techniques like multi-locus sequence typing, pulse field gel electrophoresis, and mass spectroscopy are preferred (Morris et al., 2019). The characterization of clinical and non-clinical isolates by these methods has provided new insights into the classification of strains, the development of drug candidates for clinical species, and using non-environmentalnonspecies for human significance (Wong et al., 2017).

1.2 The *Acinetobacter baumannii* complex (ACB complex)

The *Acinetobacter baumannii* complex (ACB complex) comprises five species that are both phenotypically and genotypically similar: *A. baumannii*, *A. calcoaceticus*, *A. pitti*, *A.*

nosocomialis, and *A. seifertii*. *A. lactucae*, and A. *oleivorans* have all been identified as members of this complex in recent investigations (Almeida et al., 2021; Dahal et al., 2023). Traditional phenotypic identification methods face challenges in differentiating these species within the complex. However, recent advancements in DNA identification techniques have definitively recognized them as distinct and unique species (Oelschlaeger, 2024).

1.3 Some Pathogenic Species

Among the more than 60 species of *Acinetobacter*, the clinically most significant is the *Acinetobacter baumannii* complex (comprising *A. nosocomialis*, *A. pitti*, and *A. baumannii*), followed by *A. haemolyticus*, *A. junni*, *A. johnsonii*, and *A. lwoffi*. Recent findings also indicate the presence of *A. ursingii* and *A. schindleri* in clinical infections (Kee et al., 2018; Mlynarcik et al., 2019). *A. baumannii* accounts for over 90% of infections in human hosts, with other species in the genus contributing to the remaining 10%. Epidemics caused by *Acinetobacter* species are driven by antibiotic resistance and the ability to persist in harsh hospital environments, including resistance to desiccation and disinfectants (Wong et al., 2017).

Members of the *Acinetobacter* genus typically cause a range of infections, including pneumonia, septicemia, endocarditis, meningitis, and infections in wounds, the urinary tract, and lungs (Huang et al., 2019). *Acinetobacter* employs various putative virulence factors, including outer membrane proteins, cell surface hydrophobicity, toxic slime polysaccharides, and verotoxins. The hydrophobicity of the cell surface is crucial for bacterial attachment and aids in evading phagocytosis by the host. Outer membrane proteins mediate antibiotic resistance and adaptability in host cells. *Acinetobacter* endotoxins trigger the release of inflammatory mediators in the host upon activation of white blood cells. Additionally, extracellular enzymes and cytotoxins play a role in the pathogenesis of *Acinetobacter* species (C. Liu et al., 2018).

1.3.1 *Acinetobacter baumannii*

Acinetobacter baumannii is a gram-negative, aerobic coccobacillus bacterium commonly found in hospitals worldwide. Recognized as one of the "ESKAPE" pathogens due to its multidrug resistance, *A. baumannii* is a clonal pathogen capable of causing epidemics, particularly in intensive care patients. Its presence can be identified using 16s ribosomal RNA and seven housekeeping genes (*rpoD, gyrB, gdhB, recA, gltA, gpi,* and *cpn60*) through multilocus sequence typing (MLST). *A. baumannii* is responsible for various diseases, including ventilator-associated pneumonia, sepsis, urinary tract infections, and skin and soft-tissue infections (C. Liu et al., 2018).

Apart from causing diseases, *A. baumannii* is a common colonizer of the skin and upper respiratory tract and has been identified in human sputum, blood, urine, and feces. Notably, *A. baumannii* can persist on hospital surfaces for extended periods and has been isolated from various sources such as tap water faucets, angiography catheters, ventilators, air, gloves, and bedside urinals (López et al., 2019; Morris et al., 2019).

Furthermore, *Acinetobacter baumannii* exhibits a distinctive ability to survive in clinical environments and develop resistance to antibiotics, leading to clinical outbreaks and contributing to approximately one-fifth of infections in intensive care units globally (Sarshar et al., 2021). Various genomic and phenotypic factors have been discovered that contribute to *A. baumannii's* successful pathogenicity. Some key factors include 1. Biofilm Formation Potential: *A. baumannii* possesses the capability to form biofilms, aiding in its resilience to drying on non-living surfaces, particularly on medical equipment. 2. Horizontal Gene Transfer: The ability to adapt foreign genes allows *A. baumannii* to counteract antibiotics and host defense systems effectively. 3. Host Attachment and Colonization: *A. baumannii* exhibits the potential to attach, colonize, and infect the host's body, contributing to its pathogenicity. 4. Rapid Regulation of Multidrug Resistance (MDR) Systems: *A. baumannii* can swiftly regulate its MDR systems in response to antibiotic exposure, allowing it to develop resistance within a short timeframe (Gedefie et al., 2021; Sarshar et al., 2021).

1.3.2 *Acinetobacter calcoaceticus*

Acinetobacter calcoaceticus, another member of the ACB complex, is a non fermentative aerobic, gram-negative, naturally transformable, and metabolically active rod widely distributed in nature. It is commonly found as part of the normal flora in humans, with up to 25% of healthy individuals harboring it on their skin and in the respiratory tract. *A. calcoaceticus* is recognized as an opportunistic pathogen, and several nosocomial infection outbreaks have been documented, often linked to contamination of hospital equipment and personnel's hands. In clinical laboratories, many *A. calcoaceticus* isolates are associated with skin colonization or contamination rather than genuine infection (Irankhah et al., 2019; Retailliau et al., 1979).

While *A. calcoaceticus* is generally considered harmless, infections caused by this organism have been reported to result in septicemia, meningitis, endocarditis, brain abscess, pneumonia, lung abscess, empyema, tracheobronchitis, wound infections, and more (El Gharib et al., 2021; Figueiredo et al., 2012). The emergence of antibiotic resistance in *A. calcoaceticus* is a growing concern. Resistance to β-lactams is primarily attributed to the development of a chromosomally encoded cephalosporinase. Additionally, reduced outer membrane permeability significantly contributes to *A. calcoaceticus'* natural resistance to extended-spectrum antibiotics. The poor antibiotic permeability across the outer membrane is attributed to the limited number of porins in *A. calcoaceticus* (El Gharib et al., 2021).

1.3.3 *Acinetobacter pitti*

A. pittii, another member of the ACB complex, is gaining recognition as a clinically significant species, thanks to advancements in identification technologies that better differentiate between *A. pittii* and *A. baumannii*. Also known as *Acinetobacter* genomic species three, *A. pittii* is increasingly prevalent in various settings, including food, clinical environments, and non-clinical surroundings (Vijayakumar et al., 2019a). While *A. pittii*

shares the ACB complex with *A. baumannii*, it is generally considered less pathogenic (Wong et al., 2017).

Recently *A. pittii* has exhibited heightened carbapenem resistance, accompanied by shifts in its resistance mechanisms. Notably, the emergence of carbapenem-hydrolyzing lactamases, such as NDM1, in *A. pittii* has become a significant medical concern. Carbapenem-resistant *A. pittii* (CRAP) has been extensively documented and disseminated globally, with strong links to human infection and intestinal carriage. It stands as a major contributor to nosocomial infections in hospitals worldwide, particularly in intensive care units (Iimura et al., 2020).

1.3.4 *Acinetobacter seifertii*

A. seifertii, a recently discovered member of the ACB complex, was first isolated in Denmark in 1990/91 from samples (ulcer and blood) of a patient officially identified *A. seifertii* as a new member of the ACB complex, formerly known as gen sp "near to 13TU" (Kishii et al., 2016). Subsequently, *A. seifertii* has been found in various clinical samples globally, as well as in environmental samples both within and outside hospital settings. While *A. seifertii* initially seemed to have less clinical significance than other members of the complex, the incidence of infections attributed to it is on the rise (Cayô et al., 2016; Kishii et al., 2016).

Phenotypically, *A. seifertii* shares similarities with other *Acinetobacter* species, particularly within the ACB complex. Colonies exhibit circular, convex, smooth, and somewhat opaque characteristics with complete borders, measuring 1 to 1.5 mm in diameter. The ideal temperature range for growth is 15 to 41 degrees Celsius, with 37 degrees Celsius being optimal. Growth thrives in environments with an ideal pH and NaCl concentration between 5..5 to 9 and 0 to 4%, respectively (Yang et al., 2019). *A. seifertii* isolates are aerobic, gram-negative, oxidase-negative, catalase-positive, and non-motile and can grow well in mineral medium with acetate and ammonia as the sole

sources of carbon and nitrogen, respectively. However, relying solely on phenotypic testing proves insufficient for distinguishing *A. seifertii* from the broader ACB complex (Vijayakumar et al., 2019b).

A. seifertii is equipped with the AdeB/AdeJ and MdtB/MuxB families of RND and MFS systems and the Bcr/CflA and DHA2 families of MFS systems. Resistances to erythromycin and telithromycin are conferred through mutations in the 23S rRNA gene. Abundant metal tolerance genes are present, including copper genes labeled with the prefix "cop" (designated as C, D, E), arsenic genes with the prefix "ars" (B, C, H), magnesium/cobalt genes, cadmium/zinc/cobalt genes, and chromium (chrB) (terD). Furthermore, Resistome analysis has unveiled antibiotic resistance genes for β-lactams (blaADC25 and blaTEM) and multidrug efflux mechanisms in *A. seifertii* (Furlan et al., 2019).

1.3.5 *Acinetobacter nosocomialis*

A. nosocomialis, a Gram-negative opportunistic pathogen, is part of the ACB complex. While *A. baumannii* takes the lead in the ACB complex in terms of infection frequency, clinical outcomes, and multidrug resistance, *A. nosocomialis* remains a significant pathogen in the realm of infections. The infective potential of *A. nosocomialis* in humans has been thoroughly examined, revealing a repertoire of potential virulence factors, including a protein O-glycosylation system, CTFR inhibitory factor (Cif), two types of secretion systems, the OmpA protein, the CpaA protease, and the secretion of outer membrane vesicles (Nithichanon et al., 2022). Despite the similarities in phenotype and genotype between *A. baumannii* and *A. nosocomialis*, distinctions arise in terms of infection frequency, multidrug resistance capability, carbapenem, and aminoglycoside resistance systems, clinical features of infection, and the mortality rates of infected patients (Memesh et al., 2024).

A. nosocomialis pathogenesis is orchestrated through two crucial type secretion systems: Type I (T1SS) and Type II (T2SS). The Type I secretion system is employed by *A. nosocomialis* to export two putative T1SS effectors, namely an RTX-serralysin-like toxin and the biofilm-associated protein (Bap). Remarkably, the T1SS plays a vital role in biofilm development (Amaral et al., 2023). Equally significant is the Type II secretion system, the first secretion system identified as necessary for virulence in *Acinetobacter* species, including *A. nosocomialis*, particularly for full virulence in Galleria mellonella. Among the substrates exported by T2SS are the lipases Lip (A, H) and the protease CpaA. Deletion of cpaA in moth and mouse models has demonstrated a reduction in *A. nosocomialis* pathogenicity (Amaral et al., 2023; Jing et al., 2022).

Multidrug efflux pumping systems exert influence on various aspects of *A. nosocomialis*, encompassing antibiotic resistance mechanisms, pathogenesis, cell multiplication, and biofilm development. AcrR serves as a regulator overseeing the transcription of the AcrAB efflux pump in *A. nosocomialis*. The acrAB operon, encoding AcrA and AcrB, shares a notable resemblance with the arpAB operon discovered in *A. baumannii*, known for its involvement in aminoglycoside resistance (Yang et al., 2019).

1.4 Nonpathogenic species

Non-pathogenic *Acinetobacter* species have proven valuable in various biotechnological and environmental applications. These strains play crucial role in breaking down contaminants such as biphenyl, phenol, crude oil, and acetonitrile. Additionally, they contribute to phosphate removal from waste and the production of fermented industrial products, including lipases, proteases, bio-emulsifiers, and diverse biopolymeric compounds (Jung & Park, 2015). The capacity to produce lipase is often linked to hydrocarbon degradation, and lipolytic *Acinetobacter* can be found in sources like the human body, dairy products, and diverse environments such as polluted soil and water. Clinical strains also exhibit lipolytic activity and are frequently isolated from wastewater

treatment plants and sewage, known for their high levels of petroleum-related hydrocarbons and other xenobiotics (Dahal et al., 2023). Notably, in Thailand, the *Acinetobacter* species strain MUB1 has been identified for its remarkable ability to digest crude oil (Dahal et al., 2023). Furthermore, the *A. venetianus* species encompasses marine hydrocarbon-degrading strains, making it a recommended model system for studying alkane degradation mechanisms and an effective platform for the bioremediation of contaminated environments in general (Arteaga et al., 2021).

A.baylyi, a natural producer of wax esters, stands as a valuable model organism in synthetic biology, offering insights into the potential and modifiability of wax esters within natural hosts (Kannisto et al., 2017). *A. calcoaceticus* thrives on diesel as its sole carbon source, displaying an impressive capability for diesel degradation. Over four weeks, *A. calcoaceticus* demonstrated a significant degradation of 82 to 92 percent of aliphatic hydrocarbons, underscoring its effectiveness in diesel breakdown (Ho et al., 2020). A novel phenol degrader, *A. radioresistens* APH1, distinguished by one of the highest phenol-degrading efficiencies, has been identified and harnessed for soil bioremediation (Y. Liu et al., 2020).

The breakdown of crude oil by *Acinetobacter* sp. A3 resulted in a reduction in phytotoxicity, contributing to improved germination and growth of Mung beans (*Phaseolus aureus*) in treated soil. This enhancement is evident in the increased length and weight of the plants, as well as the elevated chlorophyll content of their leaves (Das & Sarkar, 2018). *Acinetobacter* sp. has also been instrumental in degrading sulfamethoxazole and other pharmaceutical chemicals, showcasing its potential in environmental applications (Dahal et al., 2023). Additionally, *A. toweneri* and *A. guillouiae* have demonstrated their capability to digest Skatole, thereby reducing odor in the poultry and other livestock industries (Al Atrouni et al., 2016; J. Ma et al., 2020).

1.4.1 Some Non-pathogenic Species

1.4.1.1 *Acinetobacter towneri*

Acinetobacter towneri, named in honor of the noteworthy contributions of English scientist Kevin Towner to the understanding of the genus, shares typical characteristics with other *Acinetobacter* species. Its colonies are round, convex, and smooth, thriving best at temperatures ranging from 37-41 degrees Celsius. Unlike some counterparts, *A. towneri* cannot hydrolyze gelatin or produce acid, relying exclusively on pyruvate and lactate for energy. Found in environments like activated sludge and termite guts, *A. towneri* demonstrates its adaptability across diverse and challenging environmental conditions (Maehana et al., 2021).

1.4.1.2 *Acinetobacter tandoii*

A. tandoii exhibits remarkable nitrogen removal efficiency under various culture conditions and when treating real wastewater, utilizing nitrate, nitrite, and ammonium as its sole energy sources (Van Dexter & Boopathy, 2019). This species also displays the ability to decompose organic pollutants such as dipropyl phthalate, particularly in conjunction with cadmium, within polluted environments (Dahal et al., 2023). Furthermore, *A. tandoii* positively influences the growth of plants like chickpeas and pigeon pea, enhancing shoot height and root length, and exhibiting the capacity to suppress charcoal disease (Tian et al., 2016) in sorghum.In the realm of antibiotic resistance, *A. tandoii* has been documented to harbor resistance enzymes like carbapenem-hydrolyzing OXA-type lactamases (Tian et al., 2016).

1.4.1.3 *Acinetobacter lactucae*

A. lactucae presents as gram-negative spherical rods, forming non-pigmented colonies of less than 2mm. Devoid of motility and reliant on aerobic conditions, these bacteria do

not produce spores. Despite their inability to generate spores, *A. lactucae* displays adaptability to a broad temperature range (15-44 degrees Celsius), with an optimal growth temperature of 30 ℃. They exhibit positive results in catalase tests but yield negative results in oxidase tests. Incapable of hydrolyzing gelatin, they can thrive in a citrate medium and produce acid when cultivated with L-serine. The preferred pH for development falls within the range of 6 to 9. A. lactucae can be isolated from various plants, including lettuce, as well as from the surrounding environment, such as soil (Dahal et al., 2023). Notably, *A. lactucae* possesses a distinctive capability to degrade diffusible signal factors and employs quorum quenching, effectively reducing *Xanthomonas campestris* pathogenicity through an unidentified mechanism (Dahal et al., 2023). Moreover, certain strains of *A. lactucae*, isolated from soil contaminated with waste oil, demonstrate potential in the breakdown of hydrocarbons like phenol and toluene (Dahal et al., 2023).

1.5 Codon usage

The genetic code, composed of Adenine, Guanine, Cytosine, and Thymine/Uracil bases, regulates the synthesis of 20 vital amino acids. However, due to codon degeneracy, multiple triplet sequences may encode the same amino acid, leading to a bias in codon usage. This bias is influenced by factors such as differences in synonymous codon frequencies utilized by organisms or different genes (Botzman & Margalit, 2011; Hart et al., 2018). Various elements, including random genetic drift, evolutionary rates, mutation patterns, nucleotide compositions, protein lengths, selection pressures, and environmental factors, contribute to codon use bias (Brandis & Hughes, 2016). *E. coli* and the yeast *Saccharomyces cerevisiae* were the first organisms whose codon usage was examined (Espinosa et al., 2022). Notably, organisms demonstrate varying degrees of codon use bias within their genes, primarily linked to variations in translational selection levels. The

codon preference of bacteria seems to evolve as they mature, enhancing translation efficiency (Dehlinger et al., 2021).

1.6 Significance of codon usage studies

In the genomes of many organisms, codon usage bias has been detected as an essential evolutionary factor. Investigating the synonyms of codons provides a good knowledge of the mechanisms of codon usage bias, selection of host expression systems, classification of functional amino acid chains, primer design, and many more (Parvathy et al., 2022). Considering the relationship between translational selection and codon usage pattern, codon usage data from indices can be considered to estimate the expression of gene sequences of an individual. Codon usage studies can be essential in the field of biotechnology in the investigation of gene expression (Djahanschiri et al., 2022). It is believed that important genes normally includes the assembly of highly expressed genes that are vital for physiology of cell due to their ability to encode proteins that dictate cell functions like metabolism, photosynthesis-, glycolysis, respiration and many more (Carthew, 2021). Similarly, Genomic GC content is directly related to amino acid and codon usage pattern in an organism. A high level of codon usage bias is often responsible for high or low GC composition (Barceló-Antemate et al., 2023). Initially assumed silent, the growing research activities clearly indicates that codon usage regulate gene expression by its impact on co-translational protein folding, regulates the structure of proteins and enhance translational precision and efficiency. Subsequent biochemical experiments suggested that codon usage imparts an essential role to regulate the process of protein folding and functioning. It is also associated with the regulation of pace and efficiency of translational elongation (Arora et al., 2024).

It has been suggested that mutation induced changes in protein or gene function is responsible for a change of specific codon among synonymous codons. Furthermore, in specific pathophysiological conditions, synonymous codons are used selectively and

others are neglected as confirmed in the case of cellular stress or neoplastic cellular transformations across human beings. Thus, codon usage bias can be directly connected to a disease (Fornasiero & Rizzoli, 2019). Human genome coding regions analyzation confirmed the presence of high amount of CGN arginine codons compared to AGR arginine codons in defective genes which indicated that genes preferring CHG codons are prominent to underlie single gene disorders. Therefore, arginine codon usage research gave unique ideas into the probable spots for mutation in disease (Schulze et al., 2020).

Deoptimizing the process of codon usage of a gene, the protein synthesis ability of genes can be down regulated. Therefore, it is possible to engineer viruses that contain deoptimized genes which can be an attenuated candidate for a vaccine (Baker et al., 2015). Moreover, the insufficient immunogenicity of DNA vaccines is a major concern despite its many benefits. Codon usage can give a possible idea for increasing immunogenicity of vaccines to enhance the expression ability in an immunized organism. Many research studies has proved that codon usage modification of genes significantly increased DNA vaccines immunogenicity (Costa et al., 2023). Codon usage patterns can be used to analyze the phylogeny and evolutionary relationship of an organism. For example; Codon usage analysis was utilized to deduce phylogenetic and evoluntary relationship in HCV (Patil et al., 2017).

1.7 Whole Genome Sequencing

Whole-genome sequencing (WGS) is a thorough method of analyzing whole genomes that provides important information on antibiotic resistance determinants, mutations that develop cancer, and hereditary illnesses. WGS is a powerful technique in genomics research because of the falling costs associated with sequencing and its present capacity to provide large amounts of data. It offers a comprehensive, base-by-base view of the genome, finds both big and small variations, points to possible causal variants for

additional study of gene expression and regulation, and gives a considerable amount of data rapidly, assisting in the construction of new genomes (Iacono et al., 2008).

Within the field of bacterial whole-genome sequencing (WGS), this has greatly enhanced our capacity to appraise genomes and antibiotic resistance factors. *Acinetobacter* spp. full genome sequences have been more widely available during the last 10 years, and several draft sequences have also emerged. These studies focused mostly on *A. baumannii* and the ACB complex, highlighting their differences. Although the diversity of the genus has not been thoroughly investigated, several studies reveal a substantial variation in the gene repertoires of *A. baumannii*, with fewer than half of the genes making up the species' core genomes. For example, during an epidemic, the WGS of 11 *A. baumannii* isolates identified three clonal lineages and many resistance determinants, including *blaOXA-23, blaOXA-66, blaADC-25*, and *armA* (Iacono et al., 2008; López et al., 2019). Furthermore, WGS has helped identify certain genomic resistance islands, such as AbaR22, which has aided in the study of antibiotic resistance mechanisms. Also, the Whole-genome sequencing (WGS) analysis of colistin-resistant *A. baumannii* showed that the colistin-resistant genes *lpxA, lpxC, lpxD, pmrA, pmrB*, and *mcr1* were not mutated. Using single nucleotide polymorphism (SNP) and whole-genome multi-locus sequence typing (wgMLST), two main clusters of colistin-resistant *A. baumannii* strains were identified (Iacono et al., 2008).

Similar to this, a core genome consisting of 2,688 common genes between *A. baumannii* and *A. baylyi* isolates specifies the fundamental roles associated with transcription, translation, DNA replication, and different metabolic processes. The environmental organism *A. baylyi* has an 82% ortholog presence for these key genes. The study also shows that, since the two *Acinetobacter* lineages diverged, a variety of selective forces have been operating on various genes. The genome of *A*. baylyi is notable for having islands containing genes for the catabolism of complex organic compounds, and while the isolates of *A. baumannii* exhibit rearrangements, they nevertheless contain genes for the catabolism of a variety of organic compounds. To sum up, WGS helps identify

genetic information, patterns of antibiotic resistance, and evolutionary differences between bacterial isolates (Baraka et al., 2020).

Advancements in genome sequencing technology have led to a surge in studies focused on *Acinetobacter* genomes (Almeida et al., 2021b; Sahl et al., 2013; Touchon et al., 2014). However, research regarding *Acinetobacter* codon preference has predominantly concentrated on strains of a single species, notably *A. baumannii* (Jordan et al., 2022; Rahbar et al., 2019). Since there have been no studies conducted at the whole genus level, our aim was to conduct a comprehensive analysis of codon and amino acid usage, providing the initial extensive genomic insights into the entire genus. Our investigation encompassed all the named species of *Acinetobacter* species [last assessed November 2021], totaling 56, with available genome data sourced from Ensembl bacteria. Through systematic comparison, we identified and scrutinized various factors including RSCU, RAAU, optimal and favored codons, GC content, CAI, ENC plot, parity plot, and codon pairs, as well as GC3 variation. Notably, each organism displays a preference for a pair of adjacent codons, known as a codon pair. Consequently, we endeavored to compute the relative synonymous codon pair usage (RSCPU) across all members of the genus. Additionally, we sought to delineate the overarching evolutionary driving forces and offer a more intricate understanding of the distinct evolutionary statuses of all selected species through the use of neutrality plots and translational selection assessment. We also constructed the phylogenetic tree of the whole genus *Acinetobacter* for better understanding of the genus. The comprehension of genetic codes within this diverse genus is poised to make significant strides based on our discoveries. These insights will also open up novel avenues for tailored therapeutic interventions, innovative antimicrobial strategies, and applications in synthetic biology, enhancing the battle against infectious diseases and antibiotic resistance. This exhaustive investigation also lays the foundation for forthcoming projects in microbial genomics and gene expression analysis, propelling progress in both medical and biotechnological arenas.

CHAPTER 2: REVIEW OF LITERATURE

The codons are degenerate, as is widely known. Two to six synonymous codons can encode 18 of the 20 standard amino acids except methionine and tryptophan, both being encoded by the same genetic code. Codon usage bias (CUB), a phenomenon in which particular synonymous codons are preferred over others, has been discovered in all genomes examined (Liu, 2020). CUB is present in many organisms and functions as a second genetic code inside the codons. The bias in the repetition of synonymous codons differs between genomes as well as within a single gene and among functionally related genes. The mechanisms that underlie codon usage bias across all forms of life are fascinating. CUB arises from mutations occurring in the second or third positions within specific genetic codes. This occurs when there is a substitution of one codon for another that encodes the same amino acid. Since these mutations do not alter the amino acid sequence of the protein, they are termed as synonymous or silent mutations (Oelschlaeger, 2024). As a result, biased mutational patterns lead to codon usage bias, where certain codons may be retained through selection while others may be more susceptible to mutation (Parvathy et al., 2022). The local recombination rate affects how genomic variation and GC-biased genes influence the frequency of favoured codons. Additionally, codon-anticodon interactions and codon usage bias in highly expressed genes being correlated to the specified quantity of particular tRNA, are equally significant in codon usage evolution in prokaryotes (Hia & Takeuchi, 2021; López et al., 2019; Rocha, 2004).

Similarly, the deliberate alternation of the genetic code usage within prokaryotes (codon reprogramming) plays a pivotal role in their adaptive strategies and interactions with genetic material, showcasing a dynamic response to environmental challenges and interspecies competition (De La Torre & Chin, 2021). By strategically modulating codon usage, bacteria can enhance their efficiency and specificity, thereby bolstering their resistance to viral predation (De La Torre & Chin, 2021; Parvathy et al., 2022). Furthermore, in the context of horizontal gene transfer, prokaryotes employ codon

reprogramming to facilitate the CRISPR-Cas (Clustered Regularly Interspaced Short Palindromic Repeats and CRISPR-associated proteins) defense mechanisms acquisition and integration of beneficial genetic material from other organisms (Robertson et al., 2021). Codon optimization of genes involved in antibiotic resistance or metabolic pathways can enhance the fitness of prokaryotes in challenging environments. This adaptive capability not only allows prokaryotes to thrive in diverse ecological niches but also underscores their capacity to evolve rapidly through genetic exchange (De La Torre & Chin, 2021; Robertson et al., 2021). Therefore, the equilibrium between all these factors is what leads to the development of synonymous codon usage bias, which significantly promotes genome evolution (De La Torre & Chin, 2021; López et al., 2019; Parvathy et al., 2022; Robertson et al., 2021).

A significant portion of biological diversity on Earth consists of microscopic prokaryotic creatures. Millions of distinct species make up the domains Archaea and Bacteria. Prokaryotic variety is evolved 3.8 billion years ago, which is 2 billion years longer than the history of eukaryotic creatures (Kacar, 2024). During the Hadean and Archaean Eons (before 2.5 billion years ago), characterized by extreme heat and volcanic activity, prokaryotes evolved mechanisms for survival in harsh environments. The Proterozoic Eon (2.5 billion to 5.4 million years ago) saw significant environmental shifts, including rising oxygen levels leading to the evolution of photosynthetic organisms like cyanobacteria. Furthermore, during Phanerozoic Eon (5.4 million years ago to the present day), prokaryotes continued to evolve alongside multicellular organisms, influenced by factors such as mutation rates, environmental pressures, ecological interactions like symbiosis and competition, and the widespread phenomenon of horizontal gene transfer (Tonkin-Hill et al., 2023; Zhang et al., 2020). This extended evolutionary time is the cause of amazing prokaryotic diversity and a wide range of habitats. The prokaryotes are an essential part of the biosphere as they catalyze the biogeochemical cycles that maintain all life on Earth. As a result, they are the life-sustaining agents of the biosphere (Arella et al., 2021).

To date, more than 40000 (Archaea 5000 and Bacteria 35000) species have been fully characterized, and over 200000 bacterial and archaeal genomes have been sequenced and made available in public databases (Tonkin-Hill et al., 2023; Zhang et al., 2020). These genomes, which are made up of many genes sets with different histories of origin and ancestry along with various expression tendencies constitute the living legacy of the oldest living beings on the planet. The evolutionary connections among many of the sequenced genomes are unknown, and a greater fraction of the deposited genomes remain unexplored. The query regarding how cellular units adapt their coding mechanisms to meet protein requirements, using synonymous codons in organisms with genomic GC composition normally between 20% and 80%, has been a long-standing issue. This question is highlighted by the genetic diversity observed in studies with incomplete or imprecise phylogenetic analyses (Liu et al., 2021).

2.1 Phylogeny and its relationship with Codon usage

Determining the emergence of distinct prokaryotic lineages is a significant challenge due to the lack of reliable calibration points, specifically fossils, for prokaryotes. Nevertheless, initial examinations of prokaryotic phylogeny suggest an ancient origin spanning over 3 billion years. Pioneering research led by Carl Woese and colleagues extensively employed molecular sequencing techniques, particularly the analysis of 16S rRNA sequence data across a broad spectrum of species. This research brought to light an overlooked category of prokaryotes, initially labeled Archaebacteria and later rebranded as Archaea (Clark & Kolb, 2020; Imachi et al., 2020). This group encompasses methanogens, thermoacidophiles, and halophilic organisms, exhibiting a distinct phylogenetic separation from other prokaryotes, initially referred to as eubacteria and later renamed bacteria. Archaebacteria demonstrated a genetic proximity to both eukaryotes and eubacteria based on 16S rRNA data. This discovery, along with a range of other distinguishing features of Archaebacteria, prompted Woese and colleagues to propose Archaebacteria as a distinct phylum (Imachi et al., 2020; Moody et al., 2022).

These features include the absence of muramic acid in their cell walls, unique membrane lipids with ether-linked isoprenoid side chains (instead of diacyl esters found in other bacteria), distinct RNA polymerase subunit structures, and variations in sensitivity profiles to various antibiotics. Consequently, prokaryotes are dichotomized into two primary lines of descent such as Archaea and genuine bacteria.

The phylogeny of prokaryotes, which encompasses Archaea and Bacteria, reveals evolutionary relationships based on genetic similarities and divergence over time. CUB has been observed to correlate with phylogenetic topology in several ways, reflecting both shared ancestry and adaptive divergence among different taxa. At a broad phylogenetic scale, prokaryotic lineages that share a more recent common ancestor tend to exhibit similar patterns of codon usage. This similarity arises because closely related species inherit similar genomic compositions, including codon usage preferences, from their ancestors (Du Toit, 2022). For instance, within the Firmicutes phylum, species such as *Bacillus subtilis* and *Clostridium difficile* show conserved codon preferences for certain amino acids like leucine and serine, reflecting their close evolutionary relationship and shared ecological niches. Consequently, phylogenetically related organisms often display comparable biases in codon usage due to their shared evolutionary history (Pavao et al., 2023). However, variations in codon usage bias can also occur between closely related taxa or within the same phylogenetic group. These variations may arise from adaptive evolution in response to different ecological niches, selective pressures, or specific genomic features unique to certain lineages. Environmental factors such as temperature, pH, and nutrient availability can influence codon preferences in bacterial genomes, leading to divergent codon usage patterns even among closely related species (Meysman et al., 2013). For example, *Escherichia coli* and *Salmonella enterica*, both members of the Enterobacteriaceae family, demonstrate distinct codon usage patterns influenced by their respective lifestyles and environmental adaptations. *E. coli*, commonly found in the human gut, exhibits biased codon usage favoring codons optimized for efficient translation under nutrient-rich conditions, whereas *S. enterica*,

which can cause salmonellosis in various hosts, shows adaptations for survival in diverse host environments (Knöppel et al., 2018; Meysman et al., 2013).

Moreover, horizontal gene transfer (HGT) plays a significant role in shaping codon usage bias across phylogenetic boundaries in prokaryotes. Genes acquired through HGT often retain their original codon usage patterns from their donor organisms, contributing to mosaic genomes with heterogeneous codon biases within a single species or population. This phenomenon blurs strict phylogenetic correlations in codon usage and underscores the dynamic nature of genomic evolution in prokaryotes (Arella et al., 2021; Moller et al., 2022). For instance, genes involved in antibiotic resistance in *Staphylococcus aureus* may display codon biases reflective of their origins in other bacterial species, illustrating how HGT shapes codon usage independently of strict phylogenetic relationships (Moller et al., 2022).

In summary, while codon usage bias generally reflects phylogenetic relationships among prokaryotes, its patterns can also diverge due to adaptive evolution and HGT. These insights underscore the dynamic interplay between genomic evolution, environmental adaptation, and the complex patterns of codon usage bias in shaping the diversity and evolutionary trajectories of prokaryotic life (Arella et al., 2021; Moller et al., 2022).

2.2 Codon Usage in Prokaryotes

Codon usage in prokaryotes is a fundamental aspect of genetic information processing that influences protein synthesis efficiency, fidelity, and adaptation. The genetic code is degenerate, with most amino acids encoded by multiple synonymous codons. However, prokaryotic genomes often exhibit biased usage of these codons, where certain synonymous codons are preferred over others. Multiple studies have demonstrated that translational selection, affected by parameters including abundance tRNA (De Crécy-Lagard et al., 2020; Wolff et al., 2020), environmental adaptations (Arella et al., 2021)

and genomic GC content (Y. Huang & Ren, 2019), plays a vital role in defining codon usage patterns in prokaryotes.

Codon usage bias in prokaryotes is intricately linked to environmental adaptations, including temperature tolerance and nutrient acquisition, which are often reflected in genomic GC content (Y. Huang & Ren, 2019). GC-rich genomes tend to prevail in thermophilic bacteria and archaea, where higher GC content contributes to DNA stability at elevated temperatures (Hu et al., 2022). These organisms typically exhibit codon bias favoring GC-rich codons, which encode amino acids that stabilize proteins under extreme thermal conditions. Conversely, GC-poor genomes are common in mesophiles and psychrophiles adapted to moderate or cold environments, where lower GC content may confer advantages such as enhanced DNA flexibility and reduced energy costs during replication and transcription. Moreover, Prokaryotes thriving in nutrient-rich environments often prioritize codons recognized by abundant tRNAs, promoting efficient translation and high protein yields. In contrast, microbes adapted to nutrient-poor conditions may exhibit codon bias that conserve energy by favoring less costly codons during protein synthesis (Granehäll et al., 2021; Hu et al., 2022).

Different species have different preferred codon choices depending on their tRNA repertoire and other relevant parameters (Hia & Takeuchi, 2021; Rocha, 2004). As per the "mutation-selection-drift model" random genetic drift, natural selection, and mutation work together to produce genetic variation within prokaryotes due to which prokaryote genomes show a wide range of GC content. This model balances bias through selection-based restrictions, altering GC content and codon usage. There are variations in the intragenomic codon usage of singletons and core genes in different gene sets. Selection factors, gene function, and cellular effects lead to variances in genetic code utilization within a single cell. Optimal codon-anticodon interactions, determined by the amount of a certain tRNA, correspond to the biased utilization of genetic code in prokaryotes, nonstandard codon-anticodon interactions affect the development of genetic codes. Although translational selection is present in most prokaryotes, different genes and

deciding factors have different levels of codon usage bias (Cui et al., 2019; López et al., 2019). The predominance of translational selection is indicated by some species, such as *Alkaliphilus metalliredigens* (Dahal & Bansal, 2024) and *Escherichia coli* (Wu et al., 2010), which exhibits a positive association between codon bias and protein levels. Others, like as *Helicobacter pylori* (Lauener et al., 2019), show little variation in the utilization of synonymous codons, which is explained by translational selection that is weak and mutation. The correlation between phenotypic features in many prokaryotes and codon usage bias is demonstrated by the comprehensive effect of highly adapted codons on cellular processes (Hanson & Coller, 2018).

The various factors affecting codon usage trends in prokaryotes have been illustrated in **Fig 2.1** and the role of codon usage bias in various prokaryotes has been detailed in **Table 2.1**. For instance, *Pseudomonas aeruginosa* utilizes specific codons in biofilm formation and antibiotic resistance, optimizing adaptability in various host environments (Kung et al., 2010). *Salmonella enterica* exploits codon preferences for survival and colonization within the intestinal tract (Liao et al., 2019), while *Mycobacterium tuberculosis* exhibits CUB patterns influenced by HGT in adapting to the human host and evolving virulence traits (Panda et al., 2018). Cyanobacteria, such as *Synechococcus elongates*, show specific codon preferences in genes related to photosynthesis, enhancing efficiency in protein synthesis that is crucial for their metabolic pathways (Delaye et al., 2020). Archaeal species like *Haloferax volcanii* align codon usage with the abundance of tRNAs to thrive in hypersaline environments (Dahal & Bansal, 2024).

Table 2.1: Role of CUB in various Prokaryotes

Prokaryotic organism	**Role of Codon Usage Bias**	**Findings from codon usage studies**	**Reference**
Pseudomonas aeruginosa	Contribute to the pathogen's adaptability in diverse host environments	antibiotic resistance genes use codons corresponding to abundant tRNAs	(Kung et al., 2010)

Table 2.1: Continued

Prokaryotic organism	**Role of Codon Usage Bias**	**Findings from codon usage studies**	**Reference**
Salmonella enterica	Involved in host colonization and survival within the intestinal environment	Exploit specific codons that align with the host environment	(Liao et al., 2019)
Mycobacterium tuberculosis	Adaptation to the human host and the evolution of virulence traits	CUB patterns influenced by the acquisition of genes through HGT	(Panda et al., 2018)
Neisseria meningitidis	Organization of antigen expression, ensuring the elicitation of robust immune response against bacterium	Exhibits specific codon preferences can be used in rational vaccine design	(Yee et al., 2023)
Cyanobacterium	Involve complex biochemical pathways with specific codon preferences optimized for efficient protein synthesis	HGT from another Cyanobacterium	(Pérez-Carrascal et al., 2021)
Haloferax volcannii (Archaeon)	Helps to thrive in hypersaline environments	Codon usage aligns with the abundance of tRNAs	(Dahal & Bansal, 2024)
Escherichia. coli	Enhance translational efficiency	Codons for Glycine (GGC and GGG), correspond to highly abundant tRNAs,	(Wu et al., 2010)
Bacillus subtilis	Enhance translational efficiency	Genes encoding ribosome tend to prefer codons corresponding to highly abundant tRNAs	(De Crécy-Lagard et al., 2020)

Table 2.1: Continued

Prokaryotic organism	**Role of Codon Usage Bias**	**Findings from codon usage studies**	**Reference**
Thermus thermophilus	Proper folding of transcripts at elevated temperature	Genes encoding heat-shock proteins prefer codons that contribute to the stability of mRNA secondary structures.	(Yee et al., 2023)
Mycoplasma pneumonia	Reduction in overall genome size	Exhibits CUB associated with functional constraints related to genome compactness	(Leal Zimmer et al., 2020)
Synechococcus elongates (Photosynthesis gene)	Ensuring rapid and accurate translation of proteins involved in photosynthesis	Photosynthetic exhibit a bias towards codons corresponding to highly abundant tRNAs,	(Delaye et al., 2020)
Vibrio cholera	Changes in codon usage patterns when transitioning from environment reservoirs to the human host	Genes encoding toxins and adhesion proteins, show adaptation in codon usage to optimize expression during infection.	(Ramamurthy et al., 2020)
Vibrio parahaemolyticus	Distinct genomic islands are acquired through HGT	Variations in genomic composition, pa in horizontally acquired regions	(R. Huang & Lee, 2019)
Thermococcus kodakarensis (archaeon)	Enhance the stability of mRNA secondary structures, ensuring proper translation at high temperature	Genes exhibit a preference for codons that end with G or C	(Scott et al., 2021)

Table 2.1: Continued

Prokaryotic organism	**Role of Codon Usage Bias**	**Findings from codon usage studies**	**Reference**
Caulobacter crescentus	Contribute to efficient and accurate protein synthesis, especially in highly expressed genes	Displays CUB in cell cycle-related genes, which is linked to tRNA availability	(Mohapatra et al., 2020)
Streptomyces coelicolor	Efficient translation of complex biosynthetic pathways	Genes involved in secondary metabolite biosynthesis often exhibit codon usage bias correlated with tRNA availability	(Dopson et al., 2023)
Psychrobacter arcticus	Function optimally at low temperatures	Favouring codons that match availability of cold adaptated tRNAs.	(Leonardo, 2013)
Acidithiobacillus ferrooxidans	Be adapted to highly acidic pH environment	Reflect adaptations to optimize translational efficiency	(Dopson et al., 2023)
Alkaliphilus metalliredigens	Adaptation to alkaline environment	Reflect adaptations to optimize translational efficiency	(Dahal & Bansal, 2024)
Halobacterium salinarum (arhaeon)	Adapted to high salinity environment	The codon usage patterns in genome are influenced by the need for efficient translation in a high salt environment	(Edbeib et al., 2020)
Desulfovibrio desulfuricans	Helps to thrive in absence of oxygen in its environment	Influences codon usage patterns, optimizing translation under anaerobic conditions	(Nguyen et al., 2023)

Table 2.1: Continued

Prokaryotic organism	**Role of Codon Usage Bias**	**Findings from codon usage studies**	**Reference**
Clostridium thermocellum	Optimizing translational efficiency in the niche	Codon usage reflects adaptations to both high temperature and anaerobic conditions	(Dahal & Bansal, 2024)
Nitrosomonas europaea	Helps to thrive in high concentration of ammonia	Concentration of ammonia influence codon usage patterns, optimizing translational efficiency	(Saha et al., 2019)
Geobacter sulfurreducens	Helps in biodegradation of radioactive metals	Redox potential of its environment influence codon usage in genes involved in metal reduction and electron transfer process	(Inoue et al., 2018)
Synechocystis sp	Helps in the process of photosynthesis	Light intensity and photoperiod influence codon usage patterns in genes related to photosynthesis	(Du et al., 2019)
76 different species of *Clostridium*	Clustering of pathogenic species	Pathogens use amino acids with lower biosynthetic cost	(Sharma et al., 2023)
Mycobacterium avium	Contribute to virulence	Acquisition of pathogenicity islands	(Panda et al., 2018)
Bacillus anthracis	Contribute to virulence	Acquiring plasmids carrying toxin genes	(Q. Wang et al., 2022)

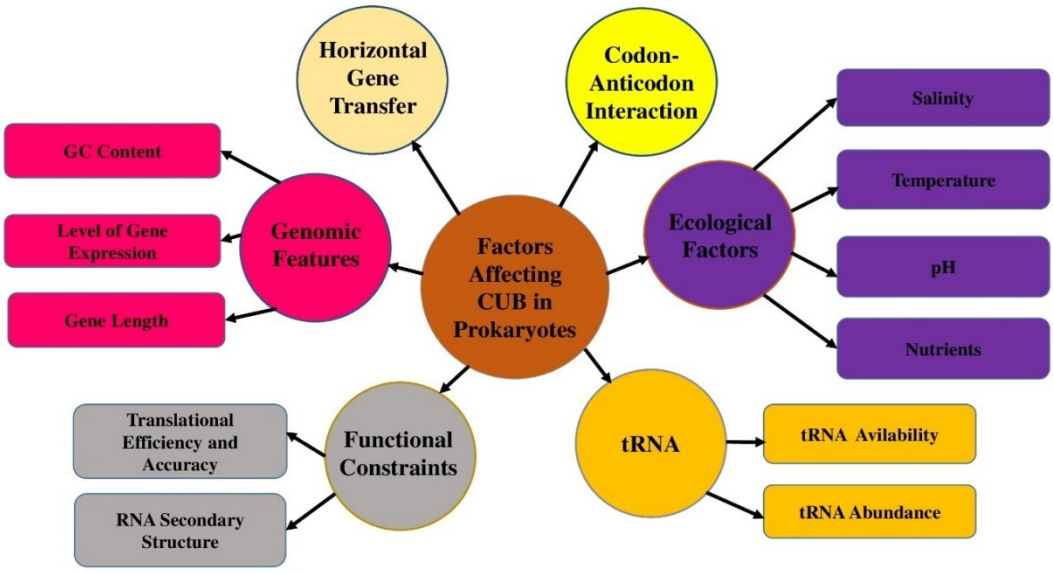

Fig 2.1: Factors Affecting Codon Usage Trends in Prokaryotes (Cano et al., 2021; Dahal & Bansal, 2024; Hia & Takeuchi, 2021; Y. Liu, 2020; Oelschlaeger, 2024; Parvathy et al., 2022; Rocha, 2004; Sharma et al., 2023; Q. Wang et al., 2022)**.**

Examining the diversity of genetic code usage in prokaryotic genomes and genes has been done in a variety of ways. Grantham and colleagues calculated the first list of codon usage frequencies in 1980 using mRNA sequences with 51 or more genetic codes. Since the 1980s, a wide range of software and indices have been created to define, examine, and quantitatively estimate genetic code use bias or genetic code usage preferences. Several software tools, such as GeneMark (Besemer & Borodovsky, 2005), CAIcal (Dahal & Bansal, 2024), EMBOSSCusp (Ata et al., 2021), and CodonW (Sharma et al., 2023), have been utilized for evaluating codon usage preferences, with many focusing on calculating indices like Codon Adaptation Index (CAI), Effective Number of Codons (ENC), and others.

The indices used for analyzing genetic code usage bias in prokaryotes has been categorized as the indices that examine the observed genetic codes use distribution of the targeted set of genetic codes against a mentioned set of highly-represented genes, that

examine data based on the supposition of equal usage of codons coding same amino acid, indices dependent on the adaptation of tRNA levels and their supply, indices dependent on complex trends of genetic code usage and also indices dependent on direct experiment analysis of translational as well as transcriptional elongation (Bahiri-Elitzur & Tuller, 2021; Dahal & Bansal, 2024). Popular most common indices applied in examination of genetic code usage bias is CAI developed by Sharp and Li in 1987 followed by ENC developed by wright 1990 and Relative Synonymous Codon Usage (RSCU) developed by sharp et al in 1986 which can be used to distinguish chromosome and plasmid in bacteria (Huo et al., 2021; Xu et al., 2024). Other commonly used indices include Frequency of optimal codons, correspondence analysis, Neutrality plot, Parity bias plot analysis, Relative codon adaptation, Codon deviation coefficient, Relative codon deoptimisation index, Synonymous codon usage order, GRAVY, and AROMO analysis (Cho et al., 2024; Dahal & Bansal, 2024; Sundar Panja, 2024; M. Wang et al., 2024). The list of the various CUB softwares and indices that has been used in prokaryotes has been illustrated in **Fig. 2.2.**

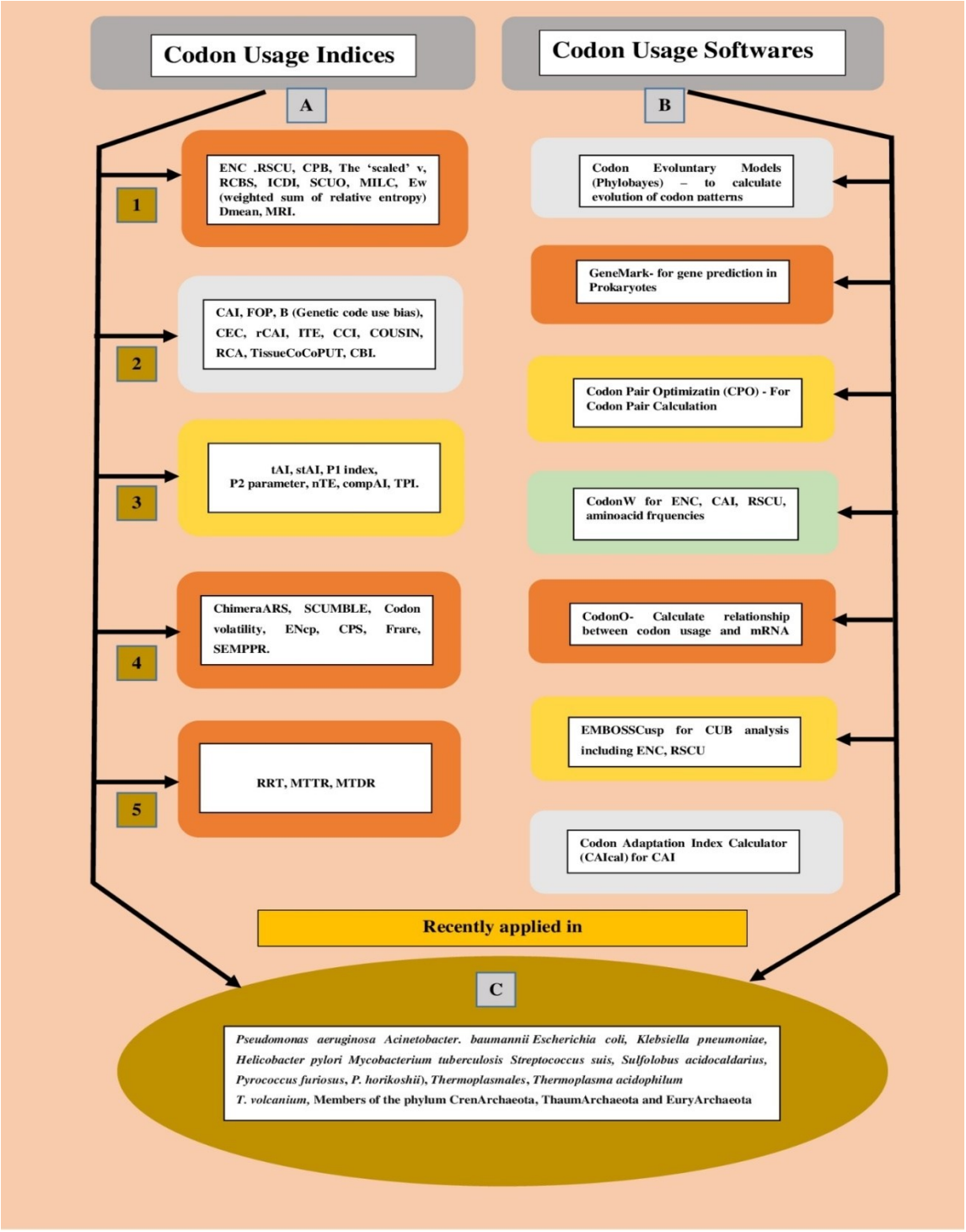

Fig 2.2: Codon usage softwares and indices used to study CUB in prokaryotic organisms.

(A). Codon usage indices dependent on (Cho et al., 2024; Huo et al., 2021; Sundar Panja, 2024; M. Wang et al., 2024; Xu et al., 2024).

1. Unequal use of synonymous genetic codes.
2. Codon frequency across a mentioned set of genes.
3. Adaptation to tRNA pool including supply.
4. Patterns of codon usage.
5. Laboratory analysis of translational and transcriptional elongation.

(B). Codon usage softwares (Dahal & Bansal, 2024)

(C). Prokaryotes in which CUB has been recently studied (Dahal & Bansal, 2024)

Note: Abbreviations Used in the figure:

Mean typical decoding rate (MTDR), Ribosome Residence Time (RRT), Mean typical transcription elongation rate (MTTR), Synonymous codon usage bias maximum-likelihood estimation (SCUMBLE), Effective number of codon-pairs (ENcp), Codon pair score (CPS), Frequency of rare codons (Frare), Stochastic evolutionary model of protein production rate (SEMPPR), tRNA adaptation index (tAI), Species-specific tRNA adaptation index (stAI), Normalized translational efficiency (nTE), Competition Adaptation Index (compAI), tRNA-pairing index (TPI), Codon adaptation index (CAI), Frequency of optimal codons (FOP), Codon bias index (CBI), Codon-enrichment correlation (CEC), Relative codon adaptation index (rCAI), Index of translation elongation (ITE), Self-Consistent Codon Index (CCI), Codon usage similarity index (COUSIN), Relative codon adaptation (RCA), Tissue specific Codon and Codon-Pair Usage Tables (TissueCoCoPUT), Effective number of codons (ENC), Relative synonymous codon usage (RSCU), Codon preference bias (CPB), Relative codon bias strength (RCBS), Intrinsic codon deviation index (ICDI), Synonymous codon usage order (SCUO), Measure independent of length and composition (MILC), Weighted sum of relative entropy (Ew), Mean dissimilarity based index (Dmean), and Mutational Response Index (MRI)

2.3 Factors affecting Codon Usage Trends in Prokaryotes

2.3.1 Genomic Features

Genomic features, such as GC content, gene length, and level of gene expression, significantly influence codon usage bias in prokaryotic organisms, reflecting adaptations to environmental conditions and evolutionary histories. However, it is to be noted that the correlation between genomic features and codon usage trends highlights their association rather than causation, emphasizing the intricate interplay between genetic features and codon selection in prokaryotic organisms (Parvathy et al., 2022; Teng et al., 2023).

The influence of genomic composition on codon usage bias is important in prokaryotes, as there is considerable variation in the frequency of individual codons. The amount of guanine (G) and cytosine (C) bases in DNA is known as the GC content, and it is one important genomic characteristic that affects codon usage. Prokaryotic genomes with high GC contents typically have biased codon usage patterns because of their propensity for codons rich in G and C. The thermodynamic stability of G-C base pairs, which supports the general stability of the mRNA secondary structure, is frequently blamed for this bias (Barceló-Antemate et al., 2023). Therefore, prokaryotes with a high GC content would prefer codons that start with G and C, which would indicate that their genomes can adapt to different environmental situations through enhanced protein stability, regulatory capabilities, and evolutionary flexibility. For instance: *Mycobacterium tuberculosis* favours G and C nucleotides across the codon due to its high GC content (Dahal & Bansal, 2024).

Gene length is another genetic characteristic that influences codon usage bias. Shorter genes are typically linked to improved translational efficiency and expression levels in prokaryotes. The "translational selection hypothesis," which explains this phenomenon, postulates that codon usage influences natural selection in a way that maximizes translation accuracy and speed. Stronger selection pressure for effective translation may be applied to genes, which might result in biased codon usage that speeds up and

improves the accuracy of protein synthesis (Lucks et al., 2008). The best example can be *B. subtilis* (Q. Wang et al., 2022) in which longer genes have a stronger preference for specific synonymous codons. The availability of tRNAs and other elements that affect translation efficiency determine the codons that are preferred in the species

Bacterial genomes frequently show differences in the bias in codon usage across genes that are highly and lowely expressed. Stronger bias towards optimal codons, which are effectively recognised by an abundance of tRNAs, is more likely to be seen in highly expressed genes, highlighting the relationship between codon selection and gene expression levels. *Caulobacter crescentus* displays CUB in cell cycle related genes (highly expressed) to contribute efficient and accurate protein synthesis (Dahal & Bansal, 2024).

2.3.2 Environment

The environment has a significant impact on the codon usage patterns of prokaryotic species, which are indicative of the adaptive methods these organisms use to survive in a variety of settings. Arella and group in 2021 suggested that prokaryotes with specific physical characteristics and residing across comparable living conditions share similar genetic codes preferences (López et al., 2019). One important environmental element that influences codon usage is temperature; prokaryotes show specialised preferences for codons that are adapted to particular temperature ranges. Due to their greater energy favorability at higher temperatures, codons rich in G and C are frequently preferred by thermophilic bacteria, which are adapted to hot temperatures. Additionally, bacteria that are psycrophiles show a predilection for codons that include G and C. These nucleotides help to stabilise DNA and RNA structures as temperatures rise. The relationship between codon usage and temperature emphasises how environmental adaptation alters the genetic code to maximise cellular functioning across a range of temperatures (Marshall et al., 2022).

Other environmental conditions that affect codon usage patterns in bacterial genomes are salt and pH. Bacteria known as extremophiles, which flourish in environments of severe salinity or pH, frequently have certain codon bias to improve their adaptability. Acidophiles like *Acidithiobacilus ferrooxidans* could choose codons with a greater GC content, which would help keep their genetic material stable in an acidic environment (Dopson et al., 2023). *Halobacterium salinarum* are acclimated to high salinities and exhibit codon preferences that are indicative of the necessity of effective protein synthesis in salt settings (Edbeib et al., 2020). Because of these modifications in codon usage, prokaryotic organisms may survive in conditions with severe pH or salinity while still maintaining optimal cellular processes like protein folding and stability. The complex relationship that exists between codon usage and environmental factors highlights the role that genetic flexibility plays in bacterial evolution (De La Torre & Chin, 2021).

Moreover, codon usage patterns of bacterial genomes can be influenced by the nutrients that are available in the surrounding environment. Prokaryotes, for example, may show a preference for codons that promote fast translation in nutrient-rich settings, maximising the use of available resources for development and reproduction. On the other hand, distinct codon preferences may result from the selection pressure for effective resource utilisation in nutrient-poor settings. The dynamic nature of codon usage patterns reflects the resilience of prokaryotic genomes on changing nutritional circumstances and shows how environmental variables aid in the expression of the genetic code in response to ecological niches (Panda & Tuller, 2023).

2.3.3 Functional Constraints

The usage of codons is subjected to functional constraints, which significantly influence the genetic code composition of organisms. The association between codons and the amino acids they encode is the main functional restriction. One or more codons are

responsible for encoding each amino acid; synonymous codons denote distinct nucleotide triplets that share the same amino acid coding. These synonymous codons can show varied usage frequency despite unchanged amino acid sequence in a protein. Therefore it is suggested that, the requirement to preserve appropriate protein folding, stability, and functionality gives rise to functional limitations (Xu et al., 2024). Because they affect the precision and speed of translation, some codons may be more advantageous than others, which in turn affect the shape and function of proteins. In *Mycobacterium tuberculosis*, overrepresentation of the alanine-coding codon GCG supports the stability of mRNA secondary structures and is thought to represent a response to the host environment (Panda et al., 2018).

Another important component that significantly contributes to codon usage bias is translational efficiency. The amount of transfer RNA (tRNA) molecules in the cellular environment affects how quickly and accurately translation proceeds, and differing amounts of tRNAs can recognize different codons. Rich tRNA-corresponding codons are frequently preferred because they promote quicker translation and lower the risk of mistakes. Natural selection optimizes translation rates by acting on codon usage patterns; this process is referred to as translational selection. The relationship between translational efficiency and codon usage emphasizes how crucial it is to strike a balance between correct amino acid incorporation and quick protein synthesis during translation (Dopson et al., 2023; Edbeib et al., 2020).

2.3.4 tRNA Abundance and Availability

The preference for codons in bacterial genomes is mostly determined by the amount of transfer RNA (tRNA) molecules. A particular amino acid is transported to the ribosome by each tRNA during translation, and the quantity of these tRNAs differs between species and even within cellular environments. Translational selection is the tendency of prokaryotic organisms to choose codons that correlate to high levels of tRNAs. High

quantity of a particular tRNA facilitates precise and efficient translation by allowing the correct codons to be quickly identified and matched with the right amino acids. This inclination towards codons linked to high tRNA abundances is indicative of an adaptive tactics to maximise translational efficiency and lower the risk of mistakes during protein synthesis. Genes involved in secondary metabolite biosynthesis often exhibit codon usage bias correlated with tRNA availability in prokaryotes like *Streptomyces coelicolor* (Dopson et al., 2023).

Furthermore, codon usage is subject to functional restrictions that go beyond the translation process itself. RNA secondary structures and binding sites for RNA-binding proteins are examples of regulatory factors that can affect the choice of particular codons within mRNA sequences. The functional consequences of codon selection are further highlighted by the fact that these components can impact mRNA stability, localization, and interactions with cellular machinery (Dahal & Bansal, 2024). Genes encoding heat-shock proteins prefer codons that contribute to the stability of mRNA secondary structures in *Thermus thermophiles* which ultimately helps in protein folding at elevated temperature (Banerjee et al., 2021; Kung et al., 2010).

In the context of codon families, the link between tRNA availability and codon usage bias is clear. Codon families are groups of synonymous codons with different nucleotide sequences that code for the same amino acid. Because related tRNAs are abundant in some codon families, some codons may be utilised more frequently than others within that family. Within these groups, prokaryotic genomes frequently display a biased use of synonymous codons, such as *Pseudomans aeruginosa* which reflects the varying availability of tRNAs. This tendency is more noticeable in highly expressed genes because there is greater selection pressure to translate a gene efficiently. The complex interaction between codon preference and tRNA abundance highlights how translational selection shapes the codon usage patterns seen in bacterial genomes (Berg & Brandl, 2021; Dahal & Bansal, 2024).

Furthermore, during evolution and adaptation, variations in tRNA abundance have shown an effect on codon usage patterns of prokaryotes like *E. coli* (Rodríguez-Beltrán et al., 2022). The cellular pool of tRNAs may change when prokaryotes experience different environmental circumstances to maximize protein production. A prokaryote may, for example, adjust the abundance of tRNAs to match codon preferences that support effective translation of genes involved in adjusting to the new conditions if it comes into contact with an environment that has a change in the availability of nutrients. The dynamic correlation between tRNA availability and codon usage highlights the functional relevance of the interaction between tRNA abundance and codon choice, reflecting the resilience of bacterial genomes to shifting selection forces. Overall, the complex mechanisms governing translational efficiency and codon usage in bacterial genomes are highlighted by the significance of tRNA abundance in these processes and environmental effect (Wei et al., 2019).

2.3.5 Horizontal Gene Transfer

In prokaryotic evolution, HGT is a ubiquitous mechanism that permits the acquisition of genetic material from unrelated species. The patterns of codon usage in bacterial genomes can be greatly impacted by this gene transfer. Foreign genes may have different codon preferences from the receiving organism when they are introduced by HGT. The integrated genes may therefore first show a bias in codon usage that is not compatible with the host genome. HGT is the process by which codon usage of acquired genes eventually aligns with the recipient genome. Selective pressures to maximize translational efficiency and protein folding are what propel HGT, which in turn helps to successfully integrate and express the foreign genes within the host organism (Emamalipour et al., 2020; Garcia-Vallve, 2000).

The effects of HGT on codon usage are seen in parts of bacterial genomes linked to mobile genetic components like phages and plasmids. These components frequently act

as carriers of new genetic material into prokaryotic communities through horizontal gene transfer. In order to conform to the preferences of the receiving organism, the genes carried by these components may alter their codon usage, enabling effective expression and functional integration (Djahanschiri et al., 2022). As a result, the dynamic and adaptable character of codon usage patterns in these microbes is partly due to the mosaic structure of prokaryotic genomes, which is the outcome of the introduction of foreign genetic material through HGT. HGT in Cyanobacterium helps them to adapt to the host environment and optimize protein synthesis (Dahal & Bansal, 2024).

The codon usage bias of particular functional gene categories is also shaped by horizontal gene transfer. Because precise control and coordination of these fundamental functions are required, genes involved in translation, transcription, and replication are frequently more conserved in terms of codon usage. On the other hand, because of the effect of horizontally transmitted genes, genes linked to adaptive functions similar to those engaged in environmental response or niche-specific metabolic pathway show more diversity in codon usage. Species like *Vibrio parahaemolyticus* (R. Huang & Lee, 2019), *Mycobacterium avium* (Panda et al., 2018) and *Bacillus anthracis* (Q. Wang et al., 2022) acquire distinct genomic islands through HGT and there is significant variation in genomic composition of horizontally acquired genes to adapt in host environment. This capacity to quickly adapt to new ecological niches and environmental obstacles is made possible by the integration of foreign genes, which enhances the overall diversity and adaptability of prokaryotic genomes (Garcia-Vallve, 2000).

2.3.6 Codon-Anticodon Interaction

Codon- anticodon interaction is one of the crucial factors that affect codon usage in prokaryotes. The interaction between codons and anticodons is essential for the formation of proteins during translation in prokaryotic organisms. On the mRNA, the codon designates a specific amino acid or a start/ stop signal. Complementary to the codon is the

anticodon, a three-nucleotide sequence on a tRNA molecule. The relevant amino acid is transported by the tRNA to the ribosome, the site of protein synthesis. The precise alignment of amino acids in the developing polypeptide chain is guaranteed by the specificity of the codon-anticodon interaction causing codon usage bias in prokaryotes (Koh & Sarin, 2018; Selleghin-Veiga et al., 2024).

The stability and specificity of the codon anticodon interaction is a key factor in determining the fidelity of translation and preventing codon reprogramming in prokaryotes (Nowak et al., 2021; Xia et al., 2020). Typically, the codon anticodon interaction is stabilized by hydrogen bonds, with the optimal interaction energy being a balance between maximizing binding strength and minimizing the risk of mismatches (Mitchener et al., 2023; Walsh et al., 2020; Yang et al., 2021). However, in certain cases, prokaryotes have evolved mechanisms to reprogram the genetic code by altering the standard codon-anticodon interactions (Nowak et al., 2021). For example, in some bacteria, the anticodon of the tRNA that recognizes the stop codon UGA can be modified to pair with the amino acid selenocysteine instead of triggering translation termination. This allows the UGA codon to specify selenocysteine incorporation, rather than acting as a stop signal. Such codon reprogramming events are crucial for the expression of specialized proteins in prokaryotes (Gaydukova et al., 2023; Nowak et al., 2021; Xia et al., 2020).

In prokaryotes like *E. coli*, *M. tuberculosis* and *B. subtilis*, interaction between codons on mRNA and anticodons on tRNA is pivotal for the precise translation of genetic information into proteins **(Fig 2.3)**. Each mRNA codon specifies a particular amino acid, and tRNA molecules carrying complementary anticodons recognize and bind to these codons through base pairing during protein synthesis (Mekonnen et al., 2019; Nowak et al., 2021). This process occurs in coordination with ribosomes, where specific amino acids like glycine and leucine are sequentially added to the growing polypeptide chain in *M. tuberculosis* and *B. subtilis* respectively. In case of *E. coli*, codon anticodon interaction (AUG-UAC) initiates the synthesis of peptide chain **(Fig 2.3).** CUB in these

prokaryotes reflects the preferential usage of certain specific synonymous codons over others, influenced by factors such as translation efficiency, accuracy, and the availability of corresponding tRNAs (Cao & Slavoff, 2020; Dahal & Bansal, 2024; L. Liu et al., 2022; O'Connor et al., 2020; Soma et al., 2023)**.** The codon anticodon preference in various prokaryotic organisms for incorporation of specific amino acids are illustrated in **Fig 2.3.**

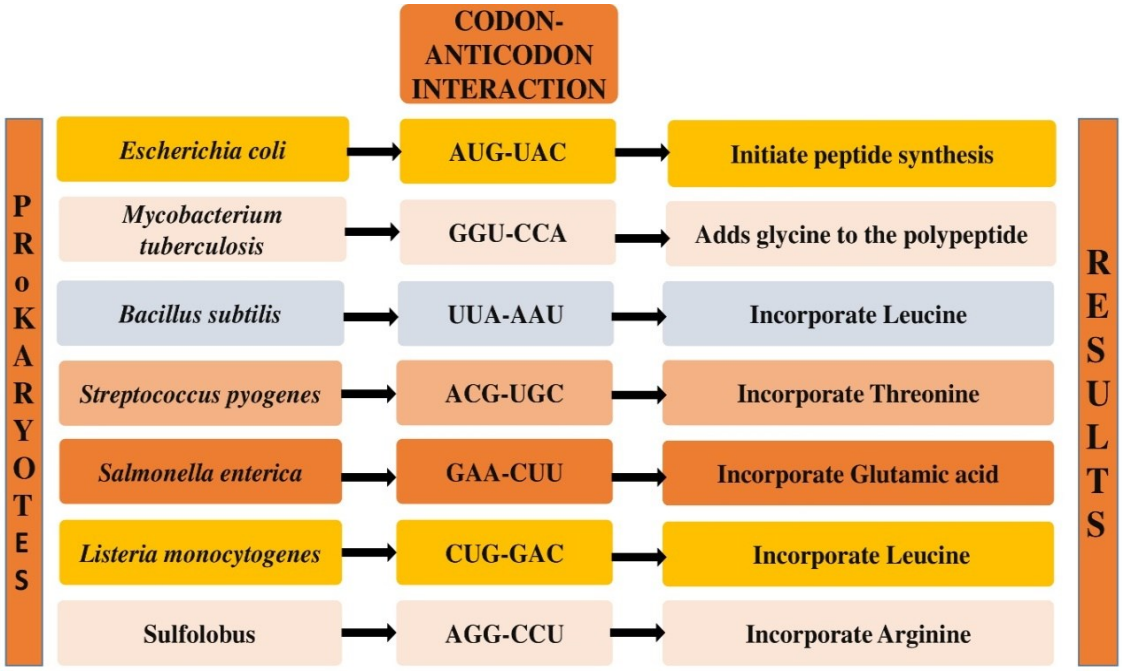

Fig 2.3: Codon-Anticodon Interaction in Prokaryotes (Cao & Slavoff, 2020; Dahal & Bansal, 2024; Espinosa et al., 2022; Koh & Sarin, 2018; L. Liu et al., 2022; Selleghin-Veiga et al., 2024; Soma et al., 2023)**.**

2.4 Codon Usage Bias in Pathogenic Prokaryotes

In pathogenic prokaryotes, CUB is a complex phenomenon with broad implications for comprehension of the complexities of host-pathogen relationships, adaptive evolution, and possible therapeutic intervention uses. Deciphering codon usage bias offers a path towards discovering critical genes and possible targets for drugs in the context of

vaccines and antibacterial treatments. Furthermore, pathogen-specific codon preferences can be used in vaccine design to generate strong immune responses. To maximise antigen expression and immunogenicity, for instance, the pathogen's codon usage patterns are taken into consideration during the design of vaccines against *Neisseria meningitides* (O'Connor et al., 2020).

A variety of variables affect the complex patterns of codon usage that are revealed by analyzing the genomes of pathogenic bacteria and archaea. In the opportunistic pathogen *Pseudomonas aeruginosa*, for example, genes linked to important processes show a translational advantage by favouring codons identified by numerous tRNAs. It is thought that this optimisation helps the bacteria adapt to a variety of host settings (Y. Huang et al., 2021). In pathogenic prokaryotes, environmental adaptability is also crucial to the dynamics of codon usage. The gastrointestinal pathogen *Salmonella enterica* has unique codon usage preferences related to its adaptability to the intestinal environment of its host. The relationship between microbial genomes and their ecological niches is shown by these adaptations, highlighting the function of CUB as an evolutionary strategy for survival and growth (Dahal & Bansal, 2024).

Moreover, it is remarkable how HGT affects codon usage patterns across pathogenic prokaryotes. Different sources of genes are frequently acquired by pathogenic prokaryotes, resulting in differences in codon preferences. The tuberculosis-causing agent, *Mycobacterium tuberculosis*, has codon usage patterns that are impacted by HGT events, which is indicative of the pathogens complicated evolutionary past (Dahal & Bansal, 2024). Additionally, it is possible to comprehend the functional importance of codon usage bias in pathogenic prokaryotes by considering its involvement in virulence modulation. A causative agent of significant respiratory infection, *Streptococcus pneumoniae* exhibits codon usage patterns linked to genes involved in immune evasion and host colonisation (Prendergast et al., 2023). The complex connection that exists between CUB and virulence highlights the possibility of using pathogen specific codon usage as a target for medicinal therapies (Antoine et al., 2021).

2.5 The future of prokaryotic codon usage studies

Codon usage patterns are very crucial to be analyzed in order to interpret the genetic codes and to predict gene expression. Codon usage studies have a very wide-ranging scope on several disciplines, including molecular biology and synthetic biology, evolutionary biology and pharmacology. Research on the analysis of codon usage have already shed light towards genetic code, the control of gene expression, and the evolutionary trends not only in prokaryotes but also in other types of organisms. However, there are a number of intriguing directions for future research that can give new insights across all forms of life available on the planet which are summarized in **Table 2.2**. Researchers can gain a deeper understanding of how prokaryotes use codons and adapt their translational machinery to various environmental conditions by leveraging developments in genomic technologies, comparative genomics, metagenomics, functional context integration, longitudinal studies, mobile genetic element analysis, synthetic biology, and multiomics approaches. Codon usage research will be essential in resolving the complexities of gene expression and evolution in prokaryotic organisms as the science develops (Dahal & Bansal, 2024; De La Fuente et al., 2023).

Table 2.2: Future direction on the codon usage research on prokaryotes

S. No.	Future Direction	Possibilities	References
1.	Analyzing comparative genomic signatures of prokaryotes	Can find conserved tendencies, species-specific adaptations, and gain better insights in the processes influencing codon usage biases	(Dahal & Bansal, 2024; De La Fuente et al., 2023)

Table 2.2: Continued

S. N	Future Direction	Possibilities	References
2.	Analyzing Codon Usage Bias in Mobile Genetic Elements of prokaryotes	Genes, transfer of plasmid and phages between various prokaryotic species and evolution can be understood by understanding the CUB in those elements. Also, examining the CUB of mobile genetic elements can provide insight into the elements interaction with the translational apparatus of the host and impact the prokaryotic host fitness.	(Parvathy et al., 2022)
3.	Metagenomic and Environmental research in prokaryotes	Possible to learn more about the genetic potential and expression methods of uncultured prokaryotes by examining the codon usage in environmental samples	(Panda & Tuller, 2023)
4.	Contextualization of Function	CUB patterns can be examined in relation to gene function, expression levels, and protein characteristics to deduce better insights of selection forces influencing trends of codon usage aiding in identifying genes susceptible to strong selection and environmental adaptation as well.	(Deb et al., 2020)
5.	Prokaryotes in genetic engineering and synthetic biology	Researchers can optimise protein expression levels, raise protein production, and create more effective genetic constructs by modifying codon usage patterns.	(Wright et al., 2022)

Table 2.2: Continued

S. N	Future Direction	Possibilities	References
6.	Bringing Multi-Omics Data of prokaryotes together	Examine how codon usage affects gene expression, protein abundance, and metabolic pathways using this integrated method. It would also aid in identifying possible relationships between codon usage biases and post-transcriptional and post-translational regulatory mechanisms.	(Bardozzo et al., 2018)
7.	Longitudinal studies in prokaryotes	Can show how the dynamics of codon usage modifications response to alterations in the environment, population constraints, and selection pressures.	(Roodgar et al., 2021)

2.6 The Genus *Acinetobacter*:

The genus *Acinetobacter* is a group of diverse organisms. It comprises of some of the most dreaded infection-causing species implicated in nosocomial as well as community acquired infections and is becoming increasingly notorious for causing opportunistic infections that may result in serious illness and even death (Almasaudi, 2018). *Acinetobacter* species have been linked to a variety of disease conditions in hospitals, especially in severely ill patients with debilitated host defense. Such species particularly infect patients using respiratory treatment equipment or catheters. Septicemia, wound sepsis, urinary tract infection (UTI), pneumonia, endocarditis, etc. are some of the critical diseases caused by *A. baumannii*, which is the most frequently encountered species in hospitals due to its ability to withstand harsh environments. Nosocomial infections are

reportedly caused by species like *A. calcoaceticus, A. nosocomialis, A. lwoffii, A. junii, A. ursingii, A. bereziniae*, and A. serfertii (Rebic et al., 2018). Presence of antibioticresistance genes is a common feature of these species, making them naturally resistant to a wide variety of antibiotics. Previously, non-*baumannii* species were considered less as pathogens due to their limited virulence. In 1970s, they were identified as major nosocomial pathogens with great sensitivity to drugs such as ampicillin, chloramphenicol, and gentamycin (Dahal et al., 2023).

The genus *Acinetobacter* harbors many environmentally important species as well, which have a wide range of metabolic capabilities, such as routes for the breakdown of contaminants like hydrocarbons, amino acid derivatives, and crude oil employing them as principal source of nutrition (Rebic et al., 2018; Xin et al., 2014). The majority of the research findings have been acquired utilizing *A. baylyi* ADP1, *A. baumannii*, and *A. calcoaceticus*. Their metabolic pathways and regulatory mechanisms have attracted substantial attention. For example, *A. calcoaceticus* can degrade up to 90% of aliphatic hydrocarbons in diesel (Dahal et al., 2023). Similarly, *A. radioresistens* APH1, a novel phenol degrader with one of the greatest phenol degrading efficiencies has been identified and used in soil bioremediation (Liu, 2020). They have also been implicated in removal of pharmaceutical wastes from the environment (Wang et al., 2018). The use of *Acinetobacter* species is not limited to biodegradation and bioremediation, they are being used as prospective bioreporters (H. Li et al., 2021), manufacturers of lipase (Fatima et al., 2021; Patel et al., 2021), biosurfactants (Oanh et al., 2020), and producers of biopolymeric substances (Dahal et al., 2023), biodiesel (Tan et al., 2022; Zhang et al., 2021), medicines, and cosmetic and other significant practical uses (Arvay et al., 2021; J. Li et al., 2017). Therefore, the environmental species also deserve special attention for the benefit of life on land and life below water.

2.6.1 Phylogeny

Acinetobacter is a complex group of saprobic bacteria that are Gram-negative coccobacilli with a GC content ranging from 39% to 47%. Members of the genus are non-fermenters, aerobic, catalase-positive, oxidase-negative, and motile in nature. *Acinetobacter* species can be found in a variety of environments, including water, inside human or animal hosts, different types of plants, and soil (Adewoyin & Okoh, 2018; Dandachi et al., 2019). Morphological traits differ according to the growth phase, e.g. appearance of rod-shaped structure is observed during the log phase, but at later stages, coccobacillus structure is displayed. The genus *Acinetobacter* comprises of 108 closely related species, but only 77 species have discretely published names according to the list of prokaryotic names with standing in nomenclature (Baraka et al., 2020; Cayô et al., 2016).

The genus *Acinetobacter* has a long history of classification. In the past, the Gram-negative non-fermenters, presently known as *Acinetobacter*, were classified under more than a dozen different generic names. The most well-known scientific names of *Acinetobacter* species in the nineteenth century were *Mima polymorpha, Morexella lwofii, M. glucidolytica*, and *Micrococcus calcoacetius.* Initially, *Acinetobacter* was suggested to be a broad group of Gram-negative, non-motile saprobes, both oxidase-positive and negative with discernable absence of pigment. Beijernick and colleagues described *M. calcoacetius* in 1911 (Dahal et al., 2023), and it is the oldest reference for *Acinetobacter* species. Birsou and Prevot proposed the new genus Achromobacter in 1954, following several revisions. With an improved explanation of the *Acinetobacter* genus, Baumann and colleagues reclassified many genera and species into the genus *Acinetobacter*ia in 1968 (Ayenew et al., 2021). Additional nutritional studies clearly demonstrated the difference between oxidase-negative and positive strains, and therefore, the subcommittee on the taxonomy of Moraxella and Allied bacteria prescribed that the genus *Acinetobacter* would solely contain oxidase-negative strains in 1971 (Towner, 2009). The use of traditional microbiological as well as numerous molecular and

biochemical approaches backed up this prescription. Some of the techniques used to identify and categorize *Acinetobacter* strains include amplified ribosomal DNA restriction analysis, DNA–DNA hybridization, and 16S DNA sequence analysis. For more than 20 years, these strategies have provided the groundwork for including various species within a genus (Adewoyin & Okoh, 2018; Enright et al., 1994).

The genus is divided into three ecologically distinct clades by combined metagenomics, comparative genomics, and phylogenomics research, which revealed two significant environmental transitions at deep phylogenetic levels. One of them has quickly turned toward host-association by acquiring genes responsible for interactions between bacteria and eukaryotes (Almeida et al., 2021; Nemec et al., 2022). Of the three clades, Clade I exhibits the most intra-clade ecological divergence. Members of the clade, such as the *Acinetobacter calcoaceticus baumannii* (ACB) complex, are more prevalent in soil and habitats where people are present. Both *A. calcoaceticus* and *A. pittii* are frequently found in soil, with the former being the most prevalent but rarely found in human hosts. *Acinetobacter baumannii*, on the other hand, is quite prevalent across the human population. The disparity in the distribution of A. *baumannii* between soil and host-associated settings raises the possibility that this species is quickly adapting to human-associated environments (including humans, human-associated hosts, and house-holds). *Acinetobacter haemolyticus, A. parvus, A. junnii, A. modestus*, and other members of clade II are frequently discovered in aquatic habitats and infrequently linked with hosts. Clade III members, such as A. lwoffii, A. generi, A. rudis, A. indicus, and others, are more frequently discovered in organicrich aquatic habitats, such as wastewater samples and marine sediments. Clade I witnessed substantially greater rates of habitat diversification compared to other groups (Garcia-Garcera et al., 2017). Recently, Almeida and group used 275 high-quality filtered protein sequences to reconstruct the phylogenic tree with more than 57 species of *Acinetobacter*. The tree corroborates with the monophyly of the genus *Acinetobacter* and illustrates four main clades on the basis of the strongest support values (**Fig. 2.4**). They also showed ACB complex as a sub clade of clade II of the genus *Acinetobacter* (Almeida et al., 2021).

The term ACB complex was coined because the species that make up the group have nearly identical morphological traits and high genetic relatedness, making precise taxonomic assignment reliant on molecular approaches. Initially, the "complex" consisted of *A. calcoaceticus*, A. *baumannii*, and two unclassified strains formerly known as *Acinetobacter* genomic species 3 and *Acinetobacter* genomic species 13TU, which were formally reclassified as *A. pitti* and *A. nosocomialis*, respectively. *Acinetobacter oleivorans, A. lactucae*, and *A. seifertii* have all been identified as members of this complex in recent investigations (Almeida et al., 2021; Mateo-Estrada et al., 2019). Phylogeny of ACB complex genomes has been verified as monophyletic, and these are frequently responsible for nosocomial infections. Environmental species are mostly from the *calcoaceticus* lineage and are not linked to nosocomial illnesses. Furthermore, the ACB complex contains both environmental and human pathogenic isolates, which can be misleading for medical treatment because most of the pathogenic isolates are equipped with antibiotic resistance genes (Djahanschiri et al., 2022; Mateo-Estrada et al., 2019).

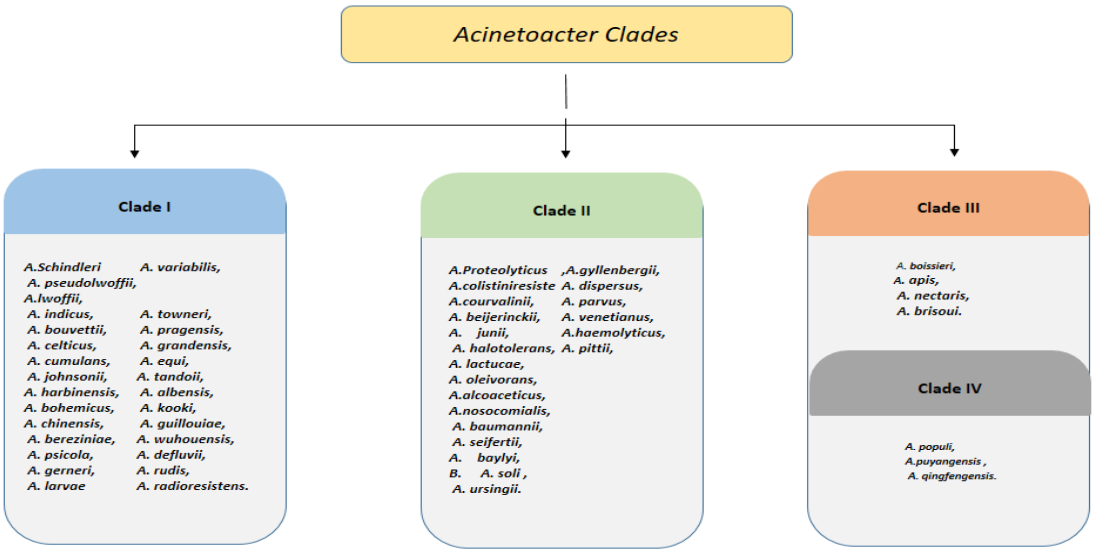

Figure 2.4: Four main clades according to the phylogenetic tree representing more than 57 species of *Acinetobacter* as given by Almeida and group in 2021 on the basis of 275 high-quality filtered protein sequences (Almeida et al., 2021)

2.6.2 Clinical significance

Among several species of *Acinetobacter*, the *Acinetobacter baumannii* complex *(A. nosocomialis, A. pitti,* and A. *baumannii*) is clinically the most important, followed by *A. haemolyticus, A. junni*, A. johnsonii, and A. lwoffi. *Acinetobacter* ursingii, and A. schindleri are also found in clinical infections (Al Atrouni et al., 2016). *Acinetobacter baumannii* alone is responsible for over 90% infections in human hosts, while other species together account for the rest. The epidemics caused by *Acinetobacter* species are due to antibiotic resistance and their ability to persist in a harsh hospital environment, including desiccation and disinfectants (Al Atrouni et al., 2016; Almasaudi, 2018; Brasiliense et al., 2019). Members of the genus usually cause pneumonia and septicemia, as well as endocarditis, meningitis, and infection in wounds, the urinary tract, and the lungs (Dahal et al., 2023). Outer membrane proteins (OMPs), cellsurface hydrophobicity,toxic slime polysaccharides, and verotoxins have been implicated in the suspected virulence mechanisms employed by members of the genus (Dandachi et al., 2019).

MDR *Acinetobacter* MDR *Acinetobacter* species are those that are resistant to at least one antimicrobial agent among fluoroquinolone, aminoglycoside, penicillin, or cephalosporin. The resistance of *Acinetobacter* species to a wide range of antibacterial drugs, including first- and second-generation cephalosporins and carbapenems, is well recognized (Ayenew et al., 2021; Ayoub Moubareck & Hammoudi Halat, 2020). Most *Acinetobacter* isolates display multiple mechanisms of drug resistance, such as enzymatic drug degradation, target alteration or protection, and decreased permeability or active efflux of antibiotics. Resistance is acquired either by horizontal transfer of genetic elements containing resistance determinants or through mutations in endogenous genes that result in the inactivation, alteration, or overexpression of cellular functions (Ibrahim et al., 2021; Maeusli et al., 2020).

In clinical settings, the selective pressure of powerful antibiotics has slowly led to a worldwide preponderance of *Acinetobacter* strains resistant to several antibiotics used to

treat infection, including impenim,sulbactam, ampicillin,second generation cephalosporins, quinolones, colistin, aminoglycosides, gentamicin, and minocycline (Al Atrouni et al., 2016; Breijyeh et al., 2020). Carbapenem-resistant A. *baumannii* has been designated as a clinically relevant pathogen for antimicrobial research and development by the World Health Organization (WHO). *Acinetobacter baumannii* is the most prevalent MDR species. Moreover, members of the ACB complex like *A. pittii* and *A. calcoaceticus* have lately emerged as MDR nosocomial pathogens (Brasiliense et al., 2019). Recent findings reveal increased carbapenem resistance as well as changes in resistance mechanisms employed by *A. pittii*. For example, carbapenem-resistant *A. pittii* (CRAP) has been reported to have disseminated worldwide. The presence of carbapenemhydrolyzing lactamases, such as NDM1, has been a major issue behind CRAP. Similarly, resistance to erythromycin- and telithromycin-like antibiotics in *A.seifertii* has been attributed to mutations in the 23S rRNA gene (Furlan et al., 2019). Resistance to β-lactams in *A. calcoaceticus* is speculated to be an outcome of chromosomally encoded cephalosporinase. Decreased outer membrane permeability is also a major factor contributing to *A. calcoaceticus* natural resistance toward broad-spectrum antibiotics (Obara & Nakae, 1991).

2.6.3 Pathogenicity

The ability of *Acinetobacter* to resist innate immune mechanisms allows them to grow in numbers, resulting in sepsis. Capsule polysaccharide and OmpA are amongst the crucial antigenic factors that permit immune evasion. Furthermore, lipopolysaccharides, the iron acquisition system, phospholipase D, outer membrane vesicles, and penicillin binding proteins facilitate in vivo survival of the pathogens by neutralizing host immune response (Ayoub Moubareck & Hammoudi Halat, 2020). Exposure to broad-spectrum antibiotics, the presence and duration of invasive surgery, burns, and other factors like ICUs, use of devices such as endotracheal tubes, catheters, and mechanical ventilation are strongly linked to *Acinetobacter* infections. *Acinetobacter* can be extremely virulent and cause an

invasive catastrophe, as seen by the incidence of fulminant community acquired infections (Meumann et al., 2019). Some of the major pathogenic species along with their key attributes have been summarized in **Table 2.3**

Table 2.3: Pathogens and their key attributes

Organism	**Average GC% and Protein count**	**Infections**	**Source**	**Antibiotic resistance genes/enzymes**	**Other Important Features**	**References**
Acinetobacter baumannii	39, 3678	Ventilator associated pneumonia, sepsis, urinary tract infections, and skin and soft-tissue infection	Clinical environment	MBLs genes of blaOXA-23, blaOXA-40, and blaOXA-58 efflux pumping systems, porins	Degradation of propanil (herbicide) MDR Monophyletic origin Member of ACB complex	Chakravarty 2020; Mea et al., 2021
Acinetobacter bereziniae	37.9, 4184	Bacteremia, especially in immunocomprom-ised patients	Clinical environment, also reported in human milk sample	blaOXA-58 reported	Formerly known as *Acinetobacter* genomospecies 10 MDR species Opportunistic pathogen	Favaro et al., 2019; Lee et al., 2020

Table 2.3: Continued

Organism	**Average GC% and Protein count**	**Infections**	**Source**	**Antibiotic resistance genes/enzymes**	**Other Important Features**	**References**
Acinetobacter calcoaceticus	38.7, 3592	Causes pneumonia and other hospital related infections	Clinical as well as natural environment including sewage treatment system	blaOXA-822(Class-D)	Cadmium and antibiotic-resistant has been reported Reported pathogenic in dogs and cat	Obara et al., 1991; Glew et al., 1977, Retailliau et al. 1979
Acinetobacter haemolyticus	39.5, 3095	Not mentioned, reported pathogenic	Across Human samples and clinical environment	blaOXA265, blaNDM-1, aphA6 and a resistance-nodulation-cell division-type efflux pump.	MDR Can produce phosphate binding exo-biopolymer Aerobic denitrification	Kaur et al.,; 2015;Bello et al., 2019; Bai et al., 2020
Acinetobacter johnsonii	41.4, 3291	Opportunistic pathogen, nematocidal activity against round worm	Distributed in clinical and natural environment	blaOXA-23	Degrades NAP (Naphthalene) and ANT (anthracene) MDR	Tian et al., 2016; Jiang et al., 2018; Jia et al., 2021
Acinetobacter junii	38.7, 3063	Urinary tract infection, Associated with outbreaks of sepsis in immuno-compromised patients	Human samples and environment	Carbapenem resistance, blaOXA-24 and blaOXA-30	Rarely pathogenic to humans	Abo-Zed et al., 2020; Kollimuttathuillam et al., 2021

Table 2.3: Continued

Organism	Average GC% and Protein count	Infections	Source	Antibiotic resistance genes/enzymes	Other Important Features	References
Acinetobacter nosocomialis	38.7, 3606	Pathogenic	Clinical specimens, soil sample	blaOXA-24/50	Member of ACB complex. Carbapenem and colistin resistant	Kim et al., 2016; Subhadra et al., 2020
Acinetobacter pittii	38.8, 3685	Causes nosocomial infections, Fish pathogenesis reported	Environment and human specimens	blaNDM-1, blaOXA-820, blaADC-43 and aphA6 reported	Member of ACB complex. Carbapenem-resistant Phosphate-solubilizing	Iimura et al., 2020; He at al., 2021
Acinetobacter seifertii	38.6, 3651	Bacteremia	Clinical samples	Produces oxa-58, metallo-β-lactamase-2	Belongs to ACB complex Resistance to Levofloxacin and carbapenems, but not colistin.	Kishii et al., 2016; Na et al., 2021
Acinetobacter towneri	41.3, 2614	Human infections	Hospital waste, sea water	Plasmid-mediated tet (X3) gene, also produce metallo-β-lactamase-1	MDR including tigecycline Causes infections in human	Ma et al., 2020; Maehana et al., 2021
Acinetobacter ursingii	40.1, 3173	Blood stream infections	Clinical environment including Human samples	Metallo-β-lactamase-producing	Affects immunocompromised and terminally-ill patients. Antibiotic resistance	Faccone et al., 2019; Daniel et al., 2021

Table 2.3: Continued

Organism	**Average GC% and Protein count**	**Infections**	**Source**	**Antibiotic resistance genes/enzymes**	**Other Important Features**	**References**
Acinetobacter kookii	43, 2828	Polyarthritis in giraffe	Soil, Rothschild's giraffe calf, Activated sludge	Unknown	Similar to *Acinetobacter beijerincki* Degrades 17α-ethinylestradiol	Schwarz et al., 2020; Palma et al., 2021
Acinetobacter lwoffii	42.95, 3100	Emerging pathogen in fish, causes bacteremia, pneumonia, meningitis and gastritis in humans	Clinical environment	Unknown	Dark green pigmentation reported	Cao et al., 2018 ;Kulkarni et al., 2021
Acinetobacter colistiniresistens	41.3 3547	Blood stream infections	Clinical environment	Produces Imp-34- and oxa-58	Previously known as *Acinetobacter* genomic species 13BJ/14TU Intrinsic resistance to colistin Carbapenem-resistant	Suzuki et al., 2019; Brasiliense et al., 2021;
Acinetobacter indicus	45.8, 2733	Not reported	Animal origin (cow, duck)	blaNDM-1 and tet(X)	Biotechnologically significant (lipase and biosurfactant production) Opportunistic pathogen	He et al., 2020; Tang et al., 2021

Table 2.3: Continued

Organism	**Average GC% and Protein count**	**Infections**	**Source**	**Antibiotic resistance genes/enzymes**	**Other Important Features**	**References**
Acinetobacter schindleri	42.5, 2956	Bacteremia in humans reported	Soil, Chicken litter (reported, water and hospital environment	Unknown	Could not use furfural as sole carbon source Opportunistic pathogen	Kee et al., 2018; Mlynarcik et al., 2019; Arteaga et al., 2021
Acinetobacter radioresistens	41.8, 2881	Bacteremia, pneumonia and hepatic hydrothorax	Soil and human samples	blaOXA-23-like gene tet(B), aph(3')-Vla, strA, and strB,	Rarely infects human Applied in soil bioremediation Resistant to ampicillin, ceftriaxone, ceftazidime, cefotaxime, streptomycin, and kanamycin	Opazo-Capurro et al., 2019; Liu et al., 2020

The most significant pathogenic species of the genus, A. *baumannii*, is one of the "ESKAPE" pathogens (*Enterococcus faecium, Staphylococcus aureus, Klebsiella pneumonia, A. baumannii, Pseudomonas aeruginosa*, and *Enterobacter spp.*) that can cause epidemics, especially in intensive care patients, and can be detected using 16s ribosomal RNA or seven housekeeping genes, *rpoD, gyrB, gdhB, recA, gltA, gpi,* and *cpn60*, through MLST. Ventilator-associated pneumonia, sepsis, UTIs, and skin and soft-tissue infections are the common diseases caused by A. *baumannii* (Dahal et al., 2023). *Acinetobacter baumannii* is a common cutaneous and upper respiratory tract colonizer that has been identified in human sputum, blood, urine, and faeces. *Acinetobacter baumannii* may survive for long durations on hospital surfaces and has been isolated from a variety of sources, including tap water faucets, angiography catheters, ventilators, air, gloves, and bed-side urinals (Ibrahim et al. 2021). One-fifth of the infections in intensive care units globally are attributed to A. *baumannii* (Dahal et al. 2023). Crucial factors that assist in the pathogenicity of *A. baumanii* and other pathogens are described in the following section.

2.6.3.1 Role of enzymes

The development of β-lactamases, particularly oxacillinases, linked to the promoter gene sequence ISAba1, is the basis of carbapenem resistance in *Acinetobacter* spp. (Bansal et al., 2020; Yazdansetad et al., 2019). The most common oxacillinase, transferred through mobile genetic elements, is blaOXA-23. The genes blaOXA-23 and blaOXA-51 had been previously linked to A. *baumannii*. However, recent reports have revealed the presence of these genes in other species as well. *Acinetobacter pittii* and *A. nosocomialis* are both reported to contain the blaOXA-23 gene (Meshkat et al. 2019). In addition, *A. calcoaceticus, A. johnsonii, and A. haemolyticus,* also contain oxacillinase-producing genes (Figueiredo et al., 2012).

Acinetobacter baumannii has an intrinsic class D type oxacillinase and a non-inducible chromosomal AmpC type cephalosporinase that is expressed at a low level. Oxacillinases from *A. baumannii* are OXA51 enzymes, which have more than 40 sequences and can hydrolyze many types of penicillin (Farajzadeh et al., 2021). In addition to this, all strains of *A. baumannii* have chromosomal cephalosporinases (AmpC enzymes), which can hydrolyze almost all derivatives of penicillin and cephalosporin (Nordmann & Poirel, 2019). Metallo-β-lactamases (MBLs) are rarely found in *A. baumannii*, but their carbapenem-degrading activity is much stronger. All the β-lactams and carbapenems are hydrolyzed by these enzymes, except for aztreonam (Ramirez et al., 2020). The presence of MBLs was described in *A. pittii* (Deglmann et al., 2019).

Other crucial enzymes encoded by genus *Acinetobacter* include phospholipase C and D. *Acinetobacter baumannii* encodes for phospholipase D, while *A. calcoaceticus* encodes phospholipase C (Lehmann, 1971). The two enzymes can be distinguished by their ability to digest a phospholipid molecule. Phospholipase D only digests the head group, whereas phospholipase C digests the phosphorylated head of a phospholipid molecule (Ayoub Moubareck & Hammoudi Halat, 2020). Phospholipases are important hydrolytic enzymes with lipolytic action against phospholipids in human cell membranes serving as crucial virulence mechanism in *A. baumannii*. Phospholipase D increases the survival rate of bacteria in human serum, whereas phospholipase C damages epithelial cells. CpaA has been acquired recently by *A. baumannii* as a virulence factor that prevents blood coagulation by inactivating factor XII. As a result, CpaA inhibits the production of thrombin at intravascular regions, allowing *A. baumannii* to spread more widely (Harding et al., 2018; Morris et al., 2019).

2.6.3.2 Outer membrane proteins

OMPs found in *Acinetobacter* species contribute significantly to their pathogenicity and evolving antibiotic resistance. OMPs reportedly modulate the uptake of antimicrobial

agents preventing them from entering the bacterial system (Nie et al., 2020; Uppalapati et al., 2020). Furthermore, OMPs promote greater cell adherence and maintain the integrity of cell membranes. OMPs regulate the generation of outer membrane vesicles, which is crucial for antibiotic resistance and in the formation of biofilms (Mozaheb & Mingeot-Leclercq, 2020). OmpA, CarO, and OmpW are the major types of porins discovered in species like *A. baumannii* and *A. nosocomialis* (Uppalapati et al., 2020). The first porin to be discovered and characterized in *Acinetobacter* was OmpA (initially identified as Omp38). OmpA is comparatively impermeable with respect to other porins of similar size (e.g. OprF from *E. coli*), implicating it in antibiotic resistance. OmpA is highly conserved across species, having 92% amino acid sequence similarity with *A. nosocomialis* (Kwon et al., 2019) and plays a key role in its pathogenesis mechanism. OmpA expressed on the outer membrane of *A. nosocomialis* helps the bacteria form biofilms on abiotic surfaces and adhere to human epithelial cells facilitating cytotoxicity (Knight et al., 2018).

CarO, or carbapenem-susceptible porin, is an outer membrane channel protein with an 8-strand β-barrel structure that does not have a continuous channel but mediates the inflow of beta-lactams (mostly imipenem) into *A. baumannii*. CarO provides carbapenem resistance to *A. baumannii* and works similarly to other OMPs in enhancing cell attachment. It can also manipulate the immunological response of host cells by inhibiting micro-tubule associated protein thereby reducing the expression of pro-inflammatory genes. Recent evidence suggests that it plays a role in enhanced bacterial endurance inside the host as it acts as a selective filter dodging antimicrobials produced by the host (Mea et al., 2021; Zhu et al., 2019).

OmpW, identified in *A. baumannii*, is highly like OmpW found in *P. aeruginosa* and *E. coli*. Although the direct role of OmpW in *A. baumannii* is unknown, colistin-resistant *A. baumannii* mutant grown in vitro exhibited a decreased expression of the porin. However, a report from 2016 revealed the porin's role in iron assimilation and its ability to accommodate colistin molecules (Gil-Marqués et al., 2022; Sarshar et al., 2021).

2.6.3.3 Biofilm

The formation of biofilms is associated with increased bacterial survival rates and therefore augments pathogenicity. Pathogenic members of the genus like *A. baumannii*, *A. pittii,* and *A. calcoaceticus* reportedly form biofilms and are more resistant to antimicrobial treatments (Bravo et al., 2018; Knight et al., 2018). Moreover, the biofilm so formed enables them to remain active on biotic and abiotic surfaces while avoiding the host reaction (Gedefie et al., 2021). The biofilm-associated protein (bap) expressed by the *bap* gene is involved in intercellular adhesion, bacterial cell accumulation, and biofilm formation. The presence and expression of the *blaPER-1* gene have also been associated with certain A. *baumannii* clinical isolates forming biofilms. Moreover, the development of pilus and exo-polysaccharide structures for defense against host is phenotypically linked to biofilm formation in A. *baumannii* strains that adhere to host cells (Yang et al. 2019, Gedefie et al. 2021, Mea et al. 2021). Similarly, as per a report, *A. pittii* may recover quickly from desiccation and express adhesion factors to infect new hosts as a result of biofilm formation (Bravo et al., 2018).

2.6.3.4 Efflux pumping systems

Efflux pumps serve as potent mechanisms for preventing antibiotics from entering the bacterial cell and induce resistance. Antimicrobials are expelled from the bacterial cell through these pumps resulting in lower drug accumulation therefore higher minimum inhibitory concentrations (MICs) for several antibiotic families such as β-lactams, quinolones, and aminoglycosides. Efflux pumps are essential for the extrusion of bile molecules, fatty acids, and peptides, as well as the active secretion of virulence factors such as siderophores in other Gram-negative bacteria. *AceI* and the AdeABC efflux pumps in *Acinetobacter* induce resistance to aminoglycosides and biocides, respectively (Morris et al., 2019).

The small multidrug resistance (SMR) family, the resistance-nodulation-division (RND) family, the major facilitator superfamily (MFS), and the multidrug and toxic compound extrusion (MATE) family are the four types of efflux pumps prevalent in *A. baumannii*. These families and their membrane-associated transporters have been shown to target specific antibiotic classes (Chakravarty, 2020). Narrow-spectrum pumps from MFS include minocycline (TetB) resistance pumps and tetracycline (TetA, TetB) pumps, as well as the CmlA system that extrudes chloramphenicol. Two RND pump systems found in *A. baumannii* are AdeABC and AdeIJK. Chloramphenicol, aminoglycosides, cefotaxime, fluoroquinolones, tetracyclines, erythromycin, and trimethoprim are all pumped out by the AdeABC efflux pump in *A. baumannii*. AdeIJK, the second RND pump, prefers amphiphilic molecules as a substrate and works in tandem with AdeABC to promote tigecycline resistance. AbeM, a pump from the MATE family, has been implicated in lowering sensitivity toward erythromycin, quinolones, gentamicin, trimethoprim, chloramphenicol, and kanamycin upon overexpression. AbeS, a member of the SMR family of bacterial integral membrane proteins is linked to Chloramphenicol, quinolone, and macrolide resistance (Darby et al., 2023; Naidu et al., 2023).

In addition to antibiotic resistance mechanisms, pathogenesis, cell multiplication, and biofilm development are all known to be influenced by multidrug efflux pumping systems in *A. nosocomialis*. AcrR regulates the transcription of the AcrAB efflux pump in *A. nosocomialis*. The acrAB operon encoding AcrA and AcrB has also been discovered in *A. nosocomialis* and is significantly similar to arpAB operon involved in aminoglycoside resistance in A. *baumannii* (Subhadra et al., 2019).

2.6.3.5 Quorum sensing

Quorum sensing (QS) is a mode of communication between bacteria in order to maintain population density, using signal molecules known as “auto-inducers.” The LuxI/LuxR system is commonly found in various Gram-negative bacteria and is analogous to the two

components of *A. baumannii*'s QS circuit: the AbaI inducer and its corresponding receptor AbaR. AbaR serves as an acyl homoserine lactone (AHL) receptor protein, while AbaI is a sensor protein that acts as an auto-inducer synthase to produce AHL signal molecules. When AHL binds to AbaR, a series of reactions are triggered. According to recent studies, QS can be crucial for the development of biofilms, which act as insulation and help organisms live in hostile conditions and develop drug resistance (Saipriya et al., 2020). In addition, AnoI/AnoR, similar to AbaI/AbaR regulatory systems, were discovered in *A. nosocomialis*. The LuxI- and LuxR-type proteins AnoI and AnoR make up the QS system. AnoI is the producer of the QS signal N-3-hydroxydodecanoyl-L-homoserine lactone in *A. nosocomialis*. The formation of *A. nosocomialis* biofilm is significantly influenced by surface motility, which is further mediated by this QS regulating network (Subhadra et al., 2019).

2.6.4 Ecological/industrial significance

Another facet of the genus *Acinetobacter* entails its role in rescuing the environment by degradation of contaminants such as biphenyl, phenol, crude oil, acetonitrile, removal of phosphate from wastes, and many more. Some species can be used for producing fermentation-based industrial goods such as lipases, proteases, bio-emulsifiers, and a variety of biopolymeric compounds (Oanh et al., 2020; Patel et al., 2021). The ability to produce lipase is associated with hydrocarbon breakdown. They are frequently isolated from waste water treatment plants and sewage, which include high levels of petroleum-related hydrocarbons and other xenobiotics (Chen et al., 2004). In Thailand, e.g. *Acinetobacter* species strain MUB1 was identified with a remarkable ability to digest crude oil (Ecker et al., 2006). Furthermore, *A. venetianus* species contain marine hydrocarbon-degrading strains and have been recommended as an attractive model system for researching the mechanisms behind the process of alkane degradation, as well as a good platform for bioremediation of contaminated environments in general (Alattraqchi et al., 2021). A short description of various ecological applications of the

Acinetobacter species has been included in the following sections and summarized in **Table 2.4**.

Table 2.4: Species with biotechnological significance

Biotechnological application	**Organisms**	**Degradation/ Production potential**	**References**
Phenol degradation	*A. calcoaceticus*	91.6% of 0.8 g/L phenol in 48 h	Dahal et al., 2023
	A. radioresistens	99% of 450 mg/kg of phenol-contaminated soil	Liu et al. 2020
	A. lwoffii	41.67 mg/L per hour	Dahal et al., 2023
	A. tandoii	100% phenol degraded at the concentration of 280 mg/L	Van Dexter & Boopathy 2019
Nitrogen assimilation and removal	*A. boisseri*	Not mentioned	Álvarez perez et al. 2021
	A. calcoaceticus	Capable of nitrogen removal under low temperature conditions	Uniyal et al., 2016
	A. nectaris	Not mentioned	Álvarez perez et al.2021
Reduces Chromium	*A. bouvetii*	Able to reduce 40% chromium absorbed by plant roots	Qadir et al. 2021

Table 2.4: Continued

Biotechnological application	**Organisms**	**Degradation/ Production potential**	**References**
Hydrocarbon degradation	*A. lwoffii*	Degraded C13- C35 n-alkanes in crude oil Can degrade 88% of crude oil	Dahal et al., 2024
	A. baumannii	Can degrade 76% diesel and 90 % paraffins	Dahal et al., 2024
Dye discoloration and degradation	*A. pittii*	Can degrade 84% methylene blue in 24 hours	Bunnoy et al., 2019
	A. calcoaceticus	azo dye amaranth degradation with 90 % efficiency	Dahal et al., 2024
	A. haemolyticus	Can degrade methylene green, basic violet and acid blue dyes	Kaur et al., 2015
	A. baumannii	Decolourized 90% of 500mg/l of azo dye	Shreedharan et al.2021
Toulene	*A. junnii*	Can degrade 80% of 50 ppm toluene within 72 hours	Sing et al. 2018
Diesel degradation	*A. vivani*	Can use diesel as a sole source of carbon	Migliaccio et al. 2023
	A. haemolyticus	Kurstakin enhances diesel degradation by this bacteria	Dahal et al. 2023
	A. baumannii	Can degrade 99% diesel at pH 7	Dahal et al. 2024
	A. lwoffii	bioremediation in marine environment	Dahal et al., 2023
	A. calcoaceticus	Presence of diesel degrading genes alkM and xcpR	Dahal et al., 2023

Table 2.4: Continued

Biotechnological application	Organisms	Degradation/ Production potential	References
Crude oil degradation	*A. venetianus*	Can degrade upto 60.6 % waxy crude oil	Bach et al., 2003
	A. pitti	36.% percent crude oil in 21 days at 10gm/lit	Wang et al. 2019
Insecticide degradation	*A. schindleri*	Can degrade insecticides α-endosulfan and α-cypermethrin with more than 60% efficiency	Dahal et al., 2023
Furfural degradation	*A. baylyi*	Can degrade 1g furfural in 1 hour	Arteaga et al., 2021
Fipronil degradation	*A. calcoaceticus*	86.6% degradation after 45 days	Uniyal et al. 2016
	A. oleivorans	89.7 % degradation after 45 days	Uniyal et al. 2016
NAP (Naphthalene) and ANT (anthracene) and other polyaromatic hydrocarbons like pyrene degradation	*A. johnsonii*	0 mg/litre NAP and ANT	Jiang et al. 2018
	A. baumannii (pyrene)	Efficient at 300mg/L concentration of pyrene	Dahal et al., 2023
Catechol production	*A. bouveti*	Produces novel biscatechol siderophores namely propanochelin , butanochelin and pentanochelin	Dahal et al., 2023
N-acetyl-β-D-glucosamine	*A. parvus*	Can convert chitin to N-acetyl-β-D-glucosamine	Dahal et al., 2023
Cellulase	*A. junnii*	capable to produce cellulase at 112.38 U/ml)	Dahal et al., 2023

Table 2.4: Continued

Biotechnological application	**Organisms**	**Degradation/ Production potential**	**References**
Mevalonate	*A. baylyi*	Produce mevalonate from lignin derived compounds by β-keto adipose pathway.	Dahal et al., 2023
Lipases	*A. indicus*	Efficient lipase producer from industrial wasters	Dahal et al., 2023
	A. radioresistens	4.16 U/ml at pH 9) of enzyme after 72 h	Dahal et al., 2023
	A. haemolyticus	Produces lipase which is highly stable at 4 °C displaying 90 % activity even after 2 months	Dahal et al., 2023
Wax esters production	*A. calcoaceticus*	Highest molecular weight (1010 Kilo Dalton) so called emulsion	Mujumdar et al., 2019
Bioemulsion and biosurfactant production	*A. pittii*	Can produce 0.57 g/l lipopeptide biosurfactant when incubated in 1%(V/V) crude oil	Mujumdar et al., 2019
	Acinetobacter beijerinckii	Produces the only bioemulsion that contains lipoprotein while other contain polysaccharides	Mujumdar et al., 2019
	A. baumannii	Produces Lipoglycan,using edible oil as carbon source	Mujumdar et al., 2019
	A. radioresistens	Produces alsan, utilizing carbon source as ethanol	Mujumdar et al., 2019
	A. bouvetii	Produce Lipo-hetero-polysaccharide bioemulsifier which is the highest molecular weight ioemulsifier	Mujumdar et al., 2019
	A. lwoffii	Produces proteoglycan in presence of castor oil as carbon source	Mujumdar et al., 2019

Table 2.4: Continued

Biotechnological application	**Organisms**	**Degradation/ Production potential**	**References**
Phenanthrene degradation	*A. venetianus*	Phenanthrenen degradation ability increased by 2.4 times in presence of Ball-milled biochar	Dahal et al., 2023
Proteases production	*A. pittii*	De-oiled neem seed cake showed yield as high as 11–12 U/ml	Dahal et al., 2023
Biohydrogen	*A. junii*	566.44 3.5 mL/L at pH 7.5	Dahal et al., 2023
Biodiesel	*A. oleivorans*	Use biodiesel as a sole source of carbon at 30° C	Deems et al. 2021
Polyhydroxy butarate	*A. nosocomialis*	Yield of 5.88 g/L 35 ° C for 54 hours	Dahal et al., 2023
Bioremediation of heavy metals	*A. indicus*	Can reduce chromium (IV) and mercury (II)	Ho et al., 2021

2.6.4.1 Phenol degradation

Due to its widespread use as a raw material, phenol makes up a sizable component of the industrial wastewater released from chemical factories. Bacterial phenol degradation involves the metabolic transformation of complicated aromatic metabolites into essential primary (3–4) carbon compounds for bacterial growth. Catechol is produced after phenol is first oxidized by phenol hydroxylase. It is then changed through a variety of ring-opening processes, such as the ortho and meta cleavage pathways, which are, respectively, mediated by catechol 1,2-dioxygenase and catechol 2,3-dioxygenase. Catechol is turned into cis-muconate and then succinyl-CoA in the ortho-cleavage process. Similarly, it is transformed into 2- hydroxymuconate semialdehyde, 2-keto-4-pentenoic acid via two pathways **(Fig. 2.5)**, and then acetyl-CoA in the metacleavage

pathway (Dahal et al., 2023). One of the most effective phenol-degrading bacteria employed in soil bioremediation is *A. radioresistens* APH1 (Liu et al. 2020). A recent study revealed the potential role of *A. lwoffii* NL1 in the breakdown of phenol in wastewater. Phenol can be used by *A. tandoii* as the only carbon source, and it can degrade phenol using both the ortho and meta pathways (Van Dexter & Boopathy 2019). When compared to loose cells, *Acinetobacter* sp. strain AQ5NOL 1 encapsulated in gellan gum has a greater ability to break down phenol (Dahal et al., 2023).

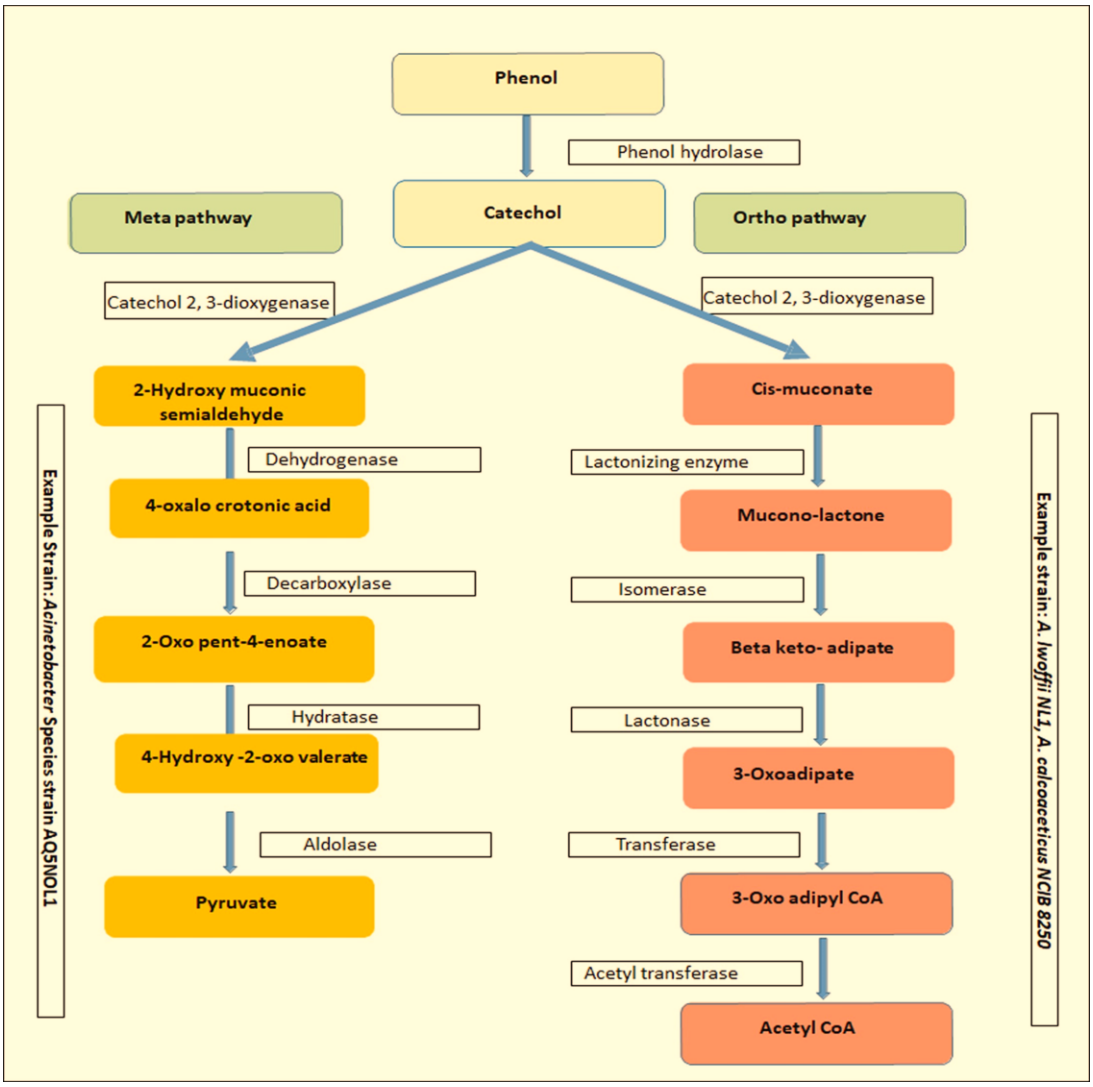

Figure 2.5: Ortho and Meta cleavage pathway for phenol degradation in *Acinetobacter* (Dahal et al., 2023, Liu et al. 2020)

2.6.4.2 Bio-emulsifier and biosurfactant production

When present in aqueous solutions and hydrocarbon mixtures, bio-emulsifiers and biosurfactants are the most significant active substances produced by microorganisms that play a crucial role in lowering surface and interfacial tensions. High-molecular-weight substances known as bio-emulsifiers are made up of intricate blends of polysaccharides, lipids, and proteins. They create stable emulsions by forging a strong bond on hydrocarbon surfaces. Contrarily, biosurfactants are low-molecular-weight substances that can lower surface and interfacial tension at the interfaces of phases, such as gas–liquid–solid interfaces. They produce stable emulsions as well and contain complex assemblages of proteins, glycolipids, and lipo-peptides (Dahal et al., 2023). Many *Acinetobacter* species, including *A. venetianus* RAG-1, *A. calcoaceticus* RAG-1, *A. calcoaceticus* BD4 RAG1, and *A. radioresistens* KA53, etc. are capable of producing polymeric bio-emulsions. The best emulsions produced by several *Acinetobacter* strains are emulsan, biodispersan, and alasan. The substrates that are insufficiently soluble in water are broken down using emulsan, generated by *A. calcoaceticus* RAG-1. It has also been claimed that the biosurfactant derived from *A. junii* B6 lowers the surface tension of cultured oil broth. Biosurfactant produced by *Acinetobacter* sp. ACMS25 was found to inhibit the growth of *Xanthomonas oryzae* XAV24. An important study revealed attenuated proliferation of lung cancer cells upon exposure to the biosurfactant produced by *A. indicus* M6, indicating its anticancer properties (Mujumdar et al. 2019).

2.6.4.3 Lipases

Lipases which hydrolyze lipids into fatty acids and glycerol at the water-oil interface and catalyze the processes of esterification and resolution find abundant use in the food, biofuel, dairy, cosmetic, and pharmaceutical industry (Dahal et al., 2023). Lipolytic *Acinetobacter* strains have been isolated from a wide range of substrates, including human skin, dairy products etc. as well as from various soil and water environments.

Lipolytic clinical strains frequently result in serious nosocomial infections in immunocompromised adults and newborns. Since bacteria use lipolysis appropriately to meet their specific needs during invasion of host cell targets, the lipase activity of pathogenic species may be a contributory factor in their pathogenicity. Together with their corresponding Lif chaperone, lipases are encoded in an operon. With the exception of A. calcoaceticus BD413, which has the reverse arrangement, the Lif chaperone is typically encoded downstream from the structural gene. For the mature lipase to be secreted, lipase genes (lip) must co-express with their cognate foldases. There have been many reports of *Acinetobacter* spp. producing lipases, including *A. beijerinckii, A. baumanii*, *Acinetobacter* nov. sp. KM109, *A. radioresistens, A. haemolyticus* CMC-1, *A. calcoaceticus* BD413, and *Acinetobacter* sp. RAG-1. Very recently, *A. indicus* strain UBT1 was proved to efficient producer of lipase and biosurfactant using industrial waste as a sole source of carbon (Patel et al. 2021).

2.6.4.5 Wax esters

Wax esters, e.g. are prospective high-value lipids for the production of a wide variety of applicants, such as cosmetics, lubricants, medicines, printing, food supplies, etc. When nitrogen is scarce and carbon is limited, bacteria collect wax esters for storage. *Acinetobacter baylyi*, a naturally existing producer of wax esters, is a suitable model organism for understanding the potential and modifiability of wax esters in natural hosts. Engineered *A. baylyi* ADP1 can produce three times as much wax via overexpression of fatty acyl-CoA reductase Acr1 and deletion of the gene *aceA* encoding for isocitrate lyase in the wax ester synthesis pathway (Dahal et al., 2023). Similar to this, *A. baylyi* ADP1 naturally catabolizes aromatic substrates derived from lignin using the β-ketoadipate pathway to produce mevalonate from lignin-derived compounds (Dahal et al., 2023).

2.6.4.6 Crude oil degradation

Large amounts of poly-aromatic hydrocarbons, alkanes, and cycloalkanes, including benzene, xylenes, and toluene, are some of the hazardous substances found in crude oil (Bach et al., 2003). There are numerous *Acinetobacter* species that are able to break down crude oil and its hazardous by products. In 2019, Pradeep and colleagues showed that toluene could be broken down into non-toxic intermediate molecules by *A. junii* in petroleum-contaminated soil. Furthermore, combined cultures of *Acinetobacter* species and hydrocarbon-degrading fungus have been shown to be effective in breaking down crude oil because the fungus has a stronger ability to break down n-alkanes while the bacteria are efficient at breaking down other components like aromatic and branched alkanes. The combined culture of A. *baumannii* and Talaromyces sp. showed exceptional resistance to alkaline environment and a high ability to degrade crude oil (Wang et al., 2019). Use of biosurfactant-producing *Acinetobacter* sp. Y2 in combination with the fungus Scedosporium doubled the breakdown of petroleum hydrocarbons in comparison to the fungus alone. *Acinetobacter* species with high methyl tolerance and lipase production ability, *A. junii* C69 and *A. pittii* C95 can also catalyze the conversion of soybean oil into biodiesel (Bach et al., 2003; Wang et al., 2019).

2.6.4.7 Diesel oil degradation

Diesel oil is an extremely complex mixture of alkanes, cycloalkanes, and aromatic hydrocarbons, including alcohols. Diesel oil and its derivatives are known soil pollutants that are phytotoxic to a range of plants and crops. Bioremediation using bacteria like *Acinetobacter* to remove toxins from the environment, can mitigate the consequences (Migliaccio et al., 2023). One of the first studies on *Acinetobacter* strains, *A. haemolyticus* and *A. johnsonii* that break down diesel oil was published in 2012. Over 90% of diesel oil could be degraded by either species (Dahal et al., 2023). In course of two weeks, *A. junii* VA2 decomposed more than 75% of the applied diesel. Another

study revealed that *A. calcoaceticus* CA16 could grow in minimal medium, including diesel as the sole source of carbon, resulting in the breakdown of more than 90% of the aliphatic hydrocarbons and alkanes in diesel (Ho et al. 2020). According to a report, a bio-emulsion produced by *A. lwoffii* selectively dissolves various chain-length hydrocarbons in diesel (Dahal et al., 2023). The degradation process of crude oil, diesel, petrol, n-alkanes, and other hydrocarbons by members of *Acinetobacter* genus have been included in **Fig 2.5 and 2.6**.

2.6.4.8 Dye degradation

Reactive dyes are manufactured and used at a rate of more than 8×10^4 tonnes annually because of their chemical stability and adaptability. Dyes are employed in textile dying as well as in tattoos, cosmetics, printing, and consumer goods. Nevertheless, once the dyes are discharged into the environment due to their endurance, contamination results. The most hazardous pollutants are synthetic textile dyes, which contaminate wastewater as part of industrial effluents. Bioremediation is more affordable and environment-friendly in comparison to chemical and physical decomposition methods. A total of 20 different types of textile dyes were previously discovered to be decolored by *A. calcoaceticus* NCIM 2890 (Kaur et al., 2015). Numerous other *Acinetobacter* species have demonstrated their effectiveness in bioremediation and decolorization of pollutant dyes. *Acinetobacter pittii*, for instance, has the ability to break down methylene blue. Within a few days of incubation, the organism showed more than 70% decolorization of the contaminated effluent as well as methylene blue degradation (Shreedharan et al., 2021). A similar investigation on *A. baumannii* by Unnikrishnan and group in 2018 demonstrated above 85% decolorization in reactive red and over 90% degradation rate in dyes like Congo red and gentian violet within three days of incubation (Dahal et al., 2023). Recent research has shown that *A. haemolyticus* may degrade dyes like methylene green, basic violet, and acid blue with an efficiency of more than 75% (Dahal et al., 2023).

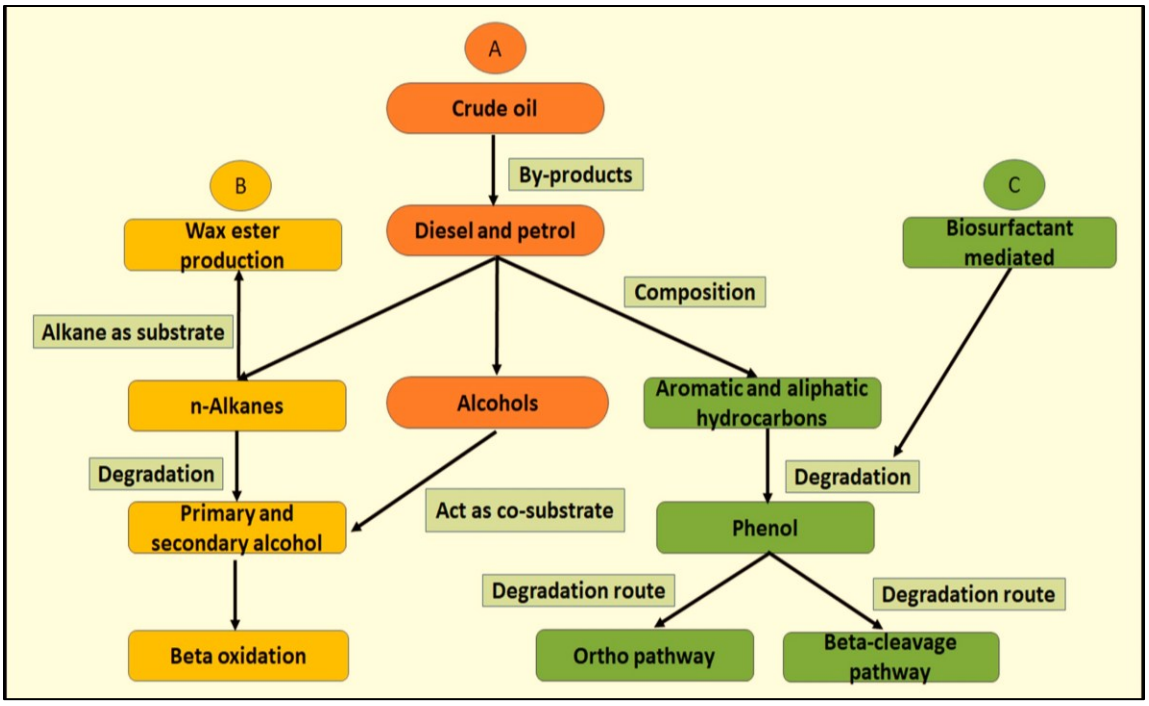

Figure 2.6: Chart for degradation of various contaminants like crude oil, diesel, petrol, n -alkanes, and other hydrocarbons by members of *Acinetobacter* genus (Kaur et al., 2015; Shreedharan et al., 2021; Dahal et al., 2023) (A) The b y -products of crude oil are diesel and petrol, which are composed of n -alkanes, alcohols, and aromatic and aliphatic hy drocarbons. (B) n -Alkanes can be used by *Acinetobacter* species for wax ester production (e.g.: *Acinetobacter* sp. strain M-1), whereas the degradation of n -alkanes forms intermediates like primary and secondary alcohols, which enter β-oxidation pathway. (C) The aliphatic and aromatic hydrocarbons from crude oils can be degraded into phenol with the help of bacterial biosurfactant (e.g.: *A. junii, A lwoffii, A. calcoaceticus* CA16). Phenol is further degraded via ortho (A. *lwoffii, A. calcoaceticus*) and β-cleavage pathway (*Acinetobacter* sp. strain AQ5NOL1), as shown in Fig. 2.5.

2.6.5 Plant-based applications

Many species of the genus Acintobacter are known to be involved in phytostimulation based on the production of hormones that promote plant growth as well as the solubilization of phosphate. *Acinetobacter calcoaceticus* has the ability to stimulate plant growth and metabolism via a positive effect on plant-produced abscisic acid and gibberellic acid (GA), amino acids, and crude protein, indicating a wider application as a biofertilizer for increased crop production and environment friendly farming practices (Gowtham et al. 2022). *Acinetobacter calcoaceticus* SE370 is a unique GA producer since it secretes ten different GAs into its environment, including a higher concentration of bioactive GA1, GA3, and GA4 (Dahal et al., 2023). *Acinetobacter calcoaceticus* has been found to colonize on plant surfaces and boost the chlorophyll content of both monocot and dicot plants. Similarly, *A. junii* can dissolve phosphate and also produces ammonia, indole acetic acid, GA, and hydrogen cyanide, all of which promote plant growth. Arbuscular mycorrhiza, together with *A. junii*, act as effective biofertilizers and promote the growth of tomato and bell pepper plants. An increase in absorbent surface area improves nutrient absorption, which in turn has improved plant development (Raimi et al. 2020). Additionally, A. rhizosphaerae strain BIHB 723 stimulates plant growth by solubilization of phosphate (Fariaet al. 2021). Some *Acinetobacter* strains indirectly promote plant growth by suppressing the growth of phytopathogenic microorganisms, including *Phytophthora capsici* and *Ralstonia solanacearum*. A recent study revealed that *Acinetobacter* sp. strain BRSI56 and ACRH80 subsequently reduce antioxidative stress in maize plant growing in hydrocarbon-contaminated environment (Dahal et al. 2023). Various plant-based applications of *Acinetobacter* species have been depicted in **Fig. 2.7.**

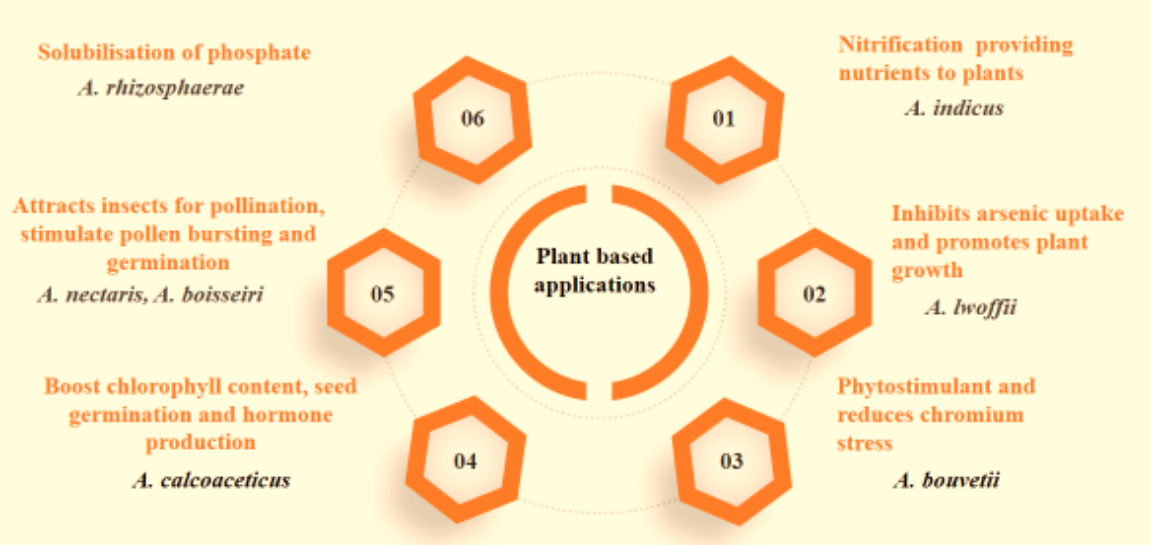

Figure 2.7: The plant-based applications of various *Acinetobacter* species (Raimi et al. 2020; Gowtham et al. 2022; Dahal et al., 2023)

2.6.6 Use as bioreporters

Bacterial whole-cell bioreporters are live microorganisms that have been genetically modified to create signals in response to stress or certain substances, allowing for the quick and accurate identification of the bioavailable fractions in samples (Dahal et al., 2023). Only small number of bacteria, like *E. coli* including certain species of *Acinetobacter*, might be utilized as bioreporters. Engineered *A. baylyi* ADP1 can emulsify mineral and crude oils into oil droplets at the microlevel and cling to the oil-water interface. ADPWHalk is able to overcome the limited solubility and accessibility of alkanes and therefore can easily detect oil spills in water and soil. The genotoxicity of phenolic chemicals in groundwater can be assessed using the bioluminescent bioreporter strain *A. baylyi* ADPWH-recA, which is capable of semi-quantitatively detecting genotoxic substances like mitomycin C and heavy metals (Dahal et al. 2023). In a contaminated environment where an *E. coli*-based reporter might not survive, Tetracycline can be detected by *A. oleivorans* strains that express bioreporters (Jiang et al., 2021). A report in 2021 suggested *A. baylyi* ADPWH recA as a potential bioreporter

for detecting the effect of heavy metals like lead and cadmium on a contaminated environment (Li et al. 2021).

2.7 Recent Developments in Acinetobacter Research (2024–2025)

In 2025, *Acinetobacter baumannii* remains a critical concern in clinical microbiology and public health. The World Health Organization reaffirmed its classification as a critical-priority pathogen in its updated Bacterial Priority Pathogens List due to its rising carbapenem resistance and life-threatening infections (lobritz er al., 2024). Recent reports emphasize its evolving resistance mechanisms, including enzymatic degradation, efflux pump overexpression, membrane permeability changes, horizontal gene transfer, and robust biofilm formation (Dahal et al., 2023). Alarming resistance rates approaching upto 90% in some regions underscore the urgency of the situation, particularly in healthcare-associated infections. On the therapeutic front, the antibiotic zosurabalpin, developed by Roche, has entered Phase III clinical trials (Dall et al., 2025; Dale et al., 2025). It represents the first new class of antibiotics specifically targeting Gram-negative pathogens like *A. baumannii* in over five decades. Simultaneously, research is intensifying on novel drug targets, such as the regulatory control of efflux systems and iron acquisition pathways that contribute to its virulence and survival. Collectively, these advances signal a global, multifaceted effort combining surveillance, drug discovery, and molecular research to address the escalating threat posed by Acinetobacter.

Research objectives

1. To inspect relative synonymous codon usage (RSCU) and relative amino acid usage (RAAU) patterns of the genomes of more than 50 *Acinetobacter* species.
2. To investigate the extent of codon usage bias and contribution of factors like mutational bias and natural selection for translational efficiency.
3. To predict the codon adaptation index and deduce the optimal codons across all genomes followed by multivariate statistical analysis.
4. To compare codon context signatures across all genomes of *Acinetobacter* genus.
5. Whole genome sequencing of selected members of the genus to compare ACB complex.

CHAPTER 3: MATERIALS AND METHODS

3.1. Retrieval of Data:

All the named species of *Acinetobacter* listed in the NCBI were considered to download their fully sequenced and annotated genomes from the Ensemble bacteria database (https://bacteria.ensembl.org/index.html). The dataset with internal stop codons or sequences with ambiguous codons at the front and/or end were excluded. To reduce sampling mistakes, only coding sequences longer than 300 base pairs were considered (Sharp et al., 1986). A thorough list of all the *Acinetobacter* species that have been analyzed in this investigation is listed in Table 3.1.

Table 3.1: Key attributes of *Acinetobacter* species under investigation.

Organism	**Assession No.**	**Coding Genes**	**Gene Transcript**	**Total no. of Codons analyzed**
Acinetobacter albensis	GCA_900095025	2,765	2,836	868254
Acinetobacter apis	GCA_900197575	2,182	2,250	707962
Acinetobacter baylyi	GCA_000046845	3,277	3,407	1050601
Acinetobacter beijerinckii	GCA_000368985	3,302	3,396	1028846
Acinetobacter bereziniae	GCA_000825165	4,493	4,493	1306879

Table 3.1: Continued

Organism	**Assession No.**	**Coding Genes**	**Gene Transcript**	**No. of Codons analyzed**
Acinetobacter bohemicus	GCA_000367925	3,324	3,430	1020199
Acinetobacter boissieri	GCA_900096955	2,502	2,563	791161
Acinetobacter bouvetii	GCA_000368865	3,112	3,209	956081
Acinetobacter brisouii	GCA_000488275	2,938	3,034	900355
Acinetobacter calcoaceticus	GCA_000368945	3,785	3,887	1181014
Acinetobacter celticus	GCA_001707755	2,829	2,969	864322
Acinetobacter colistiniresistens	GCA_000369765	3,942	4,039	1220522
Acinetobacter cumulans	GCA_003024525	3,300	3,518	1030283
Acinetobacter defluvii	GCA_001704615	3,466	3,712	1054638
Acinetobacter equi str. 114	GCA_001307195	2,707	2,829	846882

Table 3.1: Continued

Organism	**Assession No.**	**Coding Genes**	**Gene Transcript**	**No. of Codons analyzed**
Acinetobacter gandensis	*GCA_001678755*	2,888	3,044	886824
Acinetobacter genomosp.33YU	GCA_001990735	4,005	4,076	1246392
Acinetobacter gerneri	GCA_000368565	4,254	4,343	1264746
Acinetobacter guillouiae	GCA_000368145	4,613	4,710	1366166
Acinetobacter gyllenbergii	GCA_001682515	3,916	3,987	1214544
Acinetobacter haemolyticus	GCA_000164055	3,491	3,560	982156
Acinetobacter halotolerans	GCA_004208515	3,038	3,164	951296
Acinetobacter idrijaensis	GCA_000761495	3,659	3,724	1016520
Acinetobacter indicus	GCA_000488255	2,998	3,104	914956
Acinetobacter johnsonii	GCA_000368805	3,318	3,424	1013368

Table 3.1: Continued

Organism	**Assession No.**	**Coding Genes**	**Gene Transcript**	**No. of Codons analyzed**
Acinetobacter junii	GCA_003939335	3,277	3,572	1017381
Acinetobacter kookii	GCA_900096895	2,877	2,956	878452
Acinetobacter kyonggiensis	GCA_900107285	3,518	3,597	1043190
Acinetobacter lactucae	GCA_000399705	3,636	3,728	1149609
Acinetobacter larvae	GCA_001704115	3,148	3,303	1034467
Acinetobacter lwoffii	GCA_000369125	3,503	3,592	1008223
Acinetobacter marinus	GCA_900096915	2,746	2,809	869129
Acinetobacter nectaris	GCA_000488215	2,541	2,617	777104
Acinetobacter nosocomialis	GCA_002137075	3,802	4,016	1163295
Acinetobacter oleivorans	GCA_000196795	3,874	3,963	1205844

Table 3.1: Continued

Organism	**Assession No.**	**Coding Genes**	**Gene Transcript**	**No. of Codons analyzed**
Acinetobacter parvus	GCA_000368025	2,789	2,877	823616
Acinetobacter piscicola	GCA_004152775	3,542	3,719	1077745
Acinetobacter pittii	GCA_000399685	3,520	3606	1112327
Acinetobacter populi	GCA_002174125	3,292	3,420	1066499
Acinetobacter pragensis	GCA_001605895	3,393	3,593	1031412
Acinetobacter proteolyticus	GCA_001753605	3,979	4,137	1260095
Acinetobacter puyangensis	GCA_900096995	3,441	3,504	1096249
Acinetobacter qingfengensis	GCA_001753595	2,826	2,935	907802
Acinetobacter radioresistens	GCA_000368905	2,950	3,028	908795
Acinetobacter rudis	GCA_000413895	3,621	3,706	1135160

Table 3.1: Continued

Organism	**Assession No.**	**Coding Genes**	**Gene Transcript**	**No. of Codons analyzed**
Acinetobacter schindleri	GCA_000368625	3,189	3,273	958937
Acinetobacter seifertii	GCA_000368065	4,051	4,135	1080249
Acinetobacter soli	GCA_001953195	3,309	3,452	1060467
Acinetobacter tandoii	GCA_000400735	3,934	4,013	1172950
Acinetobacter tjernbergiae	GCA_000488175	3,455	3,523	1047791
Acinetobacter towneri	GCA_000368785	2,792	2,853	820258
Acinetobacter ursingii	GCA_000368845	3,559	3,650	1094467
Acinetobacter variabilis	GCA_000369625	3,348	3,438	987288
Acinetobacter venetianus	GCA_001575095	3,173	3,321	1004359
Acinetobacter wuhouensis	GCA_001696605	3,620	3,819	1105453

Table 3.1: Continued

Organism	Assession No.	Coding Genes	Gene Transcript	No. of Codons analyzed
Acinetobacter baumannii	GCA_000580515	4,425	4,572	1247286

3.2 Calculation of compositional parameters:

The frequency of several genomic compositional parameters such as adenine, guanine, cytosine, and thymine was calculated using the CodonW (http://codonw.sourceforge.net) program (Xiao et al., 2019). Total percentages of adenine (A) and thymine (T) versus guanine (G) and cytosine (C) nucleotides content, as well as the makeup of C and G nucleotides at the first (GC1), second(GC2), and third (GC3) codon locations of all the genomes, were also determined using codonW (Xiao et al., 2019).

3.3. Codon Usage Analysis

3.3.1 RSCU Evaluation

Synonymous codons are different triplet sequences of DNA or RNA nucleotides that encode the same amino acid in a protein. Relative Synonymous Codon Usage (RSCU) is a method for quantifying the uneven utilization of synonymous codons. It is expressed as the ratio of the observed frequency of codons to the expected frequency of those codons (Sharp & Li, 1986). CodonW program has been employed to determine RSCU values for the 56 different species of *Acinetoacter* (Dos Reis, 2003). RSCU values have been calculated using the following formula:

$$\text{RSCU}=\frac{\text{Observed frequency of a codon}}{\text{Expected frequencyof the codon}}$$

When the observed RSCU value equals the expected value, there is no codon bias present. Consequently, an RSCU greater than 1.0 indicates a preference for the actual high-frequency codon, while an RSCU less than 1.0 signifies the utilization of the actual low-frequency codon (Dos Reis, 2003; Nambou & Anakpa, 2020).

3.3.2 PR2-plot analysis:

Parity plot analysis is performed to determine the dominant force behind the prevalent codon usage and genomic patterns. In an ideal scenario where A equals T and C equals G at the center, the axis value would be 0.5. When the bias value falls below 0.5, it indicates a preference for pyrimidines over purines bases (Andargie & Congyi, 2022). For this analysis AT-bias (A3s/ (A3s+T3s) is plotted against GC-bias (G3s/ (G3s+C3s). Points close to the center of the plot (A = T, G = C) reflect balanced usage, while deviations from the center indicate preferences for either A/T or G/C at the third codon position (Gencer et al., 2024).

3.3.3 ENC Analysis:

The Effective Number of Codons (ENC) is a measure of codon usage bias, where a higher ENC value indicates lower codon usage bias and vice versa. ENC values typically range between 21 and 61. Typically, an ENC value below 35 suggests pronounced codon bias, reflecting selection for specific codons optimizing translational efficiency or accuracy (Chakraborty et al., 2019).Conversely, ENC values above 35 indicate less pronounced bias, where mutational pressure or genetic drift may play a more dominant role in shaping codon usage (Arora et al., 2024; Chakraborty et al., 2019).

To determine the degree of codon use bias, the Effective Number of Codons (ENC) method was used (Wright, 1990). The following formula was used to deduce the ENC values of relevant bacterial genomes:

$$ENC = 2 + \frac{9}{F2} + \frac{1}{F3} + \frac{5}{F4} + \frac{3}{F6}$$

Where F is the likelihood that two randomly chosen codons for an amino acid would be similar, and Fk (k = 2, 3, 4 or 6) denotes the average value of Fk related to k-fold degenerate amino acids. The ENC values vary from 21 to 61 and higher values indicates less bias (Chakraborty et al., 2019). The ENC values of the *Acinetoacter* genomes was estimated with CodonW.

To examine the effect of translational selection on codon usage bias, ENC-plot analysis was used. The possible importance of natural selection in influencing codon usage is shown by departures from the standard curve (Shen et al., 2020). To construct the ENC-plot, the GC3 values were employed as the horizontal axis, while the ENC values were designated as the vertical axis. A two-dimensional scatter plot was generated according to this methodology (Wright, 1990). Plot points clustering near or away from the expected ENC curve illustrate the degree to which natural selection, mutational bias, or other factors influence codon usage patterns within genomes (Wright, 1990).

3.3.4 Neutrality Plot Analysis:

Mutational pressure refers to the random occurrence of mutations influencing nucleotide sequences, while translational selection involves preferential use of codons optimizing protein synthesis efficiency and accuracy (Shen et al., 2020).To comprehend the impact of mutational pressure vs. natural selection on the relevant bacterial genomes, the neutrality plot analyses on 56 *Acinetoacter* species were performed in which frequency of GC content at third codon position (GC3) values were plotted against GC content at first and second codon position (GC12) values. Slope of the graph is indicative of magnitude of effect of neutrality i.e. mutational pressure. Value of slope close to zero suggests dominant impact of mutational pressure while close to one connote the impact of natural

selection in shaping the codon usage patterns and compositional parameters (Jia et al., 2015).

3.3.5 Assessment of Translation Selection

Assessment of Translation Selection (P2 metric), which gauges the interaction between a codon and its corresponding anticodon, was applied to quantify translational selection (Gouy & Gautier, 1982). P2 was calculated as:

$$P2=\frac{WWC+SSU}{WWY+SSY}$$

Where W stands for the prevalence of Adenine (A) or Thymine (T), S for Cytosine (C) or Guanine (G), and Y for either Cytosine (C) or Thymine (T). P2 values larger than 0.50 indicate that natural selection had a significant influence on translation (Gatherer & McEwan, 1997).

3.3.6 Analysis of Codon Adaptation Index (CAI):

Codon adaptive index is a measure of synonymous codon usage bias in genes of an organism. Highly expressed genes (PHX) typically exhibit higher CAI values, indicating their codon usage is optimized for efficient translation, while lowly expressed genes (PLX) tend to have lower CAI values, suggesting less optimized codon usage. Therefore, this numerical metric that varies between 0 to 1 where values approaching 1 indicate a strong bias towards the use of highly preferred codons (PHX) and vice versa (Sharp & Li, 1986). DAMBE software (http://dambe.bio.uottawa.ca/DAMBE/dambe.aspx) has been used in this investigation to estimate the CAI values for the all the *Acinetoacter* genomes with reference to highly expressed ribosomal genes (Xia, 2018).

The Codon Adaptation Index (CAI) for a genome is determined by calculating the geometric mean of the relative adaptiveness (W) for all the codons within the genome. The relative adaptiveness (W_a) of a codon (b) coding for an amino acid is computed as the ratio of the occurrence of a codon to the maximum occurrence for amino acid (Xia, 2018). In equation it can be expressed as:

$$W_a = X_{ab} / X_{amax}$$

Where X_{ab} is the number of codons (b) in the gene and represents the value for the th codon in the gene. In practical computer calculations, CAI is expressed as follows:

$$CAI = exp \frac{1}{L} \sum_{K=1}^{L} Ln\mathrm{Wc(k)}$$

Where L is the number of codons in the gene, and $W_{c(k)}$ represents the value for the k-th codon in the gene. This formula is commonly used in bioinformatics to assess the similarity of codon usage in a gene to a reference set of highly expressed genes, providing insights into the potential expression level of the gene (Sharp et al., 1987).

3.3.7 Analysis of Relative Synonymous Codon Pair Usage and Codon Pair Score (RSCPU)

Relative Synonymous Codon Pair (RSCPU) analysis and Codon Pair Score (CPS) are computational tools used to evaluate the non-random usage of codon pairs within nucleotide sequences. RSCPU examines the frequency of adjacent codon pairs, providing

insights into potential translational efficiency and co-evolutionary relationships between codons (Kunec & Osterrieder, 2016).

The following formula has been used to determine the RSCPU of relevant bacterial genomes (Behura & Severson, 2012):

$$\text{RSCPU} = \frac{\text{Observed frequency of a codon pair}}{\text{Expected frequencyof the codon pair}}$$

On the other hand, CPS quantifies the bias in codon pair preferences, with higher scores indicating a greater preference for specific codon pairs. To determine whether codon pairings were overrepresented and underrepresented, codon pair scores were computed (Behura & Severson, 2012).

3.3.8 Estimation of Relative Abundance of Dinucleotides:

Dinucleotides are pairs of adjacent nucleotides within DNA or RNA sequences, forming fundamental units that often exhibit specific patterns or biases in their occurrence due to underlying genetic, evolutionary, or structural constraints. Using the method suggested by Kariin and Burge, the relative dinucleotide abundance in the genomes of *Acinetoacter* were determined. To determine overrepresented and underrepresented dinucleotides, odds ratios were computed (Kariin & Burge, 1995).

$$Pxy = \frac{fxy}{fxfy}$$

$P_{xy} = (f_{xy}/f_x f_y)$ use equation box

The measured frequencies of the X and Y nucleotides are given here as fx and fy, respectively. The terms fxy and fxfy stand for the observed and predicted xy dinucleotide frequencies, respectively. When the fxy value is less than 0.78, the dinucleotides are

underrepresented, and when it is larger than 1.25, the dinucleotides are overrepresented (Kunec & Osterrieder, 2016).

3.4. Amino acid Usage Analysis:

3.4.1 Estimation of L_sym and L_aa:

Lsym represents the number of synonymous codons in a sequence while L_aa represents the number of aminoacid in the protein sequence. Using CodonW, L_sym and L_aa were estimated to reflect the quantity of synonymous codons and the segment of amino acids, respectively (Patil et al., 2017).

3.4.2 Estimation of RAAU, GRAVY, and AROMO

Using the CodonW tool, RAAU, Aromo, and GRAVY were assessed. RAAU is a method for quantifying the uneven utilization of amino acids. It is expressed as the ratio of the observed frequency of amino acid to the expected frequency of same amino acid (Snellman & Colwell, 2004).

RAAU values can be calculated using following formula:

$$RAAU = \frac{frequency\ of\ aminoacid}{expected\ frequency\ of\ aminoacid\ (in\ case\ of\ uniform\ usage)}$$

GRAVY score represents the collective hydropathy values of all amino acids within a sequence, divided by the total number of residues. Hydropathy values typically range from -2.0 to +2.0, with positive values indicating protein hydrophobicity and negative values indicating hydrophilicity. From GRAVY, it is possible to calculate the average hydropathicity rating of a translated gene by the use of the scores of the singlet amino

acids that go into protein formation (Snellman & Colwell, 2004). The GRAVY was determined as follows:

$$\text{GRAVY}=[\frac{1}{N}\sum_{i=1}^{n} Ki]$$

N stands for the exact frequency of amino acids, while ki is regarded as i^{th} amino acid's hydrophobic index.

Aromaticity (AROMO) is determined by the frequency of aromatic amino acids like Trp, Tyr, and Phe in a given amino acid sequence. Both the overall GRAVY and AROMO values were computed utilizing the CodonW tool, available for download on SourceForge.net. A translated gene product's aromaticity is shown by the average aromatic score of each individual amino acid, which has been stated as follows:

$$\text{Aromo}=[\frac{1}{N}\sum_{i=1}^{n} Vi]$$

Where N is the total numerical value of amino acids, and Vi is either 0 or 1 depending on whether the amino acid is aromatic or not (Kyte & Doolittle, 1982).

3.4.3 Estimation of Individual frequency of amino acids:

Individual frequencies of the amino acids were also calculated with the help of codonW program. First, of all, the nucleotide sequences were converted to amino acid sequences with the help of biopython and then addressed on codonW for amino acid frequencies estimation (Sharma et al., 2023).

3.5. Statistical Analysis:

To support the findings from the acquired data, inferential statistics was applied. Correlations between different compositional parameters were evaluated by Spearman's

rank correlation analysis. (*) for p-values between 0.01 and 0.05 and (**) for p-values less than 0.01 (Song et al., 2017). All mathematical evaluations were performed using IBM SPSS Statistics 28.0.0.0 (https://www.ibm.com/spss).

3.6. Sequence alignment analysis and phylogenomic tree construction

The gyrB gene sequences were shortlisted manually from the downloaded genomes. Sequence alignment studies of gyrB genes were performed with the help of MULTALIN *(*Multiple *sequence alignment tool (*http://multalin.toulouse.inra.fr/multalin/*) website* (Mitchell, 1993) a multiple sequence alignment tool. The process commences with the hierarchical clustering of sequences utilizing the provided scores. Subsequently, clusters of aligned sequences undergo pairwise comparisons to achieve a comprehensive multiple alignment. Following this, MULTALIN constructs a hierarchical clustering of sequences by incorporating scores from all pairwise comparisons using BLOSUM62 within the multiple alignments, serving as a measure of sequence similarity. Furthermore, the Clustal Omega program was used to construct the phylogenomic tree from gyrB gene sequences (Sievers & Higgins, 2014).

3.7. Whole Genome Sequence (WGS) Analysis:

3.7.1 Raw materials:

Nutrient broth, DNA extraction buffer, and glass wares like test tubes and flasks required for culture maintenance and DNA extraction were provided by the School of Bioengineering and Biosciences, Lovely Professional University, Punjab, India. In-house laboratory equipment including laminar flow, incubator, autoclave, and refrigerator were used from Biotechnology lab, Block 57(A) room no. - 401, Lovely Professional University. Whole genome sequencing was performed on Illumina 2*150 (Sadeghi 2015) from Eurofins Scientific, Bangalore India.

3.7.2 Culture Collection, maintenance, and transport:

Bacterial species devoid of contaminants and in a viable state have been procured from the National Centre for Cell Science (NCMR), Pune, and the Microbial Type Culture Collection and Gene Bank (Chandigarh) for subsequent whole genome sequencing and were grown on a nutrient medium. Fresh tubes were cultured by inoculating the dissolved samples with the help of inoculating wire. The tubes for *A. baumannii* and *A. balyii* were incubated at 37 °C and 30 °C respectively. An ice pack box with dry ice was used for transportation of samples for WGS. The plates were subcultured and stored at -40°C for future studies (Fernando et al. 2016).

3.7.3 Genomic DNA extraction, analysis and WGS

Bacterial cells were lysed in a suitable lysis buffer. Following lysis, DNA purification from cellular components has been achieved through phenol-chloroform extraction method. In order to aid in the detachment of lipids and cellular debris, a 25:24:1 combination of phenol, chloroform, and isoamyl alcohol was added. This facilitated their partitioning, with isolated DNA staying in the aqueous phase and lipids and debris going into the organic phase. The purified DNA in the aqueous phase was moved to a separate tube for further examination following centrifugation (Sadeghi 2015). Subsequently, the extracted DNA was sent to Euro fins Scientific (Bangalore, India) for genome sequence analysis.

Using the Sanger sequencing approach, the extracted DNA samples were identified based on molecular identification by focusing on the bacterial 16S region. PCR was used to amplify the bacterial 16S region fragment. On an agarose gel, a single distinct PCR amplicon band was seen. Contaminants were eliminated by purifying the PCR amplicon. PCR amplicons' DNA sequencing reaction was performed using a particular primer (Sadeghi 2015).

For samples 1425 and 9822, WGS was carried out utilizing the Illumina platform and 2*150 bp chemistry. Using Trimmomatic v0.39 (Bolger et al., 2014), the raw data of samples 1425 and 9822 was processed to eliminate adaptor sequences, ambiguous reads (readings with unknown nucleotides "N" larger than 5%), and low-quality sequences (reads with greater than 10% quality threshold (QV) < 25 phred score). Using BWA MEM (Version 0.7.1.7) (Li and Durbin 2009), the high-quality readings of samples 1425 and 9822 were aligned to the reference. With Samtools mpileup (Li et al., 2009), the consensus sequences were retrieved.

3.7.4 Genes and Variant Annotation

GFF3-formatted reference genome annotation files were obtained from NCBI. Gene coordinates from the reference genome were utilized to derive gene sequences from consensus sequences using Bedtools (Quinlan and Hall 2010). The annotations for the genes in the samples were obtained using the reference genome GFF3 file. At least 10% of ambiguous nucleotides in a gene were eliminated.
The sorted BAM file of the mappings was used to find SNPs and InDels using the mileup utility of Samtools (V 0.1.1.18) (Li et al., 2009). Based on a minimum read depth of 15 and a quality criterion of 25, the variables were filtered. The bedtools interact tool was used to annotate the detected variants (Quinlan and Hall 2010).

The Bacterial and Viral Bioinformatics Resource Centre (BV-BRC) facilitated the investigation of bacterial genomes by combining extensive data and analytic tools with essential pathogen information offering open-source tools for genomic annotation and data analysis. *A. baumannii* 1425 and *A. baylyi* 9822 assembled genome sequences were also submitted to PATRIC (Gillespie et al., 2011; Wattam et al., 2017) for subsystem analysis and annotation of proteins and functional genes.

3.7.5 Determination of VRGs and ARGs

The virulence factor database (VFDB) analyzer was used to identify genes linked to virulence. VFDB is a comprehensive and integrated online resource for gathering data regarding the virulence factors of bacterial pathogens. VFanalyzer initiates the formation of orthologous groups within the target genome and conducts preliminary analyses of reference genomes sourced from VFDB. To accurately pinpoint potential atypical or strain-specific virulence factors, extensive sequence similarity searches are conducted across VFDB's hierarchical pre-built datasets. Moreover, employing a context-based data refinement process, VFanalyzer achieves reasonably high specificity and sensitivity in identifying virulence factors encoded by gene clusters, eliminating the need for manual curation (Chen et al., 2016).

ResFinder finds acquired genes that mediate antibiotic resistance in bacteria whole or partial DNA sequence**.** With the use of the online tool Resfinder, antibiotic resistance genes were predicted (Florensa et al., 2022).

3.7.6 Codon and amino acid Usage analysis of VRGs and ARGs

Codon and amino acid usage analysis of Virulence resistance genes (VRGs) and Antibiotic resistance genes (ARGs) were conducted using methods similar to those described for *Acinetobacter* genome in session 3.3 and 3.4.

3.7.7 Phylogenetic Analysis of VRGs and ARGs

The gene sequences of VRGS and ARGS were shortlisted manually from the WGS data in FASTA format. Phylogenetic analysis of the prepared sequences were conducted with the help of the Molecular Evolutionary Genetics Analysis Version 11 (Mega11) software (Tamura et al., 2021).

3.7.8 Protein Interaction Network Analysis of VRGs and ARGs

Protein Interaction Network Analysis of VRGs and ARGs was conducted with the help of String application (version 12.0). String is a database of anticipated and known protein-protein interactions. Gene sequences of VRGs and ARGs were uploaded as input to assess gene-set enrichment analysis and visualize protein interaction networks (Szklarczyk et al., 2019).

CHAPTER 4: RESULTS AND DISCUISSIONS

4.1 Analysis of GC composition of Genus *Acinetoacter*

The nucleotide composition analysis of *Acinetoacter* species revealed a notable variation in GC content, which is pivotal for understanding their genetic diversity, evolutionary dynamics, and pathogenicity. The observed GC content ranged from 35.71% in *Acinetoacter equi* to 46.21% in *Acinetoacter* indicus **(Table 4.1)**. The *Acinetoacter baumannii* complex (namely *Acinetoacter* calcoaceticus, *Acinetoacter baumannii*, *Acinetoacter lactucae*, *Acinetoacter nosocomialis*, *Acinetoacter oleivorans*, *Acinetoacter pittii* and *Acinetoacter seifertii*) are particularly noteworthy due to their clinical significance, (Dahal et al., 2023) showed an average GC content of 39%. This average is consistent with findings from other studies (Almeida et al., 2021; Hershberg & Petrov, 2009), which report a typical GC content around 39.6% for the genus, indicating a relatively stable genomic characteristic across various *Acinetoacter* species. The GC content in these species is crucial as it influence the stability of the genome and the functionality of genes related to virulence and antibiotic resistance (Salto et al., 2018). The biotechnologically significant non-pathogenic species *A. baylyi* (Suárez et al., 2020) exhibited a GC content of 40.99%. In comparison, other species within the *Acinetoacter* genus, namely *Acinetoacter gyllenbergii, Acinetoacter halotolerans,* and *Acinetoacter idrijaensis*, which are also non-pathogenic, showed GC percentages of 41.56%, 40.64%, and 43.89%, respectively **(Table 4.1).** Therefore, it is clear that the pathogenic ACB complex have higher AT content then non-pathogenic species. GC-rich genome is energetically disadvantageous for pathogenic microbes as AT-rich metabolites such as ATP prevail in majority within human hosts because of low cost of synthesis (Dietel et al., 2019). The easy availability of A/T rich metabolites also aides in the subsequent replication by the invading species aiding in faster replication and ease in nutrient availability from the host environment (Dietel et al., 2019; Sharma et al., 2023).

Additionally, the uniform distribution of nucleotides at the third codon positions within the *Acinetoacter baumannii* complex suggests a level of evolutionary conservation that

facilitate the maintenance of essential protein functions **(Figure 4.1).** This finding aligns with the concept of codon usage bias, where certain codons are preferred over others, potentially influencing translational efficiency and protein folding (Quax et al., 2015). The conservation observed in *Acinetoacter baumannii* complex is indicative of their evolutionary strategies, particularly in the context of horizontal gene transfer (HGT), which is prevalent in this genus and plays a significant role in the dissemination of pathogenicity (metabolic adaptation, biofilm formation and acquiring of virulence genes) and antibiotic resistance (Ayoub Moubareck & Hammoudi Halat, 2020; Da Silva & Domingues, 2016; Gedefie et al., 2021).

Table 4.1: Genomic composition and Codon Usage analysis of whole genus *Acinetobacter*

Organism	**GC12 %**	**GC %**	**ENC**	**P2**	**CAI**	**L_sym**	**L_aa**	**Gravy**	**Aromo**
A. albensis	45.02	39.47	44.44	0.45	0.62	301.96	313.93	-0.10	0.09
A. apis	45.17	39.08	43.58	0.23	0.66	312.30	323.61	-0.11	0.09
A. baumannii	44.99	39.51	45.31	0.45	0.55	281.28	291.88	-0.13	0.09
A. baylyi	45.82	41.00	46.70	0.57	0.59	307.71	319.60	-0.10	0.09
A. beijerinckii	44.69	38.82	44.26	0.44	0.59	299.17	310.59	-0.12	0.09
A. bereziniae	44.03	38.75	45.06	0.44	0.59	279.20	289.87	-0.14	0.09
A. bohemicus	45.11	40.31	44.93	0.45	0.55	295.26	306.85	-0.10	0.09
A. boissieri	44.73	38.6	44.3	0.4	0.6	304.9	316.2	-0.11	0.09

Table 4.1: Continued

Organism	**GC12 %**	**GC %**	**ENC**	**P2**	**CAI**	**L_sym**	**L_aa**	**Gravy**	**Aromo**
A. bouvetii	46.96	45.98	46.12	0.48	0.54	295.47	307.41	-0.09	0.09
A. brisouii	46.58	42.51	46.29	0.47	0.54	294.52	306.08	-0.10	0.09
A. calcoaceticus	45.12	39.35	45.34	0.39	0.57	299.95	311.36	-0.10	0.09
A. celticus	45.26	40.26	45.16	0.45	0.58	292.85	304.63	-0.11	0.09
A. colistiniresistens	45.63	41.91	46.92	0.47	0.52	298.06	309.57	-0.12	0.09
A. cumulans	45.83	41.17	45.05	0.41	0.54	299.40	311.21	-0.11	0.09
A. defluvii	44.45	39.01	43.65	0.39	0.59	292.06	303.28	-0.15	0.09
A. equi	43.69	35.71	39.51	0.41	0.62	300.49	311.85	-0.10	0.09
A. gandensis	45.73	40.62	44.68	0.46	0.57	294.63	306.39	-0.11	0.09
A. genomosp. 33YU	44.96	39.30	45.15	0.45	0.58	300.42	311.78	-0.13	0.09
A. gerneri	43.87	38.47	44.78	0.44	0.57	288.41	299.34	-0.17	0.09
A. guillouiae	44.02	38.80	45.20	0.44	0.57	285.59	296.38	-0.13	0.09

Table 4.1: Continued

Organism	**GC12 %**	**GC %**	**ENC**	**P2**	**CAI**	**L_sym**	**L_aa**	**Gravy**	**Aromo**
A. gyllenbergii	45.40	41.5	46.5	0.4	0.4	298.0	309.4	-0.10	0.09
A. haemolyticus	44.72	39.73	45.54	0.45	0.57	276.05	286.86	-0.12	0.09
A. halotolerans	45.50	40.65	46.04	0.46	0.58	302.07	313.80	-0.11	0.09
A. idrijaensis	46.50	43.90	46.71	0.47	0.53	280.31	291.37	-0.16	0.09
A. indicus	47.69	46.21	43.80	0.48	0.50	293.31	304.90	-0.14	0.09
A. johnsonii	45.92	42.21	46.79	0.47	0.52	293.04	304.69	-0.10	0.09
A. junii	45.02	39.54	45.00	0.45	0.57	299.55	310.99	-0.14	0.09
A. kookii	46.42	43.96	46.46	0.48	0.57	293.06	304.65	-0.12	0.09
A. kyonggiensis	44.72	39.78	44.79	0.45	0.61	286.70	297.91	-0.12	0.09
A. lactucae	45.29	39.46	45.14	0.45	0.57	304.08	315.61	-0.11	0.09
A. larvae	46.44	42.21	46.71	0.47	0.59	315.73	327.61	-0.11	0.09
A. lwoffii	46.36	43.55	46.59	0.47	0.52	277.59	288.72	-0.15	0.09

Table 4.1: Continued

Organism	**GC12 %**	**GC %**	**ENC**	**P2**	**CAI**	**L_sym**	**L_aa**	**Gravy**	**Aromo**
A. marinus	46.84	44.13	46.90	0.48	0.62	303.86	315.97	-0.14	0.09
A. nectaris	44.22	37.30	42.96	0.43	0.65	295.53	306.40	-0.13	0.09
A. nosocomialis	45.15	39.3	45.2	0.4	0.5	294.9	306.1	-0.12	0.09
A. oleivorans	45.13	39.29	45.20	0.45	0.57	298.93	310.27	-0.10	0.09
A. parvus	45.81	42.24	46.66	0.47	0.57	283.49	294.32	-0.16	0.09
A. piscicola	44.57	38.93	43.13	0.44	0.58	292.83	304.14	-0.14	0.09
A. pittii	45.36	39.49	45.08	0.45	0.58	304.04	315.63	-0.11	0.09
A. populi	45.61	40.97	45.79	0.46	0.61	311.89	323.36	-0.12	0.09
A. pragensis	46.72	45.11	46.95	0.48	0.54	291.47	303.25	-0.10	0.09
A. proteolyticus	45.59	41.76	46.75	0.06	0.55	304.40	316.01	-0.12	0.09
A. puyangensis	45.51	41.01	46.10	0.46	0.66	307.10	318.42	-0.12	0.09
A. qingfengensis	45.05	39.02	44.62	0.45	0.61	308.84	320.46	-0.13	0.09

Table 4.1: Continued

Organism	**GC12 %**	**GC %**	**ENC**	**P2**	**CAI**	**L_sym**	**L_aa**	**Gravy**	**Aromo**
A. radioresistens	46.85	42.69	47.93	0.47	0.58	295.93	307.48	-0.13	0.09
A. rudis	45.28	39.85	45.59	0.45	0.59	302.74	314.50	-0.10	0.09
A. schindleri	46.52	43.13	46.35	0.47	0.51	288.95	300.27	-0.13	0.09
A. seifertii	45.02	39.24	44.96	0.45	0.56	287.61	298.58	-0.12	0.09
A. soli	46.78	43.5	48.4	0.4	0.5	307.4	319.4	-0.12	0.09
A. tandoii	45.36	40.75	46.05	0.46	0.52	287.29	298.53	-0.14	0.09
A. tjernbergiae	44.69	39.16	44.52	0.44	0.59	292.60	303.68	-0.13	0.09
A. towneri	45.99	41.84	44.56	0.47	0.55	284.37	295.56	-0.14	0.09
A. ursingii	45.19	40.52	46.35	0.46	0.57	295.70	307.13	-0.15	0.09
A. variabilis	46.40	42.98	46.47	0.47	0.51	283.11	294.42	-0.15	0.09
A. venetianus	45.31	39.68	44.83	0.45	0.59	304.06	315.83	-0.12	0.09
A. wuhouensis	44.33	38.93	43.93	0.44	0.57	293.17	304.37	-0.15	0.09

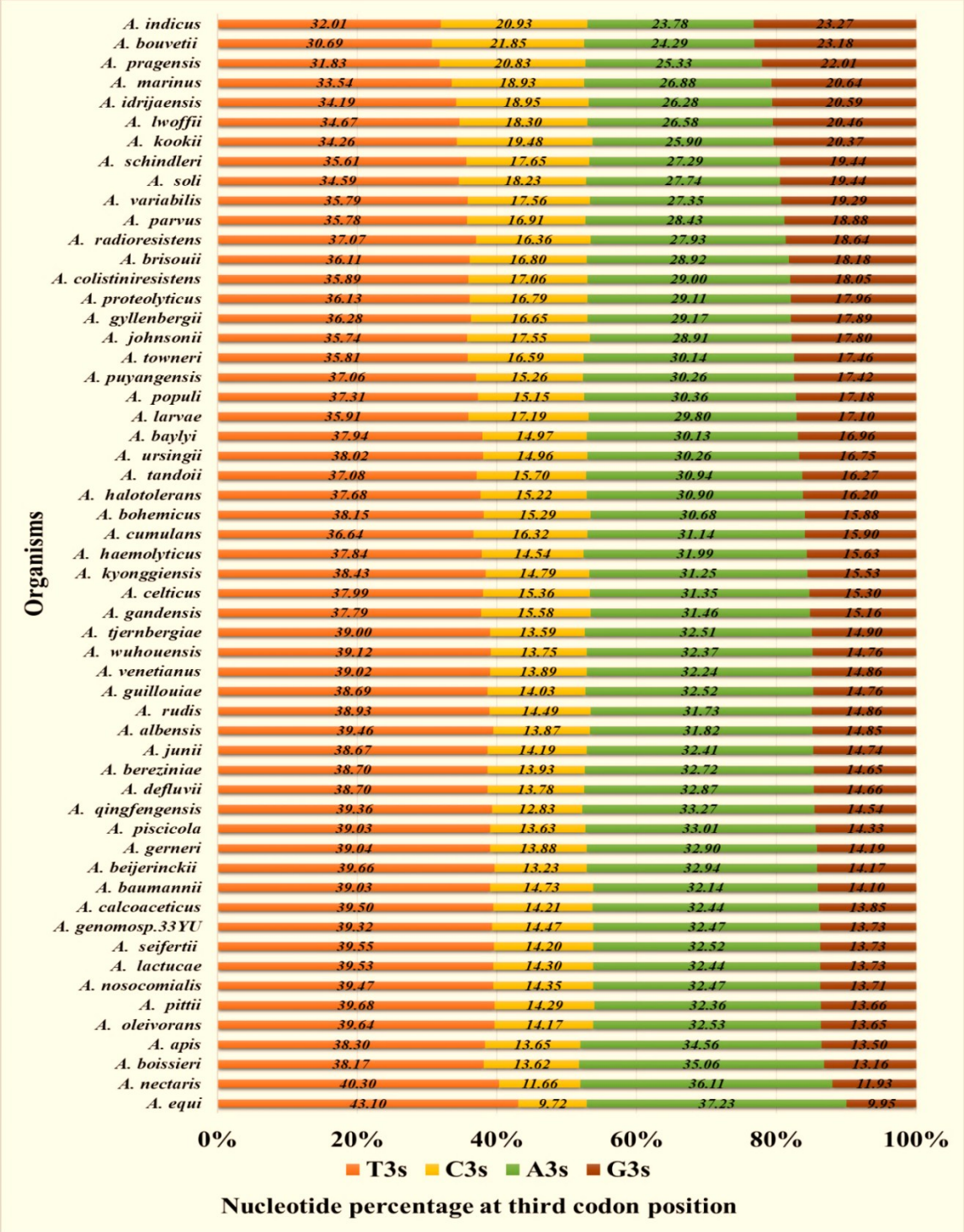

Figure 4.1: Nucleotide composition at third codon position of all the species under investigation.

4.2 Insights from preferred and optimal codons

The total count of preferred codons (those with Relative Synonymous Codon Usage, RSCU > 1) varied significantly among different species. For instance, *A. boissierii* exhibited the lowest count at 23 preferred codons, whereas both *A. variabilis* and *A. pragensis* had the highest count at 30 preferred codons each **(Table 4.2).** A notable trend observed across the majority of species is the preference for codons enriched with A and T, particularly those ending in A or T. Additionally, the significant negative correlation between GC composition and the two main axes of RSCU data **(Table 4.3)** underscores the impact of compositional constraints on the majority of bacterial genomes. These findings suggested that the composition of the genomes impart a substantial influence in determining the possibility of preferred and avoided codons (Plotkin & Kudla, 2011).

Within the *Acinetoacter baumannii* complex, all members exhibited a striking preference (>90%) for codons ending in A or T, indicating a conserved evolutionary trait within this pathogenic group. This high preference is particularly noteworthy in pathogenic species like A. *baumannii*, *A. junii*, and *A. bereziniae*, where the dominance of A/T-rich codons may be advantageous for rapid adaptation and virulence in clinical settings (Lyons et al., 2023). In contrast, non-pathogenic species such as *A. baylyi, A. gyllenbergii*, and *A. idrijaensis* showed a comparatively less pronounced preference (<85%) for A or T ending codons **(Table 4.2).** This variability in codon usage bias among non-pathogenic species reflect differences in ecological strategies, metabolic capabilities and evolutionary histories that do not necessitate high levels of A/T bias for fitness as required by pathogenic species (Sharma et al., 2023).

The codons with the highest occurrence, or the ones with the highest RSCU values, varied from 2.29 in *Acinetoacter pragensis* to 3.65 in *Acinetoacter piscicola*. All of these exhibited a preference for the CGT (Arg) codon. The preference for CGT codon is result of selective pressures that enhance the efficiency of protein synthesis and the stability of mRNA in the host environment. (Nouaille et al., 2017) as this genus is known for its genetic plasticity and ability to adapt rapidly to changing environments, such as antibiotic

pressures (Lin, 2014). Specifically, with regards to the leucine amino acid, TTA emerged as the most favored codon among all members. This preference aligns with the fact that TTA is the most abundant AT-rich codon encoding for leucine across AT rich genomes of *Acinetobacter*, lending it a logical basis (Hershberg & Petrov, 2009).

Moreover, we also noticed the preference for at least one histidine codon by all the members of the genus. The preference for at least one histidine codon across all *Acinetoacter* members can be attributed to interactions involving infection and immunity with the host. Recently, it has been demonstrated that *A. baumannii* infection relies on histidine catabolism (Dib et al., 2023; Ren & Palmer, 2023). The conserved Hut system in pathogenic *Acinetoacter* species converts histidine into glutamate, a crucial nitrogen source during infection within the host's body. This system is also connected to biofilm development, contributing to their survival within the host. (Dib et al., 2023; Ren & Palmer, 2023).

Optimal codons are those favoured by highly expressed genes over their lowly expressed counterparts. These codons are identified by positive RSCU values calculated as RSCUmeanPHX – RSCUmeanPLX (Lyons et al., 2023). The total number of optimal codons varied from 21 in *A. beijerincki* to 29 in *A. lwoffii.* However, in the case of all *Acinetoacter* species, a clear predilection for AT-rich optimal codons (<65%) was evident. **(Table 4.4)**. However, we did not notice any significant variation in optimal codon choice between the ACB complex and the other members of the genus. This trend of favoring AT-rich optimal codons was consistent throughout the genus which suggest a conserved strategy among these bacteria in utilizing AT-rich codons for optimal gene expression, irrespective of pathogenicity (Bentele et al., 2013). Moreover, our findings **(Table 4.5)** align with previous studies indicating a negative correlation between genomic GC content and Codon Adaptation Index (CAI) in related bacterial species (Sharp & Li, 1987). This negative correlation further supports our observation that AT-rich codons are favored, as lower GC content tends to correlate with increased usage of AT-rich codons to maintain high translational efficiency.

Table 4.2: Total number of preferred codons along with AT or GC nature of all the *Acinetobacter* species.

Species	**Total preferred codons**	**AT rich**	**GC rich**	**A/T ending**	**G/C Ending**
A. albensis	27	18	9	23	4
A. apis	25	17	8	22	3
A. baumannii	25	19	6	24	1
A. baylyi	27	18	9	22	5
A. beijerincki	25	17	8	23	2
A. bereziniae	24	18	6	23	1
A. bochemius	26	18	8	23	3
A. bouvetii	27	13	14	16	11
A. brisouii	29	18	7	19	6
A. calcoacetius	27	22	5	25	2
A. celticus	28	18	10	23	5
A. colistiniresistens	28	17	11	22	6
A. cumulans	29	19	10	24	5
A. defulvii	26	19	7	24	2
A. equi	25	19	6	25	0
A. generi	24	18	6	23	1
A. genomosp.33YU	26	21	5	25	1
A. guillouiae	25	18	7	23	2
A. gyllenbergii	28	18	10	22	6
A. haemolyticus	25	18	7	23	2
A. halotolerans	26	18	8	23	3
A. idrijaenesis	28	15	13	19	9

Table 4.2: Continued

Species	**Total preferred codons**	**AT rich**	**GC rich**	**A/T ending**	**G/C Ending**
A. indicus	24	11	13	16	8
A. johnsonii	27	18	9	22	5
A. junnii	25	18	7	23	2
A. kokii	28	17	11	19	9
A. kyonggiensis	26	18	8	22	4
A. lactucae	26	19	7	25	1
A. larvae	26	17	9	21	5
A. lwoffii	28	14	14	18	10
A. marinus	27	15	12	18	9
A. nectaris	25	19	6	25	0
A. nosocomialis	26	19	7	25	1
A. oleivorans	27	19	8	23	2
A. parvus	29	17	12	22	7
A. piscicola	25	18	7	23	2
A. pittii	26	19	7	25	1
A. populi	27	17	10	22	5
A. pragensis	30	15	15	19	11
A. proteolyticus	28	18	10	22	6
A. puyangensis	25	16	10	21	5
A. qingfengensis	25	19	6	24	1
A. radioresistens	28	17	11	23	5
A. rudis	26	19	7	24	2
A. schindleri	29	16	13	22	7
A. seifertii	26	18	8	25	1
A. soil	27	17	10	21	6

Table 4.2: Continued

Species	**Total preferred codons**	**AT rich**	**GC rich**	**A/T ending**	**G/C Ending**
A. tandoii	27	18	9	23	4
A. tjernbergiae	24	18	6	23	1
A. towneri	27	17	10	21	6
A. ursingii	27	18	9	23	4
A. variabilis	30	22	8	22	8
A. venetianus	25	18	7	23	2
A. wuhouensis	25	18	7	23	2
A. boissierii	23	17	6	23	0
A. gandensis	28	17	11	24	4

Table 4.3: Correlation of RAAU and RSCU with ENC, CAI, Gravy and Aromo, G3s and GC content of all the *Acinetobacter* species

Organism		**ENC**	**GC3s**	**GC**	**L_aa**	**GRAVY**	**Aromo**	**CAI**
A. apis	RAAU(Axis1)	.045*	-.182**	-.330**	-.151**	-.799**	-.147**	.246**
	RAAU(Axis2)	.395**	.079**	-.567**	-.093**	.111**	.636**	-.165**
	RSCU(Axis1)	.466**	-.118**	-.475**	-.071**	0.01666	.247**	-.443**
	RSCU(Axis2)	-.383**	-.394**	-.084**	-.109**	-.133**	-.119**	.541**
A. albensis	RAAU(Axis1)	.045*	-.182**	-.330**	-.151**	-.799**	-.147**	.246**
	RAAU(Axis2)	.395**	.079**	-.567**	-.093**	.111**	.636**	-.165**
	RSCU(Axis1)	.466**	-.118**	-.475**	-.071**	0.01666	.247**	-.443**
	RSCU(Axis2)	-.383**	-.394**	-.084**	-.109**	-.133**	-.119**	.541**
A. baumannii	RAAU(Axis1)	0.00394	-.064**	-.156**	-.145**	-.820**	-.250**	.159**
	RAAU(Axis2)	.279**	0.00332	-.614**	-.220**	-.032*	.621**	-.210**
	RSCU(Axis1)	-.415**	.117**	.482**	.232**	.039*	-.281**	.570**
	RSCU(Axis2)	.528**	.554**	.272**	.092**	.104**	.083**	-.604**

Table 4.3: Continued

Organism		**ENC**	**GC3s**	**GC**	**L_aa**	**GRAVY**	**Aromo**	**CAI**
A. baylyi	RAAU(Axis1)	-0.0061	-.142**	-.181**	-.143**	-.787**	-.273**	.253**
	RAAU(Axis2)	.359**	0.00982	-.461**	-.169**	0.03186	.565**	-.050**
	RSCU(Axis1)	.363**	-.349**	-.567**	-.169**	-0.0008	.265**	-.140**
	RSCU(Axis2)	-.535**	-.482**	-.182**	-.115**	-.139**	-.124**	.741**
A. bereziniae	RAAU(Axis1)	.097**	-.178**	-.509**	-.233**	-.734**	.049**	.206**
	RAAU(Axis2)	-.299**	-.100**	.538**	.145**	-.284**	-.693**	.101**
	RSCU(Axis1)	-.396**	.130**	.479**	.168**	.064**	-.274**	.373**
	RSCU(Axis2)	.500**	.540**	.182**	.083**	.090**	.099**	-.644**
A.beijerinckii	RAAU(Axis1)	-.220**	.087**	.433**	.174**	.648**	-.090**	-0.0274
	RAAU(Axis2)	-.373**	-.117**	.402**	.089**	-.393**	-.685**	.342**
	RSCU(Axis1)	-.486**	.152**	.525**	.137**	0.02308	-.286**	.526**
	RSCU(Axis2)	.412**	.510**	.209**	.109**	.086**	.077**	-.614**

Table 4.3: Continued

Organism		**ENC**	**GC3s**	**GC**	**L_aa**	**GRAVY**	**Aromo**	**CAI**
A. bochemicus	RAAU(Axis1)	-.119**	.217**	.409**	.164**	.783**	.073**	-.153**
	RAAU(Axis2)	-.364**	-.113**	.465**	.123**	-.193**	-.667**	.265**
	RSCU(Axis1)	.433**	-.272**	-.543**	-.190**	-.054**	.251**	-.410**
	RSCU(Axis2)	.453**	.540**	.156**	.108**	.149**	.153**	-.700**
A. boissieri	RAAU(Axis1)	-0.0353	0.02876	.111**	-.078**	-.748**	-.431**	.155**
	RAAU(Axis2)	-.321**	-.109**	.370**	.164**	-.046*	-.444**	.271**
	RSCU(Axis1)	-.357**	.223**	.524**	.142**	-0.0305	-.262**	.402**
	RSCU(Axis2)	.200**	.288**	.104**	.145**	.150**	.048*	-.523**
A. bouvetti	RAAU(Axis1)	.042*	.126**	.118**	.118**	.798**	.334**	-.141**
	RAAU(Axis2)	.221**	.204**	-.143**	-.167**	0.01474	.522**	-.348**
	RSCU(Axis1)	-.188**	.872**	.636**	.177**	.085**	.048**	-.534**
	RSCU(Axis2)	-.365**	-0.0228	.204**	.103**	-0.0208	-.301**	.626**

Table 4.3: Continued

Organism		**ENC**	**GC3s**	**GC**	**L_aa**	**GRAVY**	**Aromo**	**CAI**
A. brisouii	RAAU(Axis1)	-0.0142	.109**	.113**	.132**	.783**	.340**	-.162**
	RAAU(Axis2)	-.409**	-.290**	.095**	.079**	-.054**	-.436**	.378**
	RSCU(Axis1)	-.182**	.596**	.614**	.247**	.079**	-.098**	-.040*
	RSCU(Axis2)	-.524**	-.527**	-.207**	-0.0309	-.120**	-.203**	.825**
A. calcoaceticus	RAAU(Axis1)	-.069**	-.112**	-.137**	-.135**	-.823**	-.288**	.238**
	RAAU(Axis2)	-.322**	-0.0033	.660**	.215**	.095**	-.598**	.192**
	RSCU(Axis1)	-.425**	.170**	.514**	.208**	-0.013	-.286**	.533**
	RSCU(Axis2)	-.545**	-.508**	-.197**	-.092**	-.117**	-.089**	.651**
A. celticus	RAAU(Axis1)	.061**	.153**	.159**	.137**	.807**	.343**	-.241**
	RAAU(Axis2)	.410**	.065**	-.551**	-.146**	-.100**	.558**	-.215**
	RSCU(Axis1)	-.510**	.066**	.437**	.130**	-0.0287	-.283**	.594**
	RSCU(Axis2)	-.296**	-.490**	-.170**	-.128**	-.132**	-.098**	.556**

Table 4.3: Continued

Organism		**ENC**	**GC3s**	**GC**	**L_aa**	**GRAVY**	**Aromo**	**CAI**
A. colistiniresistens	RAAU(Axis1)	-.163**	.119**	.270**	.151**	.714**	.093**	-.108**
	RAAU(Axis2)	-.317**	-.284**	.124**	.062**	-.376**	-.572**	.333**
	RSCU(Axis1)	-.412**	.398**	.575**	.258**	.076**	-.223**	.239**
	RSCU(Axis2)	-.444**	-.584**	-.244**	-.113**	-.158**	-.164**	.801**
A. cumulans	RAAU(Axis1)	-.101**	.171**	.349**	.117**	.812**	.107**	-.147**
	RAAU(Axis2)	-.442**	-.236**	.305**	.093**	-.149**	-.635**	.402**
	RSCU(Axis1)	-.525**	-0.0188	.374**	.122**	.050**	-.299**	.589**
	RSCU(Axis2)	.348**	.636**	.291**	.070**	.164**	.135**	-.681**
A. defulvii	RAAU(Axis1)	-.257**	.190**	.603**	.179**	.652**	-.181**	-.061**
	RAAU(Axis2)	.318**	.048**	-.436**	-.036*	.418**	.709**	-.231**
	RSCU(Axis1)	-.484**	.230**	.532**	.145**	.075**	-.276**	.459**
	RSCU(Axis2)	.566**	.675**	.196**	0.0252	0.02829	.124**	-.565**

Table 4.3: Continued

Organism		**ENC**	**GC3s**	**GC**	**L_aa**	**GRAVY**	**Aromo**	**CAI**
A. equi	RAAU(Axis1)	.249**	-.072**	-.395**	0.03249	.630**	.616**	-.323**
	RAAU(Axis2)	.353**	-.047*	-.734**	-.215**	-.406**	.399**	-.189**
	RSCU(Axis1)	-.380**	.191**	.599**	.106**	-0.0148	-.296**	.643**
	RSCU(Axis2)	-.370**	-.202**	.063**	.140**	.043*	-.156**	.091**
A. gandensis	RAAU(Axis1)	-.115**	-.203**	-.120**	-.095**	-.810**	-.401**	.266**
	RAAU(Axis2)	-.456**	-.120**	.521**	.146**	.166**	-.521**	.325**
	RSCU(Axis1)	.571**	.044*	-.399**	-.110**	0.00781	.308**	-.723**
	RSCU(Axis2)	-.370**	-.520**	-.162**	-.063**	-.120**	-.115**	.578**
A. genomos. 33YU	RAAU(Axis1)	-.032*	.110**	.381**	.198**	.806**	.071**	-.168**
	RAAU(Axis2)	.333**	0.01087	-.674**	-.144**	.059**	.720**	-.235**
	RSCU(Axis1)	-.484**	.084**	.477**	.183**	0.01989	-.281**	.607**
	RSCU(Axis2)	.551**	.703**	.372**	.082**	.123**	.071**	-.566**

Table 4.3: Continued

Organism		**ENC**	**GC3s**	**GC**	**L_aa**	**GRAVY**	**Aromo**	**CAI**
A. generi	RAAU(Axis1)	-.172**	.161**	.486**	.236**	.743**	-.038*	0.01022
	RAAU(Axis2)	-.326**	-.103**	.532**	.124**	-.278**	-.721**	.233**
	RSCU(Axis1)	-.471**	.094**	.517**	.189**	.106**	-.297**	.567**
	RSCU(Axis2)	-.473**	-.563**	-.199**	-.101**	-.080**	-.050**	.598**
A.guilouiae	RAAU(Axis1)	-.144**	.176**	.476**	.234**	.718**	-.051**	-.173**
	RAAU(Axis2)	-.325**	-.144**	.427**	.135**	-.330**	-.642**	.191**
	RSCU(Axis1)	.405**	-.195**	-.526**	-.220**	-.040**	.270**	-.370**
	RSCU(Axis2)	-.492**	-.524**	-.146**	-.113**	-.106**	-.149**	.663**
A. gyllenbergii	RAAU(Axis1)	0.01278	-.184**	-.219**	-.122**	-.826**	-.227**	.331**
	RAAU(Axis2)	-.396**	-.200**	.228**	.110**	-.065**	-.429**	.286**
	RSCU(Axis1)	.390**	-.388**	-.562**	-.275**	-.043**	.252**	-.282**
	RSCU(Axis2)	.515**	.569**	.199**	.096**	.129**	.140**	-.740**

Table 4.3: Continued

Organism		**ENC**	**GC3s**	**GC**	**L_aa**	**GRAVY**	**Aromo**	**CAI**
A. haemolyticus	RAAU(Axis1)	-.048**	.140**	.261**	.131**	.819**	.196**	-.154**
	RAAU(Axis2)	.325**	.036*	-.578**	-.227**	.078**	.641**	-.180**
	RSCU(Axis1)	-.398**	.170**	.519**	.262**	0.02846	-.272**	.408**
	RSCU(Axis2)	-.480**	-.513**	-.188**	-.109**	-.107**	-.107**	.733**
A. halotolerans	RAAU(Axis1)	0.01278	-.184**	-.219**	-.122**	-.826**	-.227**	.331**
	RAAU(Axis2)	-.396**	-.200**	.228**	.110**	-.065**	-.429**	.286**
	RSCU(Axis1)	.390**	-.388**	-.562**	-.275**	-.043**	.252**	-.282**
	RSCU(Axis2)	.515**	.569**	.199**	.096**	.129**	.140**	-.740**
A. idrijaensis	RAAU(Axis1)	-.110**	.170**	.340**	.199**	.825**	.150**	-.162**
	RAAU(Axis2)	-.341**	-.157**	.296**	.059**	-.101**	-.595**	.264**
	RSCU(Axis1)	-.062**	.796**	.682**	.275**	.168**	-0.0282	-.413**
	RSCU(Axis2)	.484**	.240**	-.063**	-.127**	-0.0107	.214**	-.736**

Table 4.3: Continued

Organism		ENC	GC3s	GC	L_aa	GRAVY	Aromo	CAI
A. indicus	RAAU(Axis1)	-.168**	.142**	.248**	.135**	.791**	.092**	-.061**
	RAAU(Axis2)	-.219**	-.457**	-.208**	0.00742	-.254**	-.474**	.497**
	RSCU(Axis1)	.327**	-.878**	-.714**	-.217**	-.192**	-.085**	.553**
	RSCU(Axis2)	.393**	.102**	-.101**	-.071**	-.060**	.255**	-.638**
A. johnsonii	RAAU(Axis1)	0.0196	-.217**	-.241**	-.131**	-.828**	-.299**	.230**
	RAAU(Axis2)	.403**	.196**	-.371**	-.145**	-0.0306	.538**	-.324**
	RSCU(Axis1)	.466**	-.078**	-.404**	-.134**	-0.02	.272**	-.537**
	RSCU(Axis2)	.435**	.678**	.312**	.100**	.144**	.142**	-.735**
A. junnii	RAAU(Axis1)	.222**	-.062**	-.484**	-.149**	-.739**	.065**	0.03148
	RAAU(Axis2)	.378**	.124**	-.486**	-.057**	.273**	.720**	-.303**
	RSCU(Axis1)	-.590**	-.178**	.305**	.115**	0.0313	-.294**	.720**
	RSCU(Axis2)	.230**	.715**	.524**	.058**	0.02773	-.046**	-.213**

Table 4.3: Continued

Organism		ENC	GC3s	GC	L_aa	GRAVY	Aromo	CAI
A. kookii	RAAU(Axis1)	-0.013	.166**	.213**	.122**	.817**	.242**	-.170**
	RAAU(Axis2)	.337**	.173**	-.337**	-.112**	0.00434	.604**	-.275**
	RSCU(Axis1)	.275**	.776**	.431**	.161**	.134**	.165**	-.706**
	RSCU(Axis2)	.520**	-.203**	-.443**	-.218**	-0.0329	.250**	-.485**
A. kyonggiensis	RAAU(Axis1)	.158**	-.212**	-.528**	-.172**	-.738**	.058**	.093**
	RAAU(Axis2)	-.313**	-.101**	.444**	.087**	-.301**	-.692**	.218**
	RSCU(Axis1)	-.358**	.311**	.563**	.203**	.122**	-.236**	.340**
	RSCU(Axis2)	-.472**	-.506**	-.141**	-.084**	-.138**	-.138**	.679**
A. lactucae	RAAU(Axis1)	-0.0204	-.101**	-.184**	-.158**	-.812**	-.236**	.221**
	RAAU(Axis2)	-.346**	-.048**	.565**	.190**	-0.0009	-.575**	.251**
	RSCU(Axis1)	.467**	-.112**	-.484**	-.178**	0.01304	.286**	-.596**
	RSCU(Axis2)	.513**	.578**	.294**	.123**	.116**	.083**	-.603**

Table 4.3: Continued

Organism		ENC	GC3s	GC	L_aa	GRAVY	Aromo	CAI
A. larvae	RAAU(Axis1)	.290**	.286**	.149**	0.00574	.198**	.213**	-.249**
	RAAU(Axis2)	-0.0247	.262**	.295**	.160**	.849**	.172**	-.171**
	RSCU(Axis1)	.239**	-.458**	-.483**	-.193**	-.132**	.174**	-.239**
	RSCU(Axis2)	-.375**	-.417**	-.199**	-.099**	-.186**	-.103**	.652**
A. lwoffii	RAAU(Axis1)	.146**	-.190**	-.410**	-.188**	-.757**	0.00878	.079**
	RAAU(Axis2)	.316**	.195**	-.231**	-.072**	.262**	.654**	-.357**
	RSCU(Axis1)	.125**	-.768**	-.691**	-.307**	-.188**	.061**	.360**
	RSCU(Axis2)	-.445**	-.309**	0.0243	.054**	-0.0292	-.241**	.752**
A. marinus	RAAU(Axis1)	.199**	-.199**	-.320**	-.119**	-.692**	-.087**	-.052**
	RAAU(Axis2)	-.337**	-.204**	.228**	.074**	-.335**	-.568**	.337**
	RSCU(Axis1)	-.333**	.529**	.476**	.239**	.075**	-.149**	.252**
	RSCU(Axis2)	.467**	.382**	0.01808	0.00135	.105**	.243**	-.717**

Table 4.3: Continued

Organism		**ENC**	**GC3s**	**GC**	**L_aa**	**GRAVY**	**Aromo**	**CAI**
A. nectaris	RAAU(Axis1)	-.091**	.129**	.184**	-.103**	-.721**	-.466**	.172**
	RAAU(Axis2)	.348**	0.03745	-.665**	-.190**	-.169**	.542**	-.180**
	RSCU(Axis1)	-.310**	.194**	.557**	.134**	-.069**	-.262**	.563**
	RSCU(Axis2)	.321**	.115**	-.093**	-.139**	-.068**	.096**	.102**
A. nosocomialis	RAAU(Axis1)	0.03119	-.066**	-.210**	-.176**	-.803**	-.212**	.168**
	RAAU(Axis2)	-.345**	-.048**	.608**	.190**	-0.0302	-.661**	.230**
	RSCU(Axis1)	-.515**	.073**	.468**	.199**	0.0171	-.296**	.622**
	RSCU(Axis2)	.475**	.637**	.347**	.102**	.121**	.055**	-.561**
A. oleivorans	RAAU(Axis1)	-.078**	-.122**	-.137**	-.139**	-.826**	-.295**	.263**
	RAAU(Axis2)	-.365**	-.056**	.601**	.225**	.080**	-.571**	.218**
	RSCU(Axis1)	.488**	-.091**	-.481**	-.199**	0.02561	.283**	-.584**
	RSCU(Axis2)	-.519**	-.523**	-.232**	-.119**	-.137**	-.093**	.624**

Table 4.3: Continued

Organism		**ENC**	**GC3s**	**GC**	**L_aa**	**GRAVY**	**Aromo**	**CAI**
A. parvus	RAAU(Axis1)	.303**	-0.0327	-.379**	-.168**	-.518**	.263**	-.086**
	RAAU(Axis2)	-.272**	-.185**	.045*	-0.0087	-.578**	-.591**	.334**
	RSCU(Axis1)	-.221**	.600**	.679**	.274**	.115**	-.191**	.065**
	RSCU(Axis2)	-.552**	-.610**	-.262**	-.045*	-.084**	-.208**	.794**
A. piscicola	RAAU(Axis1)	-.251**	.173**	.561**	.190**	.628**	-.196**	-0.0183
	RAAU(Axis2)	-.321**	-.122**	.354**	0.02402	-.413**	-.695**	.297**
	RSCU(Axis1)	.512**	-.098**	-.463**	-.147**	-.060**	.282**	-.563**
	RSCU(Axis2)	.279**	.435**	.110**	.116**	.155**	.103**	-.542**
A. pittii	RAAU(Axis1)	.051**	.124**	.187**	.171**	.822**	.269**	-.227**
	RAAU(Axis2)	.373**	.058**	-.573**	-.168**	-.053**	.580**	-.239**
	RSCU(Axis1)	-.496**	.124**	.494**	.184**	-0.0062	-.281**	.595**
	RSCU(Axis2)	.495**	.554**	.281**	.129**	.146**	.083**	-.608**

Table 4.3: Continued

Organism		**ENC**	**GC3s**	**GC**	**L_aa**	**GRAVY**	**Aromo**	**CAI**
A. populi	RAAU(Axis1)	-.208**	0.01416	.234**	.202**	.492**	0.01534	.044*
	RAAU(Axis2)	.300**	.250**	-.080**	-.040*	.588**	.519**	-.247**
	RSCU(Axis1)	.228**	-.513**	-.581**	-.179**	-.055**	.224**	-.121**
	RSCU(Axis2)	.515**	.481**	.139**	0.02913	.111**	.119**	-.666**
A. pragensis	RAAU(Axis1)	-0.033	-.160**	-.175**	-.124**	-.820**	-.310**	.187**
	RAAU(Axis2)	.225**	.116**	-.290**	-.134**	-.040*	.555**	-.215**
	RSCU(Axis1)	.151**	-.872**	-.668**	-.199**	-.097**	-0.0098	.464**
	RSCU(Axis2)	-.376**	-.131**	.118**	.067**	-.056**	-.252**	.640**
A. proteolyticus	RAAU(Axis1)	-.198**	.145**	.385**	.189**	.671**	-.032*	-.082**
	RAAU(Axis2)	-.358**	-.305**	.103**	.050**	-.446**	-.547**	.340**
	RSCU(Axis1)	.451**	-.331**	-.523**	-.221**	-.072**	.233**	-.364**
	RSCU(Axis2)	-.460**	-.629**	-.275**	-.109**	-.161**	-.145**	.755**

Table 4.3: Continued

Organism		**ENC**	**GC3s**	**GC**	**L_aa**	**GRAVY**	**Aromo**	**CAI**
A. puyangensis	RAAU(Axis1)	.136**	-.130**	-.268**	-.182**	-.691**	-.154**	.039*
	RAAU(Axis2)	-.298**	-.235**	.131**	.128**	-.360**	-.408**	.266**
	RSCU(Axis1)	-.254**	.599**	.615**	.195**	.090**	-.195**	0.02589
	RSCU(Axis2)	-.471**	-.426**	-.095**	-.037*	-.112**	-.128**	.641**
A. qingfengensis	RAAU(Axis1)	.158**	-.058**	-.256**	-.158**	-.705**	-.127**	-.243**
	RAAU(Axis2)	.277**	.065**	-.432**	-.060**	.296**	.552**	-.165**
	RSCU(Axis1)	.274**	-.235**	-.475**	-.072**	0.03545	.247**	-.112**
	RSCU(Axis2)	-.469**	-.534**	-.236**	-.076**	-.076**	-.058**	.179**
A. radioresistens	RAAU(Axis1)	0.02696	-.078**	-.192**	-.147**	-.828**	-.228**	.202**
	RAAU(Axis2)	.377**	.089**	-.405**	-.112**	0.03333	.600**	-.169**
	RSCU(Axis1)	.362**	-.373**	-.565**	-.214**	-0.0283	.220**	-.295**
	RSCU(Axis2)	-.484**	-.618**	-.324**	-.165**	-.146**	-.119**	.703**

Table 4.3: Continued

Organism		ENC	GC3s	GC	L_aa	GRAVY	Aromo	CAI
A. rudis	RAAU(Axis1)	-.075**	-.141**	-.201**	-.122**	-.852**	-.232**	.239**
	RAAU(Axis2)	-.346**	-.222**	.147**	.064**	-0.004	-.237**	.205**
	RSCU(Axis1)	.368**	-.205**	-.526**	-.128**	-0.0114	.299**	-.494**
	RSCU(Axis2)	-.454**	-.410**	-.116**	-.065**	-.137**	-.100**	.660**
A. schindleri	RAAU(Axis1)	.120**	-.144**	-.322**	-.173**	-.791**	-.126**	.085**
	RAAU(Axis2)	-.391**	-.239**	.231**	.097**	-.197**	-.624**	.439**
	RSCU(Axis1)	-.385**	.502**	.638**	.279**	.128**	-.189**	.265**
	RSCU(Axis2)	.511**	.610**	.262**	.039*	.102**	.191**	-.827**
A. seifertii	RAAU(Axis1)	-0.0228	.085**	.257**	.195**	.813**	.148**	-.143**
	RAAU(Axis2)	-.332**	0.00107	.681**	.181**	0.01006	-.696**	.233**
	RSCU(Axis1)	-.501**	.086**	.485**	.215**	.038*	-.303**	.607**
	RSCU(Axis2)	.537**	.665**	.344**	.082**	.093**	.065**	-.588**

Table 4.3: Continued

Organism		**ENC**	**GC3s**	**GC**	**L_aa**	**GRAVY**	**Aromo**	**CAI**
A. soil	RAAU(Axis1)	-0.0259	-.230**	-.260**	-.187**	-.822**	-.244**	.276**
	RAAU(Axis2)	.308**	.128**	-.203**	-.117**	.078**	.498**	-.227**
	RSCU(Axis1)	-0.0268	.776**	.662**	.241**	.181**	-.054**	-.339**
	RSCU(Axis2)	.481**	.315**	.061**	0.00749	.123**	.212**	-.745**
A. tandoii	RAAU(Axis1)	.118**	-.161**	-.381**	-.192**	-.789**	-.071**	.155**
	RAAU(Axis2)	.354**	.114**	-.371**	-.073**	.218**	.613**	-.301**
	RSCU(Axis1)	.408**	-.265**	-.508**	-.180**	-.100**	.242**	-.391**
	RSCU(Axis2)	-.449**	-.591**	-.269**	-.081**	-.136**	-.124**	.733**
A. tjernbergiae	RAAU(Axis1)	-.249**	.096**	.485**	.168**	.633**	-.170**	0.01948
	RAAU(Axis2)	-.343**	-.147**	.270**	.070**	-.421**	-.648**	.318**
	RSCU(Axis1)	-.380**	.293**	.587**	.179**	.081**	-.287**	.407**
	RSCU(Axis2)	.438**	.465**	.164**	.099**	.093**	.096**	-.679**

Table 4.3: Continued

Organism		**ENC**	**GC3s**	**GC**	**L_aa**	**GRAVY**	**Aromo**	**CAI**
A. towneri	RAAU(Axis1)	.172**	-.140**	-.336**	-.158**	-.774**	-.107**	-0.0188
	RAAU(Axis2)	.391**	.216**	-.245**	-0.0346	.211**	.589**	-.431**
	RSCU(Axis1)	-.542**	.131**	.407**	.181**	.098**	-.254**	.621**
	RSCU(Axis2)	-.282**	-.599**	-.282**	-.143**	-.127**	-.143**	.607**
A. urisingii	RAAU(Axis1)	.111**	-.206**	-.390**	-.175**	-.798**	-.082**	.187**
	RAAU(Axis2)	.332**	.063**	-.428**	-.100**	.198**	.619**	-.154**
	RSCU(Axis1)	-.327**	.400**	.567**	.185**	.091**	-.222**	.152**
	RSCU(Axis2)	-.419**	-.407**	-.150**	-.088**	-.153**	-.125**	.729**
A. variabilis	RAAU(Axis1)	-.126**	.158**	.327**	.191**	.820**	.107**	-.106**
	RAAU(Axis2)	.400**	.173**	-.331**	-.096**	.107**	.648**	-.377**
	RSCU(Axis1)	.476**	-.371**	-.594**	-.273**	-.100**	.216**	-.392**
	RSCU(Axis2)	.412**	.649**	.319**	.089**	.130**	.184**	-.760**

Table 4.3: Continued

Organism		ENC	GC3s	GC	L_aa	GRAVY	Aromo	CAI
A. venetianus	RAAU(Axis1)	.195**	-.064**	-.392**	-.187**	-.650**	0.02775	0.01481
	RAAU(Axis2)	-.407**	-.200**	.315**	.045*	-.390**	-.677**	.371**
	RSCU(Axis1)	.533**	-.099**	-.480**	-.142**	0.00934	.305**	-.632**
	RSCU(Axis2)	.309**	.488**	.247**	.115**	.109**	.036*	-.536**
A. wuhouensis	RAAU(Axis1)	.225**	-.162**	-.501**	-.194**	-.662**	.143**	0.02177
	RAAU(Axis2)	.358**	.097**	-.419**	-.058**	.429**	.709**	-.295**
	RSCU(Axis1)	-.532**	.158**	.541**	.195**	.077**	-.315**	.555**
	RSCU(Axis2)	-.448**	-.517**	-.140**	-.083**	-.090**	-.117**	.588**

Table 4.4: Total number of optimal codons along with AT or GC nature of all the *Acinetobacter* species.

Species	**Total optimal codons**	**AT rich**	**GC rich**	**A/T ending**	**G/C ending**
A. albensis	24	14	10	17	7
A. apis	28	18	10	20	8
A. baumannii	25	17	8	17	8
A. byalyi	24	15	9	17	7
A. beijerincki	21	14	7	15	6
A. bereziniae	22	14	8	15	7
A. bochemius	24	16	8	18	6
A. boissierii	25	16	9	20	5
A. bouvetii	25	18	7	19	6
A. brisouii	25	18	7	19	6
A. calcoacetius	24	14	10	16	8
A. celticus	24	13	11	16	8
A. colistiniresistens	22	15	7	17	5
A. cumulans	25	16	9	19	6
A. defulvii	24	16	8	19	5
A. equi	23	14	9	15	8
A. gandensis	22	15	7	18	4
A. genomosp.33YU	25	17	8	19	6
A. generi	23	15	8	16	7
A. guillouiae	25	17	8	20	5
A. gyllenbergii	25	16	9	19	6
A. haemolyticus	24	15	9	17	7
A. halotolerans	23	15	8	17	6
A. idrijaenesis	24	18	6	20	2

Table 4.4: Continued

Species	**Total optimal codons**	**AT rich**	**GC rich**	**A/T ending**	**G/C ending**
A. indicus	25	18	7	18	7
A. johnsonii	24	16	8	18	6
A. junnii	24	16	8	18	6
A. kokii	26	18	8	18	8
A. kyonggiensis	25	17	8	19	6
A. lactucae	23	16	7	17	6
A. larvae	28	17	11	19	9
A. lwoffii	29	20	9	21	8
A. marinus	23	15	8	16	7
A. nectaris	28	17	11	18	10
A. nosocomialis	25	16	9	18	7
A. oleivorans	25	16	9	17	8
A. parvus	24	17	7	18	6
A. piscicola	25	13	12	16	9
A. pittii	25	16	9	18	7
A. populi	26	18	8	19	7
A. pragensis	26	19	7	21	5
A. proteolyticus	25	16	9	18	7
A. puyangensis	25	17	8	19	6
A. qingfengensis	25	17	8	20	5
A. radioresistens	25	17	8	18	7
A. rudis	24	14	10	16	8
A. schindleri	27	17	10	18	9
A. seifertii	26	17	9	18	8
A. soil	25	16	9	18	7

Table 4.4: Continued

Species	**Total optimal codons**	**AT rich**	**GC rich**	**A/T ending**	**G/C ending**
A. tandoii	25	16	9	19	6
A. tjernbergiae	25	16	9	17	8
A. towneri	23	16	7	17	6
A. ursingii	25	17	8	18	7
A. variabilis	28	18	10	19	9
A. venetianus	23	14	9	15	8
A. wuhouensis	23	16	7	16	7

Table 4.5: Correlation of ENC, CAI, Gravy and Aromo with other codon usage bias analysis parameters

Organism		**ENC**	**GC3s**	**GC**	**L_aa**	**GRAVY**	**Aromo**	**CAI**
A. apis	ENC	1.00	.388**	-.061**	.042*	.075**	.190**	-.566**
	CAI	-.566**	-.539**	-.227**	-.107**	-.301**	-.064**	1.00
	GRAVY	.075**	.201**	.116**	.046*	1.00	.077**	-.301**
	Aromo	.190**	.041*	-.353**	.046*	.077**	1.00	-.064**
A. albensis	ENC	1.00	.388**	-.061**	.042*	.075**	.190**	-.566**
	CAI	-.566**	-.539**	-.227**	-.107**	-.301**	-.064**	1.00
	GRAVY	.075**	.201**	.116**	.046*	1.00	.077**	-.301**
	Aromo	.190**	.041*	-.353**	.046*	.077**	1.00	-.064**
A. baumannii	ENC	1.00	.468**	.067**	0.01	.041**	.163**	-.628**
	CAI	-.628**	-.416**	-.106**	0.02	-.170**	-.119**	1.00
	Gravy	.041**	.070**	.080**	.069**	1.00	.072**	-.170**
	Aromo	.163**	.037*	-.369**	-0.01	.072**	1.00	-.119**
A. baylyi	ENC	1.00	.355**	0.01	0.00	.062**	.191**	-.487**
	CAI	-.487**	-.594**	-.407**	-.165**	-.257**	0.01	1.00
	Gravy	.062**	.161**	.112**	.047**	1.00	.067**	-.257**
	Aromo	.191**	-0.02	-.363**	0.00	.067**	1.00	0.01
A. bereziniae	ENC	1.00	.390**	-0.01	0.03	0.02	.170**	-.529**
	CAI	-.529**	-.481**	-.270**	-.115**	-.176**	-0.01	1.00
	Gravy	0.02	.195**	.151**	.065**	1.00	.047**	-.176**
	Aromo	.170**	-0.01	-.401**	-0.03	.047**	1.00	-0.01
A.beijerinckii	ENC	1.00	.387**	-.073**	-0.01	0.02	.234**	-.602**
	CAI	-.602**	-.421**	-.103**	-.046**	-.206**	-.128**	1.00
	Gravy	0.02	.127**	.103**	0.03	1.00	.052**	-.206**
	Aromo	.234**	.034*	-.386**	-0.03	.052**	1.00	-.128**

Table 4.5: Continued

Organism		ENC	GC3s	GC	L_aa	GRAVY	Aromo	CAI
A. bochemicus	ENC	1.00	.368**	-0.03	-0.02	0.00	.192**	-.578**
	CAI	-.578**	-.517**	-.200**	-.076**	-.223**	-.114**	1.00
	Gravy	0.00	.209**	.151**	.040*	1.00	.063**	-.223**
	Aromo	.192**	.034*	-.330**	0.00	.063**	1.00	-.114**
A. boissieri	ENC	1.00	.454**	0.00	0.00	0.00	.162**	-.572**
	CAI	-.572**	-.512**	-.109**	-0.03	-.169**	-.116**	1.00
	Gravy	0.00	-.041*	-0.02	0.03	1.00	.096**	-.169**
	Aromo	.162**	0.01	-.407**	0.01	.096**	1.00	-.116**
A. bouvetti	ENC	1.00	-.131**	-.214**	-.088**	0.02	.131**	-.256**
	CAI	-.256**	-.531**	-.346**	-.046*	-.181**	-.099**	1.00
	Gravy	0.02	.146**	.107**	.051**	1.00	.089**	-.181**
	Aromo	.131**	0.03	-.240**	-0.01	.089**	1.00	-.099**
A. brisouii	ENC	1.00	.366**	.044*	-0.01	0.01	.193**	-.532**
	CAI	-.532**	-.610**	-.397**	-.076**	-.206**	-.090**	1.00
	Gravy	0.01	.160**	.119**	.088**	1.00	.093**	-.206**
	Aromo	.193**	.093**	-.240**	0.02	.093**	1.00	-.090**
A. calcoaceticus	ENC	1.00	.469**	0.02	-0.03	.085**	.211**	-.639**
	CAI	-.639**	-.428**	-.105**	-0.01	-.238**	-.146**	1.00
	Gravy	.085**	.109**	.087**	.060**	1.00	.068**	-.238**
	Aromo	.211**	.072**	-.357**	-0.02	.068**	1.00	-.146**
A. celticus	ENC	1.00	.372**	-.077**	-.078**	.042*	.216**	-.596**
	CAI	-.596**	-.495**	-.143**	-0.02	-.236**	-.098**	1.00
	Gravy	.042*	.150**	.107**	.066**	1.00	.084**	-.236**
	Aromo	.216**	.066**	-.347**	0.00	.084**	1.00	-.098**

Table 4.5: Continued

Organism		**ENC**	**GC3s**	**GC**	**L_aa**	**GRAVY**	**Aromo**	**CAI**
A. colistiniresistens	ENC	1.00	.280**	-.032*	-.041*	-0.01	.167**	-.491**
	CAI	-.491**	-.534**	-.286**	-.107**	-.234**	-.108**	1.00
	Gravy	-0.01	.223**	.168**	.039*	1.00	.075**	-.234**
	Aromo	.167**	.067**	-.311**	-0.02	.075**	1.00	-.108**
A. cumulans	ENC	1.00	.412**	-0.02	-.077**	0.01	.227**	-.611**
	CAI	-.611**	-.601**	-.218**	-0.02	-.204**	-.183**	1.00
	Gravy	0.01	.170**	.153**	.037*	1.00	.074**	-.204**
	Aromo	.227**	.122**	-.299**	0.01	.074**	1.00	-.183**
A. defulvii	ENC	1.00	.346**	-.116**	-.056**	-0.02	.216**	-.534**
	CAI	-.534**	-.433**	-.153**	-0.03	-.159**	-.062**	1.00
	Gravy	-0.02	.160**	.131**	.059**	1.00	.074**	-.159**
	Aromo	.216**	-0.02	-.404**	-0.03	.074**	1.00	-.062**
A. equi	ENC	1.00	.416**	-.159**	-.082**	0.03	.216**	-.597**
	CAI	-.597**	-.234**	.179**	.059**	-.165**	-.149**	1.00
	Gravy	0.03	-0.02	0.01	.053**	1.00	.084**	-.165**
	Aromo	.216**	0.00	-.437**	0.00	.084**	1.00	-.149**
A. gandensis	ENC	1.00	.409**	-.092**	-.056**	.059**	.243**	-.652**
	CAI	-.652**	-.481**	-.057**	0.01	-.215**	-.194**	1.00
	Gravy	.059**	.177**	.114**	.041*	1.00	.097**	-.215**
	Aromo	.243**	.130**	-.325**	0.00	.097**	1.00	-.194**
A. genomosp 33YU	ENC	1.00	.500**	0.02	-.039*	.071**	.192**	-.637**
	CAI	-.637**	-.415**	-.096**	0.01	-.219**	-.129**	1.00
	Gravy	.071**	.092**	.122**	.086**	1.00	.053**	-.219**
	Aromo	.192**	.060**	-.364**	0.00	.053**	1.00	-.129**

Table 4.5: Continued

Organism		ENC	GC3s	GC	L_aa	GRAVY	Aromo	CAI
A. generi	ENC	1.00	.450**	-.040**	-0.02	-.031*	.192**	-.609**
	CAI	-.609**	-.454**	-.083**	-0.01	-.075**	-.070**	1.00
	Gravy	-.031*	.179**	.161**	.081**	1.00	.062**	-.075**
	Aromo	.192**	-0.01	-.404**	-0.01	.062**	1.00	-.070**
A. guilouiae	ENC	1.00	.424**	-.035*	-0.01	0.02	.186**	-.541**
	CAI	-.541**	-.508**	-.210**	-.081**	-.214**	-.059**	1.00
	Gravy	0.02	.188**	.149**	.059**	1.00	.040**	-.214**
	Aromo	.186**	0.02	-.381**	-0.02	.040**	1.00	-.059**
A. gyllenbegii	ENC	1.00	.308**	-.033*	-.044**	0.03	.191**	-.456**
	CAI	-.456**	-.474**	-.178**	-.065**	-.398**	-.104**	1.00
	Gravy	0.03	.223**	.168**	.038*	1.00	.045**	-.398**
	Aromo	.191**	0.01	-.363**	-.041*	.045**	1.00	-.104**
A. haemolyticus	ENC	1.00	.405**	0.00	0.02	0.01	.163**	-.553**
	CAI	-.553**	-.479**	-.198**	-.046**	-.182**	-.066**	1.00
	Gravy	0.01	.163**	.093**	0.02	1.00	.090**	-.182**
	Aromo	.163**	0.01	-.375**	-.084**	.090**	1.00	-.066**
A. halotolerans	ENC	1.00	.308**	-.033*	-.044**	0.03	.191**	-.456**
	CAI	-.456**	-.474**	-.178**	-.065**	-.398**	-.104**	1.00
	Gravy	0.03	.223**	.168**	.038*	1.00	.045**	-.398**
	Aromo	.191**	0.01	-.363**	-.041*	.045**	1.00	-.104**
A. idrijaensis	ENC	1.00	.169**	-.067**	-.056**	-0.03	.161**	-.435**
	CAI	-.435**	-.560**	-.381**	-0.02	-.184**	-.085**	1.00
	Gravy	-0.03	.169**	.175**	.118**	1.00	.089**	-.184**
	Aromo	.161**	0.03	-.265**	0.02	.089**	1.00	-.085**

Table 4.5: Continued

Organism		ENC	GC3s	GC	L_aa	GRAVY	Aromo	CAI
A. indicus	ENC	1.00	-.177**	-.249**	-.108**	-.065**	.130**	-.201**
	CAI	-.201**	-.627**	-.480**	-.092**	-.214**	-.154**	1.00
	Gravy	-.065**	.261**	.222**	.049**	1.00	.069**	-.214**
	Aromo	.130**	.110**	-.156**	.065**	.069**	1.00	-.154**
A. johnsonii	ENC	1.00	.378**	0.02	-0.02	0.00	.171**	-.564**
	CAI	-.564**	-.571**	-.244**	-.075**	-.235**	-.168**	1.00
	Gravy	0.00	.228**	.156**	.041*	1.00	.094**	-.235**
	Aromo	.171**	.117**	-.280**	0.01	.094**	1.00	-.168**
A. junnii	ENC	1.00	.443**	-.059**	-0.03	-.035*	.233**	-.604**
	CAI	-.604**	-.460**	-.138**	-0.01	-.140**	-.124**	1.00
	Gravy	-.035*	.079**	.124**	.047**	1.00	.057**	-.140**
	Aromo	.233**	.098**	-.369**	-0.02	.057**	1.00	-.124**
A. kooki	ENC	1.00	.168**	-.083**	-.065**	0.01	.185**	-.489**
	CAI	-.489**	-.549**	-.322**	-.077**	-.191**	-.123**	1.00
	Gravy	0.01	.200**	.158**	.058**	1.00	.073**	-.191**
	Aromo	.185**	.097**	-.235**	0.02	.073**	1.00	-.123**
A. kyonggiensis	ENC	1.00	.395**	0.00	0.00	0.00	.167**	-.564**
	CAI	-.564**	-.541**	-.254**	-.047**	-.164**	-.056**	1.00
	Gravy	0.00	.185**	.158**	.040*	1.00	.050**	-.164**
	Aromo	.167**	0.01	-.342**	-0.01	.050**	1.00	-.056**
A. lactucae	ENC	1.00	.486**	.039*	-0.02	.071**	.210**	-.644**
	CAI	-.644**	-.422**	-.092**	-0.03	-.236**	-.168**	1.00
	Gravy	.071**	.109**	.098**	.051**	1.00	.061**	-.236**
	Aromo	.210**	.070**	-.349**	-0.01	.061**	1.00	-.168**

Table 4.5: Continued

Organism		ENC	GC3s	GC	L_aa	GRAVY	Aromo	CAI
A. larvae	ENC	1.00	.357**	.106**	-0.01	0.02	.121**	-.508**
	CAI	-.508**	-.453**	-.324**	-.048**	-.168**	0.00	1.00
	Gravy	0.02	.269**	.185**	.057**	1.00	.058**	-.168**
	Aromo	.121**	-.065**	-.374**	0.03	.058**	1.00	0.00
A. lwoffii	ENC	1.00	.174**	-.051**	-.036*	-0.01	.162**	-.429**
	CAI	-.429**	-.597**	-.377**	-.096**	-.211**	-.103**	1.00
	Gravy	-0.01	.233**	.204**	.062**	1.00	.069**	-.211**
	Aromo	.162**	.045**	-.267**	0.03	.069**	1.00	-.103**
A. marinus	ENC	1.00	.182**	-.060**	-.051**	-0.03	.181**	-.567**
	CAI	-.567**	-.377**	-.189**	-0.02	-.104**	-.149**	1.00
	Gravy	-0.03	.274**	.171**	0.02	1.00	.059**	-.104**
	Aromo	.181**	.045*	-.327**	0.02	.059**	1.00	-.149**
A. nectaris	ENC	1.00	.479**	-0.03	-0.02	0.02	.217**	-.538**
	CAI	-.538**	-.358**	0.00	0.02	-.137**	-.132**	1.00
	Gravy	0.02	-.113**	-0.04	.060**	1.00	.105**	-.137**
	Aromo	.217**	0.04	-.388**	.043*	.105**	1.00	-.132**
A. nosocomialis	ENC	1.00	.474**	0.00	-.065**	.037*	.197**	-.643**
	CAI	-.643**	-.434**	-.091**	0.01	-.186**	-.148**	1.00
	Gravy	.037*	.073**	.080**	.069**	1.00	.075**	-.186**
	Aromo	.197**	.045**	-.376**	-0.01	.075**	1.00	-.148**
A. olievorans	ENC	1.00	.481**	0.01	-0.02	.084**	.228**	-.637**
	CAI	-.637**	-.421**	-.087**	-0.03	-.252**	-.160**	1.00
	Gravy	.084**	.111**	.087**	.051**	1.00	.073**	-.252**
	Aromo	.228**	.081**	-.349**	-0.01	.073**	1.00	-.160**

Table 4.5: Continued

Organism		**ENC**	**GC3s**	**GC**	**L_aa**	**GRAVY**	**Aromo**	**CAI**
A. parvus	ENC	1.00	.342**	.049*	-.047*	-0.01	.204**	-.533**
	CAI	-.533**	-.541**	-.328**	-0.01	-.174**	-.096**	1.00
	Gravy	-0.01	.173**	.185**	.059**	1.00	0.04	-.174**
	Aromo	.204**	0.01	-.296**	-0.01	0.04	1.00	-.096**
A. piscicola	ENC	1.00	.374**	-.062**	-.054**	-0.03	.209**	-.562**
	CAI	-.562**	-.473**	-.127**	-0.01	-.175**	-.089**	1.00
	Gravy	-0.03	.185**	.140**	.071**	1.00	0.03	-.175**
	Aromo	.209**	0.00	-.391**	-0.01	0.03	1.00	-.089**
A. pittii	ENC	1.00	.461**	0.00	-0.02	.087**	.233**	-.656**
	CAI	-.656**	-.425**	-.101**	-0.03	-.245**	-.164**	1.00
	Gravy	.087**	.127**	.122**	.089**	1.00	.066**	-.245**
	Aromo	.233**	.084**	-.333**	0.01	.066**	1.00	-.164**
A. populi	ENC	1.00	.340**	0.01	-0.03	.062**	.150**	-.501**
	CAI	-.501**	-.504**	-.278**	-.072**	-.130**	-0.03	1.00
	Gravy	.062**	.228**	.144**	.040*	1.00	.064**	-.130**
	Aromo	.150**	-.049**	-.377**	0.03	.064**	1.00	-0.03
A. pragensis	ENC	1.00	-0.03	-.157**	-.042*	0.02	.120**	-.332**
	CAI	-.332**	-.570**	-.416**	-.068**	-.210**	-0.03	1.00
	Gravy	0.02	.169**	.136**	.045**	1.00	.081**	-.210**
	Aromo	.120**	0.02	-.256**	0.01	.081**	1.00	-0.03
A. proteolyticus	ENC	1.00	.301**	-0.03	-.069**	0.02	.194**	-.526**
	CAI	-.526**	-.521**	-.276**	-.084**	-.230**	-.089**	1.00
	Gravy	0.02	.258**	.208**	.044**	1.00	.038*	-.230**
	Aromo	.194**	.057**	-.334**	0.00	.038*	1.00	-.089**

Table 4.5: Continued

Organism		ENC	GC3s	GC	L_aa	GRAVY	Aromo	CAI
A. puyangensis	ENC	1.00	.248**	-0.02	-.051**	0.02	.125**	-.509**
	CAI	-.509**	-.535**	-.312**	-.083**	-.134**	-0.03	1.00
	Gravy	0.02	.220**	.144**	0.01	1.00	.066**	-.134**
	Aromo	.125**	-.060**	-.361**	.039*	.066**	1.00	-0.03
A. qingfengensis	ENC	1.00	.481**	.083**	-.063**	0.00	.113**	-.251**
	CAI	-.251**	-.390**	-.118**	.094**	.090**	0.00	1.00
	Gravy	0.00	.102**	.070**	.052**	1.00	.059**	.090**
	Aromo	.113**	-.065**	-.395**	.056**	.059**	1.00	0.00
A. radioresistens	ENC	1.00	.352**	0.02	0.03	.062**	.194**	-.522**
	CAI	-.522**	-.444**	-.288**	-.094**	-.232**	-.050**	1.00
	Gravy	.062**	.109**	.100**	.078**	1.00	.093**	-.232**
	Aromo	.194**	0.00	-.334**	0.03	.093**	1.00	-.050**
A. rudis	ENC	1.00	.472**	0.02	-0.03	.057**	.183**	-.586**
	CAI	-.586**	-.421**	-.097**	-0.01	-.204**	-.136**	1.00
	Gravy	.057**	.140**	.111**	.035*	1.00	.052**	-.204**
	Aromo	.183**	-0.01	-.407**	0.00	.052**	1.00	-.136**
A. schindleri	ENC	1.00	.271**	-.041*	-.104**	0.01	.193**	-.575**
	CAI	-.575**	-.489**	-.213**	-.037*	-.208**	-.180**	1.00
	Gravy	0.01	.209**	.183**	.054**	1.00	.092**	-.208**
	Aromo	.193**	.091**	-.254**	0.01	.092**	1.00	-.180**
A. seifertii	ENC	1.00	.464**	0.00	-.046**	.058**	.194**	-.654**
	CAI	-.654**	-.429**	-.087**	0.02	-.180**	-.140**	1.00
	Gravy	.058**	.077**	.085**	.091**	1.00	.054**	-.180**
	Aromo	.194**	.051**	-.362**	-0.02	.054**	1.00	-.140**

Table 4.5: Continued

Organism		ENC	GC3s	GC	L_aa	GRAVY	Aromo	CAI
A. soil	ENC	1.00	.258**	.044*	-0.02	.035*	.172**	-.462**
	CAI	-.462**	-.593**	-.441**	-.116**	-.281**	-.039*	1.00
	Gravy	.035*	.222**	.181**	.107**	1.00	.072**	-.281**
	Aromo	.172**	.038*	-.284**	.040*	.072**	1.00	-.039*
A. tandoii	ENC	1.00	.373**	0.01	-.033*	-0.02	.191**	-.538**
	CAI	-.538**	-.504**	-.238**	-.035*	-.207**	-.111**	1.00
	Gravy	-0.02	.128**	.117**	.083**	1.00	.064**	-.207**
	Aromo	.191**	0.02	-.312**	0.02	.064**	1.00	-.111**
A. tjernbergiae	ENC	1.00	.391**	-0.03	-0.03	-0.02	.204**	-.564**
	CAI	-.564**	-.472**	-.165**	0.01	-.154**	-.074**	1.00
	Gravy	-0.02	.130**	.133**	0.02	1.00	0.02	-.154**
	Aromo	.204**	-0.01	-.377**	-0.02	0.02	1.00	-.074**
A. towneri	ENC	1.00	.275**	-.053**	-0.02	-.039*	.220**	-.567**
	CAI	-.567**	-.456**	-.161**	-0.04	-.116**	-.151**	1.00
	Gravy	-.039*	.170**	.140**	.082**	1.00	.068**	-.116**
	Aromo	.220**	.084**	-.296**	0.02	.068**	1.00	-.151**
A. urisingii	ENC	1.00	.328**	-.041*	-0.02	0.00	.194**	-.490**
	CAI	-.490**	-.502**	-.317**	-.119**	-.188**	-0.02	1.00
	Gravy	0.00	.194**	.132**	.072**	1.00	.079**	-.188**
	Aromo	.194**	0.00	-.364**	0.01	.079**	1.00	-0.02
A. variabilis	ENC	1.00	.222**	-.108**	-.078**	-0.01	.209**	-.534**
	CAI	-.534**	-.473**	-.191**	-0.02	-.199**	-.164**	1.00
	Gravy	-0.01	.203**	.185**	.090**	1.00	.057**	-.199**
	Aromo	.209**	.096**	-.253**	0.03	.057**	1.00	-.164**

Table 4.5: Continued

Organism		**ENC**	**GC3s**	**GC**	**L_aa**	**GRAVY**	**Aromo**	**CAI**
A. venetianus	ENC	1.00	.391**	-.102**	-.039*	0.03	.264**	-.623**
	CAI	-.623**	-.415**	-.068**	-0.01	-.213**	-.148**	1.00
	Gravy	0.03	.149**	.134**	.058**	1.00	.061**	-.213**
	Aromo	.264**	.068**	-.378**	0.00	.061**	1.00	-.148**
A. wuhouensis	ENC	1.00	.363**	-.107**	-.064**	-0.01	.236**	-.594**
	CAI	-.594**	-.442**	-.067**	0.00	-.159**	-.113**	1.00
	Gravy	-0.01	.166**	.116**	.050**	1.00	.083**	-.159**
	Aromo	.236**	-0.01	-.400**	-0.01	.083**	1.00	-.113**

4.3 Insights from ENC-GC3s analysis

The ENC-GC3 figure unveiled a diminished codon usage bias within the genomes. Genes showed a deviation just below the curve **(Table 4.1, Figure 4.2),** indicating a weak impact of mutational bias on codon usage in all studied *Acinetoacter* genomes. This observation suggests that translational selection pressure exerts a more dominant impact compared to other factors. Additionally, when the average ENC value for given set of genes exceeds 35, it indicates a reduced bias in codon usage (Andargie & Congyi, 2022). The average ENC levels for *Acinetoacter* genomes ranged from 39.5 to 48.4. **(Table 4.1, Figure 4.2).** We observed a consistent ENC value among members of the *Acinetoacter baumannii* complex, ranging from 44.11 in *A. lactucae* to 45.55 in *A. calcoaceticus.* Additionally, *A. baylyi* exhibited an ENC value of 46.7, slightly higher than the pathogenic members of the ACB complex **(Table 4.1).** Consequently, these data point towards a low codon usage bias within the genus *Acinetoacter.* Here the CUB is higher in ACB complex because non- pathogenic species like *A. baylyi* does not face the same stringent selection pressures related to virulence and host adaptation (Beceiro et al., 2013).

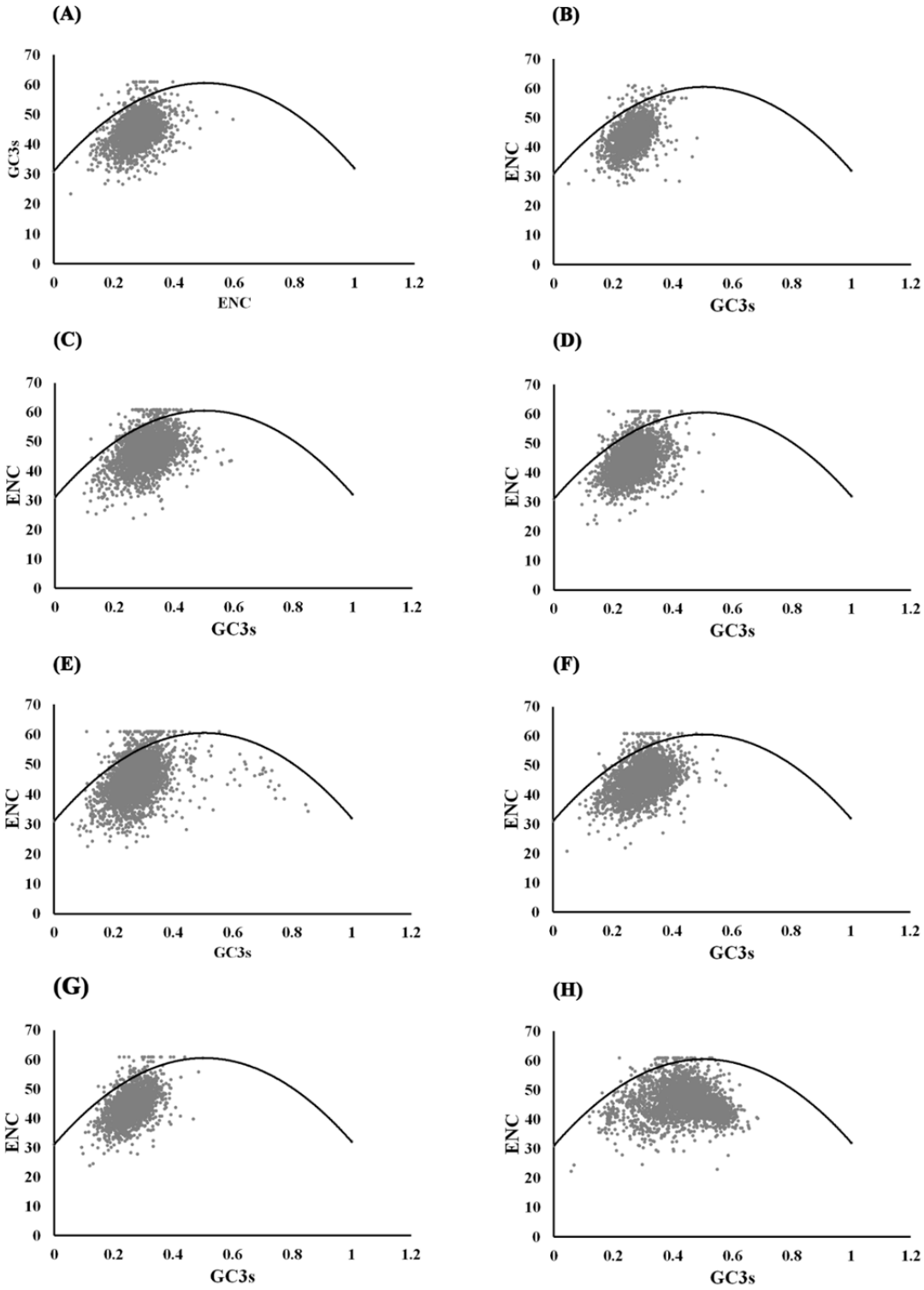
(A)
GC3s
ENC
(B)
ENC
GC3s
(C)
ENC
GC3s
(D)
ENC
GC3s
(E)
ENC
GC3s
(F)
ENC
GC3s
(G)
ENC
GC3s
(H)
ENC
GC3s

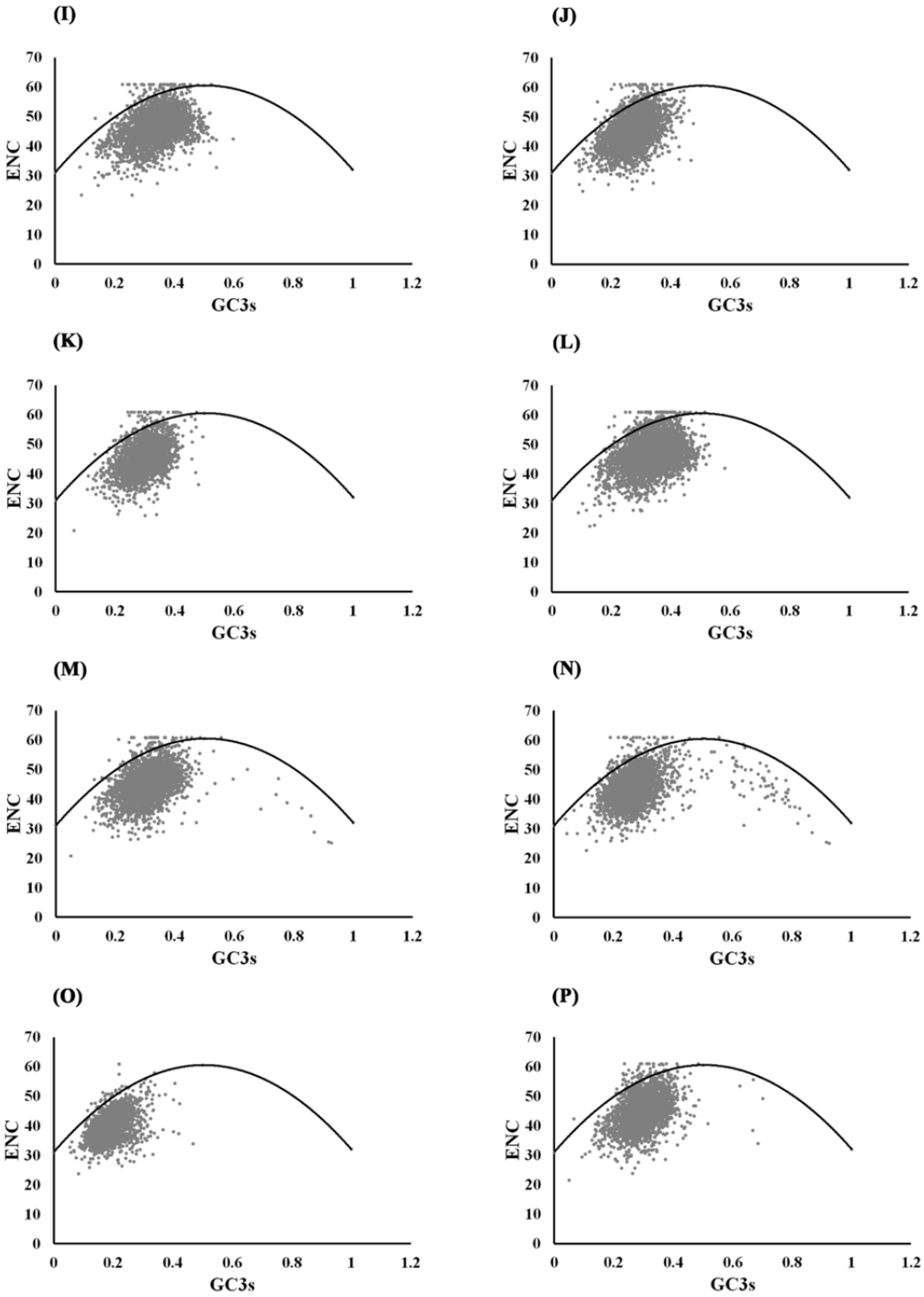
(I)
(J)
(K)
(L)
(M)
(N)
(O)
(P)
ENC
GC3s
0
10
20
30
40
50
60
70
0.2
0.4
0.6
0.8
1
1.2

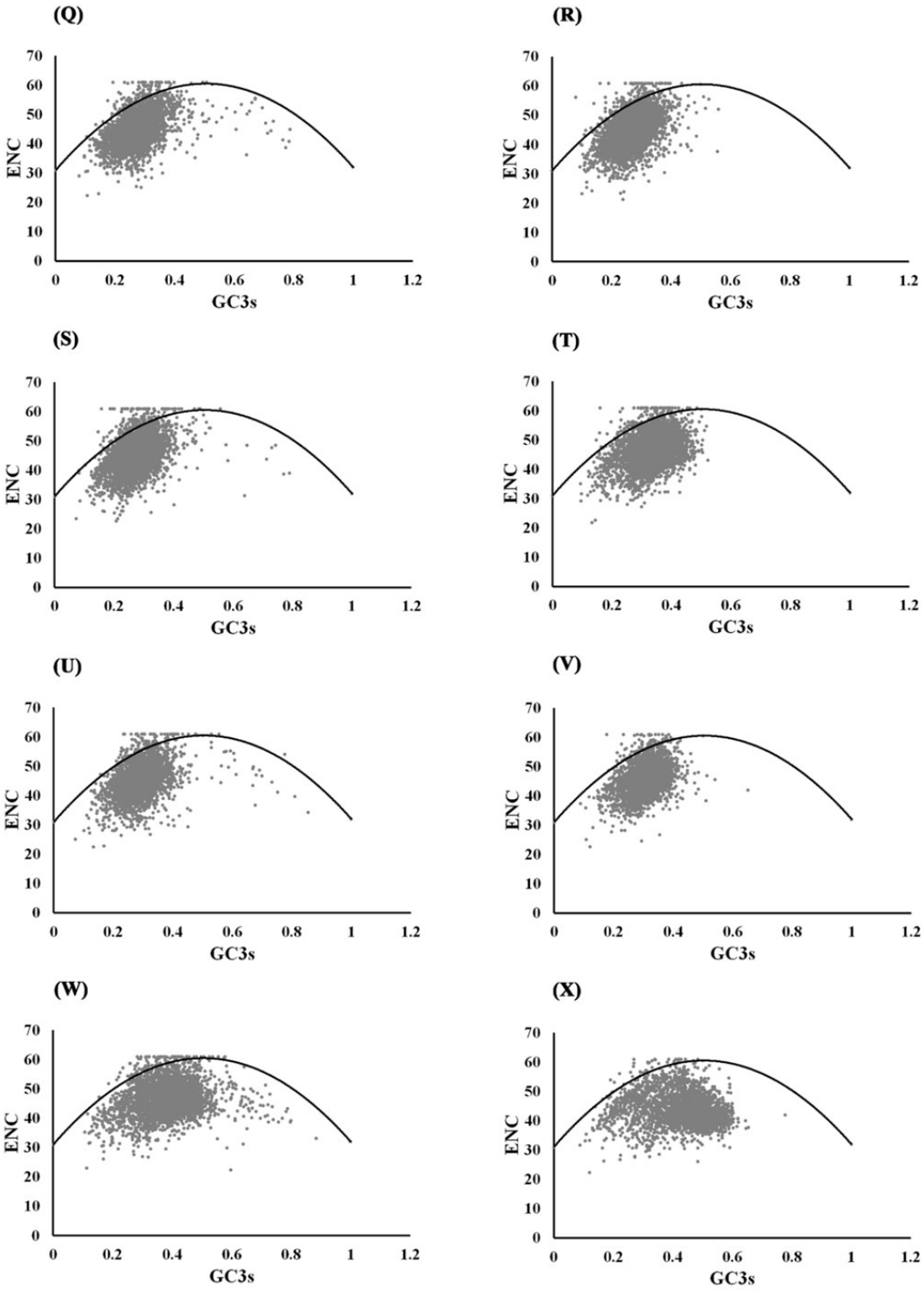
(Q)
(R)
(S)
(T)
(U)
(V)
(W)
(X)
ENC
GC3s
0
10
20
30
40
50
60
70
0.2
0.4
0.6
0.8
1
1.2

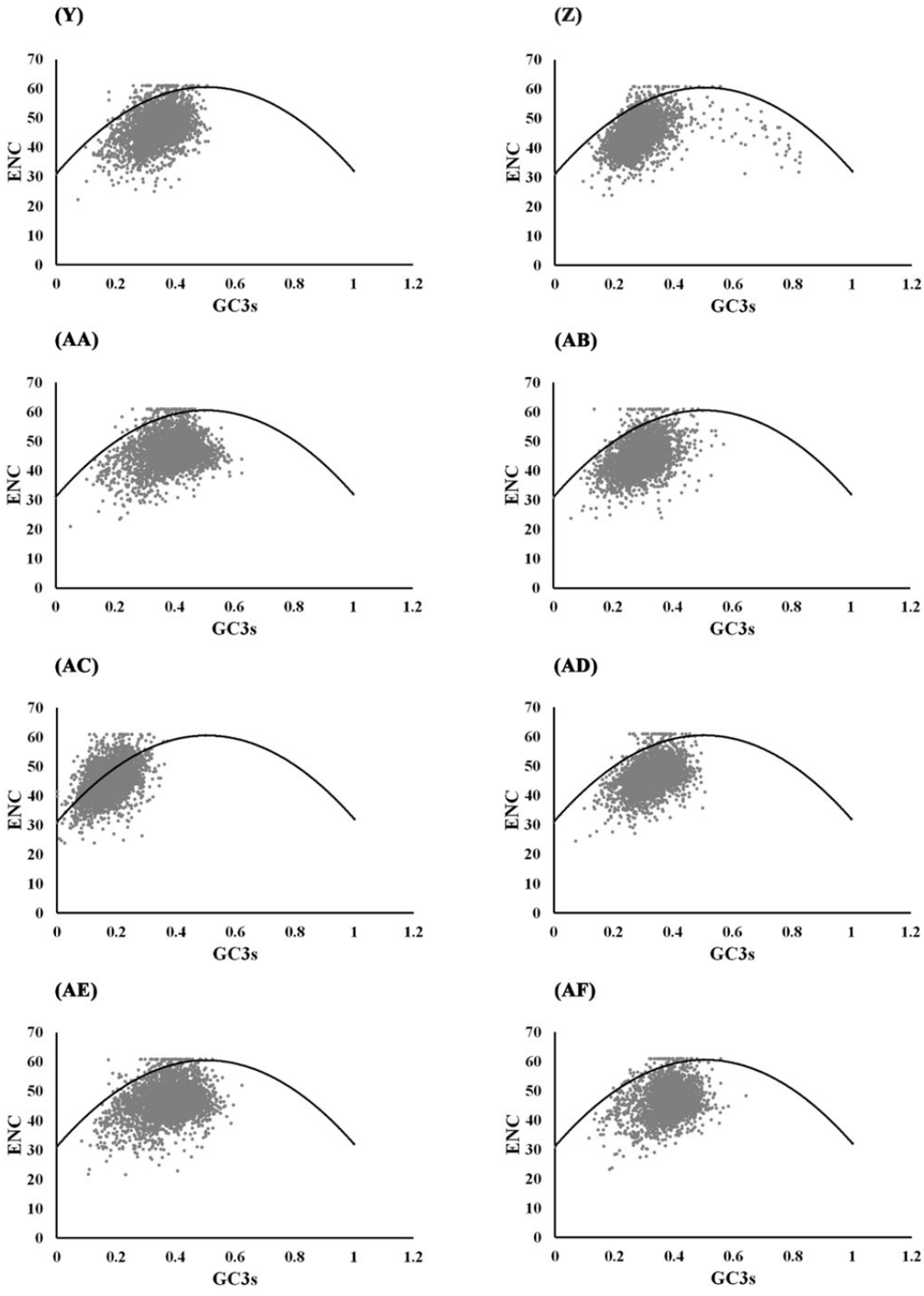
(Y)
(Z)
(AA)
(AB)
(AC)
(AD)
(AE)
(AF)
ENC
GC3s
0
10
20
30
40
50
60
70
0.2
0.4
0.6
0.8
1
1.2

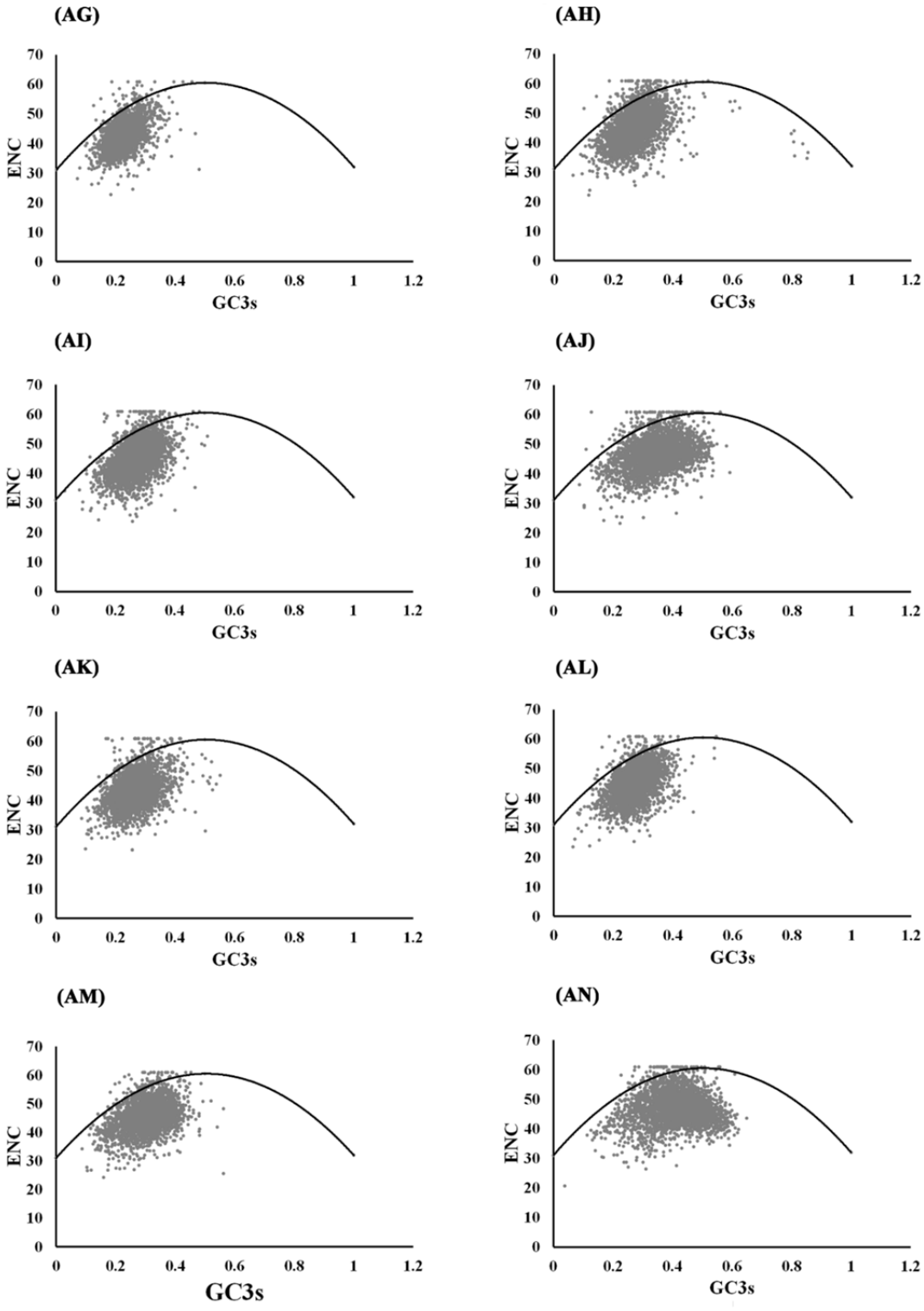
(AG)
(AH)
(AI)
(AJ)
(AK)
(AL)
(AM)
(AN)
ENC
GC3s
0
10
20
30
40
50
60
70
0.2
0.4
0.6
0.8
1
1.2

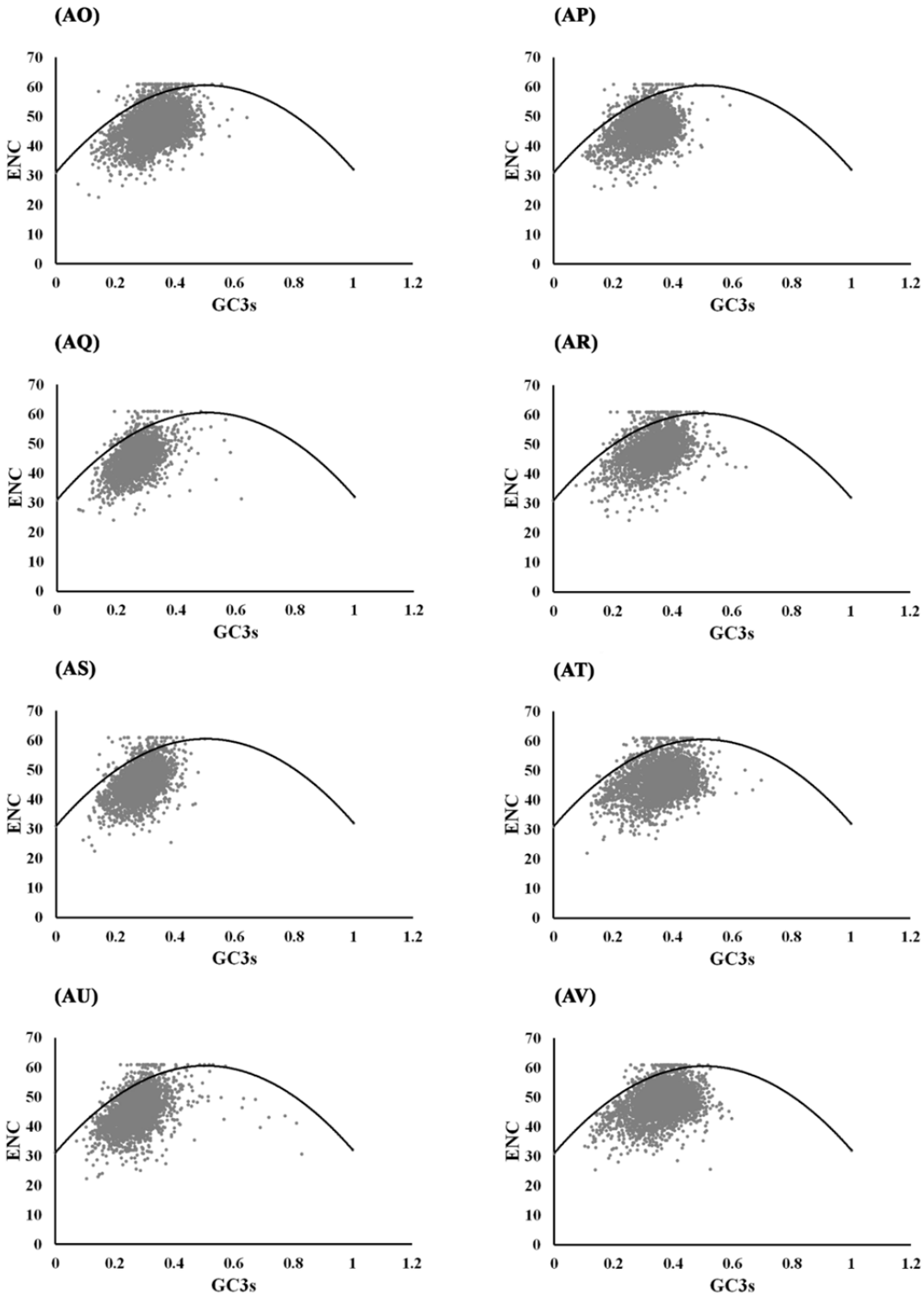
(AO)
(AP)
(AQ)
(AR)
(AS)
(AT)
(AU)
(AV)
ENC
GC3s
0
10
20
30
40
50
60
70
0.2
0.4
0.6
0.8
1
1.2

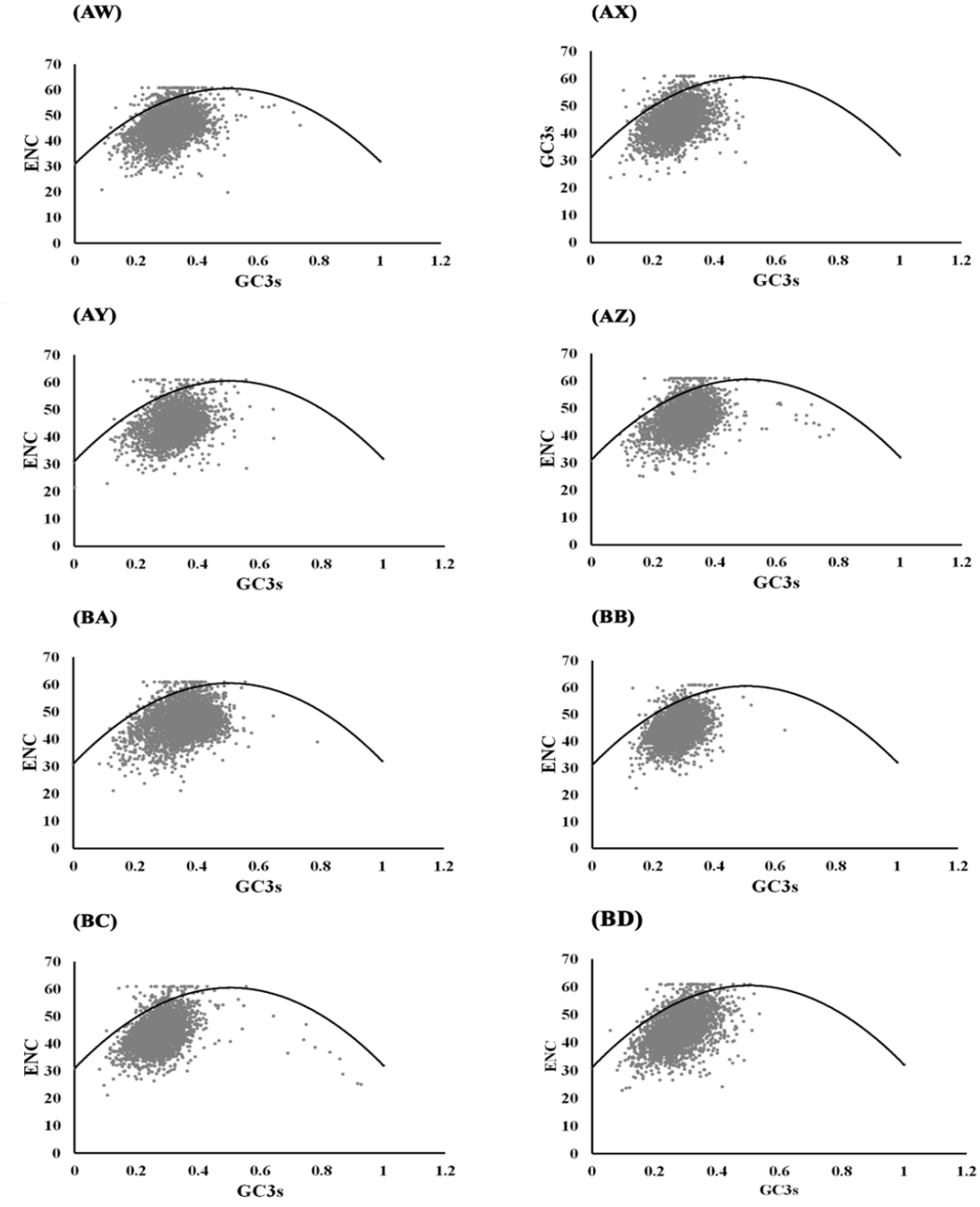

Figure 4.2: ENC plot analysis of various *Acinetobacter* species.

(Note: The ENC vs GC3s graphs of the Acinetobacter species are arranged serially according to table 3.1)

4.4 Insights from Neutrality plot analysis

Upon examining the neutrality plot across *Acinetoacter* genome species, we observed regression line slopes **(Figure 4.3)** close to zero, indicating minimal influence of mutational pressure on codon usage bias. Specifically, slopes ranged from 0.05 in *Acinetoacter apis* to 0.27 in *Acinetoacter* populi, corresponding to mutational pressure effects ranging from 0.5% to 27%, respectively. Notably, members of the ACB complex exhibited lower mutational pressure effects compared to other *Acinetoacter* species. For instance, species like *A. haemolyticus, A. junii, A. nosocomialis*, and *A. oleivorans* showed mutational pressure effects of 12%, while A. *baumannii*, *A. pittii*, and A. *lactucae* exhibited 14%. In contrast, *A. calcoaceticus* and *A. serifertii* registered 17%, while *A. baylyi*, being a non-pathogenic species showed a higher impact of 23% from mutational pressure. These results underscore the predominant influence of translational selection over mutational pressure in shaping codon usage patterns within the *Acinetoacter* genus. Translational selection is evident in the consistent codon preferences observed across species, reflecting adaptive strategies for efficient protein synthesis and functional optimization (Plotkin & Kudla, 2011). Conversely, the higher impact of mutational pressure on non-pathogenic species compared to the pathogenic ACB complex suggests differential evolutionary pressures and ecological niches that influence genomic stability and codon usage bias (Sharp & Li, 1987).

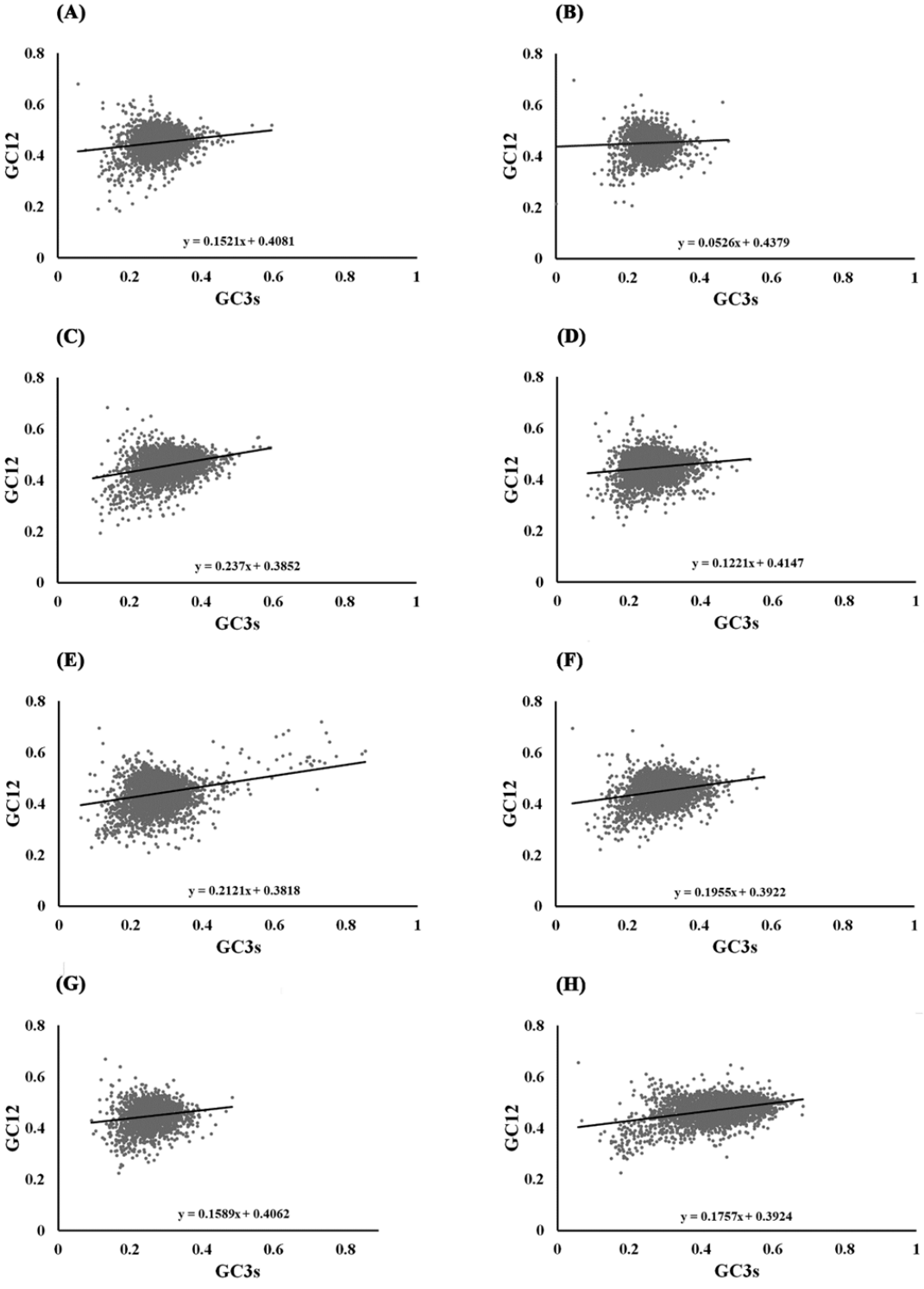
(A)
y = 0.1521x + 0.4081
(B)
y = 0.0526x + 0.4379
(C)
y = 0.237x + 0.3852
(D)
y = 0.1221x + 0.4147
(E)
y = 0.2121x + 0.3818
(F)
y = 0.1955x + 0.3922
(G)
y = 0.1589x + 0.4062
(H)
y = 0.1757x + 0.3924
GC12
GC3s
0
0.2
0.4
0.6
0.8
1

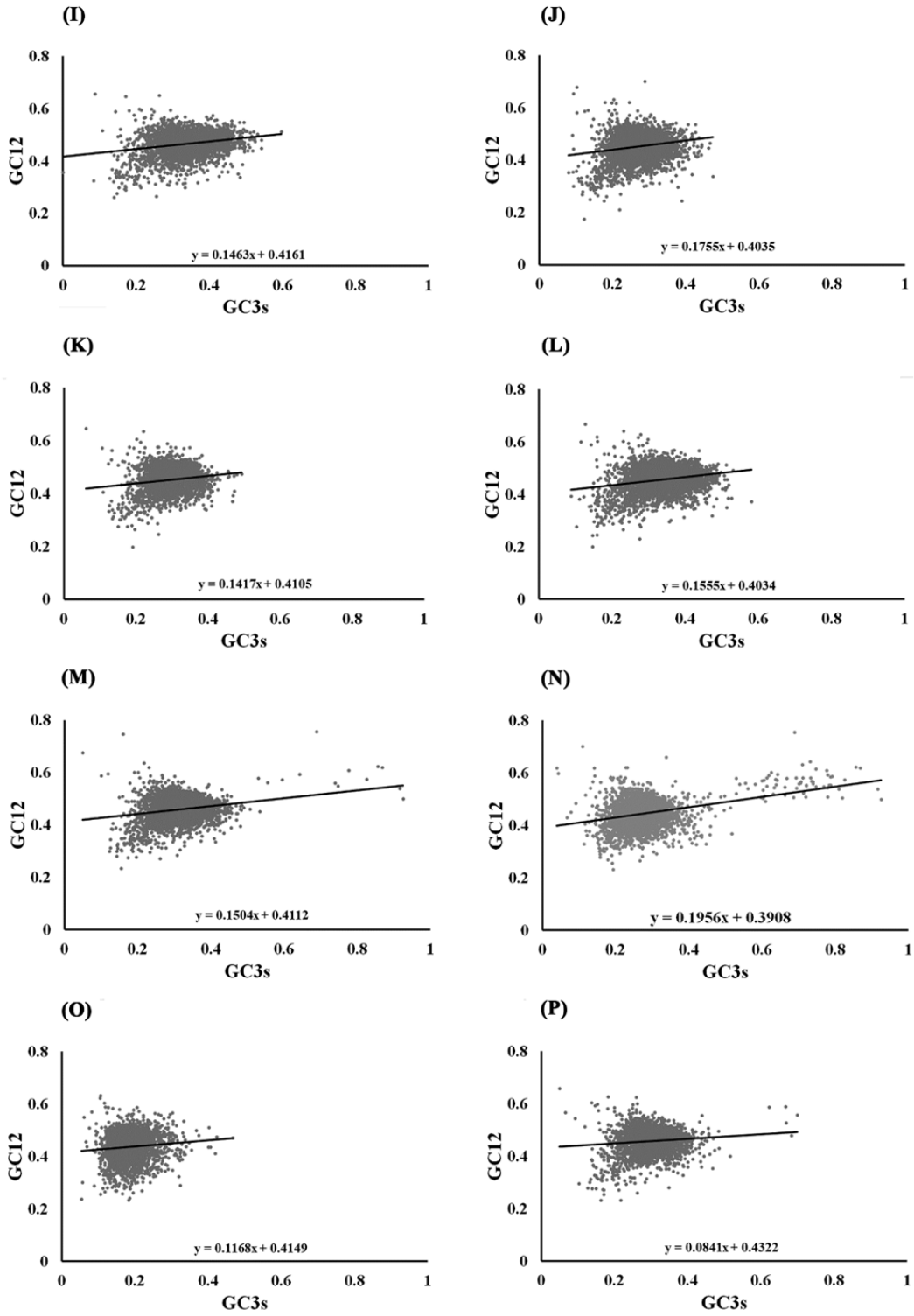
(I)
y = 0.1463x + 0.4161
(J)
y = 0.1755x + 0.4035
(K)
y = 0.1417x + 0.4105
(L)
y = 0.1555x + 0.4034
(M)
y = 0.1504x + 0.4112
(N)
y = 0.1956x + 0.3908
(O)
y = 0.1168x + 0.4149
(P)
y = 0.0841x + 0.4322
GC12
GC3s
0
0.2
0.4
0.6
0.8
1

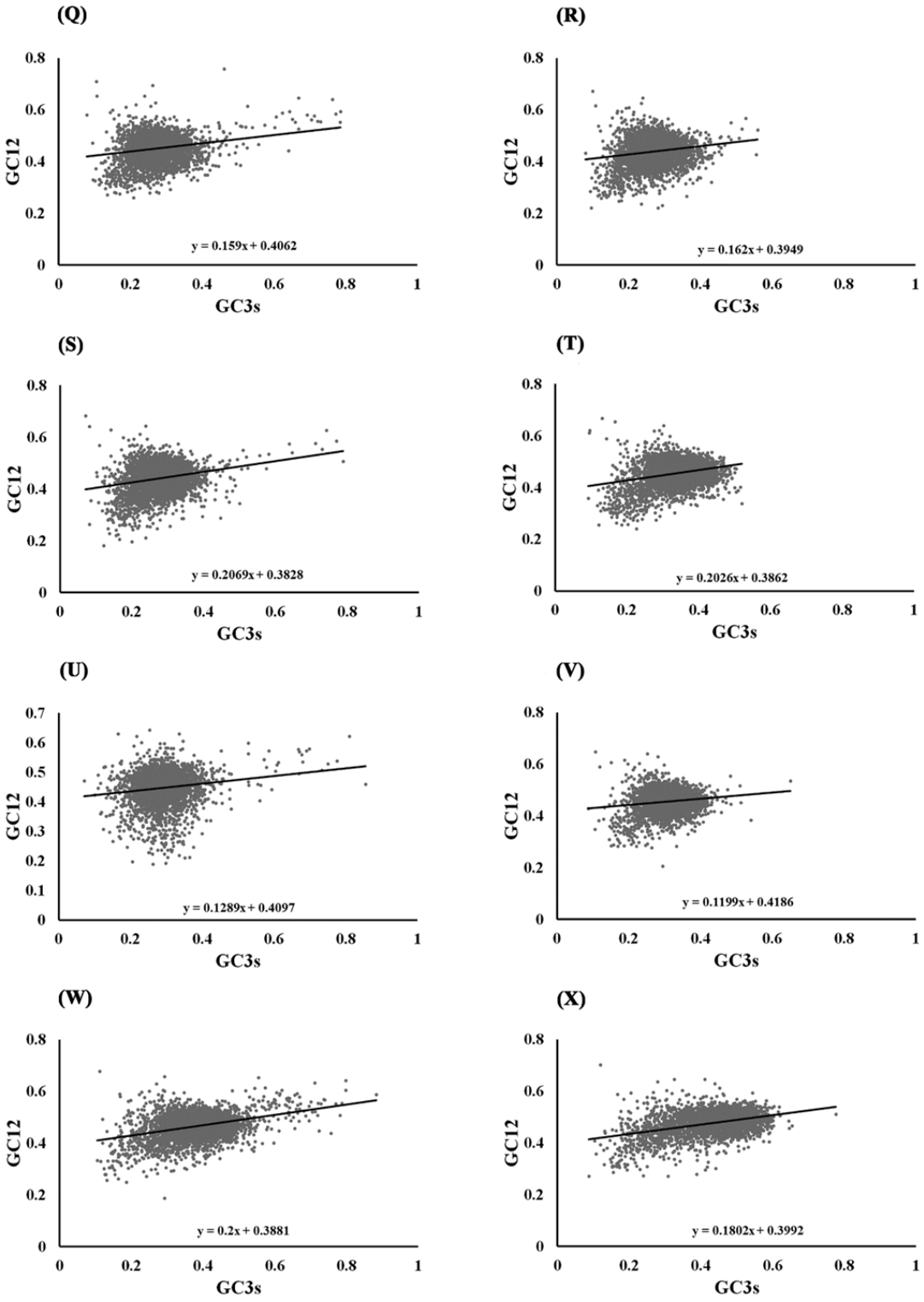
(Q)
y = 0.159x + 0.4062
(R)
y = 0.162x + 0.3949
(S)
y = 0.2069x + 0.3828
(T)
y = 0.2026x + 0.3862
(U)
y = 0.1289x + 0.4097
(V)
y = 0.1199x + 0.4186
(W)
y = 0.2x + 0.3881
(X)
y = 0.1802x + 0.3992
GC12
GC3s

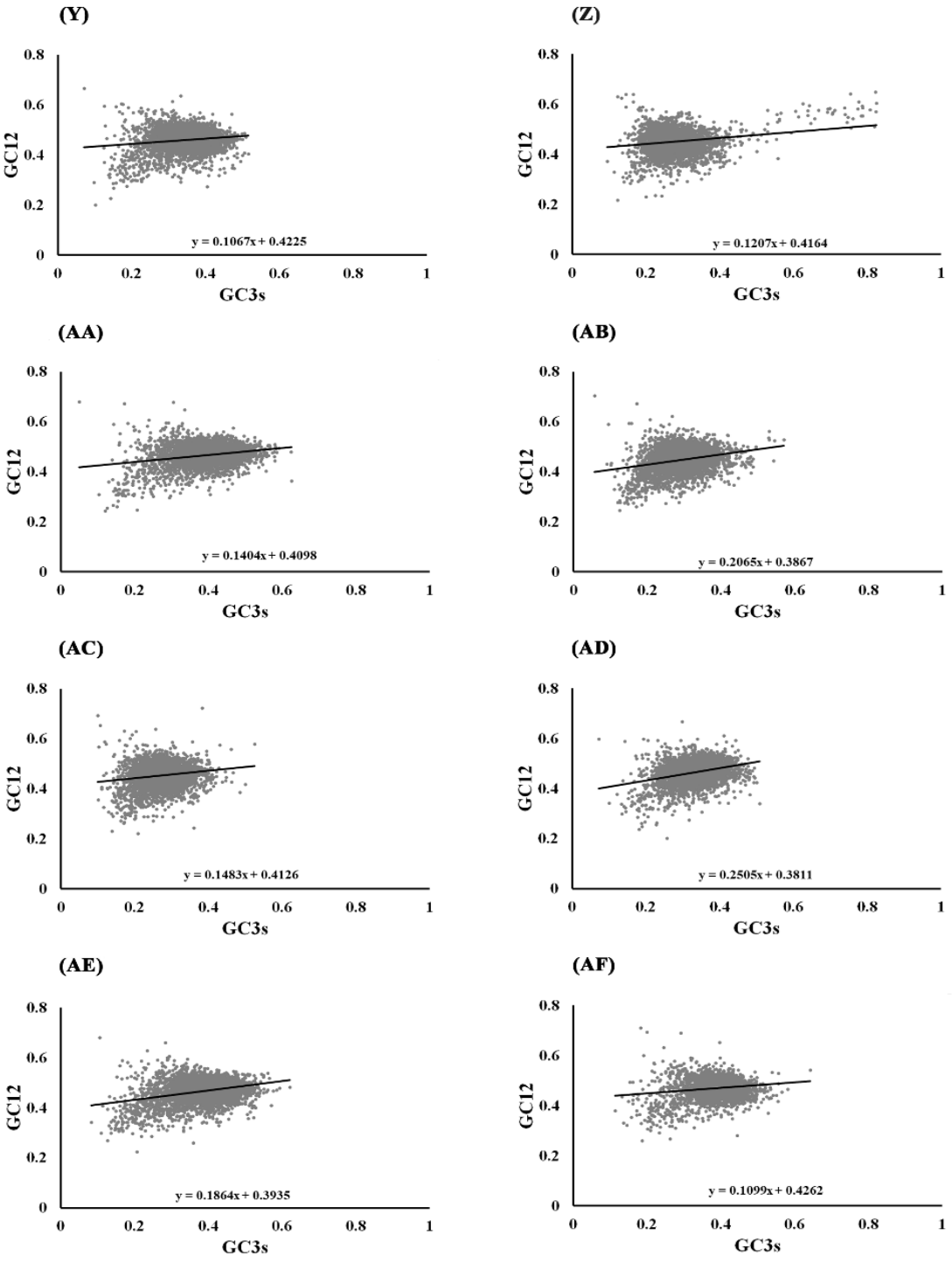
(Y)
y = 0.1067x + 0.4225
(Z)
y = 0.1207x + 0.4164
(AA)
y = 0.1404x + 0.4098
(AB)
y = 0.2065x + 0.3867
(AC)
y = 0.1483x + 0.4126
(AD)
y = 0.2505x + 0.3811
(AE)
y = 0.1864x + 0.3935
(AF)
y = 0.1099x + 0.4262
GC12
GC3s
0
0.2
0.4
0.6
0.8
1

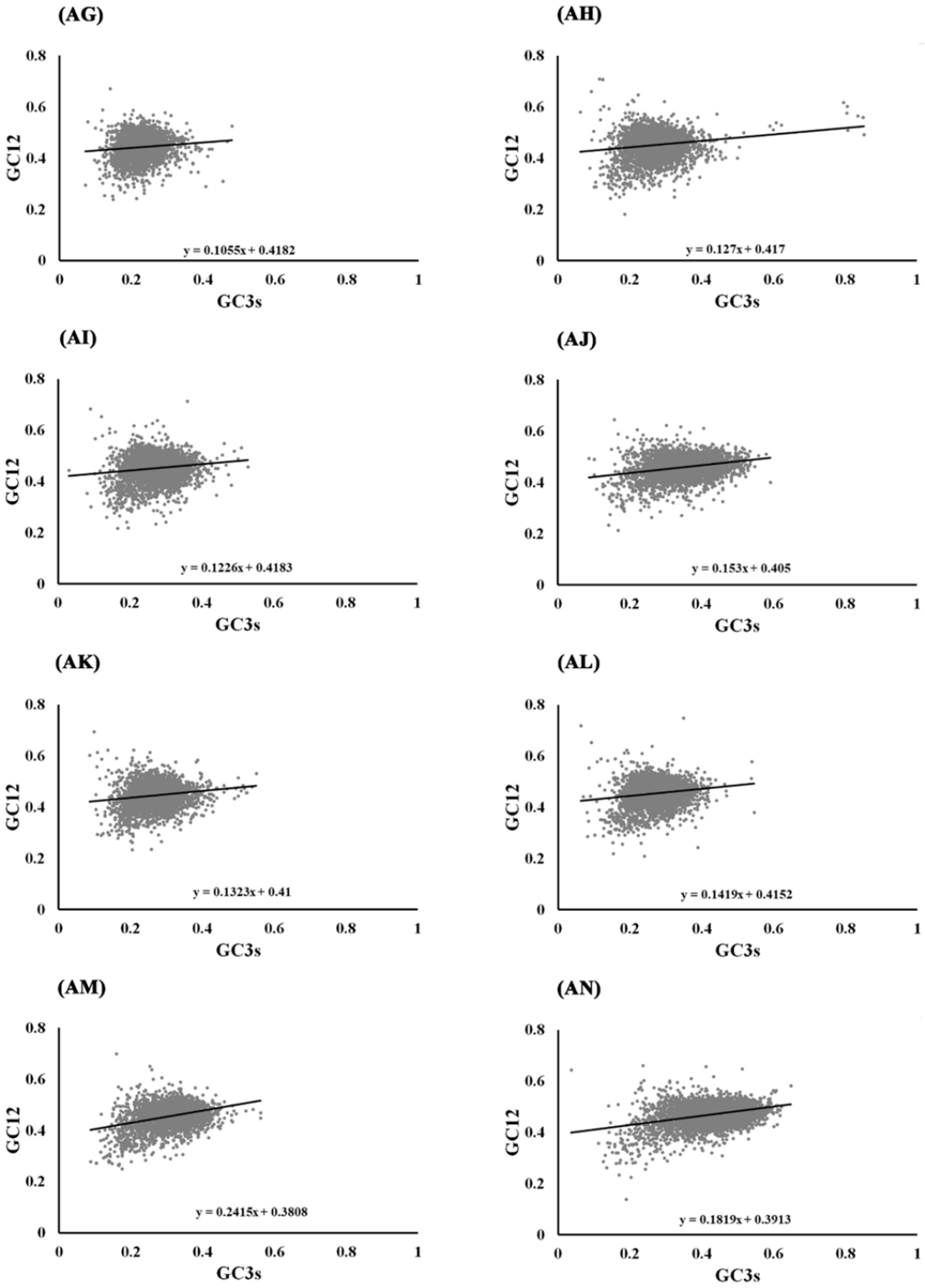
(AG)
y = 0.1055x + 0.4182
(AH)
y = 0.127x + 0.417
(AI)
y = 0.1226x + 0.4183
(AJ)
y = 0.153x + 0.405
(AK)
y = 0.1323x + 0.41
(AL)
y = 0.1419x + 0.4152
(AM)
y = 0.2415x + 0.3808
(AN)
y = 0.1819x + 0.3913
GC12
GC3s
0
0.2
0.4
0.6
0.8
1

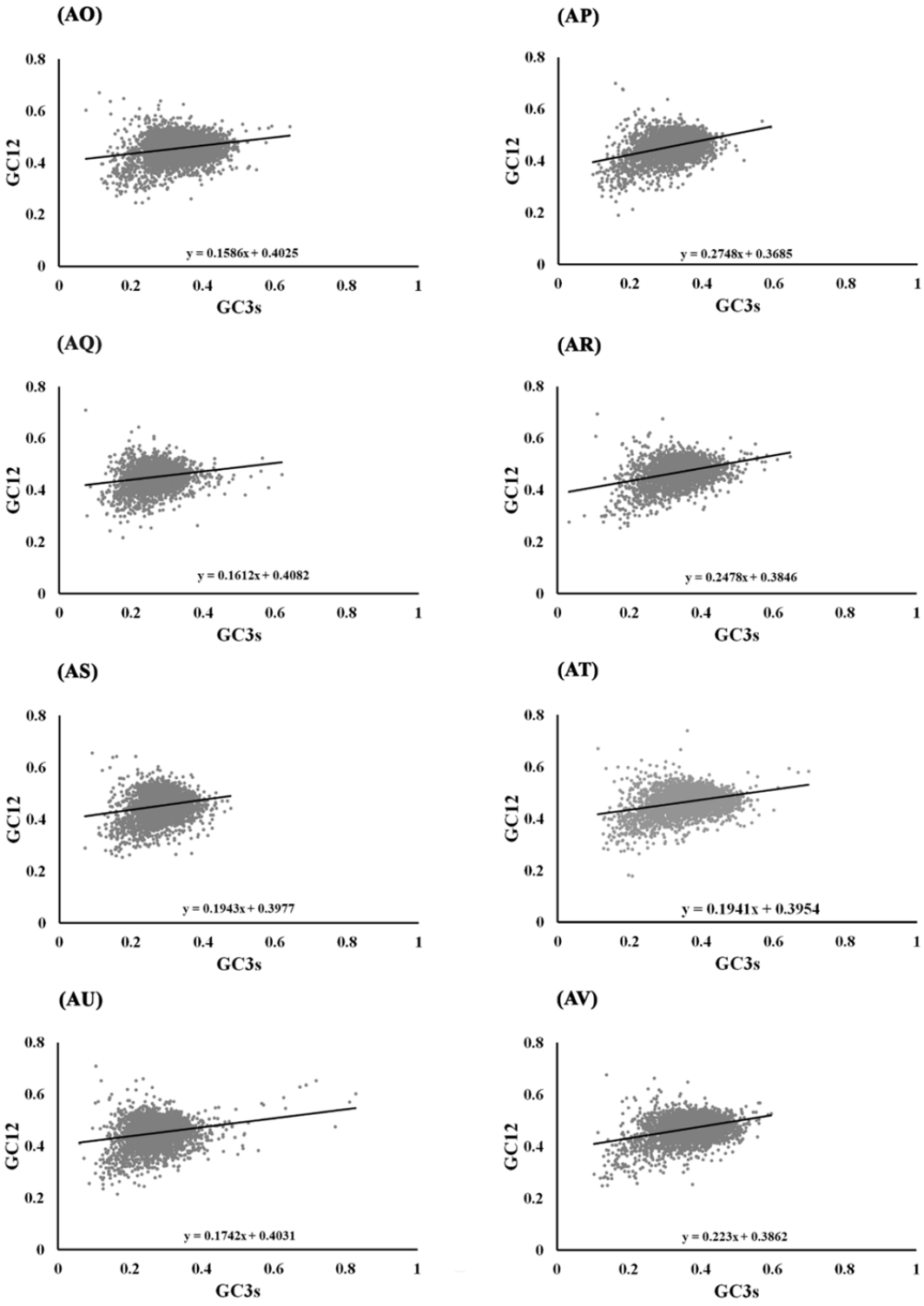
(AO)
y = 0.1586x + 0.4025
(AP)
y = 0.2748x + 0.3685
(AQ)
y = 0.1612x + 0.4082
(AR)
y = 0.2478x + 0.3846
(AS)
y = 0.1943x + 0.3977
(AT)
y = 0.1941x + 0.3954
(AU)
y = 0.1742x + 0.4031
(AV)
y = 0.223x + 0.3862
GC12
GC3s
0
0.2
0.4
0.6
0.8
1

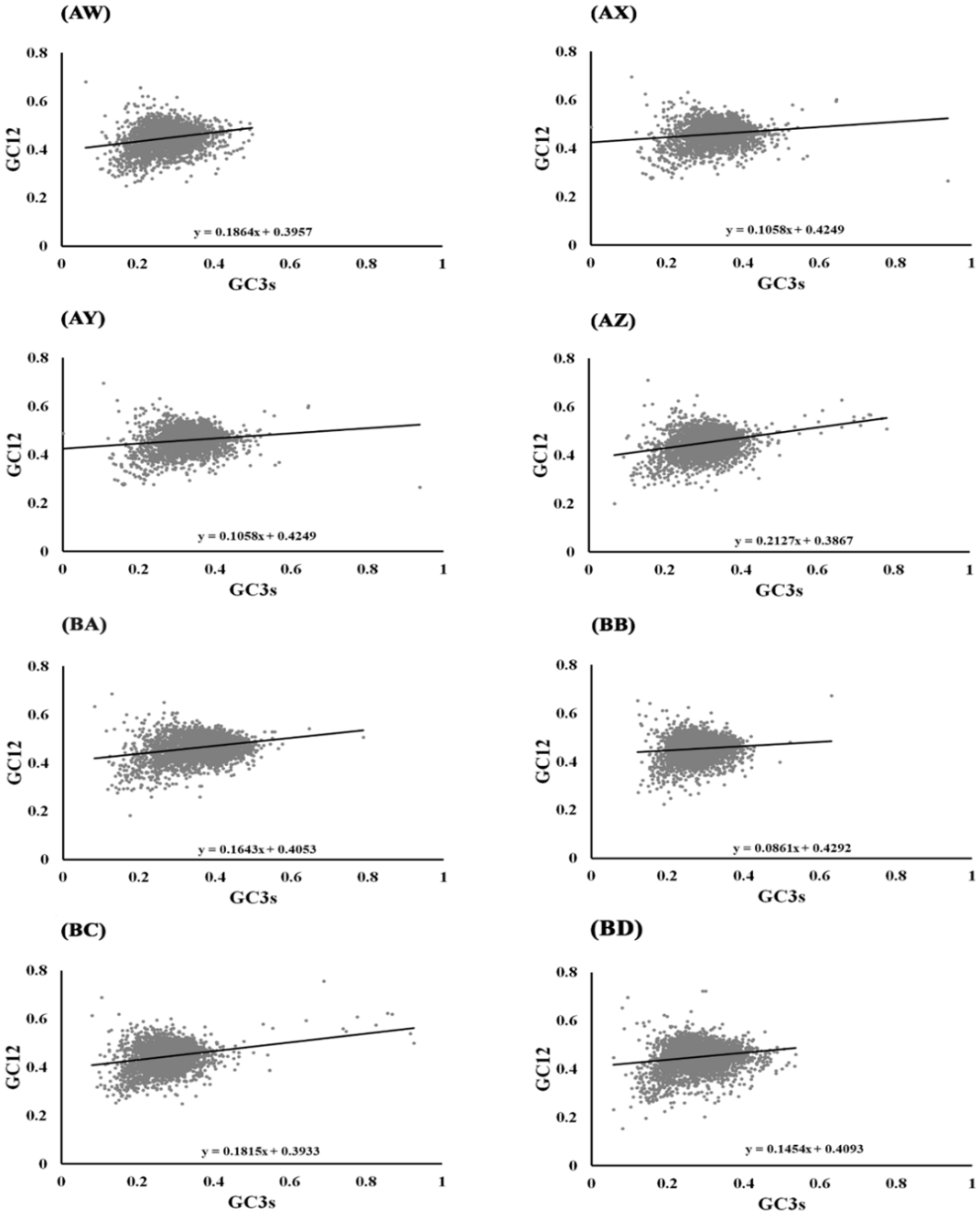

Figure 4.3: Neutral plot analysis of all the *Acinetobacter* species under investigation.

(Note: The Neutral plot graphs of the Acinetobacter species are arranged according to the table 3.1)

4.5 Insights from Parity plot analysis

Parity plot analysis was employed to estimate the bias between A or T and C or G nucleotides at the third codon position. In an ideal scenario where A equals T and C equals G at the center, the axis value would be 0.5 (Jamil et al., 2022). However, in this investigation, the mean position of x was 0.49 (suggests an AT bias) and y was 0.44 (pointing towards a GC bias) **(Figure 4.4).** All members of the ACB complex exhibited a GC bias of 0.48, except for *A. baumannii* itself, which has a slightly higher GC bias of 0.49. Similarly, the AT bias was 0.45 across all ACB complex members, except for *A. pittii*, which showed an AT bias of 0.44. In contrast, the biotechnologically significant nonpathogenic species *A. baylyi* displayed a higher GC bias of 0.52 in their genome. A bias value below 0.5 indicates a preference for pyrimidine bases (thymidine over adenine and cytosine over guanosine) (Andargie & Congyi, 2022). Therefore, it is evident that all members of the genus *Acinetoacter* favor thymidine over adenine and cytosine over guanosine in their genomic compositions except *A. baylyi.* This justifies the lower preference of AT rich favoured codons by *A. baylyi* reflecting specific adaptive strategies in the genome of *A. baylyi*, potentially related to its ecological niche or metabolic adaptations which makes it different from other pathogenic ACB members (De Oliveira et al., 2021).

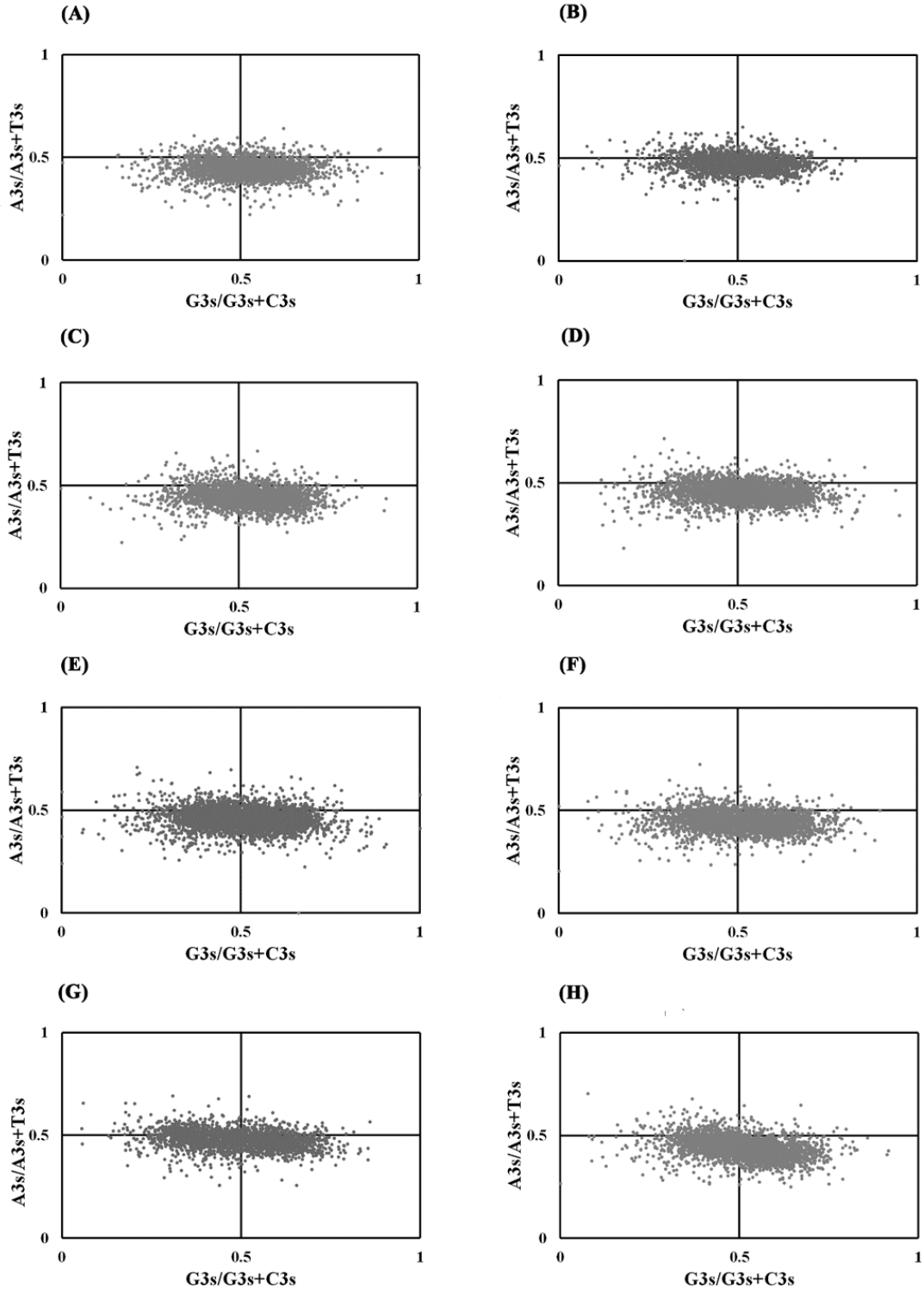
(A)
(B)
(C)
(D)
(E)
(F)
(G)
(H)
A3s/A3s+T3s
G3s/G3s+C3s
0
0.5
1

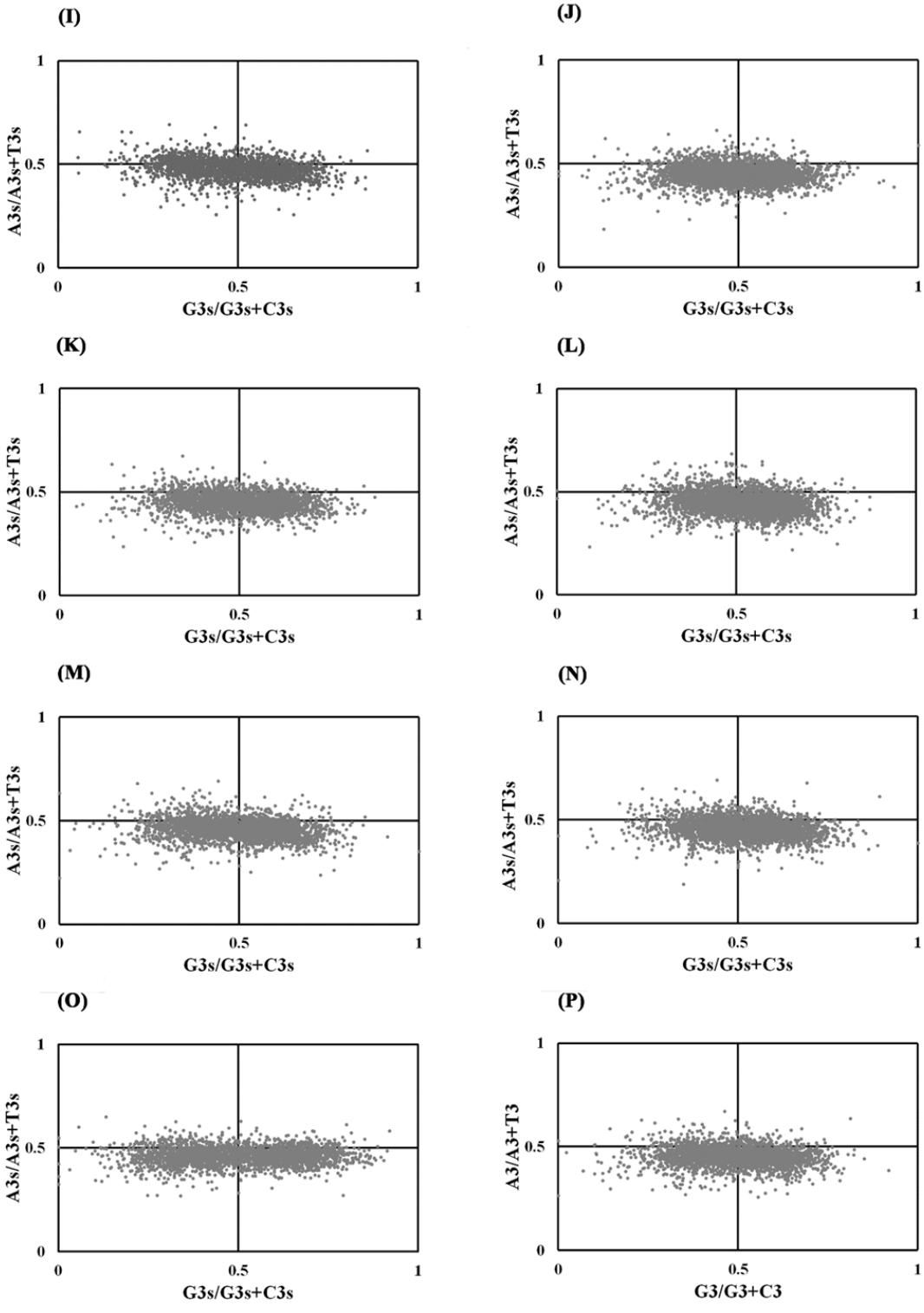
(I)
(J)
(K)
(L)
(M)
(N)
(O)
(P)
A3s/A3s+T3s
A3/A3+T3
G3s/G3s+C3s
G3/G3+C3
0
0.5
1

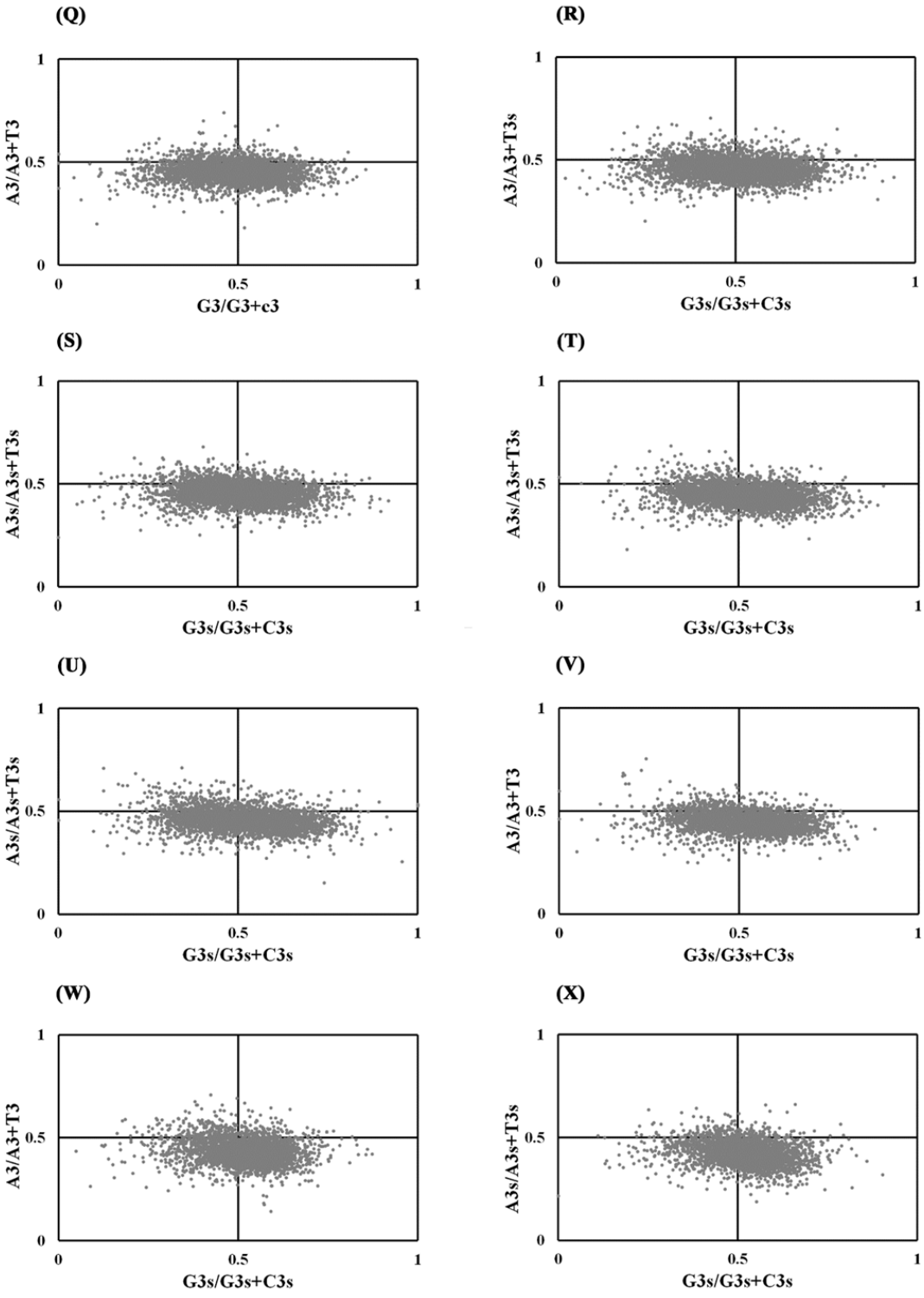
(Q)
A3/A3+T3
G3/G3+c3
(R)
A3/A3+T3s
G3s/G3s+C3s
(S)
A3s/A3s+T3s
G3s/G3s+C3s
(T)
A3s/A3s+T3s
G3s/G3s+C3s
(U)
A3s/A3s+T3s
G3s/G3s+C3s
(V)
A3/A3+T3
G3s/G3s+C3s
(W)
A3/A3+T3
G3s/G3s+C3s
(X)
A3s/A3s+T3s
G3s/G3s+C3s
0
0.5
1

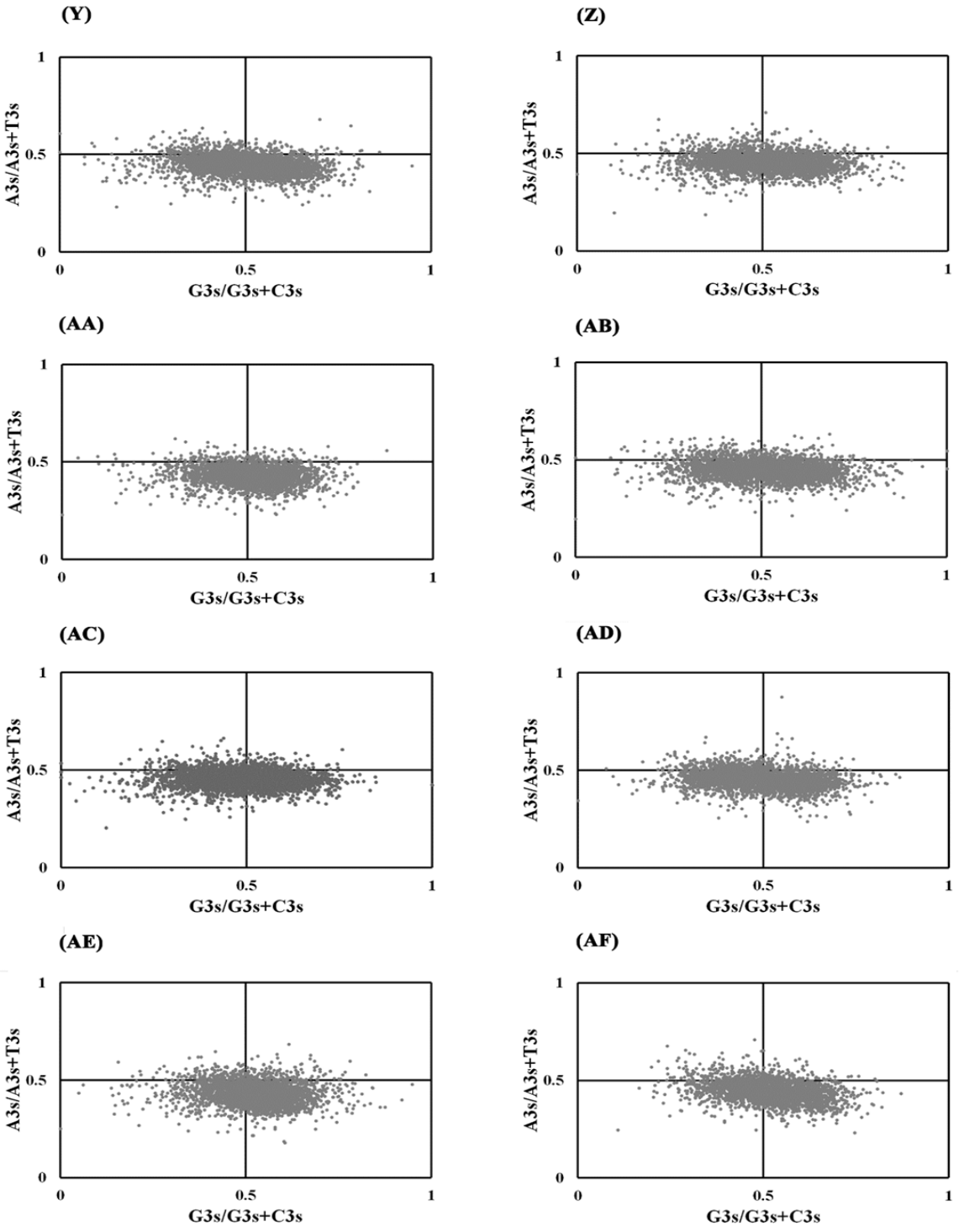
(Y)
(Z)
(AA)
(AB)
(AC)
(AD)
(AE)
(AF)
A3s/A3s+T3s
G3s/G3s+C3s
0
0.5
1

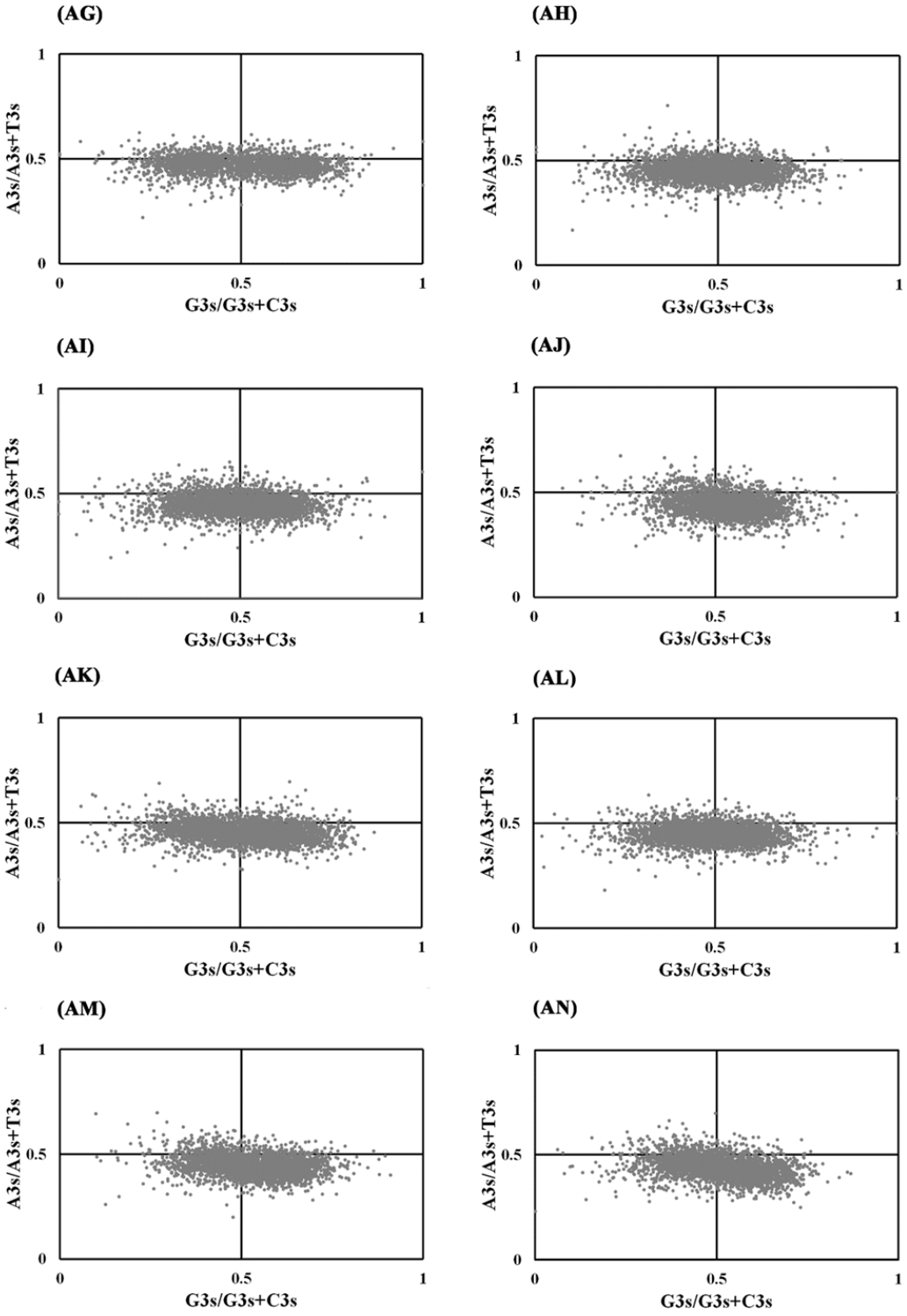
(AG)
(AH)
(AI)
(AJ)
(AK)
(AL)
(AM)
(AN)
A3s/A3s+T3s
G3s/G3s+C3s
0
0.5
1

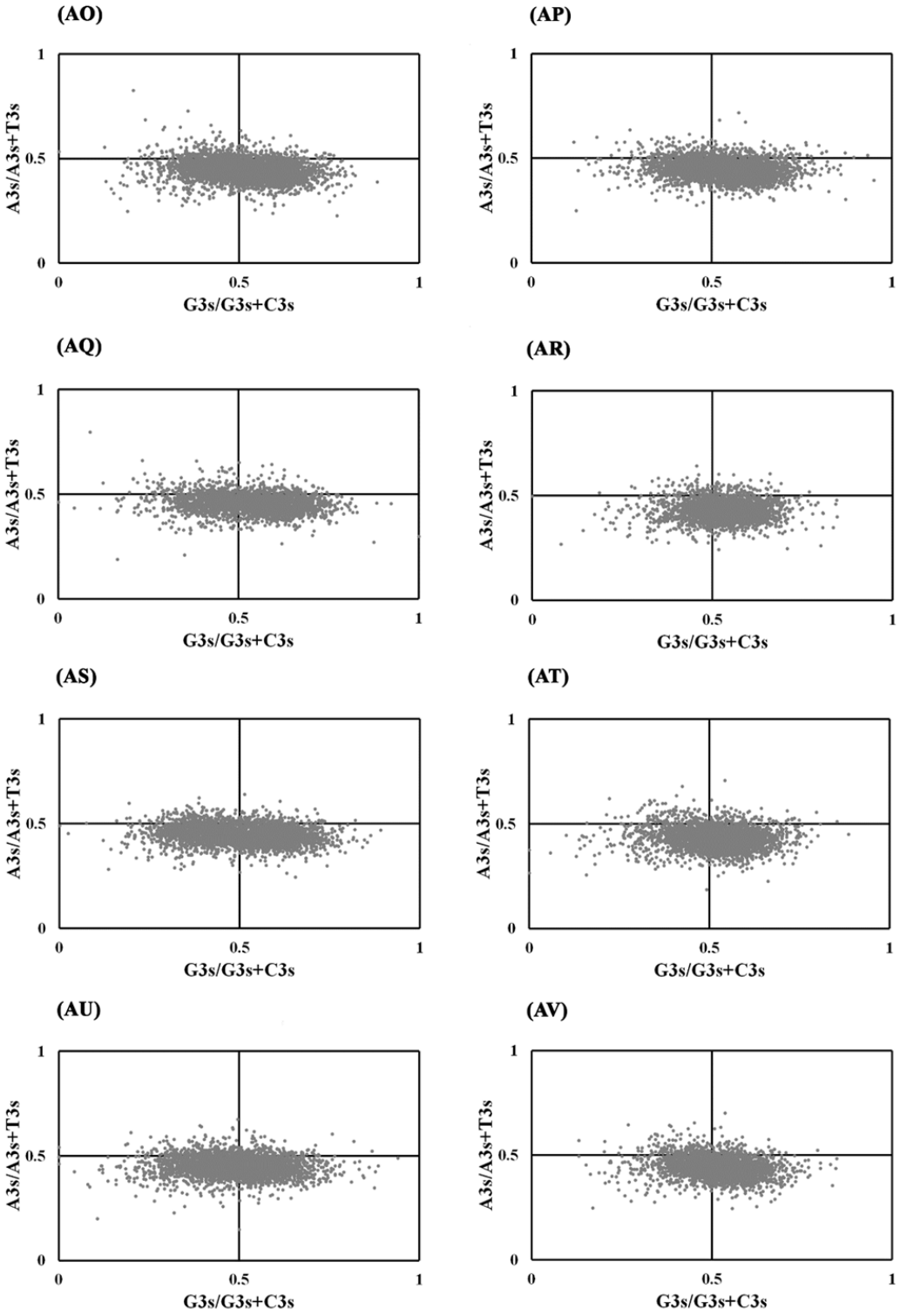
(AO)
(AP)
(AQ)
(AR)
(AS)
(AT)
(AU)
(AV)
A3s/A3s+T3s
G3s/G3s+C3s
0
0.5
1

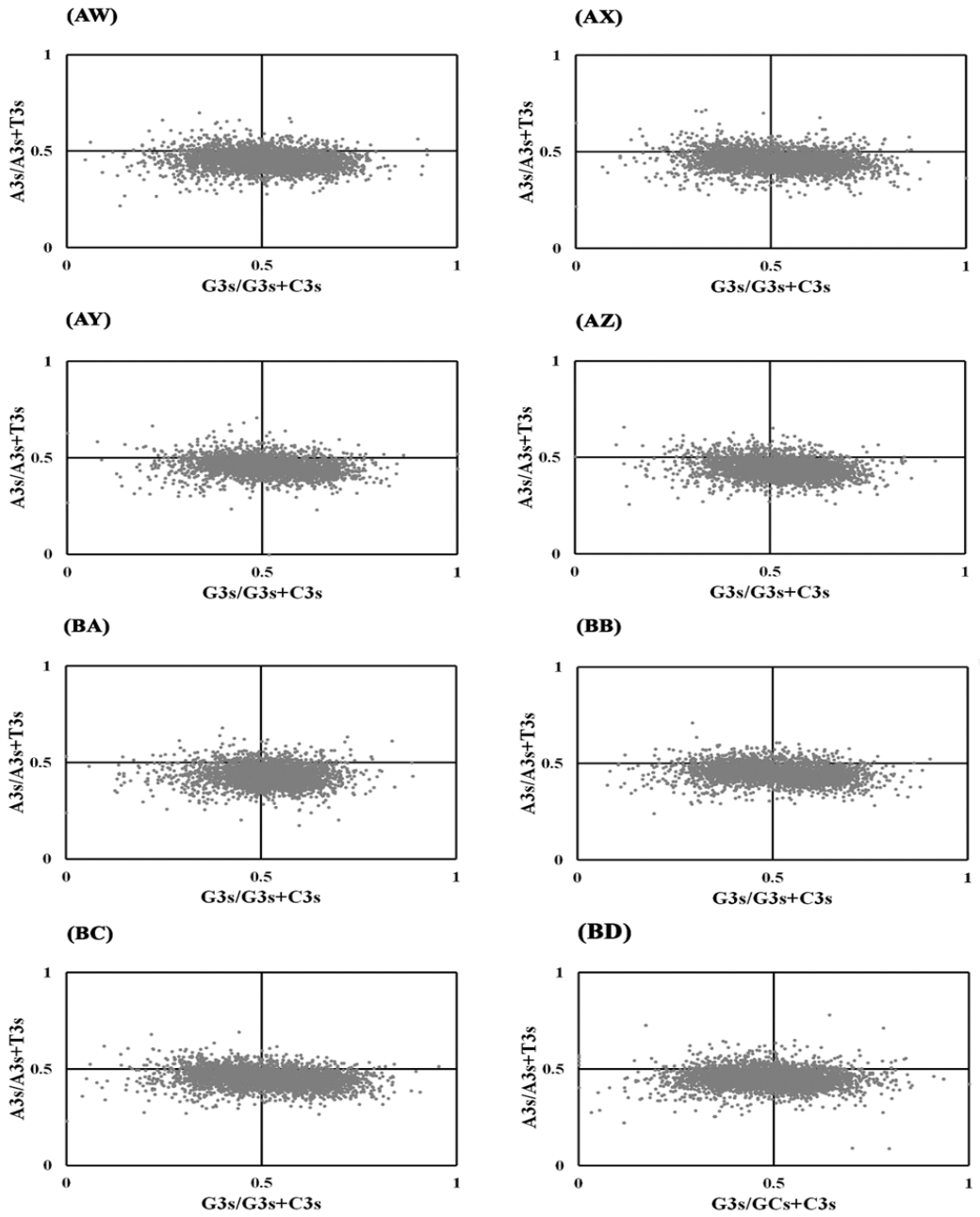

Figure 4.4: Parity plot analysis of all the *Acinetobacter* species under investigation

(Note: The parity graphs of the Acinetobacter species are arranged serially according to the table 3.1)

4.6 Insights from analysis of Translational selection

Insights from the analysis of translational selection using P2 values (Roy et al., 2015) revealed significant variation in codon usage bias across *Acinetoacter* genomes. Across all species, P2 values were notably low, ranging from 0.48 in *A. bouvetii* to 0.06 in *A. proteolyticus*, indicating a modest influence of natural selection on codon usage. However, *A. baylyi* stood out with a higher P2 value of 0.57 **(Table 4.1),** suggesting stronger translational selection pressure compared to other species within the genus. This could reflect specific adaptations related to efficient translation, gene expression regulation and environmental adaptations unique to *A. baylyi* (De Oliveira et al., 2021). Furthermore, within the ACB complex, P2 values were consistently low at 0.44 for all the members except for *A. calcoaceticus* which exhibited a even lower value (0.39). This indicates that translational selection plays a significant role in shaping codon usage across the *Acinetoacter* genus, the degree of influence varies among pathogenic and non-pathogenic species.

4.7 Insights from CAI

The assessment of gene expression levels in *Acinetoacter* genomes were conducted using the Codon Adaptative Index (CAI) parameter. CAI values were computed using a reference set comprised of genes encoding ribosomal subunits (Saha et al., 2019; Ueda et al., 2004). Among the species under investigation, CAI values ranged from 0.49 for *A. gyllenbergii* to 0.66 for *A. boissieri*. The members of ACB complex has the CAI values between 0.55-0.58 while *A. baylyi* have a CAI value of 0.59 **(Table 4.1).** In many bacterial genomes, a strong positive correlation between RSCU and RAAU with CAI indicates that genes with higher expression levels tend to utilize optimal codons more frequently (Dos Reis, 2003; Sharp & Li, 1987). In a majority of *Acinetoacter* genomes, a highly significant correlation was observed between Axis 1 and Axis 2 of RSCU and RAAU data with CAI **(Table 4.3).** This relationship suggests that natural selection favors

codons that maximize translational efficiency, reflecting the adaptation of these genus to their specific environmental and physiological requirements. Furthermore, a high negative correlation of CAI with ENC provided additional evidence of the substantial influence of gene expression on the codon usage patterns within bacterial genomes **(Table 4.5)** as a lower ENC value indicates greater codon bias towards optimal codons and suggests that selective pressure for efficient translation drives the observed codon preferences (Sharp & Li, 1987).

4.8 Insights from RSCPU

The examination of codon context patterns in bacterial genomes involved computing RSCPU values for a total of 3721 codon pairs (61 * 61), excluding Amb, Och, and Opa. A comprehensive analysis of RSCPU values displayed that *A. junii* exhibited the lowest number of overrepresented codon pairs within the genus, with 288 (the minimum among the species), while *A. marinus* had the highest at 577 (the highest among the genus). Moreover, within the ACB complex, there were relatively similar numbers of overrepresented codon pairs, ranging from 320 in *A. calcoaceticus* to 342 in *A. seifertii*. This variability suggests that different species within the same genus may employ distinct strategies in codon pair usage, possibly reflecting evolutionary adaptations or niche-specific selection pressures (Novoa et al., 2019).

Significant variations were observed in terms of favored and unfavoured codon pairs across the species. However, the total number of highly favored and unfavoured codon pairs within the ACB complex was quite similar compared to other species **(Table 4.6).** Further investigation into the dominant dinucleotide bias at the junction (CP3-CP1) of codon pairs in *Acinetoacter* genomes revealed both similarities and differences in these preferences. All the species showed a preference for either GC or CA as overrepresented pairs, and most species favored CG or GT as underrepresented pairs. However, species like *A. towneri* and *A. marinus* preferred TC and TA as the most overrepresented pairs,

respectively **(Table 4.7 and 4.8).** These preferences potentially reflect differential mRNA secondary structures, translational efficiency and interactions with specific tRNA pools, all of which are critical for cellular adaptation and fitness. (De Oliveira et al., 2021; Novoa et al., 2019).

A very similar pattern of codon pair preferences was found among the ACB complex. All the species within the ACB preferred the GC codon pair, followed by CT as the most preferred codon pair. The third most preferred codon pair was CC in all ACB members. This consistent preference for GC and CT as the top two codon pairs across all species suggests a shared adaptive strategy. Similarly, the most avoided codon pair across the ACB complex was GC, followed by GG and CC, except in the case of *A. baumanni*, which avoided GG more than the CC codon pair **(Table 4.7 and 4.8).** The uniform avoidance of these codon pairs underscores their potential detrimental effects on translation or mRNA stability in these bacteria (De Oliveira et al., 2021; Novoa et al., 2019).

Table 4.6: Most favoured and most avoided codon pairs for all the species under investigation.

Organism	**Most favoured codon pair**	**CPS mod**	**Most avoided codon pair**	**CPS mod**
A. albensis	AGG-AGG	2.5331	CCG-GAG	-4.0611
A. apis	AGG-CTG	2.50593	ACC-TGG	-4.9281
A. baumannii	AGA-AGG	1.93903	CCC-TGG	-3.6696
A. baylyi	TCC-AGA	2.53697	CCG-GAG	-5.8385
A. beijerinckii	GGG-CGA	1.77586	ACC-GGG	-6.2357
A. bereziniae	GCC-AAT	1.69652	GGC-CAA	-4.5296
A. bohemicus	AGA-AGG	2.24215	GCC-TGG	-4.747
A. boissieri	CGC-CGT	2.01773	TGC-GGG	-4.237

Table 4.6: Continued

Organism	**Most favoured codon pair**	**CPS mod**	**Most avoided codon pair**	**CPS mod**
A. bouvetii	CTC-AGC	2.20731	CGT-CGG	-4.9499
A. brisouii	ATA-AGG	2.08642	ACC-GGC	-4.9221
A. calcoaceticus	AAG-CTC	1.38834	GCC-AGG	-3.3337
A. celticus	AGG-CGA	1.92159	GTC-CGG	-4.3125
A. colistiniresistens	TTA-AGA	1.62333	CCG-GAG	-4.3113
A. cumulans	AGA-AGG	3.40729	GCC-CGG	-4.4944
A. defluvii	AGA-AGG	2.92907	TTC-CGG	-3.8047
A. equi str. 114	CCC-TCG	2.27348	TCG-GCC	-3.8022
A. gandensis	AGA-AGG	2.33945	AGA-CAC	-3.731
A. genomosp.33YU	AGG-AGG	2.07686	ACC-TGG	-2.9358
A. gerneri	AGA-CGG	1.97171	CCG-GCG	-5.3755
A. guillouiae	AGG-AGG	2.20222	CCG-GCG	-3.454
A. gyllenbergii	AGG-AGG	1.92483	CCG-GAG	-4.447
A. haemolyticus	AGG-AGG	2.31209	CCG-GAG	-3.1875
A. halotolerans	AGG-AGG	3.07884	TCC-TGG	-5.1206
A. idrijaensis	AGG-AGG	2.06565	GGG-TCC	-3.3917
A. indicus	AGA-AGA	3.02993	CGG-TAC	-5.449
A. johnsonii	AGG-AGG	2.23479	ACC-GGG	-3.6508
A. junii	ATA-AGG	1.73409	TCC-GGG	-4.2075
A. kookii	TCC-AGG	2.58281	CGG-TGT	-4.1355
A. kyonggiensis	AGA-AGG	1.78311	CCG-GCG	-5.3734
A. lactucae	AGG-CCC	1.67628	TCC-TGG	-4.9186
A. larvae	AGG-AGG	2.64337	GGC-CAC	-4.8825
A. lwoffii	ATA-AGG	2.90111	AGG-GGC	-4.1912

Table 4.6: Continued

Organism	**Most favoured codon pair**	**CPS mod**	**Most avoided codon pair**	**CPS mod**
A. marinus	CCG-GGA	2.05606	GCC-TGG	-4.5375
A. nectaris	AGG-AGG	1.83792	AGG-CGC	-2.9999
A. nosocomialis	AGA-AGG	1.68991	TCC-TGG	-3.9719
A. oleivorans	CTC-AGG	2.33315	GCC-GGG	-5.6873
A. parvus	CGG-CGG	2.39887	ACC-GGG	-5.2188
A. piscicola	ATA-CGG	1.72672	TCC-TGG	-4.8103
A. pittii	TCC-AGA	2.09935	CTG-CAG	-6.8834
A. populi	CTC-AGC	2.13633	AGG-TGG	-3.5436
A. pragensis	AGA-AGG	1.87998	GCC-CGG	-3.6745
A. proteolyticus	TCC-AGA	2.22215	CTG-CAG	-6.8797
A. puyangensis	TCC-AGA	2.90773	CTG-CAG	-3.8874
A. qingfengensis	CTC-AGG	2.32147	AAG-AGG	-3.09
A. radioresistens	AGA-AGG	1.75393	CCC-TGG	-5.7239
A. rudis	AGA-AGA	2.31002	TCG-TAC	-1.8013
A. schindleri	TGC-TGC	1.59023	CTC-CGG	-3.5139
A. seifertii	TTC-AGG	2.54338	GGG-TCC	-3.5863
A. soli	AGA-AGG	1.75702	ACC-GGC	-4.1435
A. tandoii	ATA-AGG	1.75861	ACC-GGG	-5.2148
A. tjernbergiae	AGG-AGG	3.68161	ACC-GGG	-5.0479
A. towneri	TCC-AGA	2.49808	CTC-CGG	-4.2661
A. ursingii	CTC-AGG	1.91931	GGG-TCC	-3.307
A. variabilis	GGG-CGG	1.59508	ACC-TGG	-5.9501
A. venetianus	AGA-AGG	3.67466	GGC-CTC	-5.7531
A. wuhouensis	AGA-ATA	2.23958	GGC-CTC	-7.8047

Table 4.7: Percentage of Over- represented nucleotides of all the *Acinetobacter* species under investigation

Organisms	**Over-represented nucleotides at Codon Pair Junction**				
A. albensis	CA	GC	AC	CT	GA
	19.90	18.66	8.71	8.21	8.21
A. apis	GC	CA	TG	AC	CC
	23.56	18.77	10.34	8.05	7.09
A. baumannii	GC	CT	CC	CA	GG
	22.15	12.92	12.92	8.92	8.31
A. baylyi	CA	GC	CT	AC	GA
	21.47	19.90	11.26	8.64	7.85
A. beijerinckii	GC	CA	GA	CT	TG
	18.32	14.66	10.73	9.95	7.07
A. bereziniae	CA	GC	GA	CT	AC
	19.42	17.59	10.50	9.45	8.40
A. bochemius	GC	CA	AC	CT	CC
	17.42	16.74	10.18	8.60	7.92
A. boissieri	GC	CA	CC	AC	CT
	18.83	15.27	11.92	11.30	10.25
A. bouvetti	GC	CA	AA	TT	TG
	25.87	14.39	10.20	9.47	9.29
A. brisouii	CA	GC	TG	CT	AC
	17.87	15.96	11.49	8.94	8.30
A. calcoaceticus	GC	CT	CC	GG	CA
	22.81	14.69	10.63	10.31	10.00
A. celticus	GC	CA	CC	AC	AA
	20.60	16.90	9.49	9.26	7.18

Table 4.7: Continued

Organisms	**Over-represented nucleotides at Codon Pair Junction**				
A. colistiniresistens	CA	CT	GC	TG	AC
	65.00	53.00	46.00	45.00	36.00
A. cumulans	GC	CA	CT	AC	CC
	26.29	16.20	8.69	8.45	7.04
A. defluvii	GC	CA	AC	TG	GA
	19.81	17.87	11.59	8.70	8.45
A. equi	GC	CT	CA	GA	CC
	22.84	15.23	13.20	11.42	9.39
A. gandensis	GC	CA	AC	CT	TG
	21.31	14.53	10.90	9.44	7.99
A. genomosp33YU	GC	CT	CA	CC	AA
	24.92	11.50	10.54	10.22	8.31
A. generi	GC	CA	GA	CT	TG
	18.58	14.18	12.71	9.29	7.58
A. guillouiae	GC	CA	CT	GA	AC
	17.16	16.67	10.78	9.80	8.09
A. gyllenbergii	CA	GC	CT	AC	TG
	15.68	13.64	13.18	9.77	9.32
A. haemolyticus	CA	GC	GA	CT	AA
	17.63	16.35	12.18	11.86	8.65
A. halotolerans	CA	GC	CT	GA	AC
	14.90	14.04	11.46	10.60	10.03
A. idrijaenesis	CA	CT	GC	AC	CC
	16.71	14.08	13.13	9.31	7.64
A. indicus	GC	CA	CT	AC	AA
	13.94	13.94	10.97	10.97	8.36

Table 4.7: Continued

Organisms	**Over-represented nucleotides at Codon Pair Junction**				
A. johnsonii	GC	CA	AC	CT	TG
	15.47	14.13	13.00	11.43	8.07
A. junnii	CA	GC	GA	CT	AC
	19.10	18.40	14.93	11.11	8.68
A.kookii	CA	GC	CT	TT	CC
	18.29	14.43	11.79	9.15	8.33
A. kyonggiensis	CA	GC	CT	AC	CC
	18.40	18.16	9.44	8.96	7.51
A. lactucae	GC	CT	CC	CA	GG
	22.42	14.55	11.52	9.39	8.48
A. larvae	GC	CA	AC	CT	TG
	17.76	14.04	13.82	8.99	7.68
A. lwoffii	CA	GC	CT	CC	AC
	15.63	14.02	14.02	7.82	7.82
A. marinus	GC	CA	TG	AC	CT
	15.25	14.21	12.13	11.61	9.71
A. nectaris	GC	CT	CC	CA	TG
	21.85	21.54	12.00	8.92	8.00
A. nosocomials	GC	CT	CC	CA	GG
	23.08	13.61	12.13	9.76	7.99
A. oleviorans	GC	CT	CC	CA	AA
	23.64	15.76	10.61	10.00	9.09
A.parvus	CA	CT	TG	CC	GC
	18.26	12.25	11.80	9.58	9.35
A. piscicola	CA	GC	AC	TG	GA
	17.85	17.42	10.75	9.68	8.17

Table 4.7: Continued

Organisms	**Over-represented nucleotides at Codon Pair Junction**				
A. pittii	GC	CT	CC	CA	AA
	21.92	15.92	11.11	9.61	9.01
A. populi	CA	CT	AC	GG	GC
	18.91	12.17	11.96	10.65	9.78
A. pragensis	GC	CA	TT	AA	TG
	27.57	14.08	9.86	8.85	8.45
A. proteolyticus	CA	CT	GC	AC	TG
	15.62	13.35	12.59	10.58	9.57
A. puyangensis	CA	AC	CT	GG	GC
	20.62	11.53	10.42	10.42	10.20
A. qingfengensis	CA	GC	GG	CT	TG
	24.62	13.08	11.79	10.51	8.46
A. radioresistens	CT	CA	GC	CC	GG
	18.72	17.98	17.00	13.79	7.39
A.rudis	GC	CA	CT	GA	AC
	14.78	14.78	14.52	12.10	11.56
A. schindleri	CT	CA	GC	CC	TG
	17.08	16.34	12.87	8.91	8.42
A. seifertii	GC	CT	CC	CA	AA
	23.10	14.04	10.82	9.94	7.60
A. soil	GC	CA	CT	AC	AA
	22.59	19.80	9.39	8.88	7.87
A. tandoii	CA	GC	CT	AC	CC
	21.08	17.30	10.27	8.11	7.03
A. tjernbergiae	CA	GC	CT	TG	AC
	15.08	13.76	13.23	9.52	9.52

Table 4.7: Continued

Organisms	**Over-represented nucleotides at Codon Pair Junction**				
A. towneri	GC	CA	AC	TG	CT
	18.98	17.86	9.59	8.65	6.39
A. ursingii	CA	GC	CT	GA	TG
	19.18	16.71	9.86	9.04	7.95
A. variabilis	CT	CA	GC	CC	GA
	15.96	14.96	13.22	9.48	7.23
A. venetianus	GC	GA	CT	CA	AA
	19.79	12.83	12.57	12.57	8.29
A. wuhouensis	CA	GC	GA	CT	AC
	14.51	14.29	12.02	9.75	9.75

Table 4.8: Percentage of under- represented nucleotides of all the *Acinetobacter* species under investigation.

Organisms	**Under-represented nucleotides at codon pair junction**				
A. albensis	CC	CG	TA	GT	GG
	14.84	13.54	12.80	11.13	10.02
A. apis	CG	GG	TC	CC	TA
	20.96	18.92	11.50	11.13	9.83
A. baumannii	CG	CC	GG	GT	TC
	16.96	11.45	11.45	10.79	9.91
A. baylyi	CC	CG	TA	GT	GG
	16.64	13.95	11.45	10.02	9.84
A. beijerinckii	CC	GG	CG	TA	GT
	16.10	13.06	11.99	11.27	10.02

Table 4.8: Continued

Organisms	**Under-represented nucleotides at codon pair junction**				
A. bereziniae	CG	TA	GC	GT	CT
	18.84	14.18	12.87	10.82	10.45
A. bochemius	CG	CC	GT	TA	GG
	16.64	12.52	11.53	10.71	10.54
A. boissieri	CG	TC	GG	CC	GA
	18.71	14.62	12.13	11.40	9.80
A. bouvetti	AC	TC	TA	GT	CG
	12.84	12.59	12.10	11.61	10.51
A. brisouii	CG	CC	TA	GG	TC
	14.70	11.67	11.52	10.91	10.15
A. calcoaceticus	CG	GG	CC	TA	GT
	17.57	13.88	11.50	9.98	9.11
A. celticus	CG	CC	TC	GG	TA
	16.37	14.26	13.20	10.04	9.68
A. colistiniresistens	CG	GT	TA	CC	GG
	103.00	73.00	71.00	68.00	53.00
A. cumulans	CG	TC	CC	GG	TA
	16.07	13.85	12.31	10.60	9.91
A. defluvii	CG	CC	GG	TC	TA
	19.68	11.55	11.55	11.37	11.19
A. equi	CG	GG	CC	GT	TA
	22.39	14.86	12.29	8.62	8.44
A. gandensis	CG	GG	CC	TA	TC
	17.90	16.16	14.85	14.63	12.88
A. genomosp33YU	CG	GG	CC	TA	TC
	17.14	15.26	12.91	11.03	10.33

Table 4.8: Continued

Organisms	**Under-represented nucleotides at codon pair junction**				
A. guillouiae	CG	TA	GT	GG	CC
	21.02	12.20	11.36	11.19	10.85
A. gyllenbergii	CG	TA	CC	GT	GG
	16.34	12.41	11.50	11.04	8.93
A. haemolyticus	CG	CC	TA	GG	GT
	16.59	14.63	13.32	12.45	10.92
A. halotolerans	CC	CG	TA	GG	GT
	14.81	14.23	13.27	12.31	10.96
A. idrijaenesis	GT	CG	CC	TA	TC
	14.94	13.60	12.84	11.69	9.39
A. indicus	CG	GT	CC	TC	GA
	14.18	11.75	11.32	10.60	10.17
A. johnsonii	CG	TA	CC	GG	TC
	17.13	11.86	11.37	11.04	10.21
A. junnii	CC	GG	CG	TA	GT
	15.42	15.42	14.95	13.79	10.98
A.kookii	CG	GT	TA	CC	GA
	15.30	13.91	12.67	10.82	10.51
A. kyonggiensis	CG	CC	GT	TC	GG
	18.36	12.76	11.36	10.84	10.31
A. lactucae	CG	GG	CC	GT	TA
	16.81	13.54	13.32	10.04	9.39
A. larvae	CC	CG	GT	TC	GG
	15.82	14.03	12.69	12.54	10.00
A. lwoffii	GT	CG	TA	CC	TC
	15.63	14.29	12.10	11.60	8.24

Table 4.8: Continued

Organisms	**Under-represented nucleotides at codon pair junction**				
A. marinus	CC	GG	TA	CG	TC
	14.62	11.77	11.40	11.03	9.17
A. nectaris	CG	GG	CC	TC	AG
	20.21	14.33	12.22	9.05	7.84
A. nosocomials	CG	GG	CC	TC	GT
	18.52	12.27	11.34	10.19	9.72
A. oleviorans	CG	GG	CC	TA	GT
	15.44	14.32	12.53	10.96	8.95
A.parvus	CG	GT	TA	CC	GA
	20.94	12.19	11.88	9.84	9.69
A. piscicola	CG	CC	TC	GG	TA
	18.48	12.22	11.03	11.03	10.58
A. pittii	CG	GG	CC	GT	TA
	15.50	12.95	12.10	10.19	9.55
A. populi	CG	GT	CC	GA	TC
	15.73	13.01	11.80	11.35	9.23
A. pragensis	GT	AC	TA	TC	CG
	12.29	12.29	12.03	11.50	10.85
A. proteolyticus	CG	TA	GT	CC	GG
	17.24	13.45	13.28	11.72	9.14
A. puyangensis	CG	GT	CC	GA	TC
	14.70	13.48	12.12	11.52	9.70
A. qingfengensis	CG	CC	GA	GT	AG
	17.46	11.90	11.90	11.75	8.57
A. radioresistens	CG	GT	TC	CC	GA
	21.28	13.56	12.43	10.36	7.34

Table 4.8: Continued

Organisms	Under-represented nucleotides at codon pair junction				
A. rudis	CG	CC	TC	GT	GG
	21.75	13.01	12.43	11.65	11.07
A. schindleri	CG	GT	CC	TA	TC
	18.62	15.08	11.17	10.06	9.12
A. seifertii	CG	GG	CC	TA	TC
	16.45	15.58	11.69	9.74	8.87
A. soil	CC	TA	GA	GG	CG
	18.29	11.50	11.32	10.28	10.10
A. tandoii	CG	GT	TA	CC	GG
	19.59	13.20	11.96	11.75	11.75
A. tjernbergiae	CG	CC	GG	GT	TA
	19.15	12.71	12.03	10.85	10.85
A. towneri	CC	TC	CG	GG	TA
	13.79	12.85	12.05	10.84	9.64
A. ursingii	CC	GT	TA	CG	GG
	16.05	12.18	12.18	11.62	9.96
A. variabilis	CG	GT	CC	TA	TC
	16.55	16.01	10.68	10.50	8.36
A. venetianus	CG	CC	GG	TA	GT
	15.05	14.86	14.67	12.95	11.62
A. whuouensis	CG	CC	GG	TA	GT
	16.33	12.63	11.86	11.71	9.40
A. generi	CG	CC	GT	TA	GG
	14.33	13.31	12.63	11.95	11.95

4.9 Insights from RAAU

Conducting a comprehensive analysis on the RAAU data, a CoA was peformed to investigate potential factors linked with variations in amino acid usage. The results of the multivariate statistical analysis revealed strong correlations between the aromaticity (Aromo) of encoded proteins and the two major principal axes (Axes 1 and 2) that separate genes based on RAAU data **(Table 4.3).** This suggests that the aromaticity of encoded proteins plays a pivotal role in shaping the overall amino acid composition across genes within the genus. Additionally, the GRAVY index, which indicates the mean hydropathic properties of a protein (positive values indicating hydrophobic, and negative values indicating hydrophilic) (Moura et al., 2013), exhibited notably significant correlations with Axes 1 and 2 of RAAU data. Furthermore, the significant correlation of GC content and Axes 1 and 2 of RAAU data underscored the substantial impact of compositional constraints on the amino acid usage patterns of the genus. **(Table 4.3).** A moderate impact of gene expression level on amino acid usage trends was revealed by the substantial correlation of CAI and RAAU data **(Table 4.3).** This suggests that genes with higher expression levels may exhibit distinct amino acid usage preferences, potentially linked to translational efficiency or protein folding requirements (Raghava & Han, 2005). The length of protein coding sequences (CDS) exhibited weak correlations with RAAU data, indicating a limited influence on amino acid usage in *Acinetoacter* **(Table 4.3).** This suggests that genes with higher expression levels may exhibit distinct amino acid usage preferences, potentially linked to translational efficiency or protein folding requirements (Raghava & Han, 2005).

Notably, it was observed that the aromaticity of the encoded gene products displayed significant moderate correlations with GC content in the majority of the species **(Table 4.5).** This emphasizes that GC content stands out as a key factor influencing the amino acid composition in an organism. This association further highlights the intricate interplay between genomic characteristics and protein biophysical properties in driving evolutionary strategies within the genus (Parvathy et al., 2022).

4.10 Insights from individual amino acid frequencies

We investigated the individual frequencies of aminoacids of all *Acinetoacter* members using CodonW program. Surprisingly, all the *Acinetoacter* members showed there preference towards leucine amino acid with the frequency ranging from 29.7 in *A. bereziniae* to 34.9 in *A. larvae.* This high prevalence of leucine suggests its importance in protein structure and function across diverse *Acinetoacter* species and can be linked to the he ability of *Acinetoacter* species to utilize leucine as a secondary metabolite, enable them to thrive in harsh, artificially created environments, (Ren & Palmer, 2023). Similarly, the frequency of alanine across all the members ranged from 24.08 in *A. bereziniae* to 31.6 in *A. larvae.* Alanine being a major component of peptidoglycan (bacterial cell wall) justifies the higher frequency across all *Acinetoacter* genomes (Trivedi et al., 2018). Moreover, cysteine and tryptophan amino acids were noted with extremely low frequencies across all the members of the genus. The frequency of cysteine ranged from 2.75 in *A. haemolyticus* to 3.29 *in A. larvae* while the frequency of tryptophan amino acid ranged from *3.66* in *A. haemolyticus* to .27 in *A. larvae* respectively **(Figure 4.5).** The lowest frequencies of amino acids like Tryptophan and cysteine can be linked to efficient energy costing as synthesis of tryptophan like aminoacids require higher amount of energy (Akashi & Gojobori, 2002).

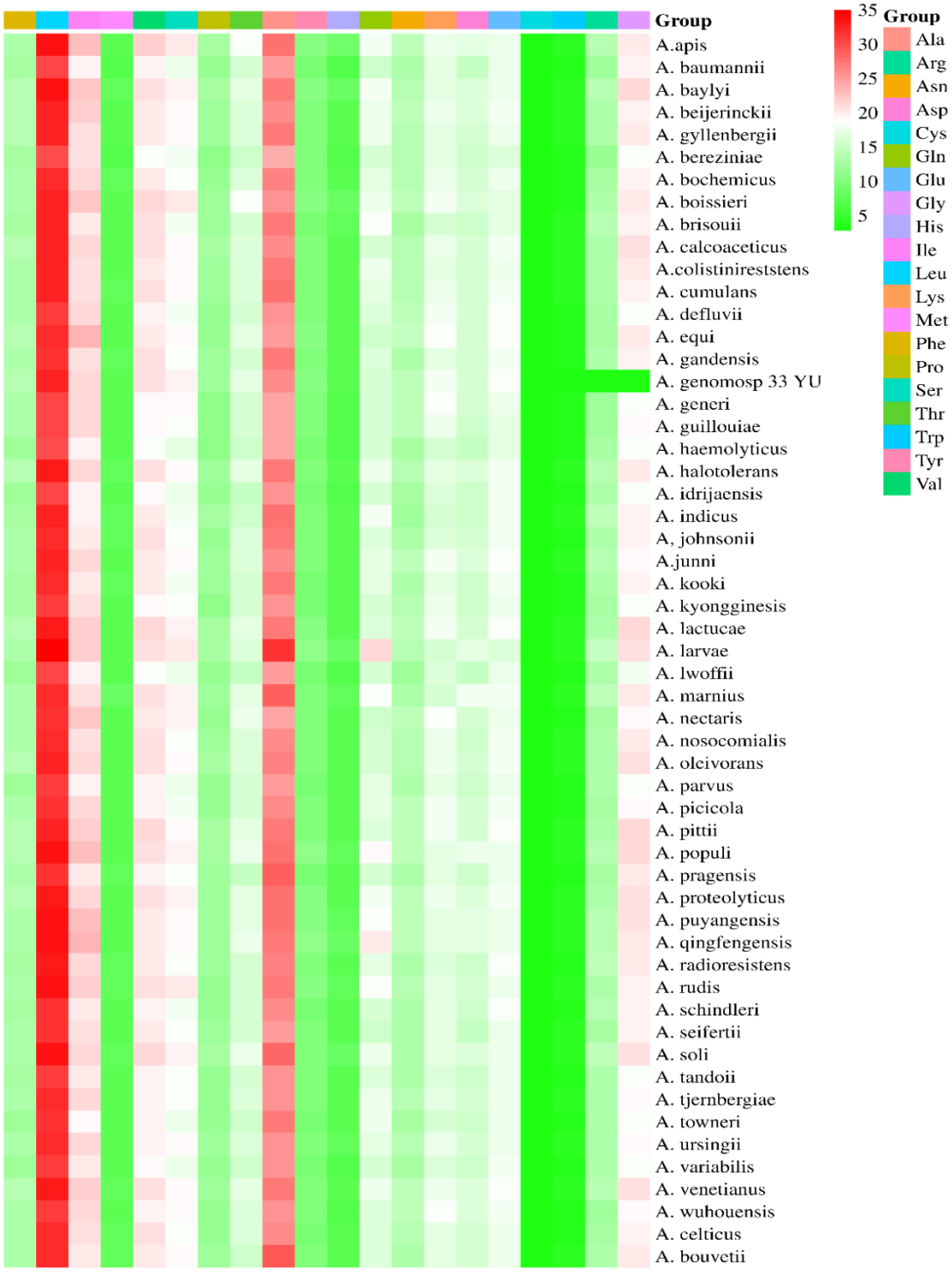

Figure 4.5: Heatmap of Amino-acids frequency of all the *Acinetobacter* species under investigation.

4.11 Insights from *gyrB* sequence alignment and phylogeny

The B component of the DNA gyrase, encoded by the *gyrB* gene has been employed as a phylogenetic marker for a number of bacterial taxon (Peeters and Willems 2011). Firstly, we studied the *gyrB* sequences alignment across all the members of the genus. We found that most of the members of genus have gaps (-----) in the alignment **(Figure 4.6)**, which indicate a variation in the start site or a sequencing gap. The beginning of protein synthesis is indicated by the codon "ATG". *A. albensis* and *A. marinus* were only the species which does not have any gap in the beginning of the alignment. The alignment red and blue colour correspond to locations that are highly (> 90% conserved) and weakly (> 50% conserved), meaning all the species share the same amino acid composition. The genetic diversity in these genomes are highlighted by the variation in the sequences indicated by black (neutral) colour **(Figure 4.6).** The average percentage identity matrix was found to be 83.16 % across the species.

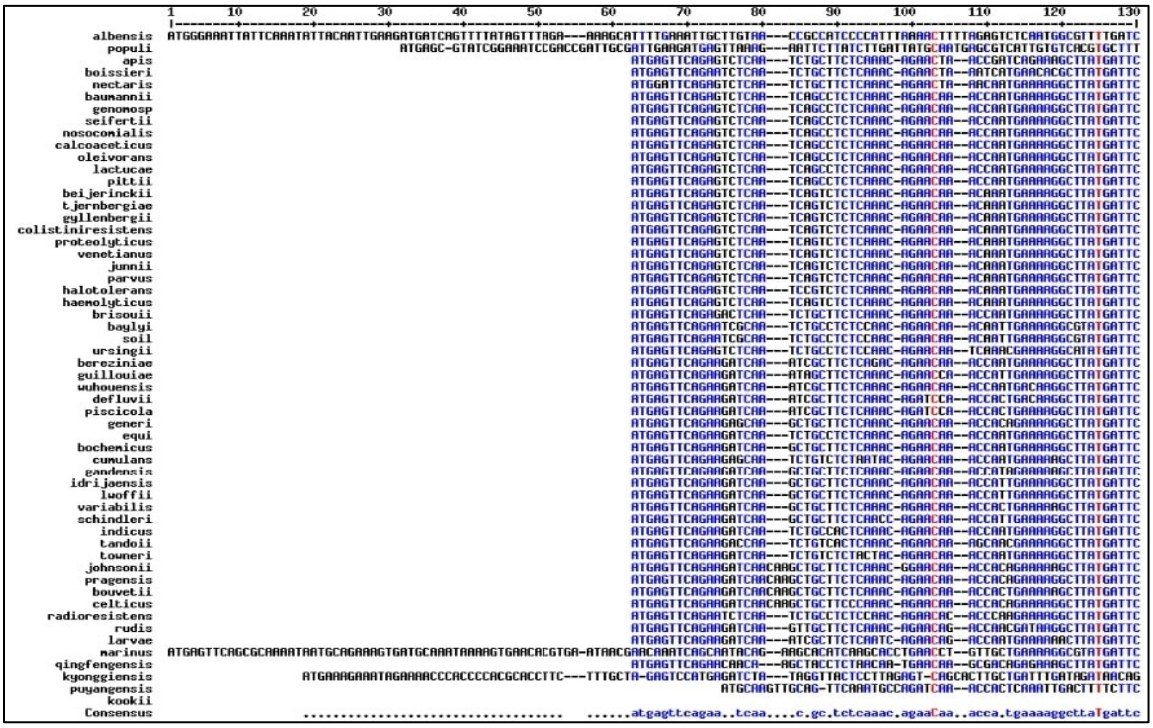

Figure 4.6: *gyrB* sequence alignment of all the *Acinetobacter* species under investigation.

Similarly, we used *gyrB* gene sequence as a phylogenetic marker to deduce the phylogeny of the whole genus *A.* and found that *A. populi* is a terminal node (sequence) with a branch length of 0.392716. The first branch contains a nested structure of internal nodes and terminal nodes, including sequences like *A. marinus, A. larvae, A. qingfengensis* and so on. The second branch contains sequences like *A. apis, boissieri, A. rudis* and so on. Each internal node represents a hypothetical common ancestor and the numbers following colon represents the branch length, which is a measure of evoluntary distance. The tree is rooted, meaning it has a starting point (often an outgroup or a distinct ancestor) **(Figure 4.7).** In the figure, the root is the node connecting *A. populi* and the rest of the tree.

The members of ACB complex were comparatively near to each other relative to genetic distance. *A. lactucae* genetic distance from its parent taxon is 0.01191 followed by *A. pittii* and *A. calcoaceticu*s with a distance of 0.01402 and 0.03028 respectively. *A. calcoaceticus* is a taxon, and the genetic distance indicates a higher level of evolutionary divergence from its parent taxon, compared to *A. lactucae* and A. *pittii*. The next member of ACB complex, *A. oleivorans* have a genetic distance of 0.2966 from its parent taxon. The main pathogenic species *A. baumannii* with a higher genetic distance of 0.045, suggest a more significant evolutionary divergence from its parent taxon compared to *A. calcoaceticus* and *A. oleivorans*. *A. nosocomialis* is a subtaxon or species within the *A. baumannii* taxon. The genetic distance reflects its evolutionary divergence within A. *baumannii group. A. seifertii* is another taxon at a similar hierarchical level to Genomosp, sharing a common parent taxon **(Figure 4.7).** All the members of ACB complex were also close to each others in terms of codon usage signatures. Therefore, we can say that the codon usage trends in these species have significant effect during the phylogenetic evolution of the genus.

Similarly, the genetic distance of *A. apis* and *A. nectaris* was found to be 0.124604 and 0.122605, while the genetic distance of A. boissieri was reported to be 0.13216. Since the presence of these species have been confirmed in flowers and insects particularly

honeybee, their genetic distance was relatively closed to each other as evident by results **(Figure 4.7).** This suggest that the evolutionary divergence of this genus is dependent on the molecular strategies employed by *Acinetoacter* in adapting to various ecological niches and environmental challenges (Touchon et al., 2014).

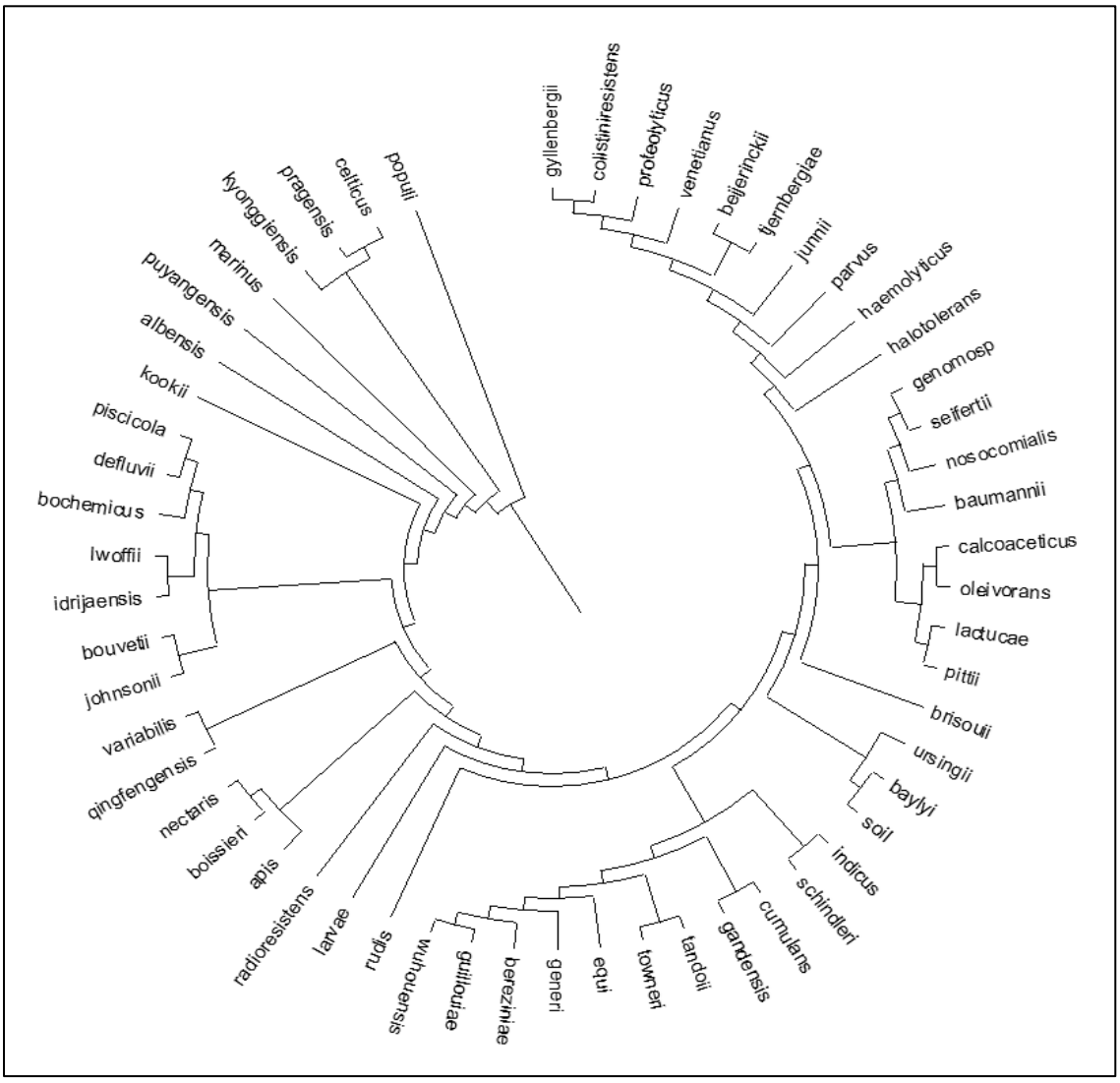

Figure 4.7: gyrB sequence phylogeny of all the *Acinetobacter* species under investigation

4.12 Whole genome sequencing of *A. baumannii* and *A. baylyi*

Molecular identification confirmed sample 1425 as *A. baumannii* and sample 9822 as *A. baylyi*. Whole-genome sequencing generated 12,508,241 and 15,363,662 raw reads for samples 1425 and 9822, respectively. Robust mapping to the reference genome, *A. baumannii* strain K09-14, showcased alignment percentages of 43.68% and 54.68% for samples 1425 and 9822, respectively, with genome coverage of 89.50% and 90.04%, respectively. Gene identification and annotation revealed 3,294 and 3,305 genes for samples 1425 and 9822, respectively, with mean gene lengths of 943 bp and 944 bp, respectively.

Variant analysis detected 59,373 and 58,729 SNPs for samples 1425 and 9822, respectively, and 33 and 27 insertions/deletions (InDels), respectively **(Table 4.9),** highlighting genetic diversity within the studied *Acinetobacter.* populations. We further analyzed SNPs density (the number of SNPs within 1Mb window size) using SRplot data visualization (Tang et al., 2023) of both *A.* species and found similar trend of SNPs distribution. The first 1Mb window size of SNPs of both genomes consists of SNPs lower than 10000 while the second, third and fourth 1Mb window size consists of SNPs lower than 16666, 19999 and around 13333 SNPs respectively **(Figure 4.8).** Similarly, there were 4 and 8 SNPs in *A. baylyi* 9822 and *A. baumannii* 1425 respectively with reference to chromosome 2 **(Figure 4.8).** Therefore, we can say that there is a consistent distribution pattern of SNPs across both species, with the density of SNPs decreasing with increasing genomic distance. Notably, analysis of SNPs within specific chromosomal regions, such as chromosome 2, revealed varying numbers of SNPs between the two species, indicating potential genomic differences even within closely related regions. These findings underscore the genetic complexity and diversity within *Acinetobacter* populations, with implications for understanding their evolutionary dynamics and adaptation mechanisms (Pu et al., 2019).

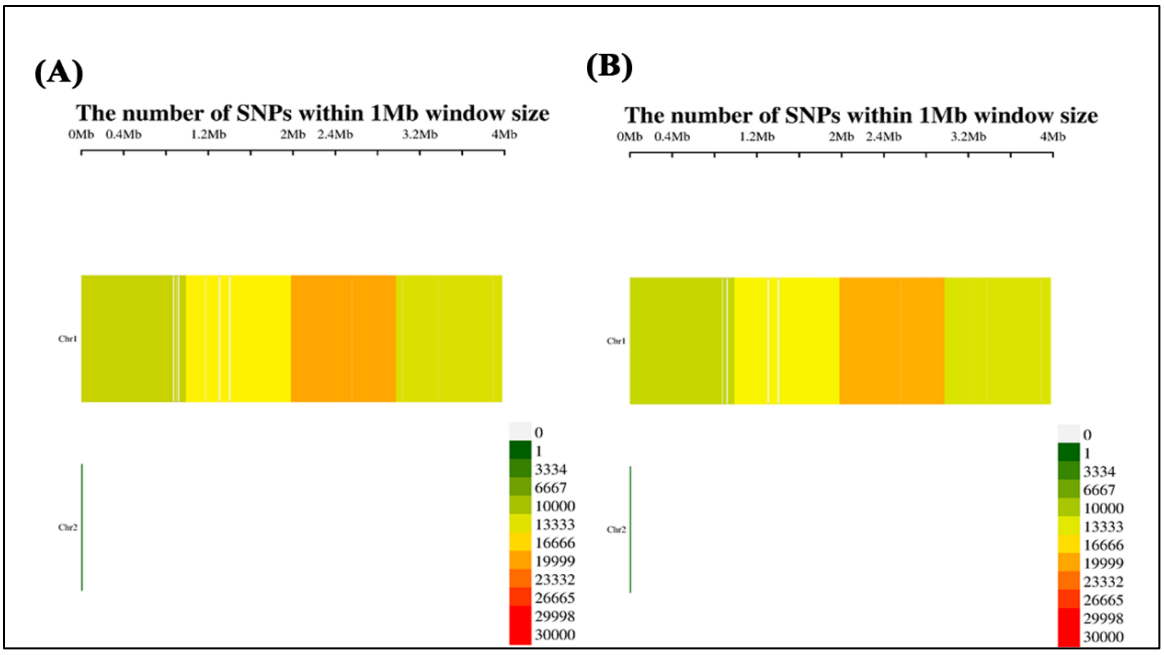

Figure 4.8: The number of SNPs present per Mb window size in investigated organism.

Figure 4.8(A): *A. baumannii* 1425, Figure 4.8(B): *A. baylyi* 9822

(Note: Chr1= NZ_CP043953.1, Chr 2= NZ_CP043954.1)

Table 4.9: SNPs and Indels identification and annotation summary

Sample	**SNP and Indels Count**				
	Total No. of SNPs and Indels	**No. of Homozygous SNPs and Indels**	**No. of Heterozygous SNPs and Indels**	**No. of Genic SNPs and Indels**	**No. of Intergenic SNPs and Indels**
1425	59373	58494	879	54271	5102
	33	31	2	6	27
9822	58729	57692	1037	53548	5181
	27	26	1	6	21

4.13 Determination of Virulence Associated Genes

We determined the presence of virulence genes in our investigated organisms with reference to *A. baumannii* strain AB00057. Each virulence factor plays a crucial role in the pathogenicity of *A. baumannii* and its ability to cause infections (Lucidi et al., 2024). All the virulence genes present in *A. baumannii* strain AB00057 were present in both of our investigated species except *hemO* and *basC* was absent in *A. baumannii* 1425 and *A. baylyi* 9822 respectively. The main types of virulence factors, their corresponding genes, and their presence in *A. baumannii* strain AB0057 are detailed in **(Table 4.10).**

Under the category of adherence, outer membrane proteins like *ompA*, facilitates adherence to host cells and colonization, thereby establishing a foothold for infection (Nie et al., 2020). Additionally, biofilm formation, a pivotal aspect of virulence, involves the expression of various genes such as *adeF, adeG, adeH, bap*, and *Csu pili* encoding proteins crucial for biofilm development and stability all of which were present in our investigated species. Moreover, the bacterium employs PNAG (Polysaccharide poly-N-acetylglucosamine) mediated by *pgaA, pgaB, pgaC*, and *pgaD* genes as a protective shield within biofilms, enhancing its resistance against host defenses and antimicrobial agents (Gedefie et al., 2021). Enzymatic virulence factors such as phospholipases C and D (*plcC* and *plcD*) contribute to membrane disruption and nutrient acquisition, while iron uptake mechanisms mediated by genes like *barA, barB*, and bas genes ensure survival within the iron-restricted host environment (Hasan et al., 2015). Furthermore, the bacterium utilizes *hemO* for heme utilization and regulatory elements including quorum sensing (*abaI and abaR*) and two-component systems (*bfmR* and *bfmS*) to modulate gene expression in accordance to environmental cues, facilitating adaptation and evasion of host defenses (Artuso et al., 2023). Lastly, the expression of *pbpG* gene confers serum resistance, a critical attribute enabling *A. baumannii 1425* to withstand host immune responses and persist within the bloodstream, contributing to its pathogenicity and virulence. Therefore, the presence of all these virulence genes in *A. baumannii* 1425 suggest strong pathogenic potential (Kyriakidis et al., 2021).

Table 4.10: Virulence genes and associated information of the *A.* species under investigation.

Virulence factor Class	**Virulence Factors**	**Related Genes**	***A. baumannii* AB0057**	***A. baylyi* 9822**	***A. baumannii* 1425**
Adherence	Outer membrane protein	*ompA*	AB57_3344	orf00598	orf00603
Biofilm formation	AdeFGH efflux pump/transport autoinducer	*adeF*	AB57_2662	orf01147	orf01140
		adeG	AB57_2663	orf01146	orf01139
		adeH	AB57_2664	orf01145	orf01138
	Biofilm-associated protein	*Bap*	AB57_3113	orf00743	orf00748
	Csu pili	*csuA/B*	AB57_2570	orf01238	orf01231
		csuA	AB57_2569	orf01239	orf01232
		csuB	AB57_2568	orf01240	orf01233
		csuC	AB57_2567	orf01241	orf01234
		csuD	AB57_2566	orf01242	orf01235
		csuE	AB57_2565	orf01243	orf01236
	PNAG (Polysaccharide poly-N-acetylglucosamine)	*pgaA*	AB57_2499	orf01309	orf01301
		pgaB	AB57_2497	orf01310	orf01302
		pgaC	AB57_2496	orf01311	orf01303
		pgaD	AB57_2495	orf01312	orf01304

Table 4.10: Continued

Virulence factor Class	**Virulence Factors**	**Related Genes**	***B. baumannii* AB0057**	***A. baylyi* 9822**	***A. baumannii* 1425**
Enzyme	Phospholipase C	*Plc*	AB57_0084	orf01427	orf01419
	Phospholipase D	*plcD*	AB57_3442	orf00497	orf00500
Iron uptake	Acinetobactin	*barA*	AB57_2806	orf01057	orf01046
		barB	AB57_2805	orf01058	orf01047
		basA	AB57_2820	orf01044	orf01033
		basB	AB57_2819	orf01045	orf01034
		basC	AB57_2812	NF	orf01040
		basD	AB57_2811	orf01052	orf01041
		basF	AB57_2809	orf01054	orf01043
		basG	AB57_2808	orf01055	orf01044
		bash	AB57_2804	orf01060	orf01049
		basI	AB57_2803	orf01061	orf01050
		basJ	AB57_2802	orf01062	orf01051
		bauB	AB57_2814	orf01050	orf01038
		bauC	AB57_2816	orf01048	orf01036
		bauD	AB57_2817	orf01047	orf01035
		bauE	AB57_2815	orf01049	orf01037
		bauF	AB57_2822	orf01043	orf01032

Table 4.10: Continued

Virulence Factor Class	**Virulence Factors**	**Related Genes**	***C. baumannii* AB0057**	***A. baylyi* 9822**	***A. baumannii* 1425**
Iron uptake	Hame Utilization	*hemO*	AB57_0991	orf02722	NF
	Quorum sensing	abaI	*AB57_0151*	orf03440	orf03430
		abaR	*AB57_0153*	orf03437	orf03427
	Two-component system	bfmR	*AB57_0796*	orf02893	orf02877
		bfmS	*AB57_0797*	orf02892	orf02876
	PbpG	pbpG	*AB57_0326*	orf03329	orf03318

(Note: NF=Not Found)

4.14 Determination Antibiotic Resistance Genes (ARGs)

Using ResFinder, several ARGs were determined in *A. baumannii* and *A. baylyi* under investigation (Florensa et al., 2022). Two important resistance genes, *blaADC-25* and *blaOXA-98*, that are crucial in granting resistance to beta-lactam antibiotics were found in our investigation. The *blaADC-25* sequence similarity study showed a 96.9% sequence similarity with the reference sequence (accession number EF016355). This gene, which is often associated with beta-lactam resistance, is one notable strategy by which *A. baumannii* evades the effects of this class of antibiotics. Comparably, our analysis showed that *blaOXA-94* had an even greater sequence identity to its reference sequence (accession number AY750907), at 99.88%. These results highlight how common antibiotic resistance is in *Acinetoacter* and how important it may be clinically.

4.15 Codon Usage Analysis in VRGs and ARGs

4.15.1 Functionally related genes have comparable genomic composition

The analysis of GC content in various virulence and antibiotic resistance genes of *A. baumannii* and *A. baylyi* revealed several distinct variation in GC content between different gene clusters and also significant similarity in GC range within same cluster and functionally related genes **(Table 4.11).** Genes involved in membrane proteins and adherence, such as *ompA*, displayed a GC content of 39%. In contrast, the *adeF*, *adeG*, and *adeH* genes, which are part of the ADEF gene cluster involved in biofilm formation and antibiotic resistance, exhibited higher but similar GC contents of 44% (for *adeH*) and 45% (for *adeF* and *adeG*), highlighting their role in the AdeABC efflux pump system. Antibiotic resistance genes like *blaADC-25* (36%) and *blaOXA-98* (39%), which are responsible for β-lactamase production, showed lower GC contents. On the other hand, the *csu* gene cluster, associated with biofilm formation, had GC contents ranging from 29% to 42% (*csuA* 29%, *csuB* 30%, *csuC* 37%, *csuD* 40%, and *csuE* 42%). The *pga* gene cluster, which also contributes to biofilm matrix development, showed GC contents closely clustered between 39% to 43% (*pgaA* 39%, *pgaB* 41%, *pgaC* 42%, and *pgaD* 43%). The *bap* gene, crucial for biofilm matrix formation, had a GC content of 37%. Iron acquisition genes within the *bau* cluster displayed relatively high and similar GC contents: *bauB* (41%), *bauC* (40%), *bauD* and *bauE* (42%), *bauF* (40%), and *hemO* (41%). The *hemO* gene, involved in iron utilization, had a GC content similar to that of the *bau* cluster genes, which may be due to functional similarity. Stress response and pathogenicity-related genes, such as *plcC* (42%), *plcD* (42%), *barA* (42%), and *barB* (43%), also exhibited higher and comparable GC contents. Finally, the genes *bfmR* and *bfmS* (both 42%), along with *pbpG* (43%), are involved in biofilm formation and peptidoglycan biosynthesis. Regulatory genes such as *abaI* (41%) and *abaR* (39%) play important roles in signaling and resistance regulation. The comparable GC content across these genes also suggest close functional relationship. Moreover, The analysis of GC content at the third codon position (GC3s) and the first and second codon positions

(GC12) also revealed notable variations among the different cluster of genes while close similarity within same cluster and functionally related genes **(Table 4.11).** Genes within the same cluster or with related functions often exhibit similar GC content due to shared evolutionary pressures and genomic environments. These similarities arise because functionally related genes are typically maintained in similar genomic contexts, which influences their GC content and contributes to their overall functional coherence. Therefore, it is clear that all the genes have higher AT content as GC-rich nucleotides are energetically unfavorable for pathogenic microbes. This is because AT-rich metabolites such as ATP are abundant in human host due to their low synthetic cost (Dietel et al., 2019). The ready availability of A/T rich metabolites also facilitates subsequent replication of the bacterium promoting rapid growth and easier access to nutrients (Dietel et al., 2019; Sharma et al., 2023).

Table 4.11: Genomic Composition of VRGs and ARGs

Genes	**T3s**	**C3s**	**A3s**	**G3s**	**GC3s**	**GC12**	**GC**
ompA	0.50	0.14	0.44	0.20	0.26	0.45	0.39
adeF	0.45	0.23	0.41	0.10	0.28	0.54	0.45
adeG	0.42	0.25	0.36	0.16	0.34	0.50	0.45
adeH	0.45	0.19	0.43	0.13	0.27	0.53	0.44
csuA	0.65	0.07	0.44	0.11	0.13	0.37	0.29
csuB	0.59	0.12	0.46	0.10	0.16	0.36	0.30
csuC	0.50	0.13	0.42	0.21	0.26	0.43	0.37
csuD	0.48	0.22	0.34	0.23	0.34	0.43	0.40
csuE	0.40	0.21	0.38	0.25	0.36	0.45	0.42
pgaA	0.55	0.15	0.41	0.22	0.27	0.45	0.39
pgaB	0.46	0.20	0.42	0.21	0.30	0.46	0.41
pgaC	0.50	0.18	0.32	0.22	0.31	0.47	0.42
pgaD	0.44	0.18	0.35	0.26	0.34	0.47	0.43
plcC	0.51	0.17	0.41	0.18	0.27	0.48	0.42

Table 4.11: Continued

Genes	**T3s**	**C3s**	**A3s**	**G3s**	**GC3s**	**GC12**	**GC**
plcD	0.50	0.17	0.42	0.18	0.27	0.49	0.42
barA	0.41	0.16	0.43	0.17	0.28	0.48	0.42
barB	0.47	0.16	0.39	0.17	0.27	0.51	0.43
basA	0.47	0.16	0.39	0.25	0.31	0.42	0.38
basB	0.51	0.20	0.43	0.16	0.27	0.44	0.38
basC	0.49	0.22	0.41	0.17	0.29	0.46	0.41
basD	0.49	0.18	0.45	0.15	0.25	0.44	0.38
basF	0.49	0.15	0.42	0.20	0.26	0.47	0.41
basG	0.51	0.22	0.35	0.21	0.32	0.43	0.39
basH	0.54	0.19	0.40	0.22	0.28	0.38	0.35
basI	0.49	0.17	0.49	0.24	0.27	0.34	0.32
basJ	0.56	0.10	0.47	0.18	0.21	0.42	0.35
bauB	0.44	0.22	0.42	0.22	0.32	0.45	0.41
bauC	0.45	0.23	0.29	0.21	0.35	0.42	0.40
bauD	0.44	0.22	0.26	0.25	0.38	0.44	0.42
bauE	0.46	0.23	0.32	0.26	0.37	0.44	0.42
bauF	0.43	0.26	0.45	0.17	0.32	0.44	0.40
hemO	0.45	0.19	0.47	0.18	0.29	0.47	0.41
abaI	0.43	0.21	0.46	0.13	0.28	0.48	0.41
abaR	0.44	0.13	0.48	0.22	0.27	0.44	0.39
bfmR	0.53	0.19	0.35	0.16	0.28	0.49	0.42
bfmS	0.47	0.20	0.36	0.23	0.33	0.46	0.42
pbpG	0.52	0.12	0.34	0.19	0.25	0.51	0.43
csuAB	0.55	0.14	0.45	0.05	0.16	0.50	0.39
bap	0.55	0.14	0.42	0.16	0.23	0.44	0.37
blaADC-25	0.49	0.18	0.47	0.16	0.26	0.41	0.36

Table 4.11: Continued

Genes	T3s	C3s	A3s	G3s	GC3s	GC12	GC
blaOXA-98	0.49	0.21	0.44	0.14	0.27	0.45	0.39

(Note: Genomic values are expressed as decimals in the table; for example, 0.39 represents 39%.)

4.15.2 Codon Usage Bias is consistent within Gene Clusters

The ENC-GC3 figure unveiled a diminished codon usage bias within the genes. Genes showed a deviation just below the curve **(Figure 4.9),** indicating a weak impact of mutational bias on codon usage in the genes. This observation suggests that translational selection pressure exerts a more dominant impact compared to other factors. Additionally, when the average ENC value for a given gene exceeds 35, it indicates a reduced bias in codon usage (Andargie & Congyi, 2022). The ENC levels of the genes ranged from 36.94 in *csuAB* to 59.79 in *bauD* **(Table 4.12).** We observed a consistent ENC values among the genes within same cluster. For instance, the genes *bauB, bauC, bauD, bauE* and *bauF* that fall within the same cluster showed the ENC value of above 50 while *ompA* gene responsible for adherence showed ENC value of only 41.5. Here the CUB in different cluster of genes are variable as they do not face the same stringent selection pressures related to virulence and host adaptation (Beceiro et al., 2013).

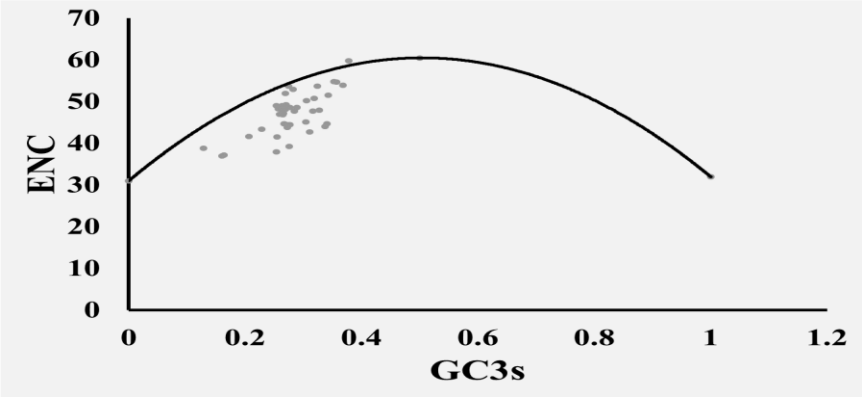

Figure 4.9: ENC plot analysis of VRGS and ARGS in *A. baumannii* 1425 and *A. baylyi* 9822.

Table 4.12: Codon usage bias analysis in ARGs and VRGs

Genes	**Nc**	**L_sym**	**L_aa**	**Gravy**	**Aromo**	**RSCU (Axis1)**	**RSCU (Axis2)**	**P2**	**CAI**
ompA	41.51	255.00	259.00	-0.35	0.09	0.22	0.15	0.45	0.80
adeF	44.50	401.00	406.00	-0.20	0.05	0.07	-0.09	0.50	0.81
adeG	44.07	1023.00	1059.00	0.32	0.08	0.20	-0.09	0.49	0.78
adeH	47.52	472.00	482.00	-0.22	0.06	-0.13	0.06	0.49	0.81
csuA	38.85	180.00	182.00	0.04	0.10	0.15	0.39	0.31	0.87
csuB	37.18	165.00	172.00	-0.32	0.11	0.05	0.35	0.36	0.85
csuC	47.01	266.00	277.00	-0.33	0.08	0.10	-0.13	0.44	0.82
csuD	51.50	817.00	832.00	-0.34	0.11	-0.03	-0.13	0.45	0.77
csuE	54.74	325.00	339.00	-0.09	0.10	-0.17	-0.11	0.47	0.74
pgaA	47.18	786.00	812.00	-0.72	0.13	0.04	0.04	0.45	0.81
pgaB	45.14	632.00	664.00	-0.50	0.10	0.16	-0.06	0.47	0.80
pgaC	42.74	386.00	419.00	0.17	0.13	0.18	-0.11	0.46	0.80
pgaD	44.70	129.00	139.00	0.02	0.11	0.16	-0.06	0.46	0.77
Plc	43.88	690.00	722.00	-0.49	0.11	0.19	-0.03	0.47	0.81
plcD	44.49	690.00	722.00	-0.50	0.11	0.17	-0.03	0.47	0.80
barA	48.65	520.00	536.00	0.43	0.06	-0.04	0.01	0.47	0.79
barB	44.68	514.00	531.00	0.32	0.06	0.03	0.06	0.47	0.80
basA	50.22	594.00	615.00	-0.15	0.08	-0.12	0.03	0.44	0.77
basB	48.20	654.00	675.00	-0.28	0.11	-0.02	-0.09	0.46	0.82
basC	48.63	425.00	436.00	-0.33	0.10	-0.03	-0.06	0.46	0.79
basD	49.04	945.00	980.00	-0.23	0.09	-0.10	0.05	0.45	0.81
basF	49.04	273.00	289.00	-0.26	0.09	-0.11	-0.01	0.46	0.80
basG	47.71	364.00	383.00	-0.22	0.12	-0.05	-0.14	0.45	0.77
bash	53.01	234.00	244.00	-0.36	0.11	-0.02	0.04	0.42	0.77
basI	49.26	248.00	251.00	-0.26	0.14	-0.48	0.31	0.39	0.76
basJ	41.69	379.00	389.00	-0.34	0.07	0.01	0.17	0.41	0.85
bauB	53.69	309.00	322.00	-0.23	0.07	-0.12	-0.13	0.48	0.77

Table 4.12: Continued

Genes	Nc	L_sym	L_aa	Gravy	Aromo	RSCU (Axis1)	RSCU (Axis2)	P2	CAI
bauC	54.83	303.00	315.00	1.09	0.13	-0.14	-0.02	0.44	0.75
bauD	59.79	304.00	313.00	1.17	0.11	-0.14	-0.27	0.45	0.74
bauE	53.96	247.00	256.00	-0.12	0.07	-0.12	-0.27	0.47	0.75
bauF	50.75	276.00	286.00	-0.42	0.09	-0.47	-0.13	0.48	0.78
hemO	47.79	193.00	199.00	-0.42	0.10	-0.13	-0.20	0.47	0.80
abaI	53.67	182.00	188.00	0.00	0.11	-0.35	0.15	0.47	0.79
abaR	51.95	223.00	238.00	-0.36	0.11	-0.20	0.23	0.45	0.79
bfmR	39.24	232.00	238.00	-0.38	0.05	0.45	-0.07	0.46	0.82
bfmS	47.95	530.00	549.00	-0.16	0.09	0.12	-0.17	0.47	0.77
pbpG	37.95	335.00	348.00	-0.16	0.05	0.32	0.01	0.47	0.84
csuAB	36.94	175.00	178.00	-0.04	0.07	0.35	0.26	0.45	0.86
Bap	43.44	3217.00	3272.00	-0.25	0.09	0.07	0.08	0.43	0.83
blaADC-25	48.34	370.00	383.00	-0.41	0.11	0.02	-0.14	0.45	0.78
blaOXA-98	46.87	260.00	274.00	-0.28	0.09	-0.08	0.18	0.46	0.79

4.15.3 Variable Impact of Mutational Pressure across different Gene Clusters

Upon examining the neutrality plot across the genes of *A. baumanii* and *A. baylyi*, we observed regression line slopes **(Figure 2, Supplementary Figures S1-1 to S1-5)** close to zero, indicating minimal influence of mutational pressure on codon usage bias. Specifically, slopes ranged from 0.06 in *bauD* to 0.284 in *csuAB*, corresponding to mutational pressure effects ranging from 6 % to 28.4 %, respectively. Notably, the impact of mutational pressure was variable across different gene clusters. For instance, the two genes *plcC* and *plcD* that encode the enzyme phospholipase have almost equal (21%) impact of mutational pressure **(Figure 4.10).** Similarly, the regulatory genes *bfmR* and

bfmS showed close (17.8% and 18.8%) of mutational pressure acting across them **(Figure 4.10).** Moreover, the genes like *bauC* (8%), *bauD* (6%), *bauE* (6.8%) responsible for biofilm formation showed lowest impact of mutational pressure amongst all the genes. Additionally, the ARGs *blaADC-25* and *blaOXA-98* also showed 18.5% and 19% effect of mutational pressure respectively **(Figure 4.10).** Therefore, we can say that the impact of mutational pressure in genes within same cluster and across functionally related genes are very similar. These results underscore the predominant influence of translational selection over mutational pressure in shaping codon usage patterns within the genes of *A. baumannii* and *A. baylyi.* Translational selection is evident in the consistent codon preferences observed across the genes, reflecting adaptive strategies for efficient protein synthesis and functional optimization (Plotkin & Kudla, 2011). Conversely, the higher impact of mutational pressure (28%) on genes like *ompA* compared to the other genes suggests differential evolutionary pressures that influence genomic stability and codon usage bias (Sharp & Li, 1987).

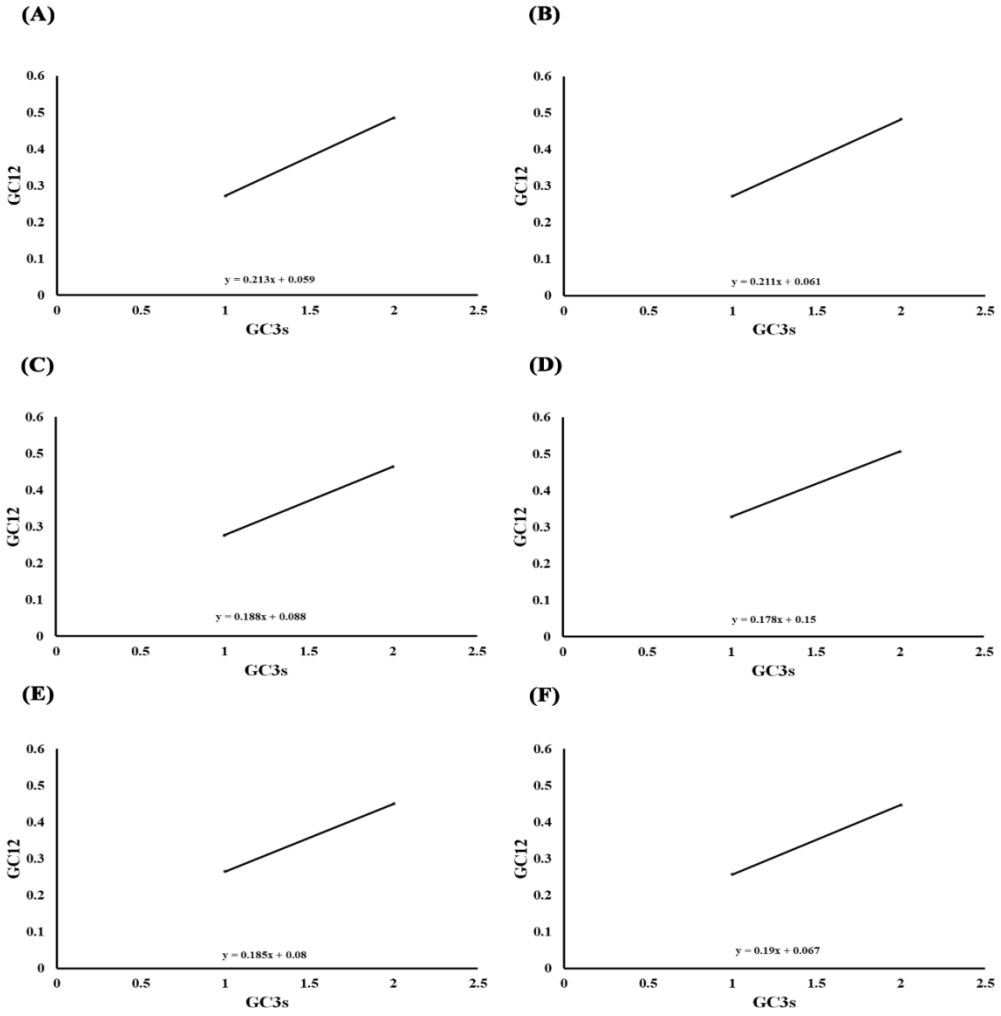

Figure 4.10: Neutral Plot analysis of VRGs and ARGS

Gene identification: A *(plcC),* B *(plcD*), C (*bfmR)*, D (*bfmS),* E *(blaADC-25)* and F (*blaOXA-98).*

(Note: The value of the slope is calculated as, y=mx+c which gives the impact of mutational pressure on the genes.)

4.15.4 Similarity in Translational Selection Levels within Gene Clusters and Functionally Related Genes

Insights from the analysis of translational selection using P2 values (Peng et al., 2022) revealed significant variation in codon usage bias across the cluster of virulence and antibiotic resistance genes. Across all the genes, P2 values were notably low, ranging from 0.31 in *cusA* to 0.50 in *adeF* **(Table 4.12)** indicating a modest influence of natural selection on codon usage. In translational selection, values below 0.5 indicate weaker selection pressure, while values above 0.5 reflect stronger selection pressure. *adeF* was the only gene with a value of 0.50. This suggests that there is a moderate level of selection pressure acting on the translational process. The level of translational selection within specific gene clusters and functionally related genes were very close to each other. For instance, the two genes in the cluster *plcC* and *plcD* have a p2 value of exactly 47 while the regulatory genes namely *abaL, and abaR* involved in quorum sensing have a p2 values of 47 and 45 respectively **(Table 4.12).** Similarly, the other two regulatory genes *bfmR* and *bfmS* also showed a very close p2 value of 46 and 47 respectively **(Table 4.12**). Therefore, we can say the selection is strong enough to have a noticeable effect on the efficiency of translation or the evolutionary dynamics of the genes investigated. In other words, translational selection has played a significant role in shaping codon usage across the virulence and antibiotic-resistance genes and the degree of influence varies among different gene clusters.

4.15.5 Uniform CAI Values in Gene Clusters and their Correlation with RSCU and RAAU

The assessment of gene expression levels in *Acinetobacter* genes was conducted using the Codon Adaptative Index (CAI) parameter. CAI values were computed using a reference set comprised of genes encoding ribosomal subunits (Saha et al., 2019; Ueda et al., 2004). Among the genes under investigation, CAI values ranged from 0.74 for *cusE*

to 0.87 for *cusA* **(Table 4.12).** We also observed a close similarity in CAI values within the genes falling under the same gene cluster as seen in the case of GC content and ENC. Furthermore, in the genes, a strong positive correlation between RSCU and RAAU with CAI indicates that genes with higher expression levels tend to utilize optimal codons more frequently (Dos Reis, 2003; Sharp & Li, 1987). In a majority of virulence genes, a highly significant correlation was observed between Axis 1 and Axis 2 of RSCU and RAAU data with CAI **(Figure 4.11).** This relationship suggests that natural selection favors codons that maximize translational efficiency, reflecting the adaptation of *A. baumannii* and *A. baylyi* to their specific environmental and physiological requirements. Furthermore, a high negative correlation of CAI with ENC provided additional evidence of the substantial influence of gene expression on the codon usage patterns within the virulence and antibiotic resistance genes **(Figure 4.11)** as a lower ENC value trends greater codon bias towards optimal codons and suggests that selective pressure for efficient translation drives the observed codon preferences (Sharp & Li, 1987).

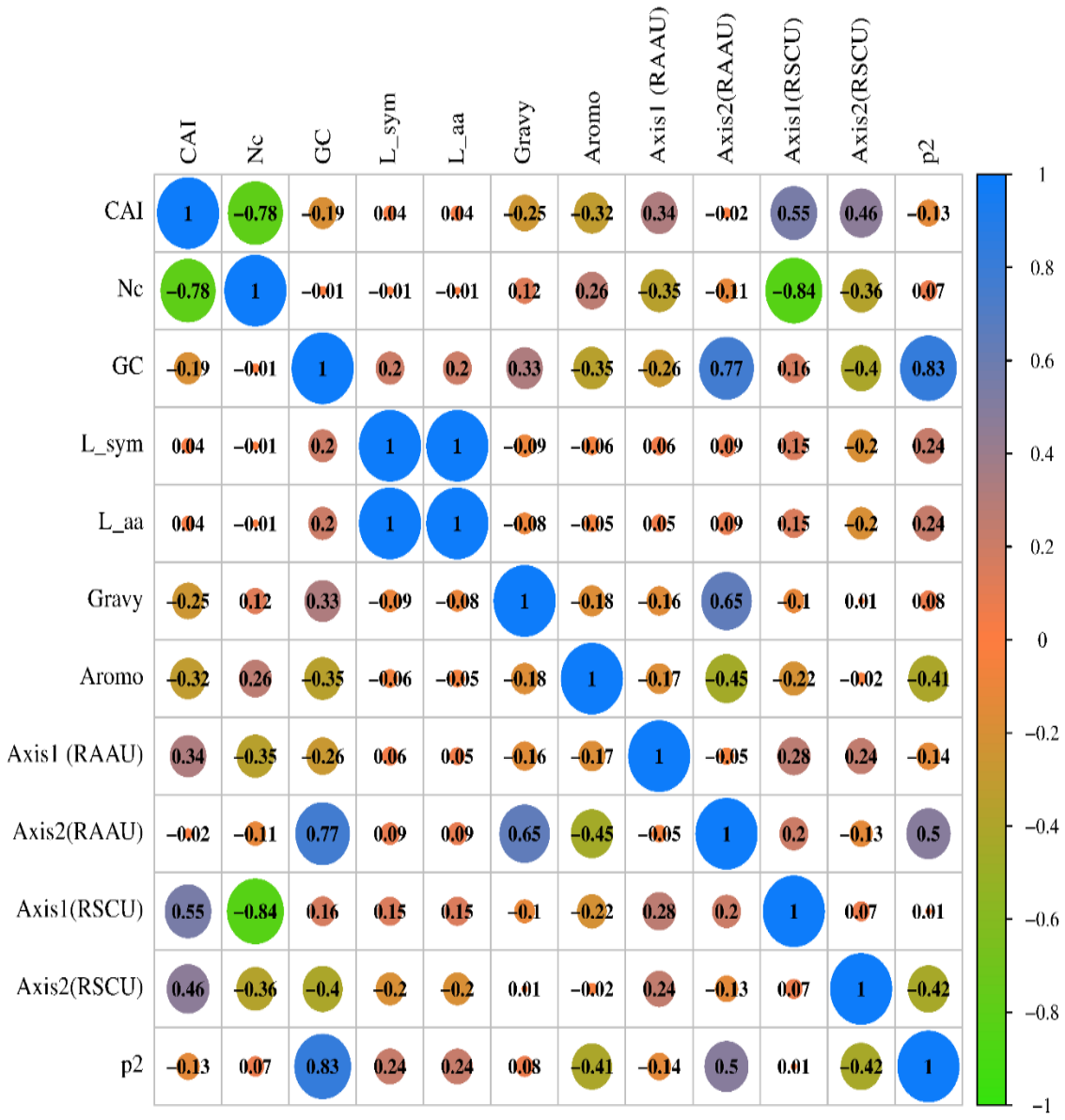

Figure 4.11: Correlation analysis of genomic and codon usage parameters of ARGS and VRGS

(Note: Significant correlations are indicated by colored circles in the numerical values. The colors highlight the strength and direction of the correlation: higher or lower positive and negative correlations. All correlations shown are significant α = 0.01 level)

4.15.6 GC Content and Protein Aromaticity Drive RAAU in the genes

Conducting a comprehensive analysis on the RAAU data, a CoA was peformed to investigate potential factors linked with variations in amino acid usage across all the genes. The results of the multivariate statistical analysis revealed strong correlations between the aromaticity (Aromo) of encoded proteins and the two major principal axes (Axes 1 and 2) that separate genes based on RAAU data **(Figure 4.11).** This suggests that the aromaticity of encoded proteins plays a pivotal role in shaping the overall amino acid composition across genes in *A. baumannii 1425* and *A. baylyi* 9822. Additionally, the GRAVY index, which indicates the mean hydropathic properties of a protein (positive values indicating hydrophobic, and negative values indicating hydrophilic) (Moura et al., 2013), exhibited notably significant correlations with Axes 1 and 2 of RAAU data. Furthermore, the significant correlation of GC content and Axes 1 and 2 of RAAU data underscored the substantial impact of compositional constraints on the amino acid usage patterns in the genes of the bacterium. **(Figure 4.11).** A moderate impact of gene expression level on amino acid usage trends was revealed by the substantial correlation of CAI and RAAU data **(Figure 4.11).** This suggests that genes with higher expression levels may exhibit distinct amino acid usage preferences, potentially linked to translational efficiency or protein folding requirements (Raghava & Han, 2005). The length of protein coding sequences (CDS) exhibited weak correlations with RAAU data, indicating a limited influence on amino acid usage in the genes of *A. baumannii 1425***(Figure 4.11).** This suggests that genes with higher expression levels may exhibit distinct amino acid usage preferences, potentially linked to translational efficiency or protein folding requirements (Raghava & Han, 2005).

Notably, it was observed that the aromaticity of the encoded gene products displayed significant moderate correlations with GC content in the majority of the genes **(Figure 4.11).** This emphasizes that GC content stands out as a key factor influencing the amino acid composition of all the genes in *A. baumannii 1425* and *A. baylyi 9822*. This association further highlights the intricate interplay between genomic characteristics and

protein biophysical properties in driving evolutionary strategies within the virulence and antibiotic resistance genes (Parvathy et al., 2022).

4.15.7 Leucine and Alanine are Predominant in ARGs and VRGs

We also investigated the individual frequencies of amino acids of all the ARGs and VRGs present in *A. baumannii* 1425 and *A. baylyi* 9822 using CodonW program. Surprisingly, majority of the genes showed their preference towards leucine and alanine amino acid while amino acids like cysteine, tryptophan and histidine were significantly avoided **(Figure 4.12).** The high prevalence of leucine (10 in *csuAB* to 223 in *bap*) suggests its importance in protein structure and function across *A. baumannii* and can be linked to the potential of *A. baumannii* to utilize leucine as a secondary metabolite, enable them to thrive in harsh, artificially created environments, (Ren & Palmer, 2023). Similarly, the frequency of alanine across all the members ranged from 9 in *csuAB* to 237 in *bap.* Alanine being a major component of peptidoglycan (bacterial cell wall) justifies the higher frequency across all the genes (Trivedi et al., 2018). Moreover, cysteine (0 in *hemO* to 36 in *basC*) and tryptophan (0 in *csuAB* and *bauE* to 36 in *bap)* amino acids were noted with extremely low frequencies in all the virulence and antibiotic resistance genes. The lowest frequencies of amino acids like tryptophan and cysteine can be linked to efficient energy costing as synthesis of tryptophan like aminoacids require higher amount of energy (Akashi & Gojobori, 2002).

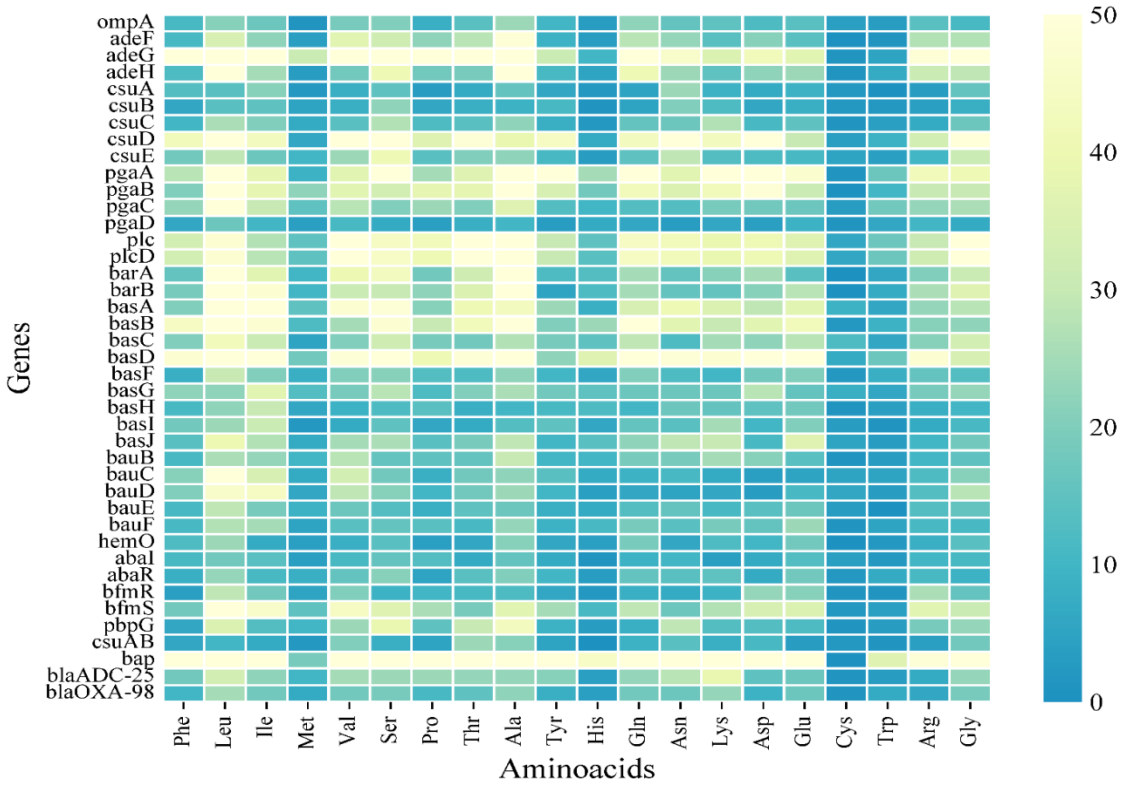

Figure 4.12: Heatmap analysis of Amino acid frequency of VRGs and ARGs present in *A. baumannii* 1425 and *A. baylyi* 9822.

4.16 Codon Usage Bias Aligns with Phylogenetic Clustering of Genes

The provided phylogenetic tree **(Figure 4.13),** constructed using Mega11(Tamura et al., 2021), offers a comprehensive view of the evolutionary relationships among VRGs and ARGs in *Acinetobacter* 1425 and *A. baylyi* under investigation. Each branch and node in the tree represents a distinct cluster of ARGs and VRGs, shedding light on their shared ancestry and evolutionary divergence.

The tree reveals distinct clusters of virulence genes, indicating both conserved evolutionary lineages and instances of gene acquisition or loss. For instance, genes such as *ompA* and *adeF* form a close cluster, suggesting a shared evolutionary history and potential functional overlap. In contrast, genes like *basC* and *blaOXA-98* appear more

distantly related, indicative of independent evolutionary trajectories or differential selection pressures. Similarly, *csuAB* and *bap* appear to be closely related, indicating potential co-evolution or horizontal gene transfer events within these virulence determinants. Conversely, genes like *adeH* and *pbpG* exhibit a separate branch, implying distinct evolutionary trajectories or functional divergence within the genomes of *A. baumannii* and *A. baylyi*. Further exploration of the tree reveals additional insights into the evolutionary dynamics of virulence genes. For instance, the clustering of genes such as *basB* and *abaI* suggests shared evolutionary pressures along with functional associations. Similarly, the grouping of genes like *basD*, *hemO,* and *bauB* implies potential co-adaptation or gene co-expression within specific physiological contexts. Additionally, the placement of genes like *plc, plcD, csuA*, and *basG* within the same clade suggests functional conservation or genetic linkage among these virulence factors **(Figure 4.13).**

The phylogeny of genomes as well as genes, reveals evolutionary relationships based on genetic similarities and divergence over time. CUB has been observed to correlate with phylogenetic topology in several ways, reflecting both shared ancestry and adaptive divergence among different genomes as well as genes. At a broad phylogenetic scale, genes that share a more recent common ancestor tend to exhibit similar patterns of codon usage. This similarity arises because closely related genes inherit similar genomic compositions, including codon usage preferences, from the ancestors (Dunn et al., 2013; Feng et al., 2024; Li et al., 2023; Yamamoto et al., 1999). In our analysis, the clustering of genes like *plcC* and *plcD*, *ompA* and *adeF* together both in phylogenic as well as codon usage context suggests effect of codon usage on the phylogeny of genes.

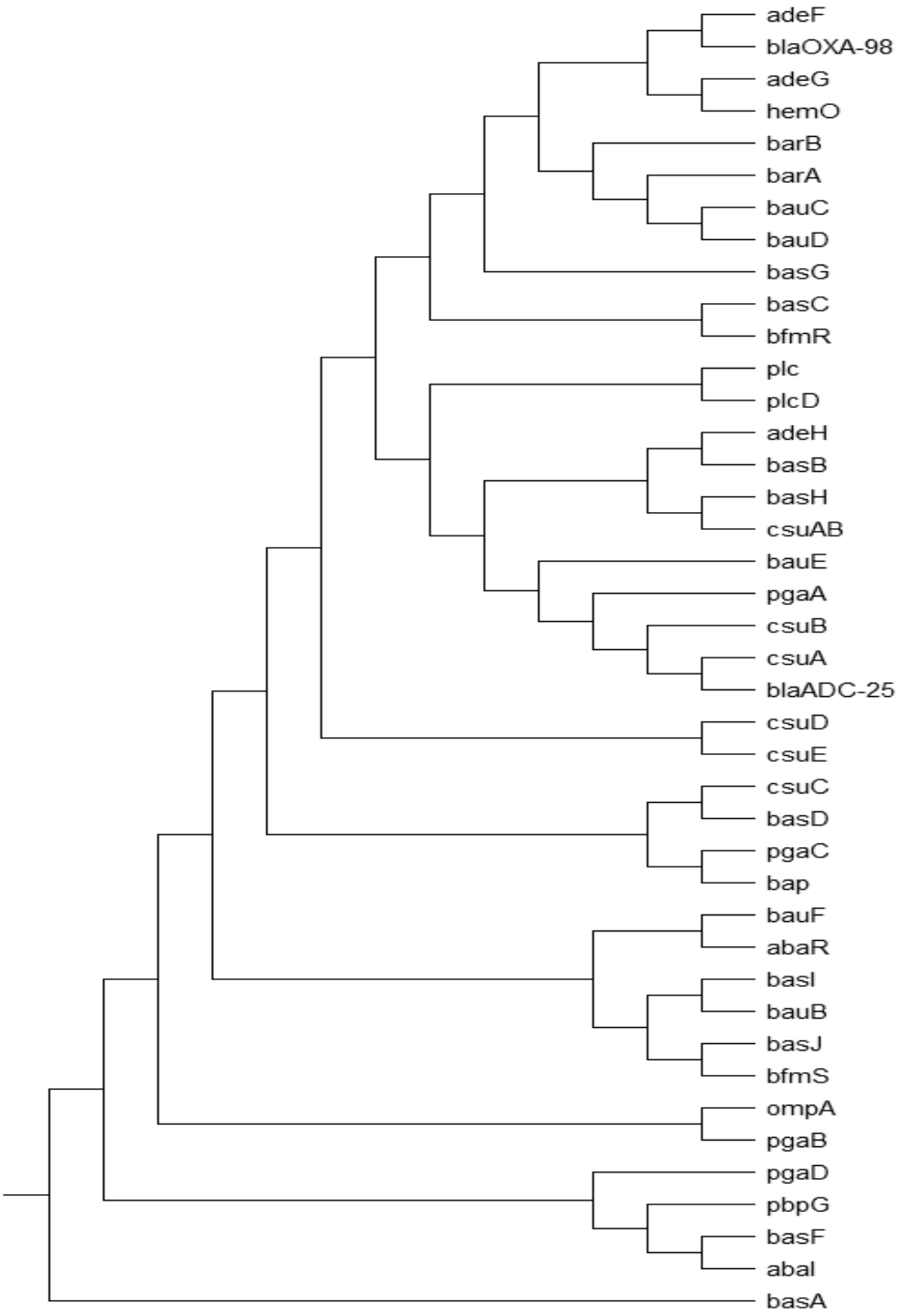

Figure 4.13: Phylogenetic tree of all the VRGs and ARGs in *A. baumannii* 1425 and *A. baylyi* 9822

4.17 Similar Codon Bias and Expression Patterns across Interconnected Genes

The network analysis of virulence genes and antibiotic resistance genes within investigated species revealed intriguing insights into the molecular interactions underlying pathogenicity and antimicrobial resistance mechanisms. With 39 nodes representing these genetic elements and 87 edges denoting their interactions, the network demonstrates a complex web of connections within these crucial components of bacterial physiology **(Figure 4.14).** The average node degree of 4.46 suggests that, on average, each virulence or antibiotic resistance gene interacts with approximately four others, highlighting a significant degree of interconnectedness within the network. For instance, *A1S_1033, A1S_2304, A1S_2305, A1S_2306* are interconnected to each other in the interaction network **(Figure 4.14)**. Apart from functional similarity, these protein genes also have identical degree of codon bias (ENC =41, 44, 44 and 47), similar GC content (39%, 44%, 44%, 45%), similar expression levels (CAI =0.80, 0.81, 0.78 and 0.81) as well as comparable effect of translational selection (45, 50, 49, 49) on them **(Table 4.11 and 4.12).** Moreover, the high average local clustering coefficient of 0.723 indicates a propensity for these genes to form tightly knit clusters, indicative of functional modules or pathways. However, the most striking observation arises from the PPI enrichment p-value, which is less than 1.0e-16, indicating a substantial deviation from random interaction patterns. This statistical significance underscores the non-random nature of the observed interactions, and strengthen our findings, to confirm that the selective pressures like translational selection and mutational forces are driving the connectivity within the network (Peng et al., 2022).

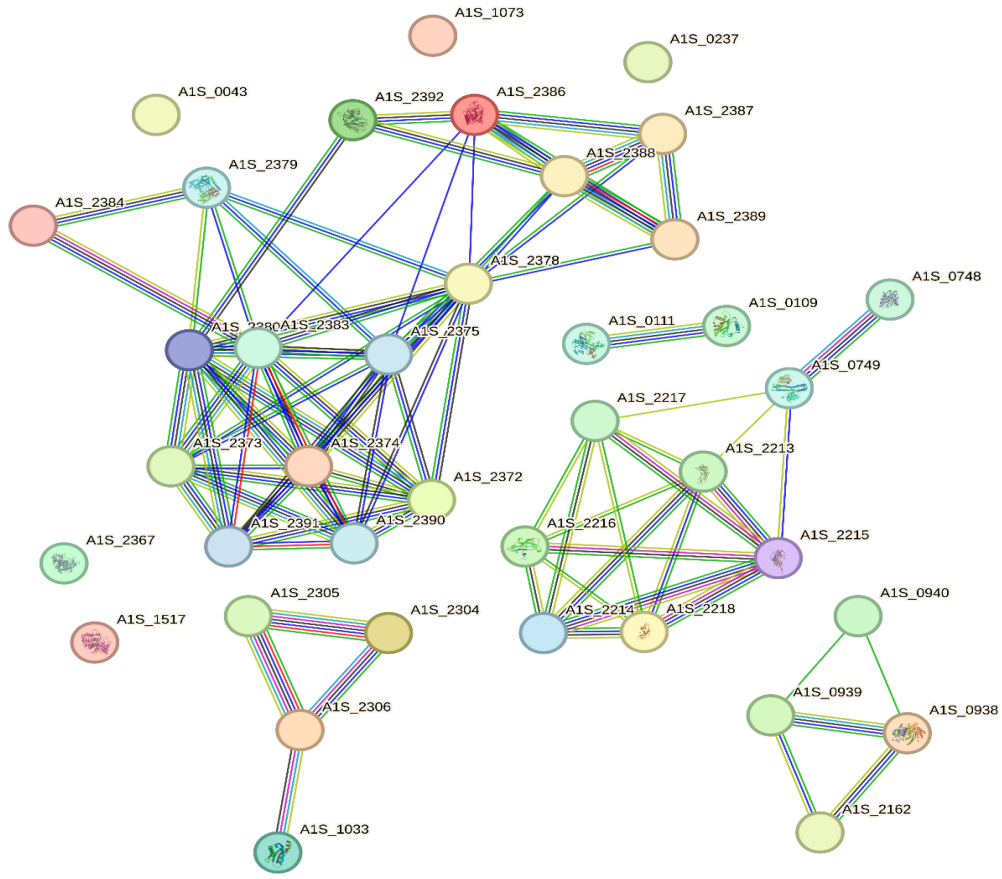

Figure 4.14: Protein Interaction Network Analysis of VRGs and ARGs present in *A. baumannii* 1425 and *A. baylyi* 9822

(*Gene Annotation :ompA = A1S_1033, adeF=A1S_2304, adeG=A1S_2305, adeH=A1S_2306, csuA=A1S_2217, csuB=A1S_2216, csuC=A1S_2215, csuD=A1S_2214, csuE=A1S_2213, pgaA=A1S_2162, pgaB=A1S_0938, pgaC=AIS_0939, pgaD=A1S_0940, plcC=A1S_0043, plcD=A1S_0043,barA=A1S_2378, barB=A1S_2375, basA=A1S_2391, basB=A1S_2390, basC=A1S_2384, basD=A1S_2383, basF=A1S_2380, basG=A1S_2379, bash=A1S_2374, basI=A1S_2373, basJ=A1S_2372, bauB=A1S_2386, bauC=A1S_2388, bauD=A1S_2389, bauE=A1S_2387, bauF=A1S_2392, abaI=A1S_0109, abaR=A1S_0111, bfmR=A1S_0748, bfmS=A1S_0749, pbpG=A1S_0237, csuAB=A1S_2218, bap=A1S_1073, blaADC-25=A1S_2367, blaOXA-98=A1S_1517*)

Therefore, we can say that codon usage bias has played a crucial role in influencing the efficiency of protein translation and expression levels. Variations in codon preferences can affect how abundantly proteins are produced, which in turn impacts their representation within a protein interaction network. This bias can lead to differential expression of network components, potentially skewing interpretations of protein interactions and their functional roles (Dilucca et al., 2021).Understanding codon usage is very essential for accurate network construction and analysis, as it helps to align experimental data with actual protein dynamics and improves the reliability of predictions in both research and therapeutic contexts.

4.18 Comparative insights and study limitations

To further contextualize these findings, it is important to compare the codon and amino acid usage patterns observed in the *Acinetobacter* members with those previously reported in pathogenic members of the *Clostridium* (Sharma et al., 2023) and Staphylococcus genera (Arora et al 2025) as well as other ESKAPE pathogens (Dahal et al., 2024). Published analyses of *Clostridium* indicate a pronounced AT-rich codon usage bias and a restricted set of preferred codons, driven largely by mutational pressure and host adaptation (Sharma et al., 2023). In contrast, pathogenic *Staphylococcus* species are characterized by a preference for energetically favorable amino acids such as leucine, isoleucine, and lysine, while avoiding costly residues like cysteine and methionine, reflecting strong translational selection (Arora et al 2025). The ACB complex of *Acinetobacter* genus exhibits a unique intermediate profile: while it shares the selective pressure for efficient translation and the under-representation of energetically expensive amino acids with these genera, it is distinguished by its intermediate GC content, moderate codon usage bias, and distinctive codon pair preferences. Compared to other ESKAPE pathogens, such as *Pseudomonas aeruginosa* and *Klebsiella pneumoniae* which display high GC content and strong GC-rich codon usage or *Enterococcus faecium*, which is more AT-rich (Dahal et al., 2024), the ACB complex balanced GC and AT content and broader codon optimization strategies stand out as intermediate and flexible.

These differences underscore the genus- and niche-specific evolutionary pressures shaping codon and amino acid usage in pathogenic bacteria. Importantly, current comparative analyses suggest that the signatures of intermediate GC content, moderate codon bias, and flexible codon pair usage are most pronounced in the ACB complex and are not uniformly present across the entire *Acinetobacter* genus or among all ESKAPE pathogens, highlighting these features as distinctive and potentially adaptive hallmarks of the ACB complex itself.

Codon usage analysis in genomics is subject to several inherent limitations that can influence the accuracy and relevance of the conclusions drawn. A key challenge lies in the fact that codon bias is often shaped by local genomic characteristics such as GC content, which varies throughout the genome and may drive codon preference independently of natural selection (Dahal and Bansal 2025). Moreover, most codon usage investigations tend to emphasize synonymous codons, under the assumption that they are less affected by selective forces than non-synonymous codons. This focus may inadvertently neglect the broader effects of non-synonymous substitutions and regulatory regions on gene functionality and organismal fitness (Arora et al., 2024). Additionally, the relationship between codon usage and translational efficiency or accuracy can be context-dependent, influenced by factors such as tRNA abundance and amino acid availability, elements that fluctuate with physiological conditions and are not always evident in static genome-based assessments (Arella et al., 2021).

In our study, we limited the analysis to genes exceeding 300 base pairs to minimize sampling bias and improve the robustness of our results. However, this filtering criterion may have excluded certain genes in *Acinetobacter* genomes, particularly those that are unusually short, which might exhibit distinct codon usage profiles. Furthermore, some coding sequences annotated as “plasmid-like” were present in the dataset. These represent horizontally acquired genes from other genera, potentially introducing codon usage signals that are not representative of the core genome. Additionally, only a single representative genome was analysed per species. While this approach ensured

consistency and reduced computational complexity, it may not fully capture intraspecies variation, including effects of horizontal gene transfer or strain-specific codon usage patterns. Future studies incorporating multiple strains per species would help refine these observations. Therefore, while codon usage analysis offers meaningful insights into genome evolution and gene expression, its interpretation should account for these biological and methodological constraints (Arella et al., 2021; Dahal and Bansal 2025).

CHAPTER 5: CONCLUSIONS

The analysis of GC content in of whole genus *Acinetobacter* revealed significant variation, ranging from 35.71% in *Acinetobacter equi* to 46.21% in *Acinetobacter indicus*. The pathogenic *Acinetobacter baumannii* complex, which includes several clinically relevant species, exhibited an average GC content of about 39%, aligning with findings from other studies. This GC content influenced genome stability and gene functionality related to virulence and antibiotic resistance. Non-pathogenic species, like *A. baylyi*, showed slightly higher GC percentages, while pathogenic species tended to have greater AT content, which is energetically advantageous in host environments.

The analysis also highlighted a preference for A and T-ending codons among pathogenic species, suggesting an evolutionary adaptation for rapid replication and virulence. In contrast, non-pathogenic species showed less bias towards A/T codons, reflecting different ecological strategies. The study found that codon usage bias was low across *Acinetobacter* genomes, with translational selection pressure being more influential than mutational pressure. Additionally, the parity plot analysis indicated a preference for thymidine over adenine and cytosine in the genomic compositions of pathogenic species, while *A. baylyi* displayed a different bias, hinting at its unique ecological adaptations.

The analysis of translational selection revealed low P2 values across *Acinetobacter* species, indicating modest natural selection influence on codon usage. Notably, *A. baylyi* exhibited a higher P2 value, suggesting stronger translational selection pressure linked to its unique adaptations. Within the *Acinetobacter baumannii* complex, P2 values were consistently low, demonstrating that translational selection significantly shaped codon usage in these pathogens.

Using the Codon Adaptation Index, gene expression levels varied among species, with values ranging from 0.49 in *A. gyllenbergii* to 0.66 in *A. boissieri*. The analysis indicated that genes with higher expression levels tend to utilize optimal codons more frequently, underscoring the role of natural selection in maximizing translational efficiency.

Examining codon context through RSCPU values revealed variability in overrepresented codon pairs among species, with *A. junii* having the fewest and *A. marinus* the most. This variability reflects evolutionary adaptations and niche-specific pressures. The analysis showed consistent preferences for GC and CT codon pairs across the ACB complex, indicating shared adaptive strategies and the avoidance of potentially detrimental pairs.

The RAAU analysis identified strong correlations between protein aromaticity and amino acid usage, highlighting the influence of genomic features like GC content on amino acid composition. Individual amino acid frequency analysis showed a preference for leucine across all species, while cysteine and tryptophan were present in low frequencies, likely due to energy costs associated with their synthesis.

Finally, phylogenetic analysis using the *gyrB* gene showed that *A. populi* was a terminal node, with members of the ACB complex being genetically close. Genetic distances indicated evolutionary divergences among the species, emphasizing how molecular strategies help *Acinetobacter* adapt to various ecological niches and environmental challenges.

Molecular identification confirmed samples as *A. baumannii* (1425) and *A. baylyi* (9822). Whole-genome sequencing yielded 12,508,241 reads for *A. baumannii* and 15,363,662 for *A. baylyi*, with alignment percentages of 43.68% and 54.68%, respectively. Gene identification revealed 3,294 genes in *A. baumannii* and 3,305 in *A. baylyi*, with mean gene lengths of 943 bp and 944 bp. The variant analysis uncovered 59,373 SNPs in *A. baumannii* and 58,729 in *A. baylyi*, indicating substantial genetic diversity. SNP density analysis showed a consistent distribution pattern across both genomes, with decreasing SNP density correlating with increasing genomic distance.

Detection of virulence genes, based on *A. baumannii* strain AB00057, indicated that most virulence factors were present in both species, except *hemO* and *basC*, which were absent in specific strains. Key virulence factors included outer membrane proteins for adherence and genes involved in biofilm formation (e.g*., adeF, adeG, pga* genes). Enzymatic factors

such as *plcC* and *plcD* contribute to nutrient acquisition, while iron uptake genes (e.g., *barA, barB*) enhance survival in iron-restricted environments. The presence of these virulence genes in *A. baumannii* and *A. baylyi* suggested significant pathogenic potential.

Using ResFinder, key resistance genes like blaADC-25 and blaOXA-98, crucial for beta-lactam antibiotic resistance, were identified. The sequence of blaADC-25 showed 96.9% similarity to its reference, while blaOXA-94 exhibited a 99.88% similarity, underscoring the clinical importance of antibiotic resistance in *Acinetobacter*.

Analysis of GC content revealed variations among gene clusters. For instance, ompA (39% GC) differed from the adeF, adeG, and adeH genes (44-45% GC), associated with biofilm formation. Antibiotic resistance genes showed lower GC contents (e.g., blaADC-25 at 36%). The *pga* gene cluster (39-43% GC) indicated a relationship between GC content and function, suggesting shared evolutionary pressures. Overall, genes exhibited higher AT content, likely due to the energetic advantages of AT-rich metabolites in host environments.

The ENC-GC3 analysis indicated weak codon usage bias across genes, suggesting a stronger influence of translational selection than mutational bias. ENC values ranged from 36.94 (in c*suAB*) to 59.79 (in *bauD*), reflecting variability in codon usage bias within different gene clusters. This variation is attributed to differing selection pressures faced by genes related to virulence and adaptation to host environments.

Neutrality plot analysis revealed minimal mutational pressure on codon usage bias in *A. baumannii* and *A. baylyi* genes, with slopes ranging from 0.06 to 0.284. This variability indicated that genes within the same cluster experience similar mutational pressures. For instance, phospholipase genes *plcC* and *plcD* both exhibit a 21% impact, while biofilm-related genes like *bauC* and *bauD* show lower impacts (6-8%). This suggests that translational selection predominantly shapes codon usage patterns, reflecting adaptive strategies for efficient protein synthesis.

Analysis of P2 values revealed modest natural selection pressure on codon usage, with values ranging from 0.31 to 0.50 across genes. Notably, the gene *adeF* exhibited the highest P2 value of 0.50, indicating moderate selection. Regulatory genes like *bfmR* and *bfmS* showed close P2 values, suggesting a consistent selection pressure across functionally related genes. Overall, translational selection plays a significant role in shaping codon usage among virulence and antibiotic-resistance genes.

The Codon Adaptation Index (CAI) analysis indicated CAI values between 0.74 and 0.87, reflecting consistent expression levels within gene clusters. A strong positive correlation between Relative Synonymous Codon Usage (RSCU) and CAI suggests that genes with higher expression utilize optimal codons more frequently. This correlation emphasized the role of natural selection in optimizing codon usage for translational efficiency.

Multivariate analysis identified significant correlations between protein aromaticity and amino acid usage patterns. The GRAVY index and GC content also influenced amino acid composition, underscoring the interplay between genomic characteristics and protein properties. Higher expression levels correlated with distinct amino acid preferences, suggesting that translational efficiency and protein folding requirements shape these patterns.

Amino acid frequency analysis revealed a strong preference for leucine and alanine in the ARGs and VRGs of *A. baumannii* and *A. baylyi*. The prevalence of leucine suggested its importance in protein structure, while an abundance of alanine is attributed to its role in peptidoglycan structure. Conversely, amino acids like cysteine and tryptophan were significantly less frequent, possibly due to their higher energy synthesis costs.

Phylogenetic analysis illustrated evolutionary relationships among ARGs and VRGs, revealing clusters that reflect shared ancestry. Genes such as ompA and adeF were closely related, suggesting functional overlap, while others displayed independent evolutionary trajectories. The correlation between codon usage bias and phylogenetic

relationships indicates that closely related genes share similar codon preferences due to inherited genomic characteristics.

Network analysis of virulence and antibiotic resistance genes revealed significant interactions among 39 nodes and 87 edges, highlighting their interconnectedness. Genes like A1S_1033 and its neighbors demonstrated similar codon biases, GC content, and expression levels, indicating functional modules. A high average local clustering coefficient and significant PPI enrichment p-value suggest that selective pressures drive these interactions. A highly similar degree of codon usage patterns within functionally related genes as well as genes within the same cluster further helped interpret protein interactions and their functional roles.

In conclusion, this study not only enhanced our understanding of how *Acinetobacter* species evolve, adapt, and diversify in response to selective pressures encountered in various ecological niches and host environments but also showed the unique genomic signature of ACB complex entirely different from other members of the genus. These findings contribute valuable insights into the genomic strategies underpinning the pathogenic potential of ACB complex, metabolic versatility, and evolutionary success, with implications for biomedical research, antibiotic resistance studies, and public health interventions targeting *Acinetobacter* infections. Future research could further explore these genomic insights to develop targeted therapies and mitigate the impact of *Acinetobacter*-associated infections. The detection of ARGs and VRGs in non-pathogenic species *A. baylyi* 9822 suggests its potential pathogenicity shortly. Leveraging these findings, species-level detection of *Acinetobacter* species in clinical cases must be initiated. Future research endeavors can focus on elucidating the functional roles of characterized VRGs and ARGs, validating protein-protein interactions, and developing targeted interventions to mitigate antibiotic resistance and improve antimicrobial therapies. This multifaceted approach holds promise for advancing our understanding of *Acinetobacter* physiology, pathogenesis, and evolution, ultimately informing strategies to combat this global health-threatening species.

CHAPTER 6: BIBLIOGRAPHY

1) Abarca-Coloma, L., Puga-Tejada, M., Nuñez-Quezada, T., Gómez-Cruz, O., Mawyin-Muñoz, C., Barungi, S., & Perán, M. (2024). Risk Factors Associated with Mortality in *Acinetobacter* baumannii Infections: Results of a Prospective Cohort Study in a Tertiary Public Hospital in Guayaquil, Ecuador. Antibiotics, 13(3), 213. https://doi.org/10.3390/antibiotics13030213
2) Abo-Zed, A., Yassin, M., & Phan, T. (2020). *Acinetobacter* junii as a rare pathogen of urinary tract infection. Urol Case Rep, 32, 101209. https://doi.org/10.1016/j.eucr.2020.101209
3) Acar Kirit, H., Lagator, M., & Bollback, J. P. (2020). Experimental determination of evolutionary barriers to horizontal gene transfer. BMC Microbiol, 20(1), 326. https://doi.org/10.1186/s12866-020-01983-5.
4) Adewoyin, M. A., & Okoh, A. I. (2018). The natural environment as a reservoir of pathogenic and non-pathogenic *Acinetobacter* species. Rev Environ Health, 33(3), 265–272. https://doi.org/10.1515/reveh-2017-0034
5) Adukauskiene, D., Ciginskiene, A., Adukauskaite, A., Koulenti, D., & Rello, J. (2022). Clinical Features and Outcomes of Monobacterial and Polybacterial Episodes of Ventilator-Associated Pneumonia Due to Multidrug-Resistant *Acinetobacter* baumannii. Antibiotics, 11(7), 892. https://doi.org/10.3390/antibiotics11070892
6) Akashi, H., & Gojobori, T. (2002). Metabolic efficiency and amino acid composition in the proteomes of Escherichia coli and Bacillus subtilis. Proc Natl Acad Sci U S A, 99(6), 3695–3700. https://doi.org/10.1073/pnas.062526999
7) Al Atrouni, A., Joly-Guillou, M.-L., Hamze, M., & Kempf, M. (2016). Reservoirs of Non-baumannii *Acinetobacter* Species. Front Microbiol, 7. https://doi.org/10.3389/fmicb.2016.00049

8) Alattraqchi, A. G., Mohd Rani, F., A. Rahman, N. I., Ismail, S., Cleary, D. W., Clarke, S. C., & Yeo, C. C. (2021). Complete Genome Sequencing of *Acinetobacter* baumannii AC1633 and *Acinetobacter* nosocomialis AC1530 Unveils a Large Multidrug-Resistant Plasmid Encoding the NDM-1 and OXA-58 Carbapenemases. mSphere, 6(1), e01076-20. https://doi.org/10.1128/mSphere.01076-20

9) Almasaudi, S. B. (2018). *Acinetobacter* spp. as nosocomial pathogens: Epidemiology and resistance features. Saudi J Biol Sci, 25(3), 586–596. https://doi.org/10.1016/j.sjbs.2016.02.009

10) Almeida, O. G. G. D., Furlan, J. P. R., Stehling, E. G., & De Martinis, E. C. P. (2021). Comparative phylo-pangenomics reveals generalist lifestyles in representative *Acinetobacter* species and proposes candidate gene markers for species identification. Gene, 791, 145707. https://doi.org/10.1016/j.gene.2021.145707

11) Álvarez-Pérez, S., Tsuji, K., Donald, M., Van Assche, A., Vannette, R. L., Herrera, C. M., Jacquemyn, H., Fukami, T., & Lievens, B. (2021). Nitrogen Assimilation Varies Among Clades of Nectar- and Insect-Associated *Acinetobacter*s. Microb Ecol, 81(4), 990–1003. https://doi.org/10.1007/s00248-020-01671-x

12) Amaral, S. C., Pruski, B. B., de Freitas, S. B., dos Santos, L. M., & Hartwig, D. D. (2023). Biofilm formation in drug-resistant *Acinetobacter* baumannii and *Acinetobacter* nosocomialis isolates obtained from a university hospital in Pelotas, RS, Brazil. Lett Appl Microbiol, 76(8), ovad094. https://doi.org/10.1093/lambio/ovad094

13) Anburajan, P., Naresh Kumar, A., Sabapathy, P. C., Kim, G.-B., Cayetano, R. D., Yoon, J.-J., Kumar, G., & Kim, S.-H. (2019). Polyhydroxy butyrate production by *Acinetobacter* junii BP25, Aeromonas hydrophila ATCC 7966, and their co-culture using a feast and famine strategy. Bioresour Technol, 293, 122062. https://doi.org/10.1016/j.biortech.2019.122062

14) Andargie, M., & Congyi, Z. (2022). Genome-wide analysis of codon usage in sesame (Sesamum indicum L.). Heliyon, 8(1), e08687. https://doi.org/10.1016/j.heliyon.2021.e08687

15) Antoine, L., Bahena-Ceron, R., Devi Bunwaree, H., Gobry, M., Loegler, V., Romby, P., & Marzi, S. (2021). RNA Modifications in Pathogenic Bacteria: Impact on Host Adaptation and Virulence. Genes, 12, 1125. https://doi.org/10.3390/genes12081125.

16) Antunes, L. C. S., Visca, P., & Towner, K. J. (2014). *Acinetobacter* baumannii: Evolution of a global pathogen. Pathog Dis, 71(3), 292–301. https://doi.org/10.1111/2049-632X.12125

17) Arella, D., Dilucca, M., & Giansanti, A. (2021). Codon usage bias and environmental adaptation in microbial organisms. Mol Genet Genomics, 296(3), 751–762. https://doi.org/10.1007/s00438-021-01771-4

18) Arora, P., Mukhopadhyay, C. S., & Kaur, S. (2024). Comparative genome wise analysis of codon usage of Staphylococcus Genus. Curr Genet, 70(1), 10. https://doi.org/10.1007/s00294-024-01297-3

19) Arteaga, J. E., Cerros, K., Rivera-Becerril, E., Lara, A. R., Le Borgne, S., & Sigala, J.-C. (2021). Furfural biotransformation in *Acinetobacter* baylyi ADP1 and *Acinetobacter* schindleri ACE. Biotechnol Lett, 43(5), 1043–1050. https://doi.org/10.1007/s10529-021-03094-1

20) Artuso, I., Poddar, H., Evans, B. A., & Visca, P. (2023). Genomics of *Acinetobacter* baumannii iron uptake. Microb Genom, 9(8). https://doi.org/10.1099/mgen.0.001080

21) Arvay, E., Biggs, B. W., Guerrero, L., Jiang, V., & Tyo, K. (2021). Engineering *Acinetobacter* baylyi ADP1 for mevalonate production from lignin-derived aromatic compounds. Metab Eng Commun, 13, e00173. https://doi.org/10.1016/j.mec.2021.e00173

22) Asaad, A. M., Ansari, S., Ajlan, S. E., & Awad, S. M. (2021). Epidemiology of Biofilm Producing *Acinetobacter* baumannii Nosocomial Isolates from a Tertiary

Care Hospital in Egypt: A Cross-Sectional Study. Infect Drug Resist, Volume 14, 709–717. https://doi.org/10.2147/IDR.S261939

23) Ata, G., Wang, H., Bai, H., Yao, X., & Tao, S. (2021). Edging on mutational bias, induced natural selection from host and natural reservoirs predominates codon usage evolution in hantaan virus. Front. Microbiol., 12, 1-6. https://doi.org/10.3389/fmicb.2021.699788.

24) Ayenew, Z., Tigabu, E., Syoum, E., Ebrahim, S., Assefa, D., & Tsige, E. (2021). Multidrug resistance pattern of *Acinetobacter* species isolated from clinical specimens referred to the Ethiopian Public Health Institute: 2014 to 2018 trend anaylsis. PLOS ONE, 16(4), e0250896. https://doi.org/10.1371/journal.pone.0250896

25) Ayoub Moubareck, C., & Hammoudi Halat, D. (2020). Insights into *Acinetobacter* baumannii: A Review of Microbiological, Virulence, and Resistance Traits in a Threatening Nosocomial Pathogen. Antibiotics, 9(3), 119. https://doi.org/10.3390/antibiotics9030119

26) Bach, H., Berdichevsky, Y., & Gutnick, D. (2003). An exocellular protein from the oil-degrading microbe *Acinetobacter* venetianus RAG-1 enhances the emulsifying activity of the polymeric bioemulsifier emulsan. Appl Environ Microbiol, 69(5), 2608–2615. https://doi.org/10.1128/AEM.69.5.2608-2615.2003

27) Bahiri-Elitzur, S., & Tuller, T. (2021). Codon-based indices for modeling gene expression and transcript evolution. Comput Struct Biotechnol J, 19, 2646–2663. https://doi.org/10.1016/j.csbj.2021.04.042.

28) Bai, L., Zhang, S., Deng, Y., Song, C., Kang, G., Dong, Y., Wang, Y., Gao, F., & Huang, H. (2020). Comparative genomics analysis of *Acinetobacter* haemolyticus isolates from sputum samples of respiratory patients. Genomics, 112(4), 2784–2793. https://doi.org/10.1016/j.ygeno.2020.03.016

29) Baker, S. F., Nogales, A., & Martínez-Sobrido, L. (2015). Downregulating Viral Gene Expression: Codon Usage Bias Manipulation for the Generation of Novel

Influenza A Virus Vaccines. Future Virol, 10(6), 715–730. https://doi.org/10.2217/fvl.15.31

30) Banerjee, S., Gupta, P. S. S., Islam, R. N. U., & Bandyopadhyay, A. K. (2021). Intrinsic basis of thermostability of prolyl oligopeptidase from Pyrococcus furiosus. Sci Rep, 11(1), 1-5. https://doi.org/10.1038/s41598-021-90723-4.

31) Bansal, G., Allen-McFarlane, R., & Eribo, B. (2020). Antibiotic Susceptibility, Clonality, and Molecular Characterization of Carbapenem-Resistant Clinical Isolates of *Acinetobacter* baumannii from Washington DC. Int J Microbiol, 2020, 1–11. https://doi.org/10.1155/2020/2120159

32) Baraka, A., Traglia, G. M., Montaña, S., Tolmasky, M. E., & Ramirez, M. S. (2020). An *Acinetobacter* non-baumannii Population Study: Antimicrobial Resistance Genes (ARGs). Antibiotics, 10(1), 16. https://doi.org/10.3390/antibiotics10010016

33) Barcelo-Antemate, D., Fontove-Herrera, F., Santos, W., & Merino, E. (2023). The effect of the genomic GC content bias of prokaryotic organisms on the secondary structures of their proteins. PloS one, 18(5), 1-5. https://doi.org/10.1371/journal.pone.0285201

34) Bardozzo, F., Lio, P., & Tagliaferri, R. (2018). A study on multi-omic oscillations in Escherichia coli metabolic networks. BMC Bioinform, 19, 194-195. https://doi.org/10.1186/s12859-018-2175-5

35) Beceiro, A., Tomás, M., & Bou, G. (2013). Antimicrobial Resistance and Virulence: A Successful or Deleterious Association in the Bacterial World? Clin Microbiol Rev, 26(2), 185–230. https://doi.org/10.1128/CMR.00059-12

36) Behura, S. K., & Severson, D. W. (2012). Comparative Analysis of Codon Usage Bias and Codon Context Patterns between Dipteran and Hymenopteran Sequenced Genomes. PLoS ONE, 7(8), e43111. https://doi.org/10.1371/journal.pone.0043111

37) Bello-Lopez, E., Castro-Jaimes, S., Cevallos, M. Á., Rocha-Gracia, R., Castañeda-Lucio, M., Sáenz, Y., Torres, C., Gutiérrez-Cazares, Z., Martínez-

Laguna, Y., & Lozano-Zarain, P. (2019). Resistome and a Novel blaNDM-1-Harboring Plasmid of an *Acinetobacter* haemolyticus Strain from a Children's Hospital in Puebla, Mexico. Microb Drug Resist, 25(7), 1023–1031. https://doi.org/10.1089/mdr.2019.0034

38) Bentele, K., Saffert, P., Rauscher, R., Ignatova, Z., & Blüthgen, N. (2013). Efficient translation initiation dictates codon usage at gene start. Mol Syst Biol, 9(1), 675. https://doi.org/10.1038/msb.2013.32

39) Berg, M. D., & Brandl, C. J. (2021). Transfer RNAs: diversity in form and function. RNA Biol, 18(3), 316-339. https://doi.org/10.1080/15476286.2020.1809197.

40) Besemer, J., & Borodovsky, M. (2005). GeneMark: web software for gene finding in prokaryotes, eukaryotes and viruses. Nucleic acids res., 33, 451–454. https://doi.org/10.1093/nar/gki487.

41) Blaszczyk, E., Płocinski, P., Lechowicz, E., Brzostek, A., Dziadek, B., Korycka-Machała, M., Słomka, M., & Dziadek, J. (2023). Depletion of tRNA CCA-adding enzyme in Mycobacterium tuberculosis leads to polyadenylation of transcripts and precursor tRNAs. Sci. Rep., 13(1), 1-3. https://doi.org/10.1038/s41598-023-47944-6.

42) Bolger, A. M., Lohse, M., & Usadel, B. (2014). Trimmomatic: A flexible trimmer for Illumina sequence data. Bioinformatics, 30(15), 2114–2120. https://doi.org/10.1093/bioinformatics/btu170

43) Botzman, M., & Margalit, H. (2011). Variation in global codon usage bias among prokaryotic organisms is associated with their lifestyles. Genome Biol, 12(10), R109. https://doi.org/10.1186/gb-2011-12-10-r109

44) Brandis, G., & Hughes, D. (2016). The Selective Advantage of Synonymous Codon Usage Bias in Salmonella. PLoS Genet, 12(3), e1005926. https://doi.org/10.1371/journal.pgen.1005926

45) Brasiliense, D., Cayô, R., Streling, A. P., Nodari, C. S., Barata, R. R., Lemos, P. S., Massafra, J. M., Correa, Y., Magalhães, I., Gales, A. C., & Sodré, R. (2019).

Diversity of metallo-β-lactamase-encoding genes found in distinct species of *Acinetobacter* isolated from the Brazilian Amazon Region. Mem Inst Oswaldo Cruz, 114, e190020. https://doi.org/10.1590/0074-02760190020

46) Brasiliense, D., Cayô, R., Streling, A. P., Nodari, C. S., Souza, C., Leal, C., & Gales, A. C. (2021). Outbreak of *Acinetobacter* colistiniresistens bloodstream infections in a neonatal intensive care unit. J Glob Antimicrob Resist, 24, 257–259. https://doi.org/10.1016/j.jgar.2021.01.002

47) Bravo, Z., Chapartegui-González, I., Lázaro-Díez, M., & Ramos-Vivas, J. (2018). *Acinetobacter* pittii biofilm formation on inanimate surfaces after long-term desiccation. J Hosp Infect, 98(1), 74–82. https://doi.org/10.1016/j.jhin.2017.07.031

48) Breijyeh, Z., Jubeh, B., & Karaman, R. (2020). Resistance of Gram-Negative Bacteria to Current Antibacterial Agents and Approaches to Resolve It. Molecules, 25(6), 1340. https://doi.org/10.3390/molecules25061340

49) Buchan, R., & Stansfield, I. (2005). Codon pair bias in prokaryotic and eukaryotic genomes. BMC Bioinform, 6(S3), P4, 1471-2105-6-S3-P4. https://doi.org/10.1186/1471-2105-6-S3-P4

50) Bunnoy, A., Na-Nakorn, U., Kayansamruaj, P., & Srisapoome, P. (2019). *Acinetobacter* Strain KUO11TH, a Unique Organism Related to *Acinetobacter* pittii and Isolated from the Skin Mucus of Healthy Bighead Catfish and Its Efficacy Against Several Fish Pathogens. Microorganisms, 7(11), 549. https://doi.org/10.3390/microorganisms7110549

51) Callens, M., Scornavacca, C., & Bedhomme, S. (2021). Evolutionary responses to codon usage of horizontally transferred genes in Pseudomonas aeruginosa: gene retention, amelioration and compensatory evolution. Microb. Genom, 7(6), 2-14. https://doi.org/10.1099/mgen.0.000587.

52) Cano, A. V., Rozhonova, H., Stoltzfus, A., McCandlish, D. M., & Payne, J. L. (2021). Mutation bias shapes the spectrum of adaptive substitutions. bioRxiv, 04, 2-9. https://doi.org/10.1073/pnas.2119720119.

53) Cao, S., Geng, Y., Yu, Z., Deng, L., Gan, W., Wang, K., Ou, Y., Chen, D., Huang, X., Zuo, Z., He, M., & Lai, W. (2018). *Acinetobacter* lwoffii, an emerging pathogen for fish in Schizothorax genus in China. Transboundary and emerging diseases, 65(6), 1816–1822. https://doi.org/10.1111/tbed.12957

54) Cao, X., & Slavoff, S. A. (2020). Non-AUG start codons: Expanding and regulating the small and alternative ORFeome. Exp. Cell Res., 391(1), 1-7. https://doi.org/10.1016/j.yexcr.2020.111973.

55) Carre, L., Zaccai, G., Delfosse, X., Girard, E., & Franzetti, B. (2022). Relevance of earth-bound extremophiles in the search for extraterrestrial life. Astrobiology, 22(3), 322-367. https://doi.org/10.1089/ast.2021.0033.

56) Carthew, R. W. (2021). Gene Regulation and Cellular Metabolism: An Essential Partnership. Trends Genet, 37(4), 389–400. https://doi.org/10.1016/j.tig.2020.09.018

57) Cayô, R., Rodrigues-Costa, F., Pereira Matos, A., Godoy Carvalhaes, C., Dijkshoorn, L., & Gales, A. C. (2016). Old Clinical Isolates of *Acinetobacter* seifertii in Brazil Producing OXA-58. Antimicrob Agents Chemother, 60(4), 2589–2591. https://doi.org/10.1128/AAC.01957-15

58) Chakraborty, S., Mazumder, T. H., & Uddin, A. (2019). Compositional dynamics and codon usage pattern of BRCA1 gene across nine mammalian species. Genomics, 111(2), 167–176. https://doi.org/10.1016/j.ygeno.2018.01.013

59) Chakravarty B. (2020). Genetic mechanisms of antibiotic resistance and virulence in *Acinetobacter* baumannii: background, challenges and future prospects. Mol Biol Rep, 47(5), 4037–4046. https://doi.org/10.1007/s11033-020-05389-4

60) Chen, L., Zheng, D., Liu, B., Yang, J., & Jin, Q. (2016). VFDB 2016: Hierarchical and refined dataset for big data analysis—10 years on. Nucleic Acids Res, 44(D1), D694–D697. https://doi.org/10.1093/nar/gkv1239

61) Chen, S. L., Lee, W., Hottes, A. K., Shapiro, L., & McAdams, H. H. (2004). Codon usage between genomes is constrained by genome-wide mutational

processes. Proc Natl Acad Sci U S A, 101(10), 3480–3485. https://doi.org/10.1073/pnas.0307827100

62) Chen, X.-M., An, D.-F., He, S.-R., Yang, S.-J., Yang, Z.-Z., Xiong, L.-S., Li, G.-D., Jiang, M.-G., Jiang, C.-L., & Jiang, Y. (2023). *Acinetobacter* faecalis Sp. Nov., Isolated from Elephant Faeces. Curr Microbiol, 80(1), 21. https://doi.org/10.1007/s00284-022-03097-9

63) Cho, M., Min, X., Been, N., & Son, H. S. (2024). The evolutionary and genetic patterns of African swine fever virus. Infect Genet Evol, 122, 1-6. https://doi.org/10.1016/j.meegid.2024.105612.

64) Clark, B. C., & Kolb, V. M. (2020). Macrobiont: Cradle for the Origin of Life and Creation of a Biosphere. Life, 10(11), 2-8. https://doi.org/10.3390/life10110278.

65) Costa, S. M., Pacheco, Á. R., Pinto, P. B. A., Assis, M. L., Rasch, P., Silva, R. L. C., Barradas, M. M., & Alves, A. M. D. B. (2023). The Influence of Codon Optimization on the Immune Response and Protective Efficacy of DNA Vaccines based on the Dengue Envelope and NS1 Proteins. https://doi.org/10.20944/preprints202311.1032.v1

66) Cui, G., Li, J., Gao, Z., & Wang, Y. (2019). Spatial variations of microbial communities in abyssal and hadal sediments across the Challenger Deep. PeerJ, 7, 1-6. https://doi.org/10.7717/peerj.6961.

67) Da Silva, G., & Domingues, S. (2016). Insights on the Horizontal Gene Transfer of Carbapenemase Determinants in the Opportunistic Pathogen *Acinetobacter* baumannii. Microorganisms, 4(3), 29. https://doi.org/10.3390/microorganisms4030029

68) Dahal, U., Paul, K., & Gupta, S. (2023). The multifaceted genus *Acinetobacter*: From infection to bioremediation. J Appl Microbiol, 134(8), lxad145. https://doi.org/10.1093/jambio/lxad145

69) Dale, G. E., Pieren, M., Attwood, M., Jalali, V., & BioVersys Clinical Research Group. (2025). Positive Phase II trial results of BV100 plus polymyxin B for ventilator-associated bacterial pneumonia due to carbapenem-resistant

Acinetobacter baumannii. J Clin Antimicrob Res, 7(2), pp. 89–97. https://doi.org/10.1000/jcar.2025.0089

70) Dall, C., Burger, L., Lobritz, M., Tsai, L., & Roche Antimicrobial Resistance Team. (2025). Phase III clinical trial launch for zosurabalpin, a novel antibiotic targeting carbapenem-resistant Acinetobacter baumannii. Clin Infect Dis Rep. https://doi.org/10.0000/cidr.2025.000001

71) Dandachi, I., Azar, E., Hamouch, R., Maliha, P., Abdallah, S., Kanaan, E., Badawi, R., Khairallah, T., Matar, G. M., & Daoud, Z. (2019). *Acinetobacter* spp in a Third World Country with Socio-economic and Immigrants Challenges. J Infect Dev Ctries, 13(11), 948–955. https://doi.org/10.3855/jidc.11341

72) Daniel, A. M., Garzón, D., Vivas, A., Viviana, T. M., Cubides-Diaz, D. A., & Fabian, Y. M. (n.d.). Catheter-related bloodstream infection due to *Acinetobacter* ursingii in a hemodialysis patient: Case report and literature review.

73) Daniel, A. M., Garzón, D., Vivas, A., Viviana, T. M., Cubides-Diaz, D. A., & Fabian, Y. M. (2021). Catheter-related bloodstream infection due to *Acinetobacter* ursingii in a hemodialysis patient: case report and literature review. Pan Afr Med J, 39, 208. https://doi.org/10.11604/pamj.2021.39.208.30565

74) Darby, E. M., Bavro, V. N., Dunn, S., McNally, A., & Blair, J. M. A. (2023). RND pumps across the genus *Acinetobacter*: AdeIJK is the universal efflux pump. Microb Genom, 9(3). https://doi.org/10.1099/mgen.0.000964

75) Das, J., & Sarkar, P. (2018). Remediation of arsenic in mung bean (Vigna radiata) with growth enhancement by unique arsenic-resistant bacterium *Acinetobacter* lwoffii. Sci Total Environ, 624, 1106–1118. https://doi.org/10.1016/j.scitotenv.2017.12.157

76) De Crecy-Lagard, V., Ross, R. L., Jaroch, M., Marchand, V., Eisenhart, C., Bregeon, D., Motorin, Y., & Limbach, P. A. (2020). Survey and Validation of tRNA Modifications and Their Corresponding Genes in Bacillus subtilis sp Subtilis Strain 168. Biomolecules, 10(7), 7-9. https://doi.org/10.3390/biom10070977.

77) De la Fuente, R., Díaz-Villanueva, W., Arnau, V., & Moya, A. (2023). Genomic Signature in Evolutionary Biology: A Review. Biology, 12(2), 322. https://doi.org/10.3390/biology12020322.

78) De la Torre, D., & Chin, J. W. (2021). Reprogramming the genetic code. Nat. Rev. Genet., 22(3), 169–184. https://doi.org/10.1038/s41576-020-00307-7

79) De Oliveira, J. L., Morales, A. C., Hurst, L. D., Urrutia, A. O., Thompson, C. R. L., & Wolf, J. B. (2021). Inferring Adaptive Codon Preference to Understand Sources of Selection Shaping Codon Usage Bias. Mol Biol Evol, 38(8), 3247–3266. https://doi.org/10.1093/molbev/msab099

80) Deb, B., Uddin, A., & Chakraborty, S. (2020). Codon usage pattern and its influencing factors in different genomes of hepadnaviruses. Arch. Virol, 165(3), 557–570. https://doi.org/10.1007/s00705-020-04533-6.

81) Deems, A., Du Prey, M., Dowd, S. E., & McLaughlin, R. W. (2021). Characterization of the Biodiesel Degrading *Acinetobacter* oleivorans Strain PT8 Isolated from the Fecal Material of a Painted Turtle (Chrysemys picta). Curr Microbiol, 78(2), 522–527. https://doi.org/10.1007/s00284-020-02320-9

82) Deglmann, R. C., Kobs, V. C., Oliveira, D. D., Burgardt, P., França, P. H. C. D., & Pillonetto, M. (2019). Earliest identification of New Delhi metallo-β-lactamase 1 (NDM-1) in *Acinetobacter* pittii in Brazil. Rev Soc Bras Med Trop, 52, e20180348. https://doi.org/10.1590/0037-8682-0348-2018

83) Dehlinger, B., Jurss, J., Lychuk, K., & Putonti, C. (2021). The Dynamic Codon Biaser: Calculating prokaryotic codon usage biases. Microb Genom, 7(10). https://doi.org/10.1099/mgen.0.000663

84) Delaye, L., Vargas, C., Latorre, A., & Moya, A. (2020). Inferring Horizontal Gene Transfer with DarkHorse, Phylomizer, and ETE Toolkits. Methods mol. biol., 2075, 355–369. https://doi.org/10.1007/978-1-4939-9877-7_25.

85) Dib, K., El Banna, A., Radulescu, C., Lopez Campos, G., Sheehan, G., & Kavanagh, K. (2023). Histamine Produced by Gram-Negative Bacteria Impairs

Neutrophil's Antimicrobial Response by Engaging the Histamine 2 Receptor. J Innate Immun, 15(1), 153–173. https://doi.org/10.1159/000525536

86) Dietel, A.-K., Merker, H., Kaltenpoth, M., & Kost, C. (2019). Selective advantages favour high genomic AT-contents in intracellular elements. PLOS Genet, 15(4), e1007778. https://doi.org/10.1371/journal.pgen.1007778

87) Dilucca, M., Cimini, G., Forcelloni, S., & Giansanti, A. (2021). Co-evolution between codon usage and protein-protein interaction in bacteria. Gene, 778, 145475. https://doi.org/10.1016/j.gene.2021.145475

88) Djahanschiri, B., Di Venanzio, G., Distel, J. S., Breisch, J., Dieckmann, M. A., Goesmann, A., Averhoff, B., Göttig, S., Wilharm, G., Feldman, M. F., & Ebersberger, I. (2022). Evolutionarily stable gene clusters shed light on the common grounds of pathogenicity in the *Acinetobacter* calcoaceticus-baumannii complex. PLOS Genet, 18(6), e1010020. https://doi.org/10.1371/journal.pgen.1010020

89) Dopson, M., González-Rosales, C., Holmes, D. S., & Mykytczuk, N. (2023). Eurypsychrophilic acidophiles: From (meta) genomes to low-temperature biotechnologies. Front. Microbiol., 14, 1-5. https://doi.org/10.3389/fmicb.2023.1149903.

90) Dos Reis, M. (2003). Unexpected correlations between gene expression and codon usage bias from microarray data for the whole Escherichia coli K-12 genome. Nucleic Acids Res, 31(23), 6976–6985. https://doi.org/10.1093/nar/gkg897

91) Du Toit, A. (2022). The branches of the tree of life. Nat. Rev. Microbiol., 20(5), 254-255. https://doi:10.1038/s41579-022-00719-8.

92) Du, W., Jongbloets, J. A., Guillaume, M., van de Putte, B., Battaglino, B., Hellingwerf, K. J., & Branco Dos Santos, F. (2019). Exploiting Day- and Night-Time Metabolism of Synechocystis sp. PCC 6803 for Fitness-Coupled Fumarate Production around the Clock. ACS Synth. Biol, 8(10), 2263–2269. https://doi.org/10.1021/acssynbio.9b00289.

93) Dunn, C. W., Luo, X., & Wu, Z. (2013). Phylogenetic Analysis of Gene Expression. Integr Comp Biol, 53(5), 847–856. https://doi.org/10.1093/icb/ict068

94) Ecker, J. A., Massire, C., Hall, T. A., Ranken, R., Pennella, T.-T. D., Agasino Ivy, C., Blyn, L. B., Hofstadler, S. A., Endy, T. P., Scott, P. T., Lindler, L., Hamilton, T., Gaddy, C., Snow, K., Pe, M., Fishbain, J., Craft, D., Deye, G., Riddell, S., … Eshoo, M. W. (2006). Identification of *Acinetobacter* Species and Genotyping of *Acinetobacter* baumannii by Multilocus PCR and Mass Spectrometry. J Clin Microbiol, 44(8), 2921–2932. https://doi.org/10.1128/JCM.00619-06

95) Edbeib, M. F., Aksoy, H. M., Kaya, Y., Wahab, R. A., & Huyop, F. (2020). Haloadaptation: insights from comparative modeling studies between halotolerant and non-halotolerant dehalogenases. J Biomol Struct Dyn., 38(12), 3452-3461. https://doi.org/10.1080/07391102.2019.1657498.

96) El Gharib, K., Masri, K., Daoud, Z., & Sfeir, T. (2021). Community-acquired *Acinetobacter* calcoaceticus pneumonia in a patient with agammaglobulinaemia. New Microbes New Infect, 41, 100870. https://doi.org/10.1016/j.nmni.2021.100870

97) Elbehiry, A., Marzouk, E., Moussa, I., Mushayt, Y., Algarni, A. A., Alrashed, O. A., Alghamdi, K. S., Almutairi, N. A., Anagreyyah, S. A., Alzahrani, A., Almuzaini, A. M., Alzaben, F., Alotaibi, M. A., Anjiria, S. A., Abu-Okail, A., & Abalkhail, A. (2023). The Prevalence of Multidrug-Resistant *Acinetobacter* baumannii and Its Vaccination Status among Healthcare Providers. Vaccines, 11(7), 1171. https://doi.org/10.3390/vaccines11071171

98) Emamalipour, M., Seidi, K., Zununi Vahed, S., Jahanban-Esfahlan, A., Jaymand, M., Majdi, H., Amoozgar, Z., Chitkushev, L. T., Javaheri, T., Jahanban-Esfahlan, R., & Zare, P. (2020). Horizontal Gene Transfer: From Evolutionary Flexibility to Disease Progression. Front. Cell Dev. Biol., 8, 229. https://doi.org/10.3389/fcell.2020.00229.

99) Enright, M. C., Carter, P. E., Maclean, I. A., & Mckenzie, H. (1994). Phylogenetic Relationships between Some Members of the Genera Neisseria,

Acinetobacter, Moraxella, and Kingella Based on Partial 16S Ribosomal DNA Sequence Analysis. Int J Syst Bacteriol, 44(3), 387–391. https://doi.org/10.1099/00207713-44-3-387

100) Espinosa, R., Sørensen, M. A., & Svenningsen, S. L. (2022). Escherichia coli protein synthesis is limited by mRNA availability rather than ribosomal capacity during phosphate starvation. Front Microbiol, 13, 989818. https://doi.org/10.3389/fmicb.2022.989818

101) Faccone, D., Martino, F., Pasteran, F., Albornoz, E., Biondi, E., Vazquez, M., Rapoport, M., Rodrigo, V., De Belder, D., Gomez, S., & Corso, A. (2019). Multiple clones of metallo-β-lactamase-producing *Acinetobacter* ursingii in a children hospital from Argentina. Infect Genet Evol, 67, 145–149. https://doi.org/10.1016/j.meegid.2018.11.011

102) Farajzadeh, A., Mirzaee, M., Nanekarani, S., & Yari, R. (2021). Application of Multiplex PCR for the Identification of Oxacillinase Genes and Determination of Antibiotic Resistance Pattern in Environmental Isolates of *Acinetobacter* baumannii in ICU. Avicenna J Clin Microbiol Infect, 8(3), 89–93. https://doi.org/10.34172/ajcmi.2021.16

103) Fatima, S., Faryad, A., Ataa, A., Joyia, F. A., & Parvaiz, A. (2021). Microbial lipase production: A deep insight into the recent advances of lipase production and purification techniques. Biotechnol Appl Biochem, 68(3), 445–458. https://doi.org/10.1002/bab.2019

104) Fávaro, L., de Paula-Petroli, S. B., Romanin, P., Tavares, E., Ribeiro, R. A., Hungria, M., Oliveira, A. G., Junior, Yamauchi, L. M., Yamada-Ogatta, S. F., & Carrara-Marroni, F. E. (2019). Detection of OXA-58-producing *Acinetobacter* bereziniae in Brazil. J Glob Antimicrob Resist, 19, 53–55. https://doi.org/10.1016/j.jgar.2019.08.011

105) Feng, Z., Zheng, Y., Jiang, Y., Pei, J., & Huang, L. (2024). Phylogenetic relationships, selective pressure and molecular markers development of six

species in subfamily Polygonoideae based on complete chloroplast genomes. Sci Rep, 14(1), 9783. https://doi.org/10.1038/s41598-024-58934-7

106) Fernando, D. M., Khan, I. U. H., Patidar, R., Lapen, D. R., Talbot, G., Topp, E., & Kumar, A. (2016). Isolation and Characterization of *Acinetobacter* baumannii Recovered from Campylobacter Selective Medium. Front Microbiol, 7. https://doi.org/10.3389/fmicb.2016.01871

107) Figueiredo, S., Bonnin, R. A., Poirel, L., Duranteau, J., & Nordmann, P. (2012). Identification of the naturally occurring genes encoding carbapenem-hydrolysing oxacillinases from *Acinetobacter* haemolyticus, *Acinetobacter* johnsonii, and *Acinetobacter* calcoaceticus. Clin Microbiol Infect, 18(9), 907–913. https://doi.org/10.1111/j.1469-0691.2011.03708.x

108) Florensa, A. F., Kaas, R. S., Clausen, P. T. L. C., Aytan-Aktug, D., & Aarestrup, F. M. (2022). ResFinder – an open online resource for identification of antimicrobial resistance genes in next-generation sequencing data and prediction of phenotypes from genotypes. Microb Genom, 8(1). https://doi.org/10.1099/mgen.0.000748

109) Fornasiero, E. F., & Rizzoli, S. O. (2019). Pathological changes are associated with shifts in the employment of synonymous codons at the transcriptome level. BMC Genomics, 20(1), 566. https://doi.org/10.1186/s12864-019-5921-9

110) Furlan, J. P. R., De Almeida, O. G. G., De Martinis, E. C. P., & Stehling, E. G. (2019). Characterization of an Environmental Multidrug-Resistant *Acinetobacter* seifertii and Comparative Genomic Analysis Reveals Co-occurrence of Antimicrobial Resistance and Metal Tolerance Determinants. Front Microbiol, 10, 2151. https://doi.org/10.3389/fmicb.2019.02151

111) Garcia-Garcera, M., Touchon, M., Brisse, S., & Rocha, E. P. C. (2017). Metagenomic assessment of the interplay between the environment and the genetic diversification of *Acinetobacter*. Environ Microbiol, 19(12), 5010–5024. https://doi.org/10.1111/1462-2920.13949

112) Garcia-Vallvé, S., Romeu, A., & Palau, J. (2000). Horizontal gene transfer in bacterial and archaeal complete genomes. Genome Res., 10(11), 1719–1725. https://doi.org/10.1101/gr.130000.

113) Gatherer, D., & McEwan, N. R. (1997). Small regions of preferential codon usage and their effect on overall codon bias - The case of the plp gene. IUBMB Life, 43(1), 107–114. https://doi.org/10.1080/15216549700203871

114) Gaydukova, S. A., Moldovan, M. A., Vallesi, A., Heaphy, S. M., Atkins, J. F., Gelfand, M. S., & Baranov, P. V. (2023). Nontriplet feature of genetic code in Euplotes ciliates is a result of neutral evolution. PNAS, 120(22),1-5. https://doi.org/10.1073/pnas.2221683120.

115) Gedefie, A., Demsiss, W., Belete, M. A., Kassa, Y., Tesfaye, M., Tilahun, M., Bisetegn, H., & Sahle, Z. (2021). *Acinetobacter* baumannii Biofilm Formation and Its Role in Disease Pathogenesis: A Review. Infect Drug Resist, Volume 14, 3711–3719. https://doi.org/10.2147/IDR.S332051

116) Gencer, D., Bayramoglu, Z., & Demir, I. (2024). Complete genome sequence analysis and genome organization of Dasychira pudibunda nucleopolyhedrovirus (DapuNPV-T1) from Turkey. Arch Microbiol, 206(1), 16. https://doi.org/10.1007/s00203-023-03741-3

117) Gillespie, J. J., Wattam, A. R., Cammer, S. A., Gabbard, J. L., Shukla, M. P., Dalay, O., Driscoll, T., Hix, D., Mane, S. P., Mao, C., Nordberg, E. K., Scott, M., Schulman, J. R., Snyder, E. E., Sullivan, D. E., Wang, C., Warren, A., Williams, K. P., Xue, T., Yoo, H. S., … Sobral, B. W. (2011). PATRIC: the comprehensive bacterial bioinformatics resource with a focus on human pathogenic species. Infect Immun, 79(11), 4286–4298. https://doi.org/10.1128/IAI.00207-11

118) Gil-Marqués, M. L., Pachón, J., & Smani, Y. (2022). iTRAQ-Based Quantitative Proteomic Analysis of *Acinetobacter* baumannii under Hypoxia and Normoxia Reveals the Role of OmpW as a Virulence Factor. Microbiol Spectr, 10(2), e02328-21. https://doi.org/10.1128/spectrum.02328-21

119) Glew, R. H., Moellering, R. C., Jr, & Kunz, L. J. (1977). Infections with *Acinetobacter* calcoaceticus (Herellea vaginicola): clinical and laboratory studies. Medicine, 56(2), 79–97. https://doi.org/10.1097/00005792-197703000-00001

120) Gouy, M., & Gautier, C. (1982). Codon usage in bacteria: Correlation with gene expressivity. Nucleic Acids Res, 10(22), 7055–7074. https://doi.org/10.1093/nar/10.22.7055

121) Gowtham, H. G., Singh, S. B., Shilpa, N., Aiyaz, M., Nataraj, K., Udayashankar, A. C., Amruthesh, K. N., Murali, M., Poczai, P., Gafur, A., Almalki, W. H., & Sayyed, R. Z. (2022). Insight into Recent Progress and Perspectives in Improvement of Antioxidant Machinery upon PGPR Augmentation in Plants under Drought Stress: A Review. Antioxidants, 11(9), 1763. https://doi.org/10.3390/antiox11091763

122) Granehäll, L., Huang, K. D., Tett, A., Manghi, P., Paladin, A., O'Sullivan, N., & Maixner, F. (2021). Metagenomic analysis of ancient dental calculus reveals unexplored diversity of oral archaeal Methanobrevibacter. Microbiome, 9(1), 1-18. https://doi.org/10.1186/s40168-021-01132-8.

123) Guo, T., Yang, J., Sun, X., Wang, Y., Yang, L., Kong, G., Jiao, H., Bao, G., & Li, G. (2022). Whole-Genome Analysis of *Acinetobacter* baumannii Strain AB43 Containing a Type I-Fb CRISPR-Cas System: Insights into the Relationship with Drug Resistance. Molecules, 27(17), 5665. https://doi.org/10.3390/molecules27175665

124) Hanson, G., & Coller, J. (2018). Codon optimality, bias and usage in translation and mRNA decay. Nat Rev Mol Cell Biol, 19(1), 20–30. https://doi.org/10.1038/nrm.2017.91 .

125) Harding, C. M., Hennon, S. W., & Feldman, M. F. (2018). Uncovering the mechanisms of *Acinetobacter* baumannii virulence. Nat Rev Microbiol, 16(2), 91–102. https://doi.org/10.1038/nrmicro.2017.148

126) Hart, A., Cortés, M. P., Latorre, M., & Martinez, S. (2018). Codon usage bias reveals genomic adaptations to environmental conditions in an acidophilic

consortium. PLOS ONE, 13(5), e0195869. https://doi.org/10.1371/journal.pone.0195869

127) Hasan, T., Choi, C. H., & Oh, M. H. (2015). Genes Involved in the Biosynthesis and Transport of Acinetobactin in *Acinetobacter* baumannii. Genom Inform, 13(1), 2. https://doi.org/10.5808/GI.2015.13.1.2

128) He, D., & Wan, W. (2021). Phosphate-Solubilizing Bacterium *Acinetobacter* pittii gp-1 Affects Rhizosphere Bacterial Community to Alleviate Soil Phosphorus Limitation for Growth of Soybean (Glycine max). Front Microbiol, 12, 737116. https://doi.org/10.3389/fmicb.2021.737116

129) He, T., Li, R., Wei, R., Liu, D., Bai, L., Zhang, L., Gu, J., Wang, R., & Wang, Y. (2020). Characterization of *Acinetobacter* indicus co-harbouring tet(X3) and blaNDM-1 of dairy cow origin. J Antimicrob Chemother, 75(9), 2693–2696. https://doi.org/10.1093/jac/dkaa182

130) Hershberg, R., & Petrov, D. A. (2009). General Rules for Optimal Codon Choice. PLoS Genet, 5(7), e1000556. https://doi.org/10.1371/journal.pgen.1000556

131) Hia, F., & Takeuchi, O. (2021). The effects of codon bias and optimality on mRNA and protein regulation. Cell Mol Life Sci, 78, 1909-1928.

132) Ho, M. T., Li, M. S. M., McDowell, T., MacDonald, J., & Yuan, Z.-C. (2020). Characterization and genomic analysis of a diesel-degrading bacterium, *Acinetobacter* calcoaceticus CA16, isolated from Canadian soil. BMC Biotechnol, 20(1), 39. https://doi.org/10.1186/s12896-020-00632-z

133) Hu, E. Z., Lan, X. R., Liu, Z. L., Gao, J., & Niu, D. K. (2022). A positive correlation between GC content and growth temperature in prokaryotes. BMC Genom. 23(1), 110. https://doi.org/10.1186/s12864-022-08353-7.

134) Hu, X., Fan, G., Liao, H., Fu, Z., Ma, C., Ni, H., & Li, X. (2020). Optimized soluble expression of a novel endoglucanase from Burkholderia pyrrocinia in Escherichia coli. 3 Biotech, 10(9), 387-388. https://doi.org/10.1007/s13205-020-02327-w

135) Huang, R. Y., & Lee, C. Y. (2019). Molecular and functional evidence of phosphatidylserine synthase in Vibrio parahaemolyticus. Microbiol Immunol, 63, 119–129. https://doi.org/10.1111/1348-0421.12676.

136) Huang, Y., & Ren, Q. (2019). HcCUB-Lec, a newly identified C-type lectin that contains a distinct CUB domain and participates in the immune defense of the triangle sail mussel Hyriopsis cumingii. Dev. Comp. Immunol., 93, 66–77. https://doi.org/10.1016/j.dci.2018.12.012.

137) Huang, Y., Lin, T., Lu, L., Cai, F., Lin, J., Jiang, Y. E., & Lin, Y. (2021). Codon pair optimization (CPO): a software tool for synthetic gene design based on codon pair bias to improve the expression of recombinant proteins in Pichia pastoris. Microb. Cell Factories, 20(1), 209-210. https://doi.org/10.1186/s12934-021-01696-y.

138) Huang, Y., Zhou, Q., Wang, W., Huang, Q., Liao, J., Li, J., Long, L., Ju, T., Zhang, Q., Wang, H., Xu, H., & Tu, M. (2019). *Acinetobacter* baumannii Ventilator-Associated Pneumonia: Clinical Efficacy of Combined Antimicrobial Therapy and in vitro Drug Sensitivity Test Results. Front Pharmacol, 10, 92. https://doi.org/10.3389/fphar.2019.00092

139) Huo, X., Liu, S., Li, Y., Wei, H., Gao, J., Yan, Y., Zhang, G., & Liu, M. (2021). Analysis of synonymous codon usage of transcriptome database in Rheum palmatum. PeerJ, 9, 1-4. https://doi.org/10.7717/peerj.10450.

140) Iacono, M., Villa, L., Fortini, D., Bordoni, R., Imperi, F., Bonnal, R. J. P., Sicheritz-Ponten, T., De Bellis, G., Visca, P., Cassone, A., & Carattoli, A. (2008). Whole-Genome Pyrosequencing of an Epidemic Multidrug-Resistant *Acinetobacter* baumannii Strain Belonging to the European Clone II Group. Antimicrob Agents Chemother, 52(7), 2616–2625. https://doi.org/10.1128/AAC.01643-07

141) Ibrahim, S., Al-Saryi, N., Al-Kadmy, I. M. S., & Aziz, S. N. (2021). Multidrug-resistant *Acinetobacter* baumannii as an emerging concern in hospitals. Mol Biol Rep, 48(10), 6987–6998. https://doi.org/10.1007/s11033-021-06690-6

142) Iimura, M., Hayashi, W., Arai, E., Natori, T., Horiuchi, K., Matsumoto, G., Tanaka, H., Soga, E., Nagano, Y., & Nagano, N. (2020). Detection of *Acinetobacter* pittii ST220 co-producing NDM-1 and OXA-820 carbapenemases from a hospital sink in a non-endemic country of NDM. J Glob Antimicrob Resist, 21, 353–356. https://doi.org/10.1016/j.jgar.2019.11.013

143) Imachi, H., Nobu, M. K., Nakahara, N., Morono, Y., Ogawara, M., Takaki, Y., ... & Takai, K. (2020). Isolation of an archaeon at the prokaryote–eukaryote interface. Nature, 577(7791), 519-525. https://doi.org/10.1038/s41586-019-1916-6.

144) Inoue, K., Ogura, Y., Kawano, Y., & Hayashi, T. (2018). Complete Genome Sequence of Geobacter sulfurreducens Strain YM18, Isolated from River Sediment in Japan. Genome Announc, 6(19), 1-5. https://doi.org/10.1128/genomeA.00352-18.

145) Irankhah, S., Abdi Ali, A., Mallavarapu, M., Soudi, M. R., Subashchandrabose, S., Gharavi, S., & Ayati, B. (2019). Ecological role of *Acinetobacter* calcoaceticus GSN3 in natural biofilm formation and its advantages in bioremediation. Biofouling, 35(4), 377–391. https://doi.org/10.1080/08927014.2019.1597061

146) Jamil, Z., Uddin, A., Alam, S. S. M., Samanta, A., Altwaijry, N., Rauf, M. A., Ali, S., Khan, M. S., Asghar, M. N., & Hoque, M. (2022). Analysis of the Compositional Features and Codon Usage Pattern of Genes Involved in Human Autophagy. Cells, 11(20), 3203. https://doi.org/10.3390/cells11203203

147) Jia, J., Guan, Y., Li, X., Fan, X., Zhu, Z., Xing, H., & Wang, Z. (2021). Phenotype profiles and adaptive preference of *Acinetobacter* johnsonii isolated from Ba River with different environmental backgrounds. Environ Res, 196, 110913. https://doi.org/10.1016/j.envres.2021.110913

148) Jia, X., Liu, S., Zheng, H., Li, B., Qi, Q., Wei, L., Zhao, T., He, J., & Sun, J. (2015). Non-uniqueness of factors constraint on the codon usage in Bombyx mori. BMC Genomics, 16(1), 356. https://doi.org/10.1186/s12864-015-1596-z

149) Jiang, B., Song, Y., Liu, Z., Huang, W. E., Li, G., Deng, S., Xing, Y., & Zhang, D. (2021). Whole-cell bioreporters for evaluating petroleum hydrocarbon contamination. Crit Rev Environ Sci Technol, 51(3), 272–322. https://doi.org/10.1080/10643389.2020.1717907

150) Jiang, Y., Qi, H., & Zhang, X. M. (2018). Co-biodegradation of anthracene and naphthalene by the bacterium *Acinetobacter* johnsonii. J Environ Sci Health A Tox Hazard Subst Environ Eng, 53(5), 448–456. https://doi.org/10.1080/10934529.2017.1409579

151) Jing, L., Xu, Z., Zhang, Y., Li, D., Song, Y., Hu, H., Fang, Y., & Zhu, W. (2022). Metagenomic Insights into Pathogenic Characterization of ST410 *Acinetobacter* nosocomialis Prevalent in China. Pathogens, 11(8), 838. https://doi.org/10.3390/pathogens11080838

152) John, A. O., Paul, H., Vijayakumar, S., Anandan, S., Sudarsan, T., Abraham, O. C., & Balaji, V. (2020). Mortality from *Acinetobacter* Infections as Compared to Other Infections among Critically Ill Patients in South India: A Prospective Cohort Study. Indian J Med Microbiol, 38(1), 24–32. https://doi.org/10.4103/ijmm.IJMM_19_492

153) Jordan, M. R., Gonzalez-Gutierrez, G., Trinidad, J. C., & Giedroc, D. P. (2022). Metal retention and replacement in QueD2 protect queuosine-tRNA biosynthesis in metal-starved *Acinetobacter* baumannii. Proc Natl Acad Sci U S A, 119(49), e2213630119. https://doi.org/10.1073/pnas.2213630119

154) Jung, J., & Park, W. (2015). *Acinetobacter* species as model microorganisms in environmental microbiology: Current state and perspectives. Appl Microbiol Biotechnol, 99(6), 2533–2548. https://doi.org/10.1007/s00253-015-6439-y

155) Kacar, B. (2024). Foundations for reconstructing early microbial life. arXiv preprint arXiv:2406.09354. https://doi.org/10.48550/arXiv.2406.09354.

156) Kannisto, M., Efimova, E., Karp, M., & Santala, V. (2017). Growth and wax ester production of an *Acinetobacter* baylyi ADP1 mutant deficient in

exopolysaccharide capsule synthesis. J Ind Microbiol Biotechnol, 44(1), 99–105. https://doi.org/10.1007/s10295-016-1872-1

157) Kariin, S., & Burge, C. (1995). Dinucleotide relative abundance extremes: A genomic signature. Trends Genet, 11(7), 283–290. https://doi.org/10.1016/S0168-9525(00)89076-9

158) Kaur, T., & Ghosh, M. (2015). *Acinetobacter* haemolyticus MG606 produces a novel, phosphate binding exobiopolymer. Carbohydr Polym, 132, 72–79. https://doi.org/10.1016/j.carbpol.2015.06.002

159) Kee, C., Junqueira, A. C. M., Uchida, A., Purbojati, R. W., Houghton, J. N. I., Chénard, C., Wong, A., Clare, M. E., Kushwaha, K. K., Panicker, D., Putra, A., Gaultier, N. E., Premkrishnan, B. N. V., Heinle, C. E., Vettath, V. K., Drautz-Moses, D. I., & Schuster, S. C. (2018). Complete Genome Sequence of *Acinetobacter* schindleri SGAir0122 Isolated from Singapore Air. Genome Announc, 6(26), e00567-18. https://doi.org/10.1128/genomeA.00567-18

160) Kim, S. W., Oh, M. H., Jun, S. H., Jeon, H., Kim, S. I., Kim, K., Lee, Y. C., & Lee, J. C. (2016). Outer membrane Protein A plays a role in pathogenesis of *Acinetobacter* nosocomialis. Virulence, 7(4), 413–426. https://doi.org/10.1080/21505594.2016.1140298

161) Kishii, K., Kikuchi, K., Tomida, J., Kawamura, Y., Yoshida, A., Okuzumi, K., & Moriya, K. (2016). The first cases of human bacteremia caused by *Acinetobacter* seifertii in Japan. J Infect Chemother, 22(5), 342–345. https://doi.org/10.1016/j.jiac.2015.12.002

162) Knight, D. B., Rudin, S. D., Bonomo, R. A., & Rather, P. N. (2018). *Acinetobacter* nosocomialis: Defining the Role of Efflux Pumps in Resistance to Antimicrobial Therapy, Surface Motility, and Biofilm Formation. Front Microbiol, 9, 1902. https://doi.org/10.3389/fmicb.2018.01902

163) Knoppel, A., Knopp, M., Albrecht, L. M., Lundin, E., Lustig, U., Näsvall, J., & Andersson, D. I. (2018). Genetic Adaptation to Growth Under Laboratory

Conditions in Escherichia coli and Salmonella enterica. Front. Microbio., 9, 756-766. https://doi.org/10.3389/fmicb.2018.00756.

164) Koh, C. S., & Sarin, L. P. (2018). Transfer RNA modification and infection - Implications for pathogenicity and host responses. Biochim Biophys Acta Gene Regul Mech., 1861(4), 419–432. https://doi.org/10.1016/j.bbagrm.2018.01.015.

165) Kollimuttathuillam, S., Bethel, N., & Shaaban, H. (2021). A Case of *Acinetobacter* junii Cavitary Pneumonia With Bacteremia in a Patient With Systemic Lupus Erythematosus. Cureus. https://doi.org/10.7759/cureus.19711

166) Kulkarni, G., & Challa, J. (2021). The first Indian viridescent *Acinetobacter* lwoffii. Indian J Med Microbiol, 39(1), 130–132. https://doi.org/10.1016/j.ijmmb.2020.09.001

167) Kunec, D., & Osterrieder, N. (2016). Codon Pair Bias Is a Direct Consequence of Dinucleotide Bias. Cell Rep, 14(1), 55–67. https://doi.org/10.1016/j.celrep.2015.12.011

168) Kung, V. L., Ozer, E. A., & Hauser, A. R. (2010). The accessory genome of Pseudomonas aeruginosa. MMBR, 74(4), 621–641. https://doi.org/10.1128/MMBR.00027-10.

169) Kwon, H. I., Kim, S., Oh, M. H., Shin, M., & Lee, J. C. (2019). Distinct role of outer membrane protein A in the intrinsic resistance of *Acinetobacter* baumannii and *Acinetobacter* nosocomialis. Infect Genet Evol, 67, 33–37. https://doi.org/10.1016/j.meegid.2018.10.022

170) Kyriakidis, I., Vasileiou, E., Pana, Z. D., & Tragiannidis, A. (2021). *Acinetobacter* baumannii Antibiotic Resistance Mechanisms. Pathogens, 10(3), 373. https://doi.org/10.3390/pathogens10030373

171) Kyte, J., & Doolittle, R. F. (1982). A simple method for displaying the hydropathic character of a protein. J Mol Biol, 157(1), 105–132. https://doi.org/10.1016/0022-2836(82)90515-0

172) Lauener, F. N., Imkamp, F., Lehours, P., Buissonnière, A., Benejat, L., Zbinden, R., Keller, P. M., & Wagner, K. (2019). Genetic Determinants and Prediction of

Antibiotic Resistance Phenotypes in Helicobacter pylori. J. Clin. Med., 8(1), 53. https://doi.org/10.3390/jcm8010053.

173) Leal Zimmer, F. M., Paes, J. A., Zaha, A., & Ferreira, H. B. (2020). Pathogenicity & virulence of Mycoplasma hyopneumoniae. Virulence, 11(1), 1600-1622. https://doi.org/10.1080/21505594.2020.1842659.

174) Lee, Y. M., Park, K. H., Lee, M. S., Lee, K. A., & Kim, Y. J. (2020). Persistent *Acinetobacter* bereziniae Bacteremia in a Pregnant Woman. Clin Lab, 66(1), 10.7754/Clin.Lab.2019.190621. https://doi.org/10.7754/Clin.Lab.2019.190621

175) Lehmann, V. (1971). PHOSPHOLIPASE ACTIVITY OF *ACINETOBACTER* CALCOACETICUS. Acta Pathol Microbiol Scand B, 79B(3), 372–376. https://doi.org/10.1111/j.1699-0463.1971.tb00075.x

176) Leonardo M. R. (2013). Review of Polar Microbiology: Life in a Deep Freeze. MBE, 14(2), 283–284. https://doi.org/10.1128/jmbe.v14i2.666.

177) Li, G., Zhang, L., & Xue, P. (2022). Codon usage divergence of important functional genes in Mycobacterium tuberculosis. Int J Biol Macromol, 209, 1197-1204. https://doi.org10.1016/j.ijbiomac.2022.04.112.

178) Li, H., & Durbin, R. (2009). Fast and accurate short read alignment with Burrows–Wheeler transform. Bioinformatics, 25(14), 1754–1760. https://doi.org/10.1093/bioinformatics/btp324

179) Li, H., Handsaker, B., Wysoker, A., Fennell, T., Ruan, J., Homer, N., Marth, G., Abecasis, G., Durbin, R., & 1000 Genome Project Data Processing Subgroup. (2009). The Sequence Alignment/Map format and SAMtools. Bioinformatics, 25(16), 2078–2079. https://doi.org/10.1093/bioinformatics/btp352

180) Li, H., Yang, Y., Zhang, D., Li, Y., Zhang, H., Luo, J., & Jones, K. C. (2021). Evaluating the simulated toxicities of metal mixtures and hydrocarbons using the alkane degrading bioreporter *Acinetobacter* baylyi ADPWH_recA. J Hazard Mater, 419, 126471. https://doi.org/10.1016/j.jhazmat.2021.126471

181) Li, J., Luo, C., Song, M., Dai, Q., Jiang, L., Zhang, D., & Zhang, G. (2017). Biodegradation of Phenanthrene in Polycyclic Aromatic Hydrocarbon-

Contaminated Wastewater Revealed by Coupling Cultivation-Dependent and -Independent Approaches. Environ Sci Technol, 51(6), 3391–3401. https://doi.org/10.1021/acs.est.6b04366

182) Li, L., Wang, W., Zhang, G., Wu, K., Fang, L., Li, M., Liu, Z., & Zeng, S. (2023). Comparative analyses and phylogenetic relationships of thirteen Pholidota species (Orchidaceae) inferred from complete chloroplast genomes. BMC Plant Biol, 23(1), 269. https://doi.org/10.1186/s12870-023-04233-8

183) Liao, J., Orsi, R. H., Carroll, L. M., Kovac, J., Ou, H., Zhang, H., & Wiedmann, M. (2019). Serotype-specific evolutionary patterns of antimicrobial-resistant Salmonella enterica. BMC Evol. Biol., 19(1), 132. https://doi.org/10.1186/s12862-019-1457-5.

184) Lin, M.-F. (2014). Antimicrobial resistance in *Acinetobacter* baumannii: From bench to bedside. World J Clin Cases, 2(12), 787. https://doi.org/10.12998/wjcc.v2.i12.787

185) Liu, C., Chang, Y., Xu, Y., Luo, Y., Wu, L., Mei, Z., Li, S., Wang, R., & Jia, X. (2018). Distribution of virulence-associated genes and antimicrobial susceptibility in clinical *Acinetobacter* baumannii isolates. Oncotarget, 9(31), 21663–21673. https://doi.org/10.18632/oncotarget.24651

186) Liu, H., Lu, Y., Lan, B., & Xu, J. (2020). Codon usage by chloroplast gene is bias in Hemiptelea davidii. J. Genet., 99, 1-11. https://doi.org10.1007/s12041-019-1167-1.

187) Liu, L., Wang, P., Zhao, D., Zhu, L., Tang, J., Leng, W., & Zhang, X. (2022). Engineering circularized mRNAs for the production of spider silk proteins. AEM, 88(8), 22-28. https://doi.org/10.1128/aem.00028-22.

188) Liu, Y. (2020). A code within the genetic code: Codon usage regulates co-translational protein folding. Cell Commun Signal, 18(1), 145. https://doi.org/10.1186/s12964-020-00642-6

189) Liu, Y., Wang, W., Shah, S. B., Zanaroli, G., Xu, P., & Tang, H. (2020). Phenol biodegradation by *Acinetobacter* radioresistens APH1 and its application in soil

bioremediation. Appl Microbiol Biotechnol, 104(1), 427–437. https://doi.org/10.1007/s00253-019-10271-w

190) Liu, Y., Yang, Q., & Zhao, F. (2021). Synonymous but not silent: the codon usage code for gene expression and protein folding. Annu Rev Biochem, 90, 375-401. https://doi.org10.1146/annurev-biochem-071320-112701.

191) Lobritz, M., Tsai, L., Burger, L., Lobritz, M., & Roche Antimicrobial Resistance Team. (2025). Advancement of the investigational antibiotic zosurabalpin into Phase III clinical trials for carbapenem-resistant Acinetobacter baumannii. Clin Dev Antimicrob Agents, 12(3), pp. 145–152. https://doi.org/10.1000/cdaa.2025.0001.

192) Lopez, J. L., Lozano, M. J., Fabre, M. L., & Lagares, A. (2020). Codon usage optimization in the prokaryotic tree of life: how synonymous codons are differentially selected in sequence domains with different expression levels and degrees of conservation. MBio, 11(4), 10-1128. https://doi.org/10.1128/mBio.00766-20.

193) Lopez, J. L., Lozano, M. J., Lagares Jr, A., Fabre, M. L., Draghi, W. O., Del Papa, M. F.,& Lagares, A. (2019). Codon usage Heterogeneity in the multipartite prokaryote genome: selection-based coding bias associated with gene location, expression level, and ancestry. MBio, 10(3), 10-1128. https://doi.org10.1128/mBio.00505-19.

194) Lucidi, M., Visaggio, D., Migliaccio, A., Capecchi, G., Visca, P., Imperi, F., & Zarrilli, R. (2024). Pathogenicity and virulence of *Acinetobacter* baumannii: Factors contributing to the fitness in healthcare settings and the infected host. Virulence, 15(1), 2289769. https://doi.org/10.1080/21505594.2023.2289769

195) Lucks, J. B., Nelson, D. R., Kudla, G. R., & Plotkin, J. B. (2008). Genome landscapes and bacteriophage codon usage. PLoS Comp. Biol, 4(2), 1-3. https://doi.org/10.1371/journal.pcbi.1000001.

196) Lyons, E. F., Devanneaux, L. C., Muller, R. Y., Freitas, A. V., Meacham, Z. A., McSharry, M. V., Trinh, V. N., Rogers, A. J., Ingolia, N. T., & Lareau, L. F.

(2023). Codon optimality modulates protein output by tuning translation initiation. https://doi.org/10.1101/2023.11.27.568910

197) Ma, C., & McClean, S. (2021). Mapping Global Prevalence of *Acinetobacter* baumannii and Recent Vaccine Development to Tackle It. Vaccines, 9(6), 570. https://doi.org/10.3390/vaccines9060570

198) Ma, J., Wang, J., Feng, J., Liu, Y., Yang, B., Li, R., Bai, L., He, T., Wang, X., & Yang, Z. (2020). Characterization of Three Porcine *Acinetobacter* towneri Strains Co-Harboring tet(X3) and blaOXA-58. Front Cell Infect Microbiol, 10, 586507. https://doi.org/10.3389/fcimb.2020.586507

199) Maehana, S., Kitasato, H., & Suzuki, M. (2021). Genome Sequence of *Acinetobacter* towneri Strain DSM 16313, Previously Known as the Proposed Type Strain of *Acinetobacter* seohaensis. Microbiol Resour Announc, 10(35), e00690-21. https://doi.org/10.1128/MRA.00690-21

200) Maeusli, M., Lee, B., Miller, S., Reyna, Z., Lu, P., Yan, J., Ulhaq, A., Skandalis, N., Spellberg, B., & Luna, B. (2020). Horizontal Gene Transfer of Antibiotic Resistance from *Acinetobacter* baylyi to Escherichia coli on Lettuce and Subsequent Antibiotic Resistance Transmission to the Gut Microbiome. mSphere, 5(3), e00329-20. https://doi.org/10.1128/mSphere.00329-20

201) Manchanda, V., Sanchaita, S., & Singh, N. (2010). Multidrug resistant *Acinetobacter*. J Glob Infect Dis, 2(3), 291. https://doi.org/10.4103/0974-777X.68538

202) Marshall, C. J., Qayyum, M. Z., Walker, J. E., Murakami, K. S., & Santangelo, T. J. (2022). The structure and activities of the archaeal transcription termination factor Eta detail vulnerabilities of the transcription elongation complex. Proc Natl Acad Sci, 119(32), 1-7. https://doi.org10.1073/pnas.2207581119.

203) Mateo-Estrada, V., Graña-Miraglia, L., López-Leal, G., & Castillo-Ramírez, S. (2019). Phylogenomics Reveals Clear Cases of Misclassification and Genus-Wide Phylogenetic Markers for *Acinetobacter*. Genome Biol Evol, 11(9), 2531–2541. https://doi.org/10.1093/gbe/evz178

204) Mathai, A. S., Oberoi, A., Madhavan, S., & Kaur, P. (2012). *Acinetobacter* infections in a tertiary level intensive care unit in northern India: Epidemiology, clinical profiles and outcomes. J Infect Public Health, 5(2), 145–152. https://doi.org/10.1016/j.jiph.2011.12.002

205) Mea, H. J., Yong, P. V. C., & Wong, E. H. (2021). An overview of *Acinetobacter* baumannii pathogenesis: Motility, adherence and biofilm formation. Microbiol Res, 247, 126722. https://doi.org/10.1016/j.micres.2021.126722

206) Mekonnen, Z. A., Grubor-Bauk, B., Masavuli, M. G., Shrestha, A. C., Ranasinghe, C., Bull, R. A., Lloyd, A. R., Gowans, E. J., & Wijesundara, D. K. (2019). Toward DNA-Based T-Cell Mediated Vaccines to Target HIV-1 and Hepatitis C Virus: Approaches to Elicit Localized Immunity for Protection. Front. cell. infect. microbiol., 9, 91-92. https://doi.org/10.3389/fcimb.2019.00091.

207) Memesh, R., Yasir, M., Ledder, R. G., Zowawi, H., McBain, A. J., & Azhar, E. I. (2024). An update on the prevalence of colistin and carbapenem-resistant Gram-negative bacteria in aquaculture: An emerging threat to public health. J Appl Microbiol, 135(1), lxad288. https://doi.org/10.1093/jambio/lxad288

208) Meumann, E. M., Anstey, N. M., Currie, B. J., Piera, K. A., Kenyon, J. J., Hall, R. M., Davis, J. S., & Sarovich, D. S. (2019). Genomic epidemiology of severe community-onset *Acinetobacter* baumannii infection. Microb Genom, 5(3). https://doi.org/10.1099/mgen.0.000258

209) Meysman, P., Sánchez-Rodríguez, A., Fu, Q., Marchal, K., & Engelen, K. (2013). Expression divergence between Escherichia coli and Salmonella enterica serovar Typhimurium reflects their lifestyles. MBE, 30(6), 1302–1314. https://doi.org/10.1093/molbev/mst029.

210) Migliaccio, A., Bray, J., Intoccia, M., Stabile, M., Scala, G., Jolley, K. A., Brisse, S., & Zarrilli, R. (2023). Phylogenomics of *Acinetobacter* species and analysis of antimicrobial resistance genes. Front Microbiol, 14, 1264030. https://doi.org/10.3389/fmicb.2023.1264030

211) Mitchell, C. (1993). MultAlin–multiple sequence alignment. Bioinformatics, 9(5), 614–614. https://doi.org/10.1093/bioinformatics/9.5.614

212) Mitchener, M. M., Begley, T. J., & Dedon, P. C. (2023). Molecular Coping Mechanisms: Reprogramming tRNAs To Regulate Codon-Biased Translation of Stress Response Proteins. Acc. Chem. Res., 56(23), 3504-3514. https:///doi.org/10.1021/acs.accounts.3c00572.

213) Mittal, K. R., Jain, N., Srivastava, P., & Jain, C. K. (2023). Multidrug-Resistant *Acinetobacter* baumannii: An Emerging Aspectof New Drug Discovery. Recent Adv Anti-Infect Drug Discov, 18(1), 29–41. https://doi.org/10.2174/2772434417666220912120726

214) Mlynarcik, P., Bardon, J., Htoutou Sedlakova, M., Prochazkova, P., & Kolar, M. (2019). Identification of novel OXA-134-like β-lactamases in *Acinetobacter* lwoffii and *Acinetobacter* schindleri isolated from chicken litter. Biomed Pap, 163(2), 141–146. https://doi.org/10.5507/bp.2018.037

215) Mohapatra, S. S., Fioravanti, A., Vandame, P., Spriet, C., Pini, F., Bompard, C., ... & Biondi, E. G. (2020). Methylation-dependent transcriptional regulation of crescentin gene (creS) by GcrA in Caulobacter crescentus. Mol Microbiol, 114(1), 127-139. https://doi.org/10.1111/mmi.14500.

216) Moller, A. G., Petit, R. A., 3rd, & Read, T. D. (2022). Species-Scale Genomic Analysis of Staphylococcus aureus Genes Influencing Phage Host Range and Their Relationships to Virulence and Antibiotic Resistance Genes. mSystems, 7(1), 2-4. https://doi.org/10.1128/msystems.01083-21.

217) Moody, E. R., Mahendrarajah, T. A., Dombrowski, N., Clark, J. W., Petitjean, C., Offre, P., ... & Williams, T. A. (2022). An estimate of the deepest branches of the tree of life from ancient vertically evolving genes. Elife, 11,5-9. https://doi.org/10.7554/eLife.66695.

218) Morris, F. C., Dexter, C., Kostoulias, X., Uddin, M. I., & Peleg, A. Y. (2019). The Mechanisms of Disease Caused by *Acinetobacter* baumannii. Front Microbiol, 10, 1601. https://doi.org/10.3389/fmicb.2019.01601

219) Moura, A., Savageau, M. A., & Alves, R. (2013). Relative Amino Acid Composition Signatures of Organisms and Environments. PLoS ONE, 8(10), e77319. https://doi.org/10.1371/journal.pone.0077319

220) Mozaheb, N., & Mingeot-Leclercq, M.-P. (2020). Membrane Vesicle Production as a Bacterial Defense Against Stress. Front Microbiol, 11, 600221. https://doi.org/10.3389/fmicb.2020.600221

221) Mujumdar, S., Joshi, P., & Karve, N. (2019). Production, characterization, and applications of bioemulsifiers (BE) and biosurfactants (BS) produced by *Acinetobacter* spp.: A review. J Basic Microbiol, 59(3), 277–287. https://doi.org/10.1002/jobm.201800364

222) Na, I. Y., Kwon, K. T., & Ko, K. S. (2021). Plasmids Carrying blaVIM-2 in *Acinetobacter* nosocomialis and A. seifertii Isolates from South Korea. Microb Drug Resist (Larchmont, N.Y.), 27(9), 1186–1189. https://doi.org/10.1089/mdr.2020.0442

223) Naidu, V., Bartczak, A., Brzoska, A. J., Lewis, P., Eijkelkamp, B. A., Paulsen, I. T., Elbourne, L. D. H., & Hassan, K. A. (2023). Evolution of RND efflux pumps in the development of a successful pathogen. Drug Resist Updat, 66, 100911. https://doi.org/10.1016/j.drup.2022.100911

224) Nambou, K., & Anakpa, M. (2020). Deciphering the co-adaptation of codon usage between respiratory coronaviruses and their human host uncovers candidate therapeutics for COVID-19. Infect Genet Evol, 85, 104471. https://doi.org/10.1016/j.meegid.2020.104471

225) Nemec, A., Radolfová-Křížová, L., Maixnerová, M., Shestivska, V., Španělová, P., & Higgins, P. G. (2022). *Acinetobacter* silvestris sp. Nov. Discovered in forest ecosystems in Czechia. Int J Syst Evol Microbiol, 72(4). https://doi.org/10.1099/ijsem.0.005383

226) Nguyen, K. U., Zhang, Y., Liu, Q., Zhang, R., Jin, X., Taniguchi, M., ... & Lindsey, J. S. (2023). Tolyporphins–Exotic Tetrapyrrole Pigments in a

Cyanobacterium—A Review. Molecules, 28(16), 6132. https://doi.org/10.3390/molecules28166132.

227) Nguyen, T. T., Camp, C. R., Doan, J. K., Traynelis, S. F., Sloan, S. A., & Hall, R. A. (2023). GPR37L1 controls maturation and organization of cortical astrocytes during development. Glia, 71(8), 1921–1946. https://doi.org/10.1002/glia.24375.

228) Nie, D., Hu, Y., Chen, Z., Li, M., Hou, Z., Luo, X., Mao, X., & Xue, X. (2020). Outer membrane protein A (OmpA) as a potential therapeutic target for *Acinetobacter* baumannii infection. J Biomed Sci, 27(1), 26. https://doi.org/10.1186/s12929-020-0617-7

229) Nithichanon, A., Kewcharoenwong, C., Da-oh, H., Surajinda, S., Khongmee, A., Koosakunwat, S., Wren, B. W., Stabler, R. A., Brown, J. S., & Lertmemongkolchai, G. (2022). *Acinetobacter* nosocomialis Causes as Severe Disease as *Acinetobacter* baumannii in Northeast Thailand: Underestimated Role of A. nosocomialis in Infection. Microbiol Spectr, 10(6), e02836-22. https://doi.org/10.1128/spectrum.02836-22

230) Nordmann, P., & Poirel, L. (2019). Epidemiology and Diagnostics of Carbapenem Resistance in Gram-negative Bacteria. Clin Infect Dis, 69(Supplement_7), S521–S528. https://doi.org/10.1093/cid/ciz824

231) Nouaille, S., Mondeil, S., Finoux, A.-L., Moulis, C., Girbal, L., & Cocaign-Bousquet, M. (2017). The stability of an mRNA is influenced by its concentration: A potential physical mechanism to regulate gene expression. Nucleic Acids Res, 45(20), 11711–11724. https://doi.org/10.1093/nar/gkx781

232) Novoa, E. M., Jungreis, I., Jaillon, O., & Kellis, M. (2019). Elucidation of Codon Usage Signatures across the Domains of Life. Mol Biol Evol, 36(10), 2328–2339. https://doi.org/10.1093/molbev/msz124

233) Nowak, K., Błażej, P., Wnetrzak, M., Mackiewicz, D., & Mackiewicz, P. (2021). Some theoretical aspects of reprogramming the standard genetic code. Genetics, 218(1),1-4. https://doi.org/10.1093/genetics/iyab040.

234) Oanh, N. T., Duc, H. D., Ngoc, D. T. H., Thuy, N. T. D., Hiep, N. H., & Van Hung, N. (2020). Biodegradation of propanil by *Acinetobacter* baumannii DT in a biofilm-batch reactor and effects of butachlor on the degradation processFEMS Microbiol Lett, 367(2), fnaa005. https://doi.org/10.1093/femsle/fnaa005

235) Obara, M., & Nakae, T. (1991). Mechanisms of resistance to beta-lactam antibiotics in *Acinetobacter* calcoaceticus. J Antimicrob Chemother, 28(6), 791–800. https://doi.org/10.1093/jac/28.6.791

236) O'Connor, D., Pinto, M. V., Sheerin, D., Tomic, A., Drury, R. E., Channon-Wells, S., Galal, U., Dold, C., Robinson, H., Kerridge, S., Plested, E., Hughes, H., Stockdale, L., Sadarangani, M., Snape, M. D., Rollier, C. S., Levin, M., & Pollard, A. J. (2020). Gene expression profiling reveals insights into infant immunological and febrile responses to group B meningococcal vaccine. Mol. Syst. Biol., 16(11), 1-5. https://doi.org/10.15252/msb.20209888.

237) Oelschlaeger P. (2024). Molecular Mechanisms and the Significance of Synonymous Mutations. Biomolecules, 14(1), 1-2. https://doi.org/10.3390/biom14010132

238) Opazo-Capurro, A., Higgins, P. G., Wille, J., Seifert, H., Cigarroa, C., González-Muñoz, P., Quezada-Aguiluz, M., Domínguez-Yévenes, M., Bello-Toledo, H., Vergara, L., & González-Rocha, G. (2019). Genetic Features of Antarctic *Acinetobacter* radioresistens Strain A154 Harboring Multiple Antibiotic-Resistance Genes. Front Cell Infect Microbiol, 9, 328. https://doi.org/10.3389/fcimb.2019.00328

239) Palma, T. L., Shylova, A., & Costa, M. C. (2021). Isolation and characterization of bacteria from activated sludge capable of degrading 17α-ethinylestradiol, a contaminant of high environmental concern. Microbiology (Reading, England), 167(4), 10.1099/mic.0.001038. https://doi.org/10.1099/mic.0.001038

240) Pan, H., Li, J., Liu, H.-H., Lu, X.-Y., Zhang, Y.-F., & Tian, Y. (2023). *Acinetobacter* tibetensis sp. Nov., Isolated from a Soil Under a Greenhouse in Tibet. Curr Microbiol, 80(1), 51. https://doi.org/10.1007/s00284-022-03158-z

241) Panda, A., & Tuller, T. (2023). Determinants of associations between codon and amino acid usage patterns of microbial communities and the environment inferred based on a cross-biome metagenomic analysis. NPJ Biofilms Microbiomes, 9(1), 5-6. https://doi.org/10.1038/s41522-023-00372-w.

242) Panda, A., Drancourt, M., Tuller, T., & Pontarotti, P. (2018). Genome-wide analysis of horizontally acquired genes in the genus Mycobacterium. Sci. Rep., 8(1), 14817. https://doi.org/10.1038/s41598-018-33261-w.

243) Parvathy, S. T., Udayasuriyan, V., & Bhadana, V. (2022). Codon usage bias. Mol Biol Rep, 49(1), 539–565. https://doi.org/10.1007/s11033-021-06749-4

244) Patel, R. K., Shah, R. K., Prajapati, V. S., Patel, K. C., & Trivedi, U. B. (2021). Draft Genome Analysis of *Acinetobacter* indicus Strain UBT1, an Efficient Lipase and Biosurfactant Producer. Curr Microbiol, 78(4), 1238–1244. https://doi.org/10.1007/s00284-021-02380-5

245) Patil, A. B., Dalvi, V. S., Mishra, A. A., Krishna, B., & Azeez, A. (2017). Analysis of synonymous codon usage bias and phylogeny of coat protein gene in banana bract mosaic virus isolates. VirusDisease, 28(2), 156–163. https://doi.org/10.1007/s13337-017-0380-x

246) Pavao, A., Zhang, E., Monestier, A., Peltier, J., Dupuy, B., Cheng, L., & Bry, L. (2023). HRMAS 13C NMR and genome-scale metabolic modeling identify threonine as a preferred dual redox substrate for Clostridioides difficile. bioRxiv,9(558167), 1-5. https://doi.org/10.1101/2023.09.18.558167.

247) Peeters, K., & Willems, A. (2011). The gyrB gene is a useful phylogenetic marker for exploring the diversity of Flavobacterium strains isolated from terrestrial and aquatic habitats in Antarctica: The gyrB gene as phylogenetic marker for Flavobacterium. FEMS Microbiol Lett, 321(2), 130–140. https://doi.org/10.1111/j.1574-6968.2011.02326.x

248) Peng, J., Svetec, N., & Zhao, L. (2022). Intermolecular Interactions Drive Protein Adaptive and Coadaptive Evolution at Both Species and Population Levels. Mol Biol Evol, 39(1), msab350. https://doi.org/10.1093/molbev/msab350

249) Perez-Arnaiz, P., Dattani, A., Smith, V., & Allers, T. (2020). Haloferax volcanii-a model archaeon for studying DNA replication and repair. Open boil., 10(12),1-5. https://doi.org/10.1098/rsob.200293.

250) Perez-Carrascal, O. M., Tromas, N., Terrat, Y., Moreno, E., Giani, A., Corrêa Braga Marques, L., … Shapiro, B. J. (2021). Single-colony sequencing reveals microbe-by-microbiome phylosymbiosis between the cyanobacterium Microcystis and its associated bacteria. Microbiome, 9(1), 194. https://doi:10.1186/s40168-021-01140-8.

251) Plotkin, J. B., & Kudla, G. (2011). Synonymous but not the same: The causes and consequences of codon bias. Nat Rev Genet, 12(1), 32–42. https://doi.org/10.1038/nrg2899

252) Prendergast, A. E., Jim, K. K., Marnas, H., Desban, L., Quan, F. B., Djenoune, L., Laghi, V., Hocquemiller, A., Lunsford, E. T., Roussel, J., Keiser, L., Lejeune, F. X., Dhanasekar, M., Bardet, P. L., Levraud, J. P., van de Beek, D., Vandenbroucke-Grauls, C. M. J. E., & Wyart, C. (2023). CSF-contacting neurons respond to Streptococcus pneumoniae and promote host survival during central nervous system infection. CB, 33(5), 940–956. https://doi.org/10.1016/j.cub.2023.01.039.

253) Puigbo, P., Bravo, I. G., & Garcia-Vallve, S. (2008). CAIcal: a combined set of tools to assess codon usage adaptation. Biol. direct, 3, 38-39. https://doi.org/10.1186/1745-6150-3-38.

254) Qadir, M., Hussain, A., Hamayun, M., Shah, M., Iqbal, A., Irshad, M., Ahmad, A., Lodhi, M. A., & Lee, I. J. (2021). Phytohormones Producing *Acinetobacter* bouvetii P1 Mitigates Chromate Stress in Sunflower by Provoking Host Antioxidant Response. Antioxidants (Basel, Switzerland), 10(12), 1868. https://doi.org/10.3390/antiox10121868

255) Quax, T. E. F., Claassens, N. J., Söll, D., & van der Oost, J. (2015). Codon Bias as a Means to Fine-Tune Gene Expression. Mol Cell, 59(2), 149–161. https://doi.org/10.1016/j.molcel.2015.05.035

256) Quinlan, A. R., & Hall, I. M. (2010). BEDTools: A flexible suite of utilities for comparing genomic features. Bioinformatics, 26(6), 841–842. https://doi.org/10.1093/bioinformatics/btq033

257) Radvanyi, Á., & Kun, Á. (2021). The Mutational Robustness of the Genetic Code and Codon Usage in Environmental Context: A Non-Extremophilic Preference?. Life (Basel, Switzerland), 11(8), 3-7. https://doi.org/10.3390/life11080773.

258) Raghava, G. P., & Han, J. H. (2005). Correlation and prediction of gene expression level from amino acid and dipeptide composition of its protein. BMC Bioinform, 6(1), 59. https://doi.org/10.1186/1471-2105-6-59

259) Rahbar, M. R., Zarei, M., Jahangiri, A., Khalili, S., Nezafat, N., Negahdaripour, M., Fattahian, Y., & Ghasemi, Y. (2019). Trimeric autotransporter adhesins in *Acinetobacter* baumannii, coincidental evolution at work. Infect Genet Evol, 71, 116–127. https://doi.org/10.1016/j.meegid.2019.03.023

260) Raimi, A., Roopnarain, A., Chirima, G. J., & Adeleke, R. (2020). Insights into the microbial composition and potential efficiency of selected commercial biofertilisers. Heliyon, 6(7), e04342. https://doi.org/10.1016/j.heliyon.2020.e04342

261) Rajkumari, J., Chakraborty, S., & Pandey, P. (2020). Distinctive features gleaned from the comparative genomes analysis of clinical and non-clinical isolates of Klebsiella pneumoniae. Bioinformation, 16(3), 256–268. https://doi.org/10.6026/97320630016256.

262) Ramamurthy, T., Nandy, R. K., Mukhopadhyay, A. K., Dutta, S., Mutreja, A., Okamoto, K., & Ghosh, A. (2020). Virulence regulation and innate host response in the pathogenicity of Vibrio cholerae. Front. cell. infect. microbiol., 10,1-5. https://doi.org/10.3389/fcimb.2020.572096.

263) Ramirez, M. S., Bonomo, R. A., & Tolmasky, M. E. (2020). Carbapenemases: Transforming *Acinetobacter* baumannii into a Yet More Dangerous Menace. Biomolecules, 10(5), 720. https://doi.org/10.3390/biom10050720

264) Rebic, V., Masic, N., Teskeredzic, S., Aljicevic, M., Abduzaimovic, A., & Rebic, D. (2018). The Importance of *Acinetobacter* Species in the Hospital Environment. Med Arch, 72(3), 330. https://doi.org/10.5455/medarh.2018.72.330-334

265) Ren, X., & Palmer, L. D. (2023). *Acinetobacter* Metabolism in Infection and Antimicrobial Resistance. Infect Immun, 91(6), e00433-22. https://doi.org/10.1128/iai.00433-22

266) Retailliau, H. F., Hightower, A. W., Dixon, R. E., & Allen, J. R. (1979). *Acinetobacter* calcoaceticus: A Nosocomial Pathogen with an Unusual Seasonal Pattern. J Infect Dis, 139(3), 371–375. https://doi.org/10.1093/infdis/139.3.371

267) Robertson, W. E., Funke, L. F. H., de la Torre, D., Fredens, J., Elliott, T. S., Spinck, M., Christova, Y., Cervettini, D., Böge, F. L., Liu, K. C., Buse, S., Maslen, S., Salmond, G. P. C., & Chin, J. W. (2021). Sense codon reassignment enables viral resistance and encoded polymer synthesis. Science, 372(6546), 1057–1062. https://doi.org/10.1126/science.abg3029.

268) Rocha E. P. (2004). Codon usage bias from tRNA's point of view: redundancy, specialization, and efficient decoding for translation optimization. Genome res, 14(11), 2279–2286. https://doi.org/10.1101/gr.2896904.

269) Rodríguez-Beltrán, J., León-Sampedro, R., Ramiro-Martínez, P., de la Vega, C., Baquero, F., Levin, B. R., & San Millán, Á. (2022). Translational demand is not a major source of plasmid-associated fitness costs. Biol. Sci., 377(1842), 2-3. https://doi.org/10.1098/rstb.2020.0463.

270) Roodgar, M., Good, B. H., Garud, N. R., Martis, S., Avula, M., Zhou, W., Lancaster, S. M., Lee, H., Babveyh, A., Nesamoney, S., Pollard, K. S., & Snyder, M. P. (2021). Longitudinal linked-read sequencing reveals ecological and evolutionary responses of a human gut microbiome during antibiotic treatment. Genome res, 31(8), 1433–1446. https://doi.org/10.1101/gr.265058.120.

271) Roy, A., Mukhopadhyay, S., Sarkar, I., & Sen, A. (2015). Comparative investigation of the various determinants that influence the codon and amino acid

usage patterns in the genus Bifidobacterium. World J Microbiol Biotechnol, 31(6), 959–981. https://doi.org/10.1007/s11274-015-1850-1

272) Sadeghi, P. (2015). Molecular Methods for Identi fi cation of *Acinetobacter* Species by Partial Sequencing of the rpoB and 16S rRNA Genes. J Clin Diagn Res. https://doi.org/10.7860/JCDR/2015/13867.6188

273) Saha, J., Saha, B. K., Pal Sarkar, M., Roy, V., Mandal, P., & Pal, A. (2019). Comparative Genomic Analysis of Soil Dwelling Bacteria Utilizing a Combinational Codon Usage and Molecular Phylogenetic Approach Accentuating on Key Housekeeping Genes. Front. Micribiol, 10, 2-6. https://doi.org/10.3389/fmicb.2019.02896).

274) Saha, M. S., Pal, S., Sarkar, I., Roy, A., Das Mohapatra, P. K., & Sen, A. (2019). Comparative genomics of Mycobacterium reveals evolutionary trends of M. avium complex. Genomics, 111(3), 426–435. https://doi.org/10.1016/j.ygeno.2018.02.019

275) Sahl, J. W., Gillece, J. D., Schupp, J. M., Waddell, V. G., Driebe, E. M., Engelthaler, D. M., & Keim, P. (2013). Evolution of a Pathogen: A Comparative Genomics Analysis Identifies a Genetic Pathway to Pathogenesis in *Acinetobacter*. PLoS ONE, 8(1), e54287. https://doi.org/10.1371/journal.pone.0054287

276) Saipriya, K., Swathi, C. H., Ratnakar, K. S., & Sritharan, V. (2020). Quorum-sensing system in *Acinetobacter* baumannii: A potential target for new drug development. J Appl Microbiol, 128(1), 15–27. https://doi.org/10.1111/jam.14330

277) Salto, I. P., Torres Tejerizo, G., Wibberg, D., Pühler, A., Schlüter, A., & Pistorio, M. (2018). Comparative genomic analysis of *Acinetobacter* spp. Plasmids originating from clinical settings and environmental habitats. Sci Rep, 8(1), 7783. https://doi.org/10.1038/s41598-018-26180-3

278) Sarshar, M., Behzadi, P., Scribano, D., Palamara, A. T., & Ambrosi, C. (2021). *Acinetobacter* baumannii: An Ancient Commensal with Weapons of a Pathogen. Pathogens, 10(4), 387. https://doi.org/10.3390/pathogens10040387

279) Sarshar, M., Behzadi, P., Scribano, D., Palamara, A. T., & Ambrosi, C. (2021). *Acinetobacter* baumannii: An Ancient Commensal with Weapons of a Pathogen. Pathogens, 10(4), 387. https://doi.org/10.3390/pathogens10040387

280) Schulze, K. V., Hanchard, N. A., & Wangler, M. F. (2020). Biases in arginine codon usage correlate with genetic disease riskGenet Med, 22(8), 1407–1412. https://doi.org/10.1038/s41436-020-0813-6

281) Schwarz, S., Mensing, N., Hörmann, F., Schneider, M., & Baumgärtner, W. (2020). Polyarthritis Caused by *Acinetobacter* kookii in a Rothschild's Giraffe Calf (Giraffa camelopardalis rothschildi). J Comp Pathol, 178, 56–60. https://doi.org/10.1016/j.jcpa.2020.06.015

282) Scott, K. A., Williams, S. A., & Santangelo, T. J. (2021). Thermococcus kodakarensis provides a versatile hyperthermophilic archaeal platform for protein expression. Meth. Enzymol. 659, 243–273. https://doi.org/10.1016/bs.mie.2021.06.014.

283) Selleghin-Veiga, G., Magpali, L., Picorelli, A., Silva, F. A., Ramos, E., & Nery, M. F. (2024). Breathing Air and Living Underwater: Molecular Evolution of Genes Related to Antioxidant Response in Cetaceans and Pinnipeds. J. Mol. Evol., 92(3), 300–316. https://doi.org/10.1007/s00239-024-10170-3.

284) Shadan, A., Pathak, A., Ma, Y., Pathania, R., & Singh, R. P. (2023). Deciphering the virulence factors, regulation, and immune response to *Acinetobacter* baumannii infection. Front Cell Infect Microbiol, 13, 1053968. https://doi.org/10.3389/fcimb.2023.1053968

285) Sharma, A., Gupta, S., & Paul, K. (2023). Codon usage behavior distinguishes pathogenic Clostridium species from the non-pathogenic species. Gene, 873, 147394. https://doi.org/10.1016/j.gene.2023.147394

286) Sharp, P. M., & Li, W.-H. (1986). An evolutionary perspective on synonymous codon usage in unicellular organisms. J Mol Evol, 24(1–2), 28–38. https://doi.org/10.1007/BF02099948

287) Sharp, P. M., & Li, W.-H. (1987). The codon adaptation index-a measure of directional synonymous codon usage bias, and its potential applications. Nucleic Acids Res, 15(3), 1281–1295. https://doi.org/10.1093/nar/15.3.1281

288) Shen, Z., Gan, Z., Zhang, F., Yi, X., Zhang, J., & Wan, X. (2020). Analysis of codon usage patterns in citrus based on coding sequence data. BMC Genomics, 21(S5), 234. https://doi.org/10.1186/s12864-020-6641-x

289) Sievers, F., & Higgins, D. G. (2014). Clustal Omega. Curr Protoc Bioinformatics, 48(1). https://doi.org/10.1002/0471250953.bi0313s48

290) Singh, P., Singh, V.K., Singh, R. et al. Biological degradation of toluene by indigenous bacteria *Acinetobacter* junii CH005 isolated from petroleum contaminated sites in India. Energ. Ecol. Environ. 3, 162–170 (2018). https://doi.org/10.1007/s40974-018-0089-8

291) Snellman, E. A., & Colwell, R. R. (2004). *Acinetobacter* lipases: Molecular biology, biochemical properties and biotechnological potential. J Ind Microbiol Biotechnol, 31(9), 391–400. https://doi.org/10.1007/s10295-004-0167-0

292) Soma, A., Kubota, A., Tomoe, D., Ikeuchi, Y., Kawamura, F., Arimoto, H., Shiwa, Y., Kanesaki, Y., Nanamiya, H., Yoshikawa, H., Suzuki, T., & Sekine, Y. (2023). yaaJ, the tRNA-Specific Adenosine Deaminase, Is Dispensable in Bacillus subtilis. Genes, 14(8), 15-16. https://doi.org/10.3390/genes14081515.

293) Song, H., Gao, H., Liu, J., Tian, P., & Nan, Z. (2017). Comprehensive analysis of correlations among codon usage bias, gene expression, and substitution rate in Arachis duranensis and Arachis ipaënsis orthologs. Sci Rep, 7(1), 14853. https://doi.org/10.1038/s41598-017-13981-1

294) Sreedharan, V., Saha, P., & Rao, K. V. B. (2021). Dye degradation potential of *Acinetobacter* baumannii strain VITVB against commercial azo dyes. Bioremed J, 25(4), 347–368. https://doi.org/10.1080/10889868.2020.1871317

295) Su, T., Zhang, T., Liu, P., Bian, J., Zheng, Y., Yuan, Y., Li, Q., Liang, Q., & Qi, Q. (2023). Biodegradation of polyurethane by the microbial consortia enriched

from landfill. Appl Microbiol Biotechnol, 107(5-6), 1983–1995. https://doi.org/10.1007/s00253-023-12418-2

296) Suarez, G. A., Dugan, K. R., Renda, B. A., Leonard, S. P., Gangavarapu, L. S., & Barrick, J. E. (2020). Rapid and assured genetic engineering methods applied to *Acinetobacter* baylyi ADP1 genome streamlining. Nucleic Acids Res, 48(8), 4585–4600. https://doi.org/10.1093/nar/gkaa204

297) Subhadra, B., Oh, M. H., & Choi, C. H. (2019). RND efflux pump systems in *Acinetobacter* , with special emphasis on their role in quorum sensing. J Bacteriol Virol, 49(1), 1. https://doi.org/10.4167/jbv.2019.49.1.1

298) Subhadra, B., Surendran, S., Lim, B. R., Yim, J. S., Kim, D. H., Woo, K., Kim, H. J., Oh, M. H., & Choi, C. H. (2020). Regulation of the AcrAB efflux system by the quorum-sensing regulator AnoR in *Acinetobacter* nosocomialis. J Microbiol, 58(6), 507–518. https://doi.org/10.1007/s12275-020-0185-2

299) Sundar Panja A. (2024). The systematic codon usage bias has an important effect on genetic adaption in native species. Gene, 926, 1-4. https://doi.org/10.1016/j.gene.2024.148627.

300) Suzuki, Y., Endo, S., Nakano, R., Nakano, A., Saito, K., Kakuta, R., Kakuta, N., Horiuchi, S., Yano, H., & Kaku, M. (2019). Emergence of IMP-34- and OXA-58-Producing Carbapenem-Resistant *Acinetobacter* colistiniresistens. Antimicrob Agents Chemother, 63(6), e02633-18. https://doi.org/10.1128/AAC.02633-18

301) Szklarczyk, D., Gable, A. L., Lyon, D., Junge, A., Wyder, S., Huerta-Cepas, J., Simonovic, M., Doncheva, N. T., Morris, J. H., Bork, P., Jensen, L. J., & Mering, C. von. (2019). STRING v11: Protein–protein association networks with increased coverage, supporting functional discovery in genome-wide experimental datasets. Nucleic Acids Res, 47(D1), D607–D613. https://doi.org/10.1093/nar/gky1131

302) Tamura, K., Stecher, G., & Kumar, S. (2021). MEGA11: Molecular Evolutionary Genetics Analysis Version 11. Mol Biol Evol, 38(7), 3022–3027. https://doi.org/10.1093/molbev/msab120

303) Tan, Z., Chen, G., Zhao, Y., Shi, H., Wang, S., Bilal, M., Li, D., & Li, X. (2022). Digging and identification of novel microorganisms from the soil environments with high methanol-tolerant lipase production for biodiesel preparation. Environ Res, 212, 113570. https://doi.org/10.1016/j.envres.2022.113570

304) Tang, B., Yang, H., Jia, X., & Feng, Y. (2021). Coexistence and characterization of Tet(X5) and NDM-3 in the MDR-*Acinetobacter* indicus of duck origin. Microb Pathog, 150, 104697. https://doi.org/10.1016/j.micpath.2020.104697

305) Tang, D., Chen, M., Huang, X., Zhang, G., Zeng, L., Zhang, G., Wu, S., & Wang, Y. (2023). SRplot: A free online platform for data visualization and graphing. PLOS ONE, 18(11), e0294236. https://doi.org/10.1371/journal.pone.0294236

306) Teng, W., Liao, B., Chen, M., & Shu, W. (2023). Genomic Legacies of Ancient Adaptation Illuminate GC-Content Evolution in Bacteria. Microbiol. Spectr., 11(1),2-5. https://doi.org/10.1128/spectrum.02145-22

307) Tian, S., Ali, M., Xie, L., & Li, L. (2016). Genome-sequence analysis of *Acinetobacter* johnsonii MB44 reveals potential nematode-virulent factors. SpringerPlus, 5(1), 986. https://doi.org/10.1186/s40064-016-2668-5

308) Tonkin-Hill, G., Corander, J., & Parkhill, J. (2023). Challenges in prokaryote pangenomics. Microb. Genom., 9(5), 1-5. https://doi:10.1099/mgen.0.001021.

309) Touchon, M., Cury, J., Yoon, E.-J., Krizova, L., Cerqueira, G. C., Murphy, C., Feldgarden, M., Wortman, J., Clermont, D., Lambert, T., Grillot-Courvalin, C., Nemec, A., Courvalin, P., & Rocha, E. P. C. (2014). The Genomic Diversification of the Whole *Acinetobacter* Genus: Origins, Mechanisms, and Consequences. Genome Biol Evol, 6(10), 2866–2882. https://doi.org/10.1093/gbe/evu225

310) Towner, K. J. (2009). *Acinetobacter*: An old friend, but a new enemy. J Hosp Infect, 73(4), 355–363. https://doi.org/10.1016/j.jhin.2009.03.032

311) Trivedi, R. R., Crooks, J. A., Auer, G. K., Pendry, J., Foik, I. P., Siryaporn, A., Abbott, N. L., Gitai, Z., & Weibel, D. B. (2018). Mechanical Genomic Studies Reveal the Role of D -Alanine Metabolism in Pseudomonas aeruginosa Cell Stiffness. mBio, 9(5), e01340-18.

312) Ueda, H. R., Hayashi, S., Matsuyama, S., Yomo, T., Hashimoto, S., Kay, S. A., Hogenesch, J. B., & Iino, M. (2004). Universality and flexibility in gene expression from bacteria to human. Proc Natl Acad Sci U S A, 101(11), 3765–3769. https://doi.org/10.1073/pnas.0306244101

313) Uniyal, S., Paliwal, R., Verma, M., Sharma, R. K., & Rai, J. P. (2016). Isolation and Characterization of Fipronil Degrading *Acinetobacter* calcoaceticus and *Acinetobacter* oleivorans from Rhizospheric Zone of Zea mays. Bull Environ Contam Toxicol, 96(6), 833–838. https://doi.org/10.1007/s00128-016-1795-6

314) Uppalapati, S. R., Sett, A., & Pathania, R. (2020). The Outer Membrane Proteins OmpA, CarO, and OprD of *Acinetobacter* baumannii Confer a Two-Pronged Defense in Facilitating Its Success as a Potent Human Pathogen. Front Microbiol, 11, 589234. https://doi.org/10.3389/fmicb.2020.589234

315) Van Dexter, S., & Boopathy, R. (2019). Biodegradation of phenol by *Acinetobacter* tandoii isolated from the gut of the termite. Environ Sci Pollut Res Int, 26(33), 34067–34072. https://doi.org/10.1007/s11356-018-3292-4

316) Vijay, G., Mandal, A., Sankar, J., Kapil, A., Lodha, R., & Kabra, S. K. (2018). Ventilator Associated Pneumonia in Pediatric Intensive Care Unit: Incidence, Risk Factors and Etiological Agents. Indian J Pediatr, 85(10), 861–866. https://doi.org/10.1007/s12098-018-2662-8

317) Vijayakumar, S., Biswas, I., & Veeraraghavan, B. (2019). Accurate Identification of Clinically Important *Acinetobacter* Spp.: An Update. Future Sci OA, 5(6), FSO395. https://doi.org/10.2144/fsoa-2018-0127

318) Walsh, I. M., Bowman, M. A., Soto Santarriaga, I. F., Rodriguez, A., & Clark, P. L. (2020). Synonymous codon substitutions perturb cotranslational protein folding in vivo and impair cell fitness. PNAS, 117(7), 3528-3534. https://doi.org/10.1073/pnas.1907126117.

319) Wang, K., Li, P., Li, J., Hu, X., Lin, Y., Yang, L., Qiu, S., Ma, H., Li, P., & Song, H. (2020). An NDM-1-Producing *Acinetobacter* towneri Isolate from Hospital

Sewage in China. Infect Drug Resist, 13, 1105–1110. https://doi.org/10.2147/IDR.S246697

320) Wang, M., Zhu, M., Qian, J., Yang, Z., Shang, F., Egan, A. N., Li, P., & Liu, L. (2024). Phylogenomics of mulberries (Morus, Moraceae) inferred from plastomes and single copy nuclear genes. Mol. Phylogenet. Evol, 197, 1-8. https://doi.org/10.1016/j.ympev.2024.108093.

321) Wang, Q., Zhang, L., Zhang, Y., Chen, H., Song, J., Lyu, M., Chen, R., & Zhang, L. (2022). Comparative genomic analyses reveal genetic characteristics and pathogenic factors of Bacillus pumilus HM-7. Front. Microbial., 13, 1-4. https://doi.org/10.3389/fmicb.2022.1008648.

322) Wang, S., Hu, Y., & Wang, J. (2018). Biodegradation of typical pharmaceutical compounds by a novel strain *Acinetobacter* sp. J Environ Manage, 217, 240–246. https://doi.org/10.1016/j.jenvman.2018.03.096

323) Wang, Y., Wang, Q., & Liu, L. (2019). Crude Oil Degrading Fingerprint and the Overexpression of Oxidase and Invasive Genes for n-hexadecane and Crude Oil Degradation in the *Acinetobacter* pittii H9-3 Strain. Int J Environ Res Public Health, 16(2), 188. https://doi.org/10.3390/ijerph16020188

324) Wattam, A. R., Abraham, D., Dalay, O., Disz, T. L., Driscoll, T., Gabbard, J. L., Gillespie, J. J., Gough, R., Hix, D., Kenyon, R., Machi, D., Mao, C., Nordberg, E. K., Olson, R., Overbeek, R., Pusch, G. D., Shukla, M., Schulman, J., Stevens, R. L., Sullivan, D. E., … Sobral, B. W. (2014). PATRIC, the bacterial bioinformatics database and analysis resource. Nucleic Acids Res, 42(Database issue), D581–D591. https://doi.org/10.1093/nar/gkt1099

325) Wei, Y., Silke, J. R., & Xia, X. (2019). An improved estimation of tRNA expression to better elucidate the coevolution between tRNA abundance and codon usage in bacteria. Sci. Rep., 9(1), 1-3. https://doi.org/10.1038/s41598-019-39369-x.

326) Wolff, P., Villette, C., Zumsteg, J., Heintz, D., Antoine, L., Chane-Woon-Ming, B., Droogmans, L., Grosjean, H., & Westhof, E. (2020). Comparative patterns of

modified nucleotides in individual tRNA species from a mesophilic and two thermophilic archaea. RNA, 26(12), 1957–1975. https://doi.org/10.1261/rna.077537.120.

327) Wong, D., Nielsen, T. B., Bonomo, R. A., Pantapalangkoor, P., Luna, B., & Spellberg, B. (2017). Clinical and Pathophysiological Overview of *Acinetobacter* Infections: A Century of Challenges. Clin Microbiol Rev, 30(1), 409–447. https://doi.org/10.1128/CMR.00058-16

328) Wright, B. W., Molloy, M. P., & Jaschke, P. R. (2022). Overlapping genes in natural and engineered genomes. Nat rev Genet, 23(3), 154–168. https://doi.org/10.1038/s41576-021-00417-w.

329) Wright, F. (1990). The 'effective number of codons' used in a gene. Gene, 87(1), 23–29. https://doi.org/10.1016/0378-1119(90)90491-9

330) Wu, X., Wu, S., Li, D., Zhang, J., Hou, L., Ma, J., Liu, W., Ren, D., Zhu, Y., & He, F. (2010). Computational identification of rare codons of Escherichia coli based on codon pairs preference. BMC Biform. 11, 61-65. https://doi.org/10.1186/1471-2105-11-61.

331) Xia, P. F., Casini, I., Schulz, S., Klask, C. M., Angenent, L. T., & Molitor, B. (2020). Reprogramming acetogenic bacteria with CRISPR-targeted base editing via deamination. ACS Synth. Biol., 9(8), 2162-2171. https://doi.org/10.1021/acssynbio.0c00226.

332) Xia, X. (2018). DAMBE7: New and Improved Tools for Data Analysis in Molecular Biology and Evolution. Mol Biol Evol, 35(6), 1550–1552. https://doi.org/10.1093/molbev/msy073

333) Xiao, J., Zhang, C., & Ye, S. (2019). *Acinetobacter* baumannii meningitis in children: A case series and literature review. Infection, 47(4), 643–649. https://doi.org/10.1007/s15010-018-1234-1

334) Xin, F., Cai, D., Sun, Y., Guo, D., Wu, Z., & Jiang, D. (2014). Exploring the diversity of *Acinetobacter* populations in river water with genus-specific primers

and probes. J Gen Appl Microbiol, 60(2), 51–58. https://doi.org/10.2323/jgam.60.51

335) Xu, Q., Cao, J., Rai, K. R., Zhu, B., Liu, D., & Wan, C. (2024). Codon usage bias of goose circovirus and its adaptation to host. Poult Sci, 103(7), 3-7. https://doi.org/10.1016/j.psj.2024.103775.

336) Xu, Q., Chen, H., Sun, W., Zhu, D., Zhang, Y., Chen, J. L., & Chen, Y. (2021). Genome-wide analysis of the synonymous codon usage pattern of Streptococcus suis. Microb Pathog, 150, 1-6. https://doi.org10.1016/j.micpath.2021.104732.

337) Yacouba, A., Sissoko, S., Tchoupou Saha, O. L. F., Haddad, G., Dubourg, G., Gouriet, F., Tidjani Alou, M., Alibar, S., Million, M., Lagier, J.-C., Raoult, D., Fenollar, F., Fournier, P.-E., & Lo, C. I. (2022). Description of *Acinetobacter* ihumii sp. Nov., Microbacterium ihumii sp. Nov., and Gulosibacter massiliensis sp. Nov., three new bacteria isolated from human blood. FEMS Microbiol Lett, 369(1), fnac038. https://doi.org/10.1093/femsle/fnac038

338) Yamamoto, S., Bouvet, P. J. M., & Harayama, S. (1999). Phylogenetic structures of the genus *Acinetobacter* based on gyrB sequences: Comparison with the grouping by DNA-DNA hybridization. Int J Syst Evol Microbiol, 49(1), 87–95. https://doi.org/10.1099/00207713-49-1-87

339) Yang, C.-H., Su, P.-W., Moi, S.-H., & Chuang, L.-Y. (2019). Biofilm Formation in *Acinetobacter* Baumannii: Genotype-Phenotype Correlation. Molecules, 24(10), 1849. https://doi.org/10.3390/molecules24101849

340) Yang, Q., Lyu, X., Zhao, F., & Liu, Y. (2021). Effects of codon usage on gene expression are promoter context dependent. Nucleic acids Res., 49(2), 818–831. https://doi.org/10.1093/nar/gkaa1253.

341) Yazdansetad, S., Najari, E., Ghaemi, E. A., Javid, N., Hashemi, A., & Ardebili, A. (2019). Carbapenem-resistant *Acinetobacter* baumannii isolates carrying blaOXA genes with upstream ISAba1: First report of a novel OXA subclass from Iran. J Glob Antimicrob Resist, 18, 95–99. https://doi.org/10.1016/j.jgar.2018.12.011

342) Yee, W. X., Barnes, G., Lavender, H., & Tang, C. M. (2023). Meningococcal factor H-binding protein: implications for disease susceptibility, virulence, and vaccines. Trends Microbiol, 31(8), 805-815. https://doi.org/10.1016/j.tim.2023.02.011.

343) Zhang, X., Kong, D., Liu, X., Xie, H., Lou, X., & Zeng, C. (2021). Combined microbial degradation of crude oil under alkaline conditions by *Acinetobacter* baumannii and Talaromyces sp. Chemosphere, 273, 129666.

344) Zhang, Z., Wang, J., Wang, J., Wang, J., & Li, Y. (2020). Estimate of the sequenced proportion of the global prokaryotic genome. Microbiome, 8(1), 1-4. https://doi.org/10.1186/s40168-020-00903-z.

345) Zheng, K., Hong, Y., Guo, Z., Debnath, S. C., Yan, C., Li, K., Chen, G., Xu, J., Wu, F., Zheng, D., & Wang, P. (2022). *Acinetobacter* sedimenti sp. Nov., isolated from beach sediment. Int J Syst Evol Microbiol, 72(11). https://doi.org/10.1099/ijsem.0.005609

346) Zhong, S., & He, S. (2021). Quorum Sensing Inhibition or Quenching in *Acinetobacter* baumannii: The Novel Therapeutic Strategies for New Drug Development. Front Microbiol, 12, 558003. https://doi.org/10.3389/fmicb.2021.558003

347) Zhu, L., Chen, X., & Hou, P. (2019). Mutation of CarO participates in drug resistance in imipenem-resistant *Acinetobacter* baumannii. J Clin Lab Anal, 33(8), e22976. https://doi.org/10.1002/jcla.22976

List of Publications

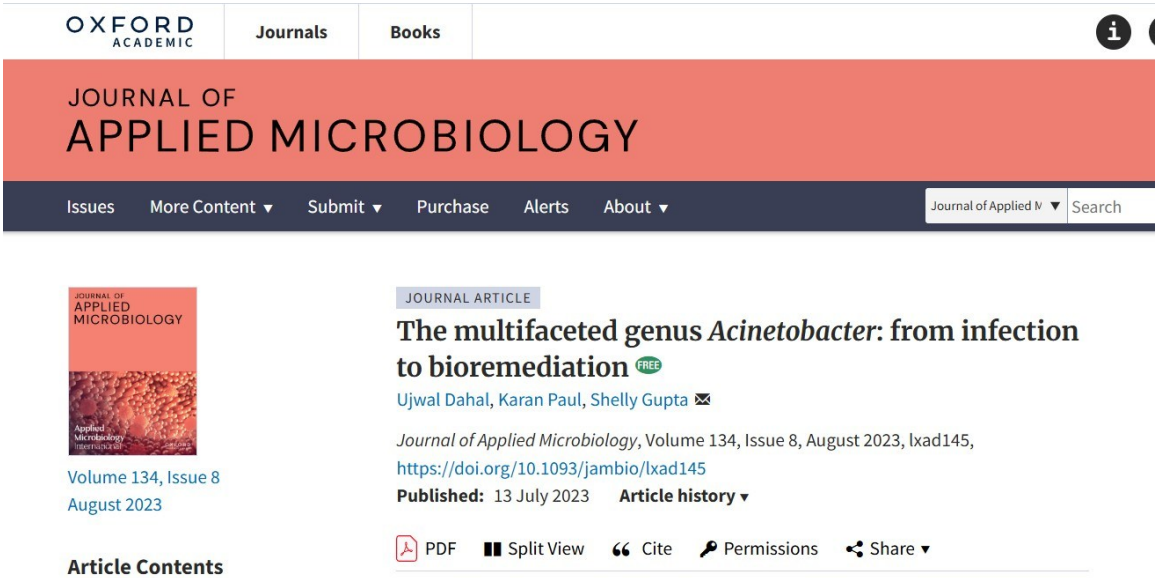

List of Publications

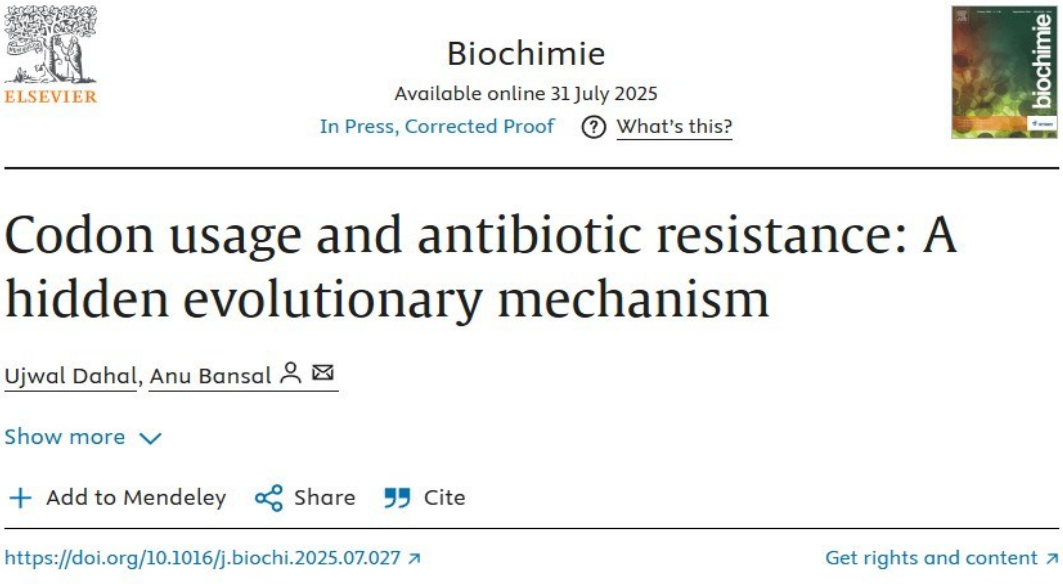

List of Publications

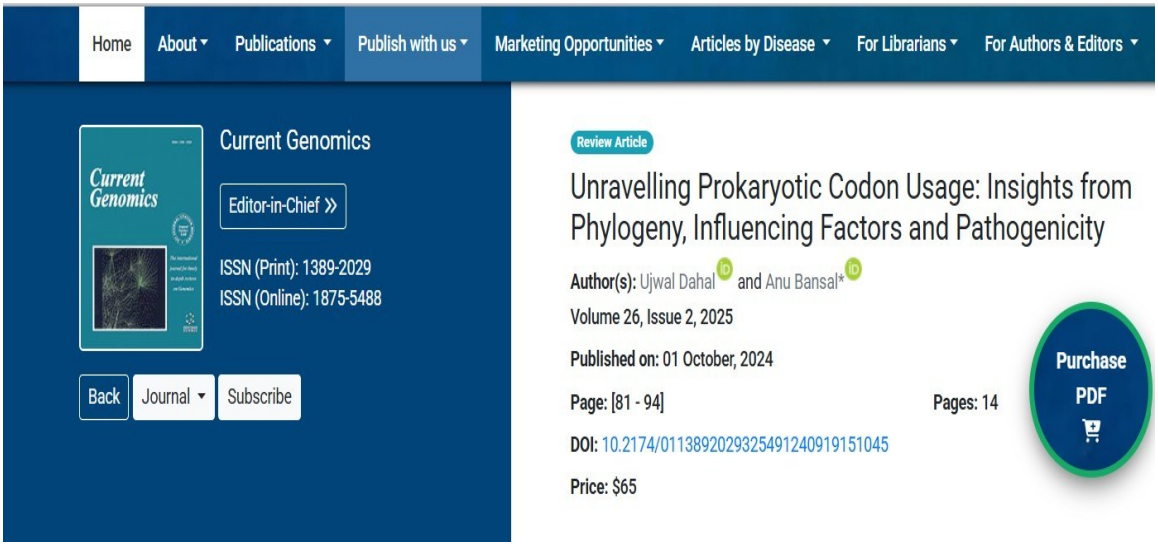

List of Conferences

VIT BHOPAL

CERTIFICATE

OF PRESENTATION

This is to certify that Ujwal Dahal of Lovely Professional University has presented a paper entitled Analysis of Codon Usage Pattern and Influencing Factors in Whole Genus Acinetobacter in the 2nd International Conference on "RECENT TRENDS IN APPLIED SCIENCES AND COMPUTING ENGINEERING (RTASCE-2023)" organized by VIT Bhopal University in association with National Institute of Technology, Warangal during July 7-9, 2023.

Dr. Senthil Kumar Arumugam, Vice Chancellor (I/C) | Dr. Bhumika Chokal, Organizing Secretary | Dr. Navneet Kumar Verma, Convener | Dr. K. Murugeswari, Co - Convener

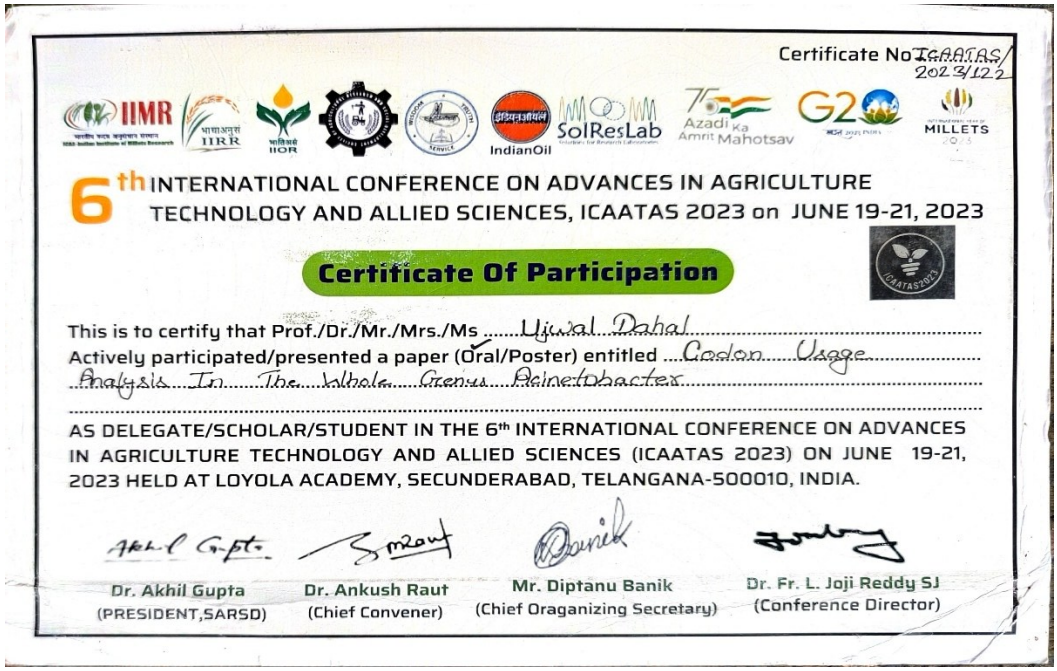

Certificate No ICAATAS/2023/122

IIMR IIRR IIOR IndianOil SolResLab Azadi ka Amrit Mahotsav G20 MILLETS 2023

6th INTERNATIONAL CONFERENCE ON ADVANCES IN AGRICULTURE TECHNOLOGY AND ALLIED SCIENCES, ICAATAS 2023 on JUNE 19-21, 2023

Certificate Of Participation

This is to certify that Prof./Dr./Mr./Mrs./Ms Ujwal Dahal
Actively participated/presented a paper (Oral/Poster) entitled Codon Usage Analysis In The Whole Genus Acinetobacter

AS DELEGATE/SCHOLAR/STUDENT IN THE 6th INTERNATIONAL CONFERENCE ON ADVANCES IN AGRICULTURE TECHNOLOGY AND ALLIED SCIENCES (ICAATAS 2023) ON JUNE 19-21, 2023 HELD AT LOYOLA ACADEMY, SECUNDERABAD, TELANGANA-500010, INDIA.

Dr. Akhil Gupta (PRESIDENT,SARSD) | Dr. Ankush Raut (Chief Convener) | Mr. Diptanu Banik (Chief Oraganizing Secretary) | Dr. Fr. L. Joji Reddy SJ (Conference Director)